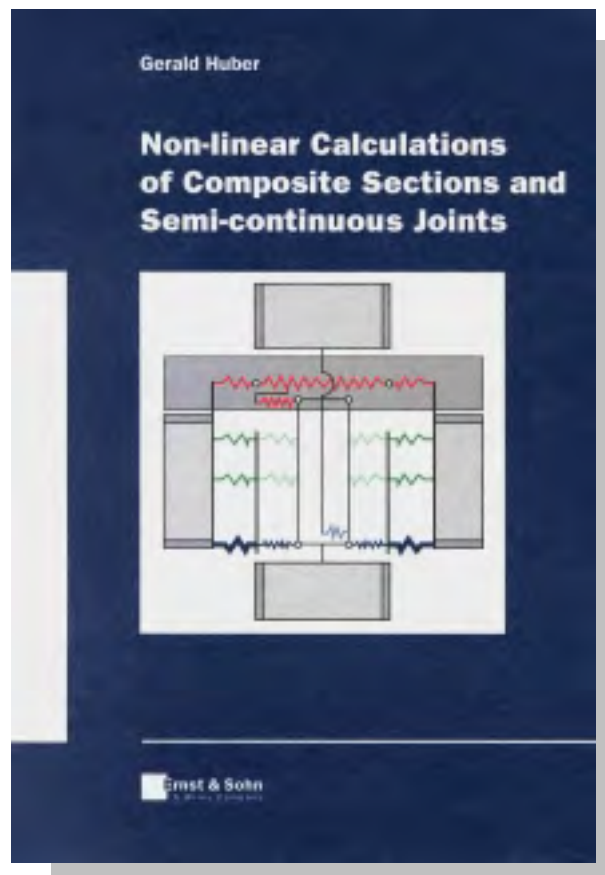


SUMMARY



Non-linear calculations of composite sections and semi-continuous joints

Nicht-lineare Berechnungen von Verbundquerschnitten und biegeweichen Knoten

Non-linear calculations of composite sections and semi-continuous joints

First of all the Eurocodes opened the door to **non-linear calculations** in view of elastic-plastic material laws and geometrical non-linearities. Using the structures up to their plastic capacity instead of the conventional elastic design philosophy enables a drastic reduction of material use at least in view of the ultimate limit state. Resulting from this reduction of construction dimensions automatically the requirements at serviceability limit state are often governing the design with the effect of increasing demands on sophisticated non-linear design tools.

In the recent decade the combined use of different materials within construction elements or even the mixture of construction methods within one structure became more and more disseminated due to the remarkable advantages in view of economy and construction time. In modern construction different materials are used consciously at those locations within the structure where they develop their specific advantages. The most frequently applied combination of construction materials for buildings as well as bridges is that of structural steel and concrete. The importance of such steel-concrete **composite sections** is stressed by the existence of an own Eurocode dedicated to this building technology.

A quite new approach is the reality-related representation of joints in the analysis of structural systems. Joints in a wider sense are connecting all kinds of non-monolithic structural elements and are therefore the crucial key points within members themselves as well as within the overall structure. Nevertheless due to a lack of more realistic knowledge on their characteristics and the way of modelling, the joints so far have been neglected badly and simplifying assumptions concerning their representation often led to time-consuming and expensive constructions. This work focuses on the joints between beam and column members with special regard to their non-linear characterisation. With the help of an analytical component approach the so-called **semi-continuous joint** response can be determined. This method has successfully been applied to steel and composite structural joints, however it could easily be enlarged to other materials.

The first chapter of this doctoral thesis - the **introduction** - contains general considerations about new building concepts and different construction methods followed by a detailed presentation of construction elements in so-called mixed structures. This covers the different types of slabs, beams, columns and – as new construction elements influencing the design calculations – the joints. To avoid misunderstandings it continues with the definitions and the terminology

used in composite and mixed construction. Special attention is paid to the differences between bare composite construction and the more general (sometimes even already unconsciously used) mixed building technology. From the shear-slip characteristic of a single connector it is led over to the behaviour of the overall shear joint between the slab and the sheeting and the slab and the beam. The joint's resistance is linked to the degree of shear connection, the so-called shear interaction concerns the stiffness and the third key value is the joint's deformation capacity. The erection sequence determines the type of composite action.

The second chapter deals with **composite floors** consisting of the slabs and the beams. In the general part the principles of composite action between the contributing elements are discussed. A further chapter is dedicated to the new composite slim-floor systems, where the steel beams are already integrated into the slabs with the result of a drastic reduction of construction height. After some construction principles the main advantages of this innovative technology are presented. The enormous flexibility is emphasised giving some examples in view of slab types, floor beams, columns and joints. A special testing programme has been worked out for the characterisation of a new dowel system, the so-called punched shear connector. First of all the principle idea and the manufacturing process of these dowels which are already integrated into the floor beam are described. For the testing programme it is distinguished between fundamental push-out tests and final beam tests, which have been carried out for the validation of the gained results. The test evaluation procedure is described in detail for the design resistance, the stiffness and the important deformation capacity applying the method of partial shear connection.

A real focal point of this thesis is the theoretical background of **joint representation** described in chapter 3. Comprehensive knowledge on this field has already available at the Institute of Steel and Timber Construction in Innsbruck. Basing on that this chapter has developed iteratively as a result of numerous proposals, which have been introduced by the author into the Drafting Group for Composite Connections, aiming at the provision of Model Clauses for ENV 1994-1-1. First general considerations are made about the new semi-continuous joint philosophy, followed by the description of the component method as an analytical method of joint characterisation. Following the explanation of the different available component models, the basic joint components are listed. Refinements in view of the tension region of composite joints has become necessary and are therefore is treated in a separate chapter. Untiring discussions within international committees about component characterisation on the basis of test results

have shown the importance of a unified test evaluation concept, which is given herein for all the key characteristics: initial stiffness, design resistance, elastic limit and rotation or deformation capacity. The assembly of contributing non-linear components to the overall joint response is one of the main tasks of this doctoral thesis. For that purpose an own computer program has been realised – details are described in chapter four, however already chapter three gives most of the theoretical background in view of translational and rotational grouping of component springs. Further comparisons are made between sophisticated and simplified assembly models. Passing different possibilities of joint modelling a lot of background considerations are made in view of the differences between joint modelling reflecting the actual behaviour and simplified joint modelling (as used in the Eurocodes). A so-called joint transformation is developed to improve accuracy when applying the simplified joint model. This is followed by comments on the joint classification concept introduced by the Eurocodes. For a first comparative judgement of joint test results a joint assessment system is proposed leading to a simple possibility to define joint families. The chapter is concluded with final guidelines on joint representation within the global frame analysis as a summary of the previous considerations.

After these theoretical and quite sophisticated investigations their practical applicability is proved by a specially developed **computer program** called CoBeJo (Composite Beams and Joints). This program is dedicated to scientists as well as innovative practitioners covering the already described three fields of modern engineering: non-linear calculations of composite sections and semi-continuous joints. Special attention is paid to an advanced and self-explaining post-processing. A lot of graphical tools are provided to inspect the various results. At present two main modules for the separate non-linear characterisation of composite sections and semi-continuous joints are available. An extension to a common action of beam and joint elements within overall semi-continuous beams and frames is planned.

At the beginning the mechanical background as well as the handling of the first module covering composite but also steel beam cross sections (BCS) is described starting with the definition of the section geometry and the respective material laws and ending with all possible calculations for the steel section alone, the concrete section alone and the overall composite section. The following non-linearities are taken into consideration: non-linear material laws of steel, reinforcing steel and concrete including the tension stiffening effect of concrete between the cracks. Furthermore a jump of the strain distribution at the layer of

shear connection between the steel section and the reinforced concrete section due to incomplete shear interaction may be considered.

The second part of the CoBeJo description is dedicated to the module of joint characterisation (*JOINT*). In the introduction the main principles of modern joint representation are repeated, maybe giving a better general overview of this new philosophy to a newcomer than the more sophisticated chapter on joint representation itself. After the explanation how a joint configuration can be defined by giving the characteristics of all contributing translational components, the iterative assembly procedure is described in detail followed by numerous graphical tools helping to explore the joint response in a quite convenient way. So on the one hand this module provides a powerful tool for scientific purposes in view of further parameter studies and on the other hand it is meant to support the promotion of the semi-continuous joint concept.



This book is available in English language:
ISBN 3-433-01250-4
Ernst & Sohn
Verlag für Architektur und techn. Wiss. GmbH
Buehringstr. 10
D-13086 BERLIN
Germany
e-mail: mktg@ernst-und-sohn.de

Nicht-lineare Berechnungen von Verbundquerschnitten und biegeweichen Knoten

Zwei Bereiche moderner Ingenieurbautechnologie waren Thema dieser Doktorarbeit: Stahl-Beton-Verbundquerschnitte für Deckenträger, Deckenplatten und Stützen und Riegel-Stützen-Verbindungen (sogenannte Knoten).

Das erste Kapitel - die **Einleitung** - beinhaltet allgemeine Überlegungen zu neuen Bauwerkskonzepten und verschiedenen Baumethoden, gefolgt von einer detaillierten Beschreibung von Bauteilen der sogenannten Mischbautechnologie. Dabei werden verschiedene Typen von Deckenplatten, Deckenträgern, Stützen und – als neue Bauteile, die die Tragwerksbemessung beeinflussen – Knoten behandelt. Um Mißverständnissen vorzubeugen, folgen Definitionen und Begriffsbestimmungen für die Verbund- und Mischbauweise. Dabei wird speziell auf die Unterschiede zwischen reinem Verbundbau und der allgemeineren (ev. sogar schon unbewußt eingesetzten) Mischbautechnologie eingegangen. Aus dem Verbund-Schlupf-Verhalten einzelner Verbindungsmittel wird danach das Verhalten der gesamten Dübelfuge zwischen Betonplatte und Stahlblech bzw. zwischen Deckenplatte und Deckenträger hergeleitet. Die Tragfähigkeit der Fuge wird als Verdübelungsgrad angegeben, die Verbundnachgiebigkeit hängt mit deren Steifigkeit zusammen, und als dritter Kennwert ist das Verformungsvermögen zu nennen. Der Bauablauf wiederum bestimmt die Verbundart.

Im zweiten Kapitel geht es um **Verbunddecken**, bestehend aus Deckenplatten und Deckenträgern. Zuerst werden die Grundlagen der Verbundwirkung zwischen den einzelnen Bauelementen im allgemeinen Teil erörtert. Ein weiteres Kapitel ist den Flachdecken (slim-floors) gewidmet, wo der stählerne Deckenträger in die Deckenplatte integriert wird und dadurch bedeutend an Bauhöhe eingespart werden kann. Im Anschluß an einige Konstruktionsprinzipien werden die Vorteile dieser innovativen Baumethode vorgestellt. Deren beeindruckende Flexibilität wird dabei anhand von Beispielen hinsichtlich Platten-, Träger-, Stützen- und Knotentypen unterstrichen. Zur Ermittlung des Verhaltens eines neuen Verbindungsmittels, des sogenannten Stanzdübels, wurde ein spezielles Versuchsprogramm ausgearbeitet. Zuerst werden die Grundlagen sowie die Herstellung dieser Dübel beschrieben, die bereits direkt aus dem Trägermaterial geformt werden. Beim

Versuchsprogramm wird zwischen grundlegenden Push-out Tests und abschließenden Trägerversuchen, die lediglich zur Bestätigung der zuvor gewonnenen Ergebnisse dienen, unterschieden. Die Testauswertung wird detailliert für die Bemessungstragfähigkeit, die Steifigkeit und die wichtige Verformungskapazität erläutert, wobei die Methode des nachgiebigen Trägerverbundes zur Anwendung kam.

Einer der Hauptschwerpunkte dieser Arbeit ist der theoretische Hintergrund der **Modellbildung von Knoten**, der in Kapitel 3 beschrieben wird. Umfassendes Wissen auf diesem Gebiet war bereits zuvor am Institut für Stahlbau und Holzbau in Innsbruck verfügbar. Darauf aufbauend entstand dieses Kapitel sukzessive aus zahlreichen Vorschlägen, die der Autor in die Drafting Group for Composite Connections – ein Gremium zur Erstellung von Model Clauses für die ENV 1994-1-1 – eingebracht hat. Nach allgemeinen Überlegungen zu biegeweichen Knoten folgt die Beschreibung der Komponentenmethode, einer analytischen Vorgangsweise zur Bestimmung des Knotenverhaltens. Zuerst werden verfügbare Komponentenmodelle vorgestellt, danach sind zahlreiche Knotenkomponenten zusammengefaßt. Die erforderlich gewordenen Verbesserungen der Modellierung der Zugregion in Verbundknoten werden detailliert in einem eigenen Kapitel beschrieben. Unermüdliche Diskussionen innerhalb internationaler Forscherkreise haben die Notwendigkeit eines vereinheitlichten Testauswerteverfahrens für die Komponentencharakterisierung gezeigt. Hierin wird ein Vorschlag für folgende Kennwerte unterbreitet: Anfangssteifigkeit, Bemessungstragfähigkeit, elastische Grenztragfähigkeit und Rotations- bzw. Deformationsvermögen. Die Gruppierung (Assembly) aller am Knotenverhalten beteiligten nichtlinearen Komponenten zum Gesamtverhalten des Knotens ist ein weiterer Hauptschwerpunkt dieser Dissertation. Zu diesem Zweck wurde ein eigenes Computerprogramm entwickelt. Details dazu werden zwar erst in Kapitel 4 beschrieben, jedoch gibt bereits dieses Kapitel Einblick in die theoretischen Hintergründe der Weg- und Drehfedergruppierung von Komponentenfedern. Darüber hinaus werden Vergleiche zwischen wissenschaftlichen und vereinfachten Assembly-Modellen angestellt. Nach einer allgemeinen Vorstellung der verschiedenen Möglichkeiten der Knotenmodellierung werden zahlreiche vergleichende Studien zwischen dem realitätsnahen und dem

vereinfachten Knotenmodell, wie es in den Eurocodes angegeben ist, durchgeführt. Eine sogenannte Knotentransformation wurde entwickelt, um die Ergebnisse bei Anwendung des vereinfachten Knotenmodells zu verbessern. Es folgen Kommentare zum Eurocode-Konzept der Knotenklassifikation. Zum Zweck einer Erstbeurteilung der Ergebnisse aus Knotenversuchen wird ein Assessment-Verfahren vorgeschlagen. Dies ermöglicht eine einfache Bestimmung von gleichartigen Knotenfamilien. Abschließend werden die vorhergehenden Erkenntnisse in Form von Richtlinien für die Modellbildung von Knoten bei der Tragwerksberechnung zusammengefaßt.

Nach diesen theoretischen Untersuchungen wird deren praktische Umsetzbarkeit anhand eines speziell für diesen Zweck entwickelten **Computerprogrammes** namens CoBeJo (Composite Beams and Joints) unter Beweis gestellt. Dieses Programm ist sowohl für Forscher als auch innovative Praktiker bestimmt und umfaßt die bereits zuvor erwähnten Bereiche moderner Bautechnologie: nichtlineare Berechnung von Verbundquerschnitten und biegeweichen Knoten. Großer Wert wurde dabei auf ein fortschrittliches und selbsterklärendes Post-Processing gelegt. Eine Vielzahl von Grafikwerkzeugen ermöglichen ein detailliertes und übersichtliches Studium der Ergebnisse. Derzeit sind zwei wesentliche Module für die getrennte nichtlineare Charakterisierung von Verbundquerschnitten und biegeweichen Knoten verfügbar. Eine Erweiterung auf ein gemeinsames Zusammenwirken von Träger- und Knotenelementen innerhalb eines biegeweichen Trägers oder Rahmens ist geplant.

Zu Beginn wird der mechanische Hintergrund sowie die Handhabung des ersten Moduls beschrieben, der zur Berechnung von Stahl- und Verbundquerschnitten (BCS-Beam Cross Section) dient. Im Anschluß an die Eingabe der Querschnitts- und Materialkennwerte sind die Berechnungsverfahren für den isolierten Stahlquerschnittsanteil, den isolierten Betonquerschnittsanteil und den Gesamt-Verbundquerschnitt erläutert. Folgende Nichtlinearitäten werden dabei berücksichtigt: das nichtlineare Stoffgesetz von Baustahl, Bewehrungsstahl und Beton unter Berücksichtigung des „Tension stiffening effects“ zwischen den Rissen, sowie ein Dehnungssprung in Höhe der Dübelfuge zwischen dem Stahl- und dem bewehrten Betonanteil infolge der Dübelnachgiebigkeit.

Der zweite Teil der CoBeJo Beschreibung behandelt das Modul zur Knotencharakterisierung (*JOINT*). In der Einleitung werden die Grundlagen moderner Knotenmodellbildung in einer praxisorientierteren Weise als in Kapitel 3 wiederholt, um einem Newcomer auf diesem Gebiet einen besseren Überblick zu geben. Die Eingabe der zu untersuchenden Knotenkonfiguration erfolgt über die Definition des Verhaltens der jeweiligen Wegfeder-Komponenten. Danach wird die iterative Assembly von den einzelnen Wegfedern zur Knotendrehfeder im Detail beschrieben, gefolgt von den zahlreichen Grafikwerkzeugen, die das Erforschen des Knotenverhaltens auf eine komfortable und spielerische Weise ermöglichen. Infolgedessen stellt dieses Modul einerseits ein leistungsfähiges Werkzeug für wissenschaftliche Zwecke hinsichtlich weiterer Parameterstudien dar, andererseits ist es auch dazu bestimmt das recht neue Konzept von biegeweichen Knoten in der Praxis zu etablieren.



Dieses Buch ist in englischer Sprache erhältlich:
ISBN 3-433-01250-4
Ernst & Sohn
Verlag für Architektur und techn. Wiss. GmbH
Bühningstr. 10
D-13086 BERLIN
Deutschland
e-mail: mktg@ernst-und-sohn.de

Extract from the doctoral thesis

NON-LINEAR CALCULATIONS OF COMPOSITE SECTIONS AND SEMI-CONTINUOUS JOINTS

which has been published by



Ernst & Sohn
Verlag für Architektur und techn. Wissenschaften GmbH
Buehringstrasse 10
D-13086 Berlin
Germany
Tel. +49 30 47031 280
mktg@ernst-und-sohn.de

ISBN 3-433-01250-4
350 pages. Format 17 x 24 cm
PB DM 148,- / ÖS 1080,- / sFr 131,- / € 78,-
Publication date: December 1999

Table of Contents

contents of the full book available at Ernst & Sohn, Berlin – the part given within this file is indicated by a green bar on the left side

PREFACE

ABSTRACT / KURZFASSUNG

TABLE OF CONTENTS

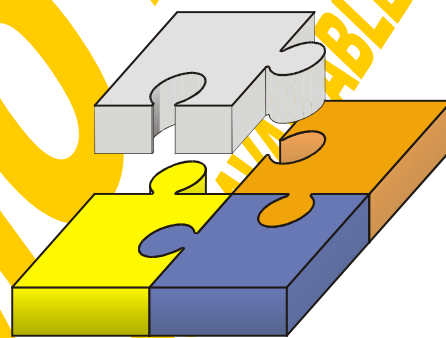
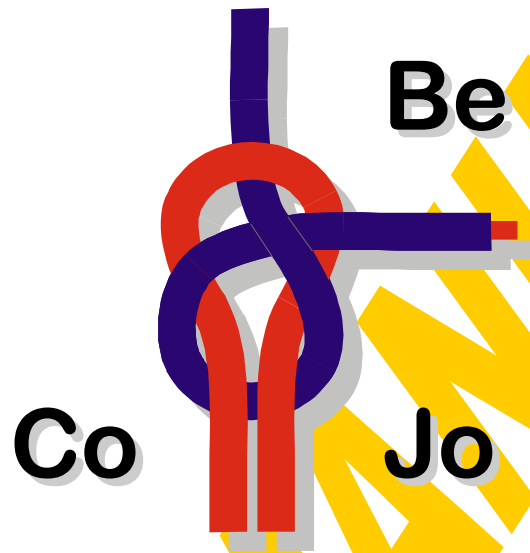
1	INTRODUCTION	1
1.1	General.....	3
1.2	Construction methods	5
1.3	Construction elements in mixed structures.....	6
1.3.1	Slabs	6
1.3.1.1	Reinforced concrete slabs.....	7
1.3.1.2	Pre-stressed concrete slabs.....	7
1.3.1.3	Profiled steel sheeting.....	7
1.3.2	Beams.....	9
1.3.3	Columns.....	10
1.3.4	Joints.....	11
1.4	Definitions and terminology	14
1.4.1	Composite construction	14
1.4.2	Mixed building technology.....	14
1.4.3	Shear-slip characteristic of a single connector.....	14
1.4.4	Degree of shear connection (resistance)	15
1.4.5	Shear interaction (stiffness)	17
1.4.6	Deformation capacity	18
1.4.7	Type of composite action	19
2	COMPOSITE FLOORS	21
2.1	General.....	23
2.2	Slim-floor systems	24
2.2.1	Construction principles.....	24
2.2.2	Advantages	25
2.2.3	Flexibility	27
2.2.3.1	Floor slab.....	27
2.2.3.2	Floor beam	28
2.2.3.3	Columns and joints.....	31
2.3	Punched shear connectors.....	32
2.3.1	Introduction	32
2.3.2	Description	32

2.3.3	Testing programme	33
2.3.3.1	Push-out tests.....	34
2.3.3.2	Beam tests.....	36
2.3.4	Test evaluation	39
2.3.4.1	Design resistance	39
2.3.4.2	Stiffness.....	40
2.3.4.3	Deformation capacity.....	40
2.3.4.4	Shear-slip characteristic	41
3	JOINT REPRESENTATION.....	43
3.1	General.....	45
3.2	Joint characterisation.....	48
3.3	Component models.....	49
3.4	Basic joint components.....	54
3.5	Tension region of composite joints	59
3.5.1	General.....	59
3.5.2	Mechanical truss model.....	60
3.5.2.1	General.....	60
3.5.2.2	Sources of deformation	61
3.5.2.3	Gap.....	64
3.5.2.4	Stiffness.....	64
3.5.3.	Model refinement in view of consistent global frame analysis	66
3.5.4.	Summary of the refined model	69
3.5.4.1	Translational stiffness.....	69
3.5.4.2	Resistance.....	69
3.5.4.3	Deformation capacity.....	70
3.6	Component characterisation and test evaluation.....	70
3.6.1	General.....	70
3.6.2	Initial stiffness.....	75
3.6.3	Design resistance	76
3.6.4	Elastic limit	77
3.6.5	Rotation capacity	78
3.6.6	Summary	78
3.7	Component assembly	79
3.7.1	Translational spring groups	79
3.7.2	Rotational spring for the connection	81
3.7.2.1	General.....	81
3.7.2.2	Bare steel joint.....	83
3.7.2.3	Composite joint with stiffened panel in compression.....	86
3.7.2.4	Composite joint with contact plate connection.....	88
3.7.3	Rotational spring for the shear panel.....	90
3.8	Joint modelling.....	90
3.8.1	CoBeJo (reflecting the actual behaviour)	90
3.8.2	Finite joint model (reflecting the actual behaviour)	91

3.8.3	Finite stub model (nearly reflecting the actual behaviour).....	94
3.8.4	Concentrated joint model (EC3 and EC4; simplified modelling)	96
3.9	Joint transformation.....	97
3.9.1	General	97
3.9.2	Connection L (bending influence)	98
3.9.3	Shear influence S.....	111
3.9.4	Entire spring C (left/right)	116
3.9.5	Continuity of the joint transformation	117
3.9.6	Summary of transformation factors.....	123
3.10	Joint classification	124
3.10.1	General	124
3.10.2	Comments on EC3 classification	126
3.10.2.1	Stiffness classification	126
3.10.2.2	Strength classification	126
3.10.2.3	Rotation classification	127
3.11	Joint assessment (German: Einstufung)	130
3.11.1	General	130
3.11.2	Dimensionless curve representation.....	131
3.11.3	Assessment by stiffness	132
3.11.4	Assessment by strength.....	136
3.11.5	Assessment by rotation capacity.....	137
3.11.6	Assessment example.....	138
3.12	Global frame analysis.....	138
3.13	Summary.....	145
4	COMPUTER PROGRAM.....	149
4.1	General.....	151
4.2	Beam Cross Section.....	153
4.2.1	General	153
4.2.2	Section management	155
4.2.3	Steel section	161
4.2.3.1	Section input.....	161
4.2.3.2	Internal forces to a given strain distribution (steelstrain).....	165
4.2.3.3	Strain distribution to a given normal force (Nsteeliteration)	166
4.2.3.4	N-M-relation for a defined curvature (NMsteel).....	170
4.2.4	Concrete section	179
4.2.4.1	Section input.....	179
4.2.4.2	Internal forces to a given strain distribution (concstrain).....	189
4.2.4.3	Strain distribution to a given normal force (Nconcriteration)	191
4.2.4.4	N-M-relation for a defined curvature (NMconcr)	193
4.2.5	Composite section	201
4.2.5.1	Section input.....	201
4.2.5.2	Theoretical background.....	202
4.2.5.3	Ni-M-relation for a defined curvature (NMcomp).....	203

4.2.5.4	Ni-M- κ -relation for a defined strain jump (DEcomp).....	223
4.2.5.5	Given M and strain jump (cross sectional design).....	232
4.2.5.6	Forces and moments to a given strain distribution.....	234
4.2.5.7	Summary.....	241
4.3	Joint characterisation.....	245
4.3.1	Introduction.....	245
4.3.1.1	General.....	245
4.3.1.2	Joint characterisation (German: Knotencharakterisierung).....	246
4.3.1.3	Joint classification (German: Knotenklassifikation).....	249
4.3.1.4	Curve idealisation (German: Kurvenidealisation).....	250
4.3.1.5	Joint modelling (German: Knotenmodellierung).....	250
4.3.1.6	Summary.....	254
4.3.2	General.....	256
4.3.3	Joint management.....	259
4.3.4	Joint input.....	265
4.3.5	Linear grouping.....	271
4.3.6	Basic joint calculations.....	279
4.3.6.1	Fundamental calculation.....	280
4.3.6.2	Fundamental graphs.....	285
4.3.6.3	Fundamental iteration.....	290
4.3.6.4	Summary.....	295
4.3.7	Main joint calculations.....	296
4.3.7.1	Assembly boundaries.....	297
4.3.7.2	Component assembly.....	298
4.3.7.3	Warnings.....	299
4.3.7.4	Presentation of results.....	301
4.3.7.5	Final comparisons.....	310
4.3.7.6	Unbalanced joint loading.....	312
4.3.8	Conclusions.....	313
5	CONCLUSIONS / SCHLUSSWORT.....	315
5.1	General / Allgemeines.....	317 / 324
5.2	Structure of this doctoral thesis / Aufbau der Dissertation.....	317 / 324
5.3	Outlook / Ausblick.....	319 / 327
	REFERENCES.....	329
	CURRICULUM VITAE / LEBENS LAUF.....	345

4	COMPUTER PROGRAM.....	149
4.1	General.....	151
4.2	Beam Cross Section.....	153
4.2.1	General.....	153
4.2.2	Section management.....	155
4.2.3	Steel section.....	161
4.2.3.1	Section input.....	161
4.2.3.2	Internal forces to a given strain distribution (steelstrain).....	165
4.2.3.3	Strain distribution to a given normal force (Nsteeliteration).....	166
4.2.3.4	N-M-relation for a defined curvature (NMsteel).....	170
4.2.4	Concrete section.....	179
4.2.4.1	Section input.....	179
4.2.4.2	Internal forces to a given strain distribution (concstrain).....	189
4.2.4.3	Strain distribution to a given normal force (Nconcriteration).....	191
4.2.4.4	N-M-relation for a defined curvature (NMconcr).....	193
4.2.5	Composite section.....	201
4.2.5.1	Section input.....	201
4.2.5.2	Theoretical background.....	202
4.2.5.3	N_i -M-relation for a defined curvature (NMcomp).....	203
4.2.5.4	N_i -M- κ -relation for a defined strain jump (DEcomp).....	223
4.2.5.5	Given M and strain jump (cross sectional design).....	232
4.2.5.6	Forces and moments to a given strain distribution.....	234
4.2.5.7	Summary.....	241



DEMO - MANUAL
AVAILABLE AT ERNST & SOHN, BERLIN

4 Computer Program

4.1 General

Within the scope of this work two of the main modules of a software-package called „CoBeJo“ (Non-linear Calculations for Composite Beams and Joints) have been worked out. The final aim of this program will be the calculation of composite beams with partial shear connection and therefore also incomplete shear interaction taking into consideration the material non-linearities, the non-linear force-deformation behaviour of the shear interface and furthermore the non-linear moment-rotation response of the composite joints. Out of this task a clear subdivision into the following basic jobs arose:

- input and characterisation of the **beam's cross-section (BCS)**
- input and characterisation of the **joint configuration (JOINT)**
- **global analysis** of the entire beam formed by finite beam elements and joints (planned for the future)

Each of these three jobs is solved by a separate computer program representing the basic modules of the CoBeJo package. That results in clear input and output windows, where the user will not get lost due to the complexity of the job. The calculation is solved step by step with a multitude of provisional results, which at one hand ease checks and at the other hand enable to adjust the analysed system interactively in view of economical optimisation. Besides especially for scientific purposes parameter studies have successfully been performed. In addition the results of the single modules can also be used as input data for other programs using the output files as interface.

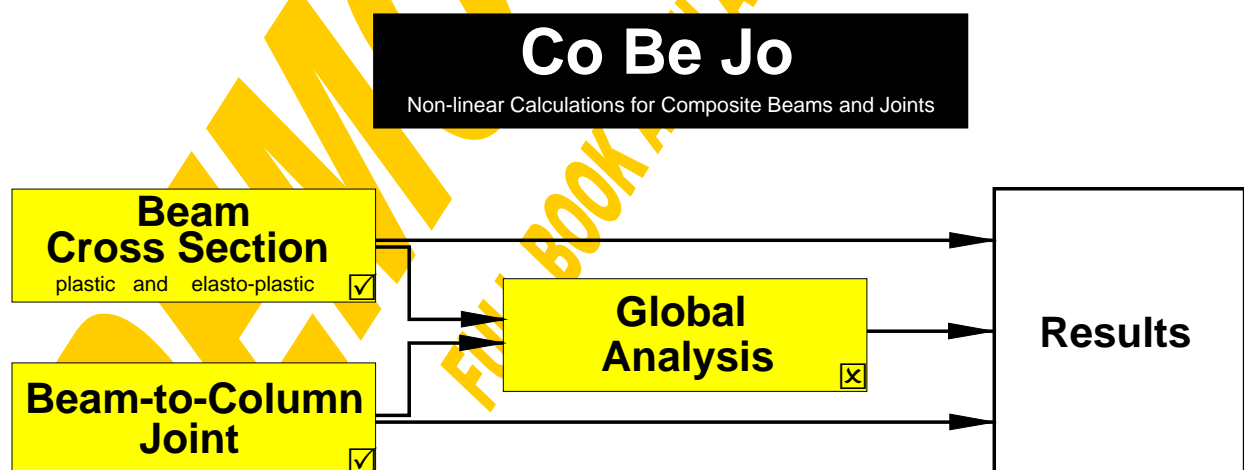


Fig.4-1 Structure of the computer program package CoBeJo

As the acceptance of a computer program mainly depends on the simplicity and clearness of the pre- and post-processing the object-orientated MS Windows-compiler Visual Basic has been chosen. In the following the theoretical background as well as the handling of the realised two main modules „Beam Cross Section“ and „Beam-to-Column Joint“ will be described in detail.

Remark: A dot (not a comma) has to be defined as decimal separator in MS Windows for all modules of this program.

DEMO - MANUAL
FULL BOOK AVAILABLE AT ERNST & SOHN, BERLIN

4.2 Beam Cross Section

4.2.1 General

First of all a comfortable procedure for the input of composite beam sections should be provided followed by calculations to study the member response. The clear separation between the steel and the reinforced concrete section part has strictly been realised throughout the whole program for the input as well as for the results. To make accessible the influences of the section parts on the entire composite member response the behaviour of the steel and concrete part at one hand can be analysed separately and at the other hand many of the composite results are given as the sum of steel and concrete. Again this eases the check of the results and also enables to examine, if both section parts, steel and reinforced concrete, are used in an efficient way or if failure of the overall composite member is dominated by one section part while the other one is only hardly stressed.

The section analysis is based on the assumption of a linear strain distribution, taking into consideration a jump of strains at the shear interface due to the incomplete interaction. Generally a constant distribution of strains in transverse direction is expected. To take account for that effective concrete widths have to be used. From the given stress-strain diagrams of the section elements the stress distribution can be derived from which the internal forces and moments, both for the section parts and for the entire composite section, can be calculated. Investigating the whole range of possible strain distributions interactions between internal forces of the entire section and that of the section parts as well as coherence between internal forces and deformations can be gained.

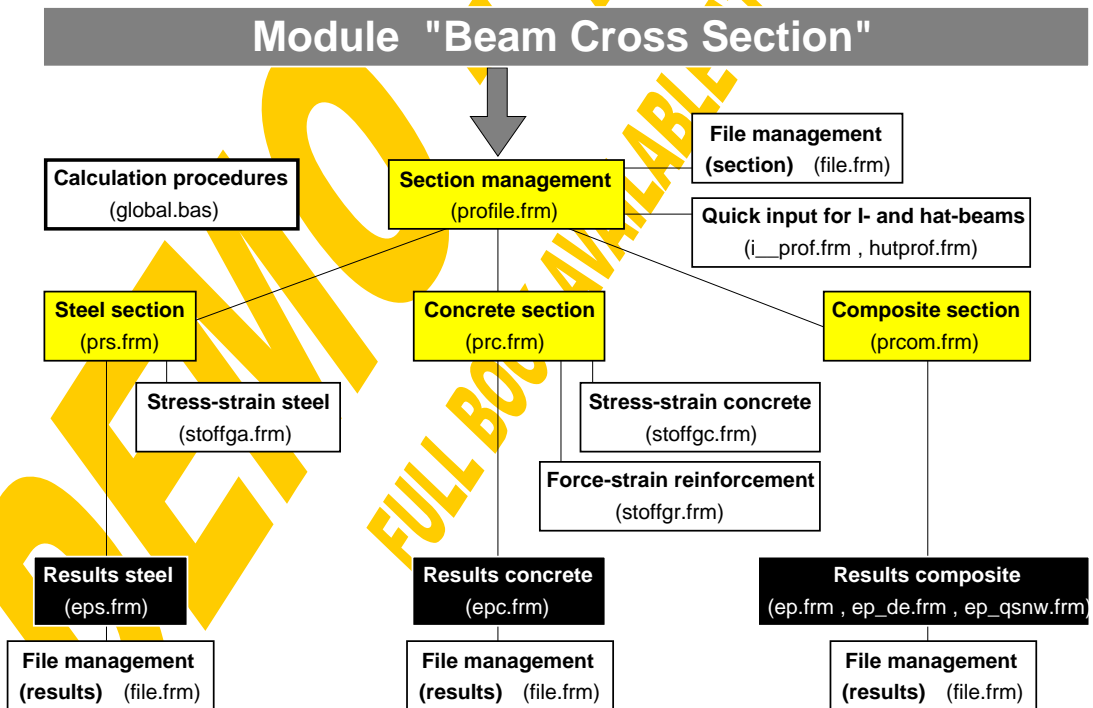


Fig.4-2 Structure of the module „Beam Cross Section“

At the beginning only the fully plastic limit state has been treated assuming a perfectly plastic behaviour of each element. In a second step the program has been extended to the whole elasto-plastic range. At one hand self-evidently the input of the material characteristics had to be extended and at the other hand the iterative calculations had to be fully changed. A special aim was to bring in the tension stiffening effect of the concrete between the cracks following the guidelines given in the new Composite Bridge Code [62] and to enable partial shear connection also in the hogging moment regions beyond the rules of ENV 1994-1 [59,109]. As the elasto-plastic calculation of course also covers the fully plastic state as an extreme limit the module for plastic section analysis will not be described herein any more. It only proved to be very useful for checks of the elasto-plastic module as both programs are based on completely different calculation methods.

Summarising the module for the Beam Cross Section represents an instrument for studying the response of composite members within the full elasto-plastic range considering the contribution of the individual section parts steel and concrete. The principle structure of this module can be seen in Fig.4-2.

DEMO - MANUAL
FULL BOOK AVAILABLE AT ERNST & SOHN, BERLIN

4.2.2 Section management

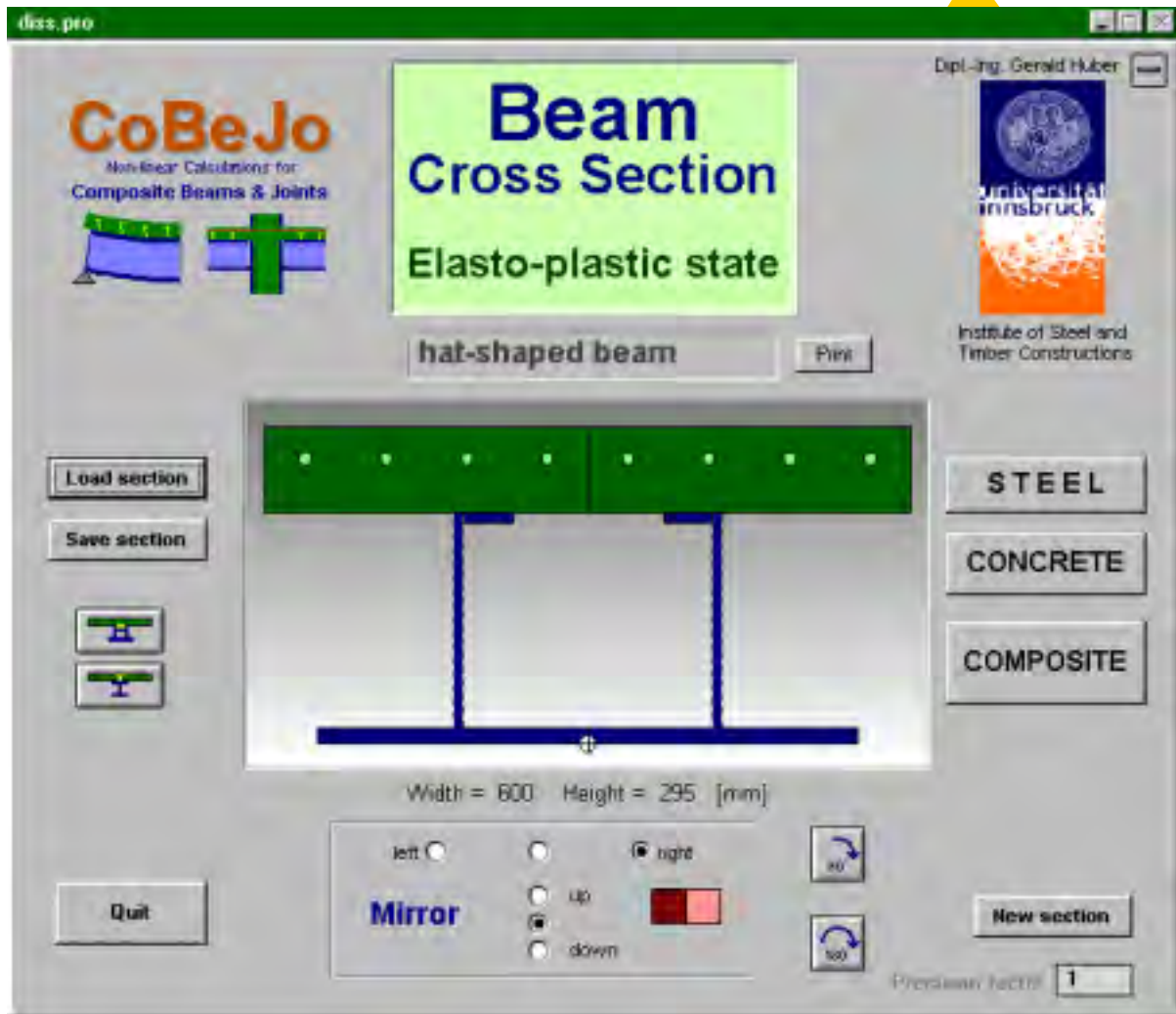


Fig.4-3 Start-up window of the module „Beam Cross Section“ (profile.frm)

Fig.4-3 shows the start-up window of the module „Beam Cross Section“. It serves for the file-management of composite sections and gives the link to the windows for the input and calculation of the steel and the concrete section part as well as to the composite calculations.

A special composite cross section consisting of a hat-shaped steel beam and an upper reinforced concrete plate has been chosen for the following examples. The cross sectional input data, which can be printed with the button „Print“, is given on page 157. All section data including section name, safety factors, geometry and material properties are saved in a file with the default-extension „*.pro“. The input file of the example section „diss.pro“ can be seen on page 158. Clicking on the „Load section“ or „Save section“ buttons activates the window for the file management (Fig.4-4). Apart from the possibility to load or save section data buttons are provided for a small variety of disk manipulation like „Create Directory“, „Remove Directory“, „Rename File“, „Copy File“ and „Delete File“.

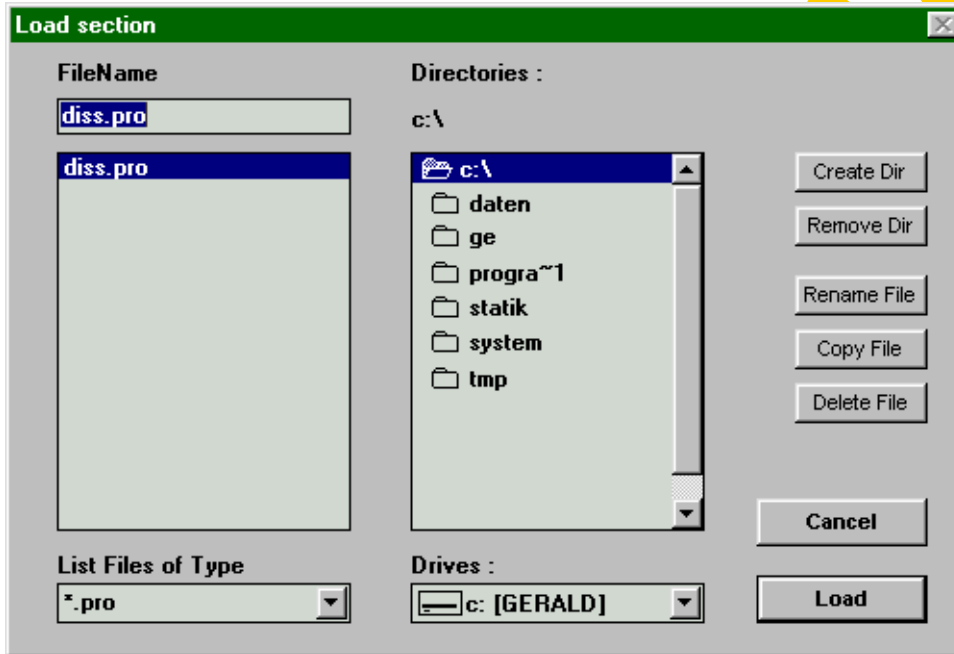


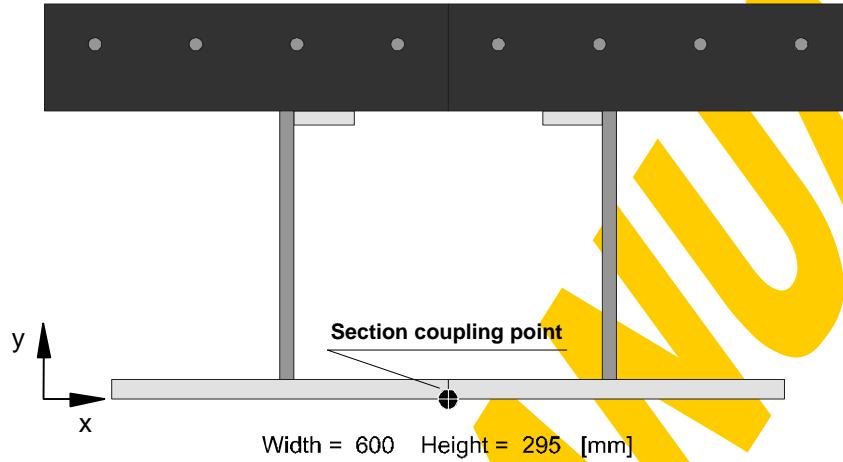
Fig.4-4 File management (file.frm)

It was tried to keep the program self-explaining, however the possible further operations concerning the start-up window should also be listed: A special text field is reserved for a section name, the button „New section“ deletes the actual profile, a section can be rotated 90° or 180° and the field for mirror options enables to reduce the input procedure for symmetrical sections (remark: the reinforced concrete section will only be mirrored horizontally and not vertically).

COMPOSITE CROSS SECTION

file = c:\ge\dynamic\diss\cobejo\files\DISS.PRO

hat-shaped beam



Width = 600 Height = 295 [mm]

Table of elements



STEEL

No	x	y	w	h	fyk	E/1000	fu	eu[o/oo]
1	50.00	0.00	250.00	15.00	355.00	210.0	510.00	100.00
w 2	175.00	15.00	10.00	200.00	380.00	210.0	450.00	100.00
3	185.00	205.00	45.00	10.00	380.00	210.0	450.00	100.00
11	300.00	0.00	250.00	15.00	355.00	210.0	510.00	100.00
w 12	415.00	15.00	10.00	200.00	380.00	210.0	450.00	100.00
13	370.00	205.00	45.00	10.00	380.00	210.0	450.00	100.00

CONCRETE

No	x	y	w	h	fck	fctm
1	0.00	215.00	300.00	80.00	30.00	3.00
11	300.00	215.00	300.00	80.00	30.00	3.00

REINFORCEMENT

No	y	no.	d	fsk	E/1000	fu	eu[o/oo]	Nshr.
1	265.00	8	10.00	550.00	200.0	620.00	100.00	0.00

Input file: diss.pro

elasto-plastic (input-file saved by plastic or elasto-plastic module)
 section (0=user,1=hat,2=I),1 (section type)
 hat-shaped beam (name of section)
 hogging mom.,0 (only necessary for plastic module)
 safety factor steel, 1.1
 safety factor, stress-factor(EC4) concrete, 1.5, 0.85
 safety factor reinforcement, 1.15
 beta-tension-stiffening, 0.4
 fcteff/fctm, 1
 symm.conditions (-1,0,1 hor.left/no/right, -1,0,1 ver.steel down/no/up), 1 , 0
elementlist steel

El.no. 1 to 40	type (0=rect.)	x (left corner) [mm]	y (lower corner) [mm]	width [mm]	height [mm]	yield strength [N/mm ²]	E-Modulus [kN/mm ²]	ultimate strength [N/mm ²]	ultimate strain [1]	flange=0 web=1
1	0	50	0	250	15	355	210	510	0.1	0
2	0	175	15	10	200	380	210	450	0.1	1
3	0	185	205	45	10	380	210	450	0.1	0
4	-	-	-	-	-	-	-	-	-	-
5	-	-	-	-	-	-	-	-	-	-
6	-	-	-	-	-	-	-	-	-	-
7	-	-	-	-	-	-	-	-	-	-
8	-	-	-	-	-	-	-	-	-	-
9	-	-	-	-	-	-	-	-	-	-
10	-	-	-	-	-	-	-	-	-	-
11	0	300	0	250	15	355	210	510	0.1	0
12	0	415	15	10	200	380	210	450	0.1	1
13	0	370	205	45	10	380	210	450	0.1	0
14	-	-	-	-	-	-	-	-	-	-
15	-	-	-	-	-	-	-	-	-	-
16	-	-	-	-	-	-	-	-	-	-
17	-	-	-	-	-	-	-	-	-	-
18	-	-	-	-	-	-	-	-	-	-
19	-	-	-	-	-	-	-	-	-	-
20	-	-	-	-	-	-	-	-	-	-
21	-	-	-	-	-	-	-	-	-	-
22	-	-	-	-	-	-	-	-	-	-
23	-	-	-	-	-	-	-	-	-	-
24	-	-	-	-	-	-	-	-	-	-
25	-	-	-	-	-	-	-	-	-	-
26	-	-	-	-	-	-	-	-	-	-
27	-	-	-	-	-	-	-	-	-	-
28	-	-	-	-	-	-	-	-	-	-
29	-	-	-	-	-	-	-	-	-	-
30	-	-	-	-	-	-	-	-	-	-
31	-	-	-	-	-	-	-	-	-	-
32	-	-	-	-	-	-	-	-	-	-
33	-	-	-	-	-	-	-	-	-	-
34	-	-	-	-	-	-	-	-	-	-
35	-	-	-	-	-	-	-	-	-	-
36	-	-	-	-	-	-	-	-	-	-
37	-	-	-	-	-	-	-	-	-	-
38	-	-	-	-	-	-	-	-	-	-
39	-	-	-	-	-	-	-	-	-	-
40	-	-	-	-	-	-	-	-	-	-

elementlist concrete

El.no. 1 to 20	type (0=rect.)	x (left corner) [mm]	y (lower corner) [mm]	width [mm]	height [mm]	compressive strength [N/mm ²]	fctm [N/mm ²]	shear connection to steel (0/1) (only for plastic module)
1	0	0	215	300	80	30	3	1
2	-	-	-	-	-	-	-	-
3	-	-	-	-	-	-	-	-
4	-	-	-	-	-	-	-	-
5	-	-	-	-	-	-	-	-
6	-	-	-	-	-	-	-	-
7	-	-	-	-	-	-	-	-
8	-	-	-	-	-	-	-	-
9	-	-	-	-	-	-	-	-
10	-	-	-	-	-	-	-	-
11	0	300	215	300	80	30	3	1
12	-	-	-	-	-	-	-	-
13	-	-	-	-	-	-	-	-
14	-	-	-	-	-	-	-	-
15	-	-	-	-	-	-	-	-
16	-	-	-	-	-	-	-	-
17	-	-	-	-	-	-	-	-
18	-	-	-	-	-	-	-	-
19	-	-	-	-	-	-	-	-
20	-	-	-	-	-	-	-	-

elementlist reinforcement

El.no. 1 to 10	number	diameter [mm]	layer height [mm]	yield strength [N/mm ²]	E-Modulus [kN/mm ²]	ultimate strength [N/mm ²]	ultimate strain [1]	shear connection to steel (0/1) (only for plastic module)	Normal force due to shrinkage [N]	Act*fctm [N]
1	8	10	265	550	200	620	0.1	1	0	144000
2	-	-	-	-	-	-	-	-	-	-
3	-	-	-	-	-	-	-	-	-	-
4	-	-	-	-	-	-	-	-	-	-
5	-	-	-	-	-	-	-	-	-	-
6	-	-	-	-	-	-	-	-	-	-
7	-	-	-	-	-	-	-	-	-	-
8	-	-	-	-	-	-	-	-	-	-
9	-	-	-	-	-	-	-	-	-	-
10	-	-	-	-	-	-	-	-	-	-

section coupling point y= , 0
 end

A special quick-input procedure has been arranged for the often-used composite sections with I-shaped (Fig.4-5) or hat-shaped (Fig.4-6) steel beams. If desired the gained section from the quick-input then can be modified in detail within the steel and concrete input windows.

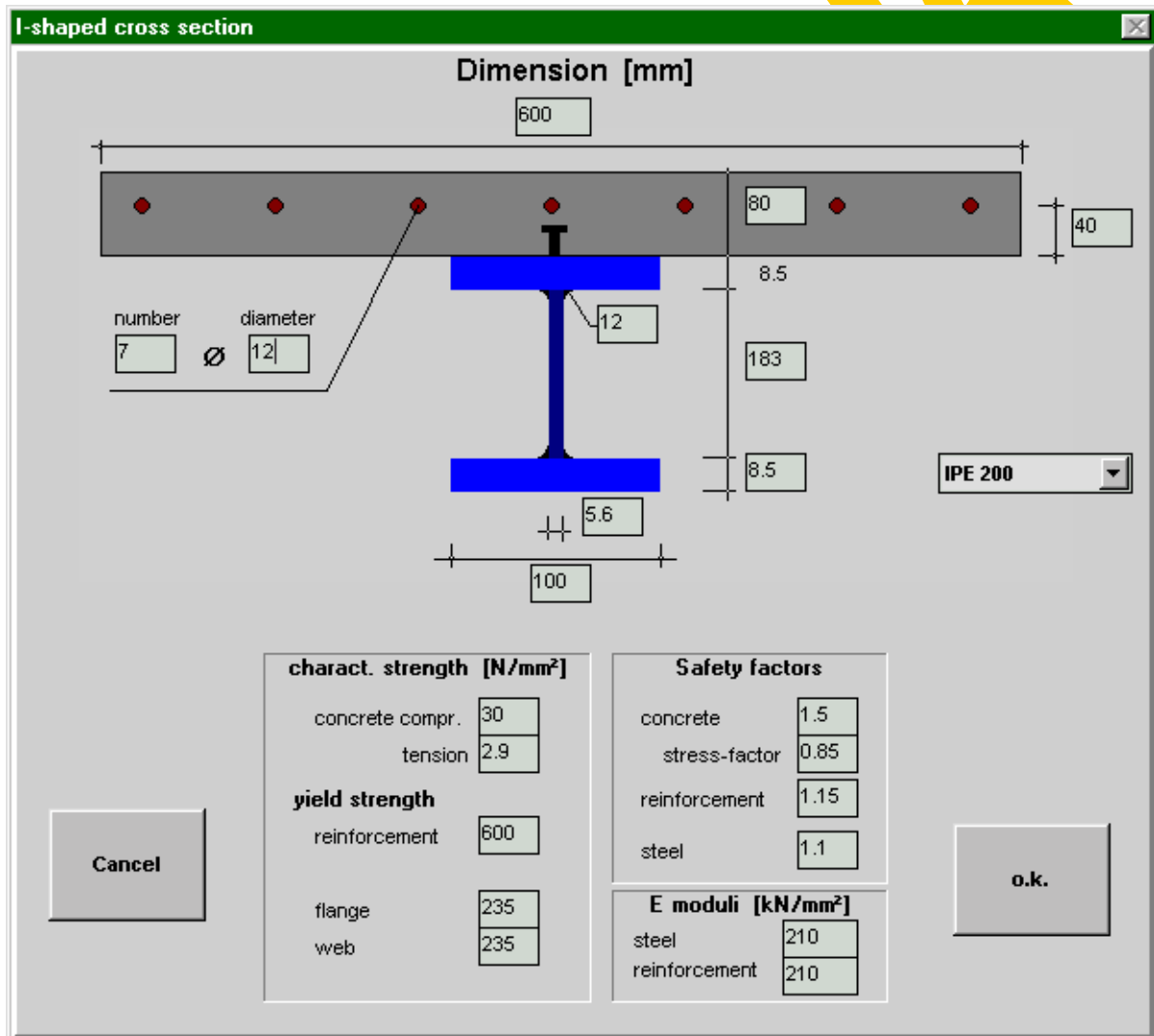


Fig.4-5 Quick-input for I-shaped steel beams (i_prof.frm)

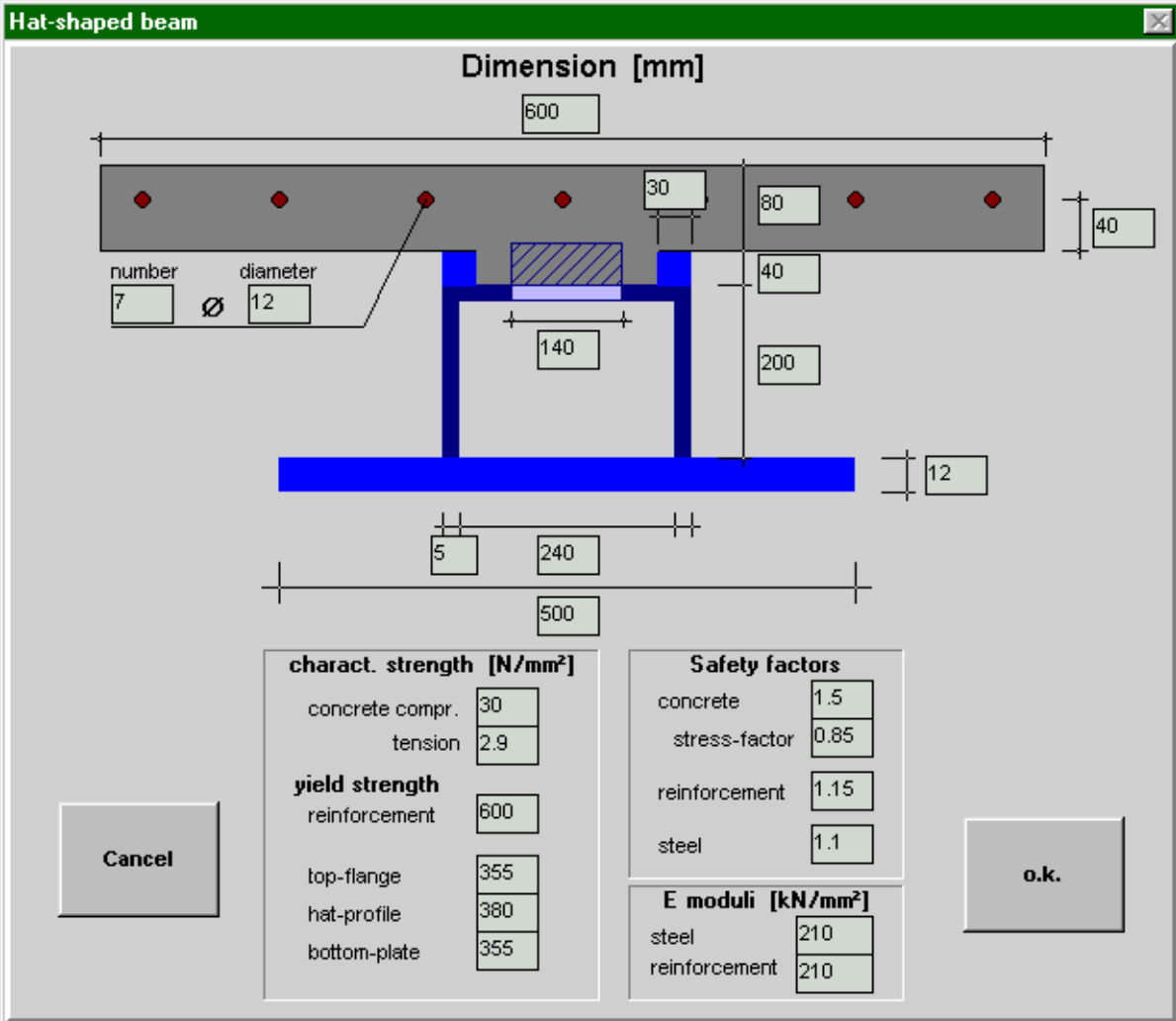


Fig.4-6 Quick-input for hat-shaped steel beams (hutprof.frm)

For I-shaped steel sections default values for IPE, HEA and HEB beams can directly be taken from the file „iprofile.dat“ in the following format: Name, height, width, thickness of web, thickness of flange, fillet radius. As the section has to be built up only by rectangular elements the fillet radius is approximated as shown in Fig.4-7.

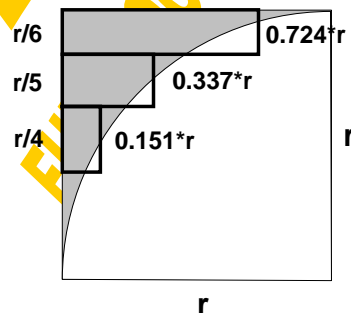


Fig.4-7 Approximation of fillet radius by rectangular elements

Finally it should not be forgotten to mention the precision factor, which is set equal to one in the start-up window. Generally all accuracy pre-settings within the iteration loops have been defined as a compromise between precision and calculation time. In the summary of this chapter the convergence criteria defined for each iteration loop are given. Further for each iteration result the final deviation will be declared. So if this indicated deviation should exceed the desired limits the accuracy can be improved by raising the precision factor. However thanks to the quick computers in most cases even the wise absolute lower accuracy limits (e.g. 1 N as absolute lower precision limit for the inner shear force) are already decisive using the pre-set precision factor 1.0.

The button „STEEL“ will close the start-up window and open that for the steel section part, which will be described in detail in the following chapter.

4.2.3 Steel section

4.2.3.1 Section input

The steel section window, shown in Fig.4-8, first of all enables the input of the steel section part consisting of up to 10 rectangular elements. In view of the possibility to mirror the section horizontally and vertically the final steel section so may consist of up to 40 elements. The 10 basic elements are marked with different colours. To point out the mirrored elements they are drawn with a more pale colour, what is also stressed in the „Mirror“-box. For each element the coordinates of one corner (x,y) and the width and height (b,h) to the other corner can be defined. Also negative values are accepted, however then the x- and y-coordinates will automatically be re-calculated for the lower left corner. To facilitate the input the coordinates of the actual mouse-position are indicated at the top of the drawing. A single click within the drawing will write the coordinates of the nearest existing element corner to the x- and y-boxes. A double-click is understood as the second corner of the actual element. Therefore the actual element width and height then are calculated as the distance between the given x- and y-values and the nearest element corner from the double-click position. Attention has to be paid that the corners of mirrored elements cannot be caught; they will automatically be transformed to the basic element corners. Pressing „shift“ while clicking on the drawing will define the height of a section coupling point (vertical section-to-section coupling for different cross section types within a beam), which will be used when placing element behind element for the global analysis.

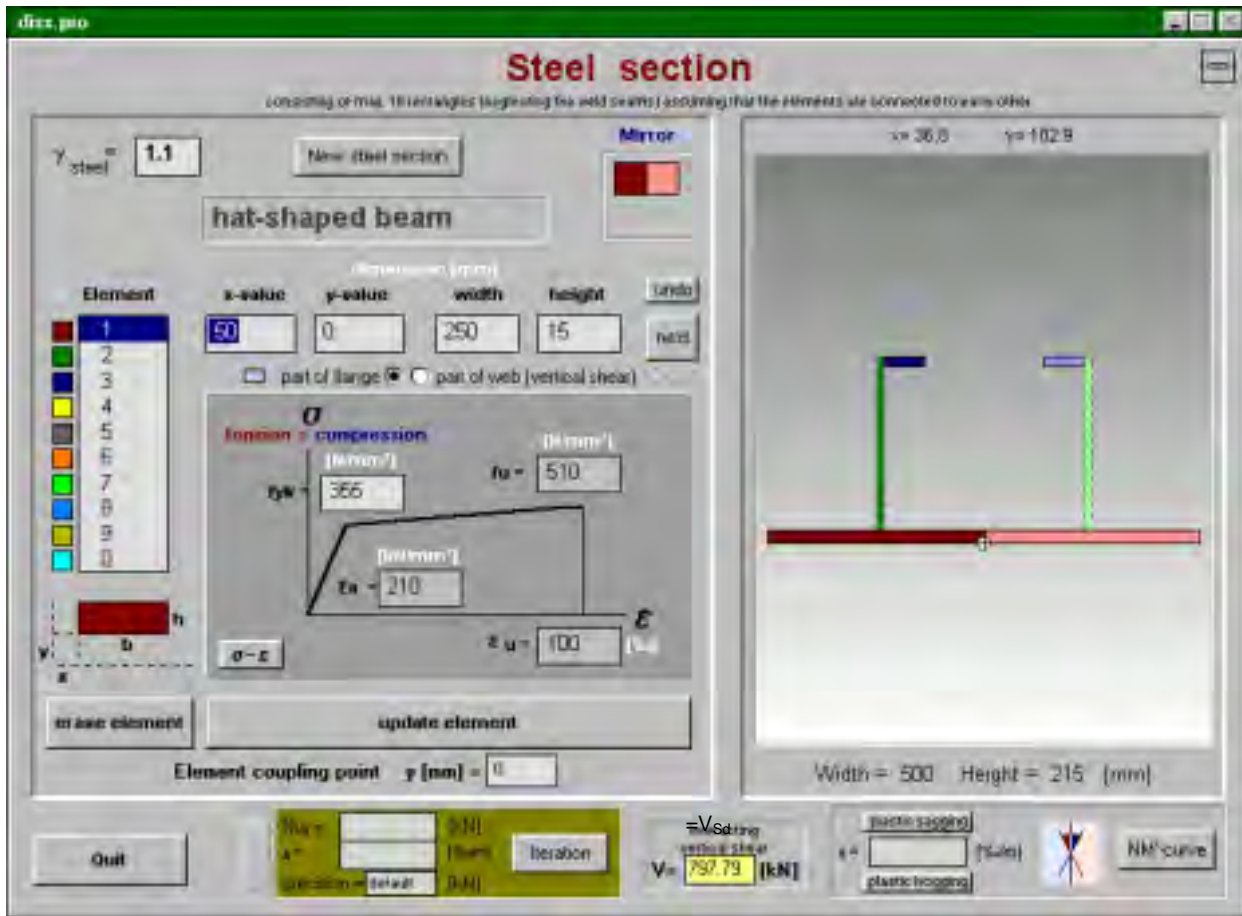


Fig.4-8 Window for the input and calculation of the steel section part (prs.fm)

Further it can be chosen if an element participates in the vertical shear transfer as a part of the „web“ or if there is no interaction between normal forces and shear forces when an element is defined as part of the „flanges“. Web elements are indicated with a dashed border in the drawings. Their reduced stress-strain-diagram is calculated using the global procedure „*querkraftsinteraktion*“ (see Fig.4-9, Fig.4-10). There the longitudinal yielding stress f_{yk} fictitiously is reduced to f_{yv} depending on the ratio between V_{sd} (actual interacting vertical shear force) and V_{Rd} (plastic shear resistance) based on the Huber-Hencky-Mises-hypothesis. Fig.4-9 shows the difference between the applied theoretical approach of σ - τ -interaction and the one according to EC3 [58,108]. Simplifying only vertical web elements may be assumed to participate in shear.

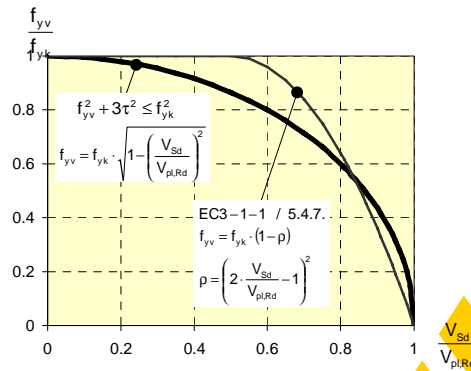
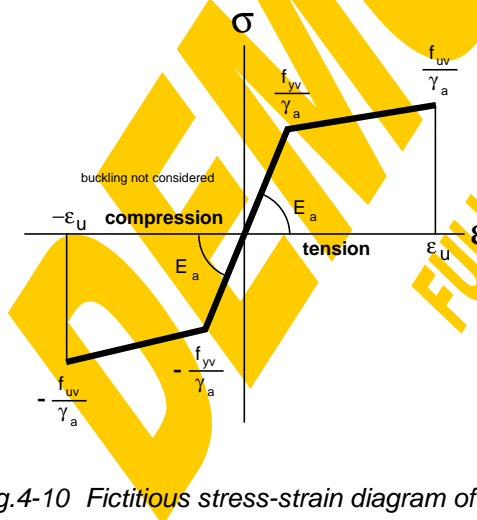


Fig.4-9 Interaction between shear and longitudinal stresses

Apart from the geometrical properties also the material properties can be defined for each element separately. The constitutive law of a steel element is assumed to be symmetrical for tension and compression and is based on the following input data: Young modulus E_a , characteristic yield strength f_{yk} , ultimate strength f_u and ultimate strain ϵ_u . Further it depends on the global partial safety factor of steel $\gamma_{steel} = \gamma_a$ (default=1.0) and if it concerns a web element of course on the actual interacting vertical shear force V_{Sd} . It will automatically be checked that the actual shear force does not exceed the plastic shear capacity of all web elements together. Buckling will not be taken into consideration.

The definition of the stress-strain diagram for steel elements used in this program is summarised in Fig.4-10. The actual stress-strain diagram of each steel element can be seen true to scale when clicking on the „ σ - ϵ “-button (Fig.4-11). There will be the possibility to calculate the corresponding stress to a given strain and vice versa by a linear interpolation. Fig.4-12 gives the diagrams for the described example section using $\gamma_a=1.1$.



flange elements: $f_{yv} = f_{yk}$, $f_{uv} = f_u$

web elements: $V_{Rd} = \sum_{\text{web elements}} b_i \cdot h_i \cdot \frac{f_{yk,i}}{\gamma_a} \cdot \frac{1}{\sqrt{3}}$

$V_{Sd} \leq V_{Rd}$: $f_{yv} = f_{yk} \cdot \rho$ $f_{uv} = f_u \cdot \rho$

$$\rho = \sqrt{1 - \left(\frac{V_{Sd}}{V_{Rd}}\right)^2}$$

according to $f_{yv}^2 + 3\tau^2 \leq f_{yk}^2$

$V_{Sd} > V_{Rd}$: beyond resistance

Fig.4-10 Fictitious stress-strain diagram of steel elements

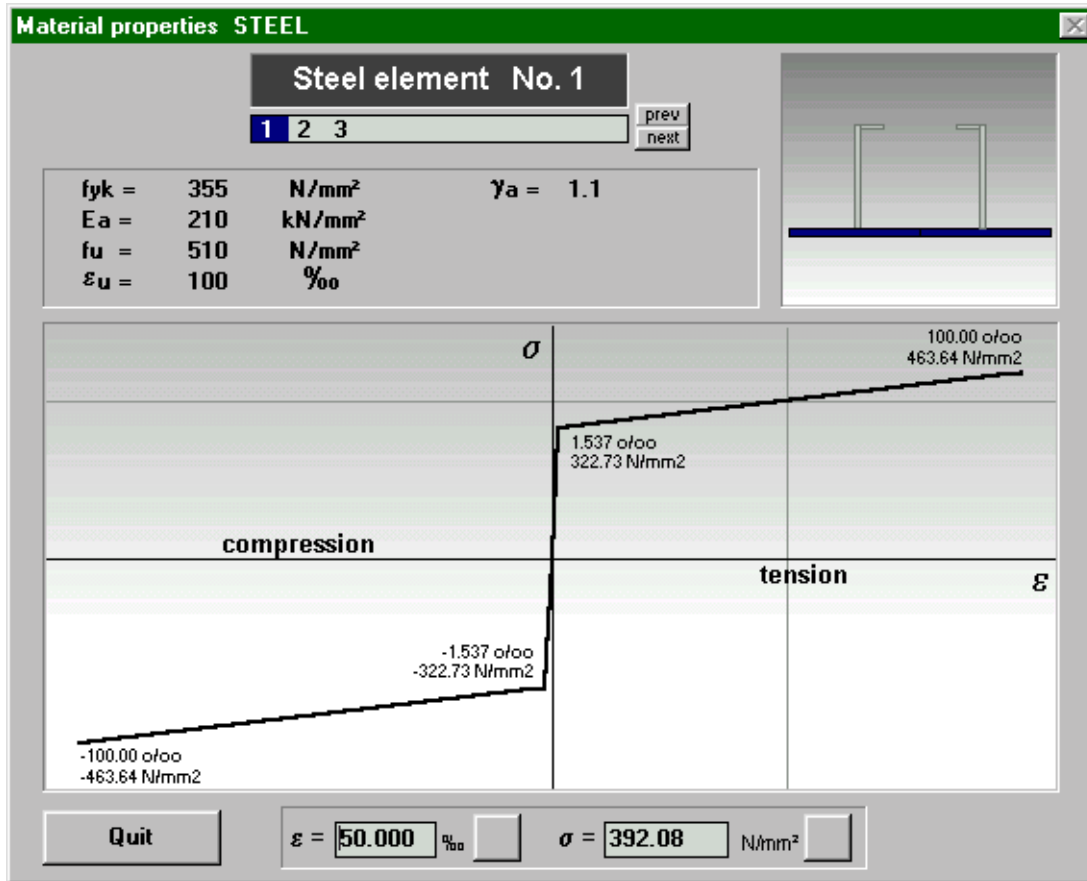


Fig.4-11 Window for the actual stress-strain diagrams of steel elements (stoffga.frm)

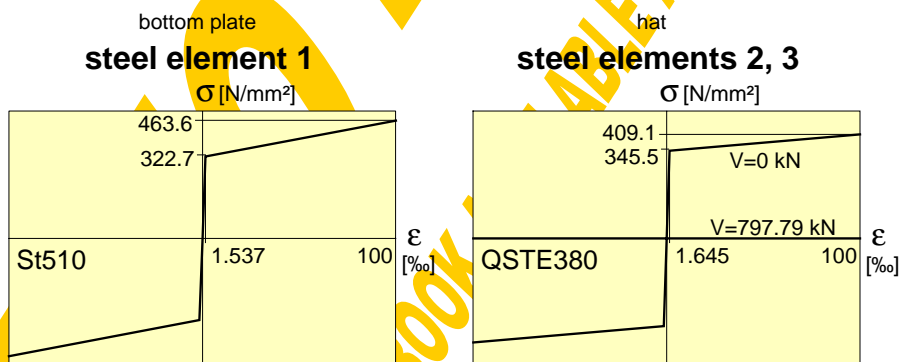


Fig.4-12 Actual stress-strain diagrams for the example section

Before returning from the steel section window to the section management window or before starting any calculation it will be checked automatically if elements are overlapping and therefore these areas would be calculated more than once. Further after each element input the entire composite cross section automatically will be moved so that the minimum x-value of the entire section and the minimum y-value of the bare steel section (datum line) are equal to 0.

Based on the so-defined steel section including geometry and material properties the following three calculations or iterations can be carried out:

- internal forces to a given strain distribution
- strain distribution to a given normal force
- N-M-relation for a defined curvature

4.2.3.2 Internal forces to a given strain distribution (*steelstrain*)

$\varepsilon (y=0) =$	0.56875	[%]	Calculation
$\kappa =$	10	[%/m]	

The actual linear strain distribution within the steel section can be defined by the strain at the steel bottom ($y=0$) ε_{0a} and the curvature κ as shown in Fig.4-13.

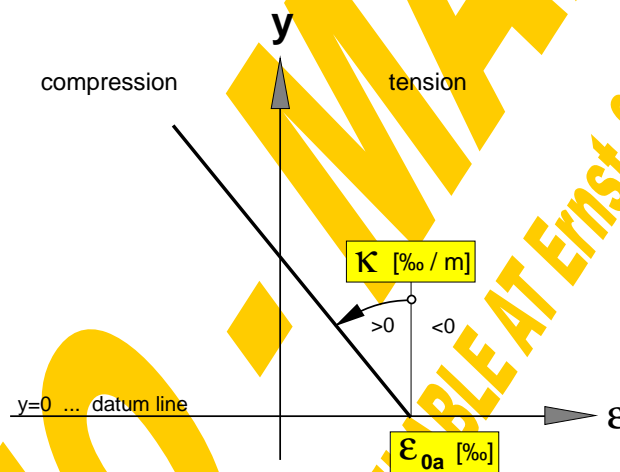
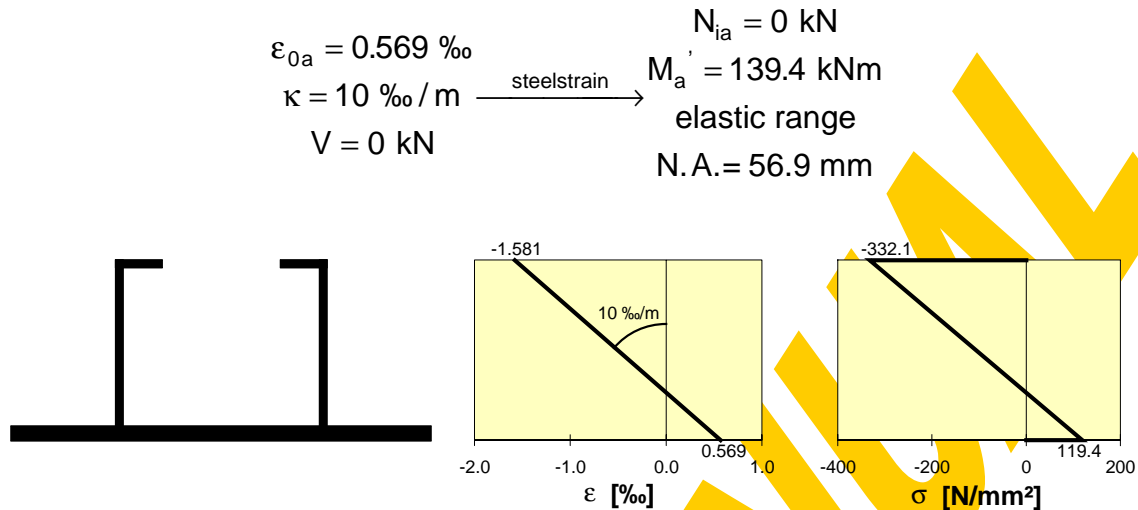


Fig.4-13 Linear strain distribution

Based on that the global procedure „*steelstrain*“ calculates the corresponding stresses of each steel element based on the material properties. If the stress at least in one point exceeds the design yield value (f_{yV}/γ_a) a non-elastic („ne“) flag is set, otherwise elastic („el“) will be indicated. An integration of the stresses over the whole steel section leads to the inner normal force N_{ia} (tension positive). Integrating the stresses multiplied by their lever arms to the steel bottom line results in the moment M_a^y , which of course is related to this datum line $y=0$ as described in [106] (sagging moments positive). Finally also the y -value of the neutral axis (N.A._a) is declared.

Fig.4-14 illustrates this basic calculation for the example section leading from strains to stresses and internal forces.

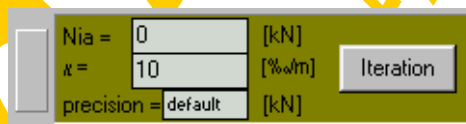


STEEL elements:

el.no.	$\varepsilon_{\text{bottom}}$ [‰]	ε_{top} [‰]	σ_{bottom} [N/mm ²]	σ_{top} [N/mm ²]	
1	0.569	0.419	119.44	87.94	elastic
2	0.419	-1.581	87.94	-332.06	elastic
3	-1.481	-1.581	-311.06	-332.06	elastic
11	0.569	0.419	119.44	87.94	elastic
12	0.419	-1.581	87.94	-332.06	elastic
13	-1.481	-1.581	-311.06	-332.06	elastic

Fig.4-14 Calculation example

4.2.3.3 Strain distribution to a given normal force (*Nsteeliteration*)



The global procedure „*Nsteeliteration*“ goes the opposite direction iterating the corresponding strain distribution for a given normal force N_{ia} and a given curvature κ . This problem is solved in two steps:

First the ultimate boundaries of datum strains (at $y=0$) depending on the curvature κ and the ultimate strain values ε_u of the steel elements are derived within the procedure „*steellimit*“. Then the yielding datum strain boundaries are calculated, from where on any parallel movement of the strain distribution would not bring any more changing of stresses. Naturally these yielding boundaries are only necessary, if for the steel elements an ideal plastic plateau without any strain hardening is given. Comparing the ultimate strain boundaries with the yielding ones leads to the decisive strain boundaries. The lower and upper ultimate normal force in the steel section depending on the given curvature κ can then be calculated with the procedure „steelstrain“ as shown in Fig.4-15.

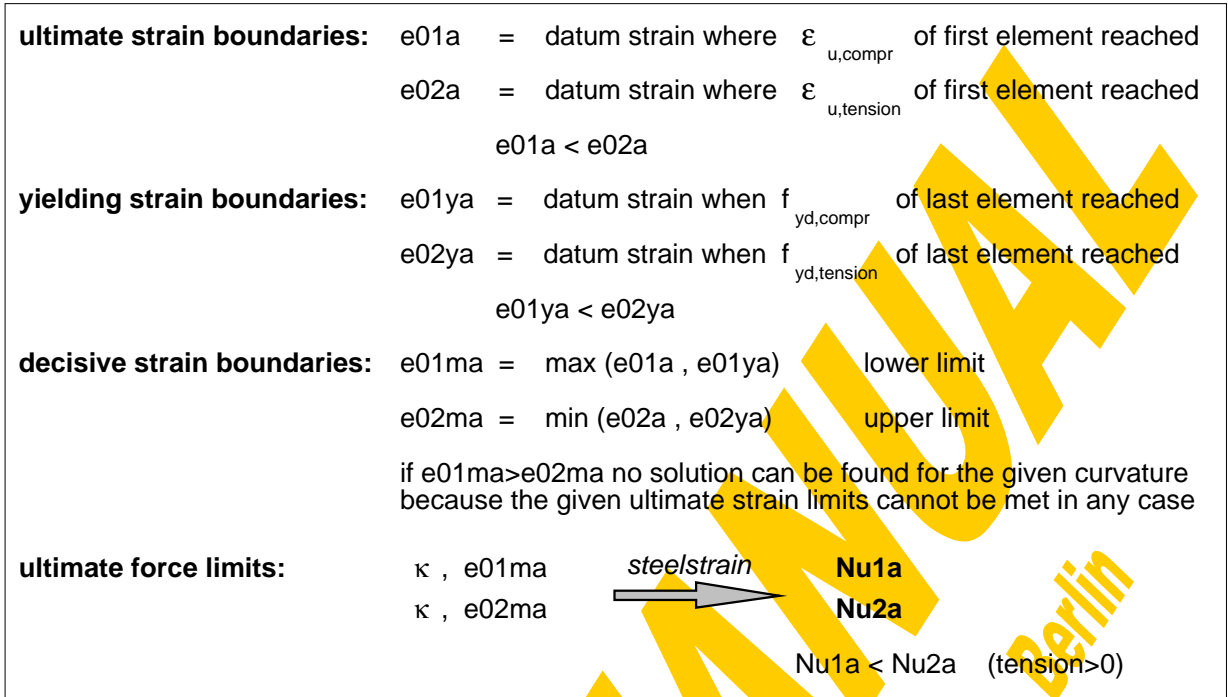
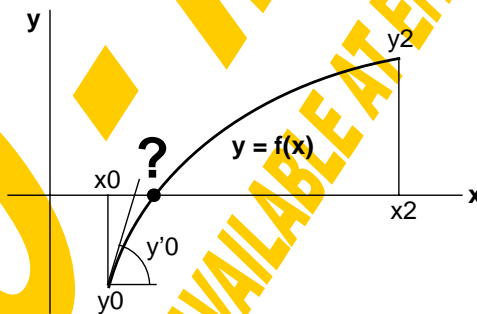


Fig.4-15 Strain boundaries from procedure „steellimit“

Iteration methods



Regula falsi

$$x_1 = x_0 - y_0 \cdot (x_2 - x_0) / (y_2 - y_0)$$

$$y_1 = f(x_1)$$

if $\text{sign}(y_1) = \text{sign}(y_0)$ then $x_0 = x_1, y_0 = y_1$ else $x_2 = x_1, y_2 = y_1$

Newton method

$$x_1 = x_0 - y_0 / y'_0$$

Bisection method

$$x_1 = (x_0 + x_2) / 2$$

$$y_1 = f(x_1)$$

if $\text{sign}(y_1) = \text{sign}(y_0)$ then $x_0 = x_1$ else $x_2 = x_1$

Fig.4-16 Iteration methods

In the second step the iteration for the corresponding datum strain in between the decisive strain boundaries will start, if the given normal force N_{ia} lies in between the just calculated limits $Nu1a$ and $Nu2a$. This is done within the procedure „itNsteel“ in the following iterative way:

Starting with the boundaries $e01ma$ and $e02ma$ the actual normal force for the bisection point of these strains is calculated using the procedure „steelstrain“. Then the strain boundaries are adapted so that the searched normal force lies in between the new boundaries. This iteration based on the bisection method is repeated until one of the following criteria is fulfilled: Either the actual normal force reaches the prescribed one with a given accuracy or the change of strains is smaller than a given tolerance or the iteration time exceeds a preset limit. A summary of the iteration accuracy criteria can be found at the end of chapter 4.2.

The method of halving the iteration interval generally has been chosen because of the big variation of gradients of the analysed curves, resulting from the relatively flat strain hardening plateau. Especially for such nearly bilinear functions the regula falsi or the Newton-method showed to be unstable, though for curves with a relatively constant gradient these methods would converge much faster (Fig.4-16).

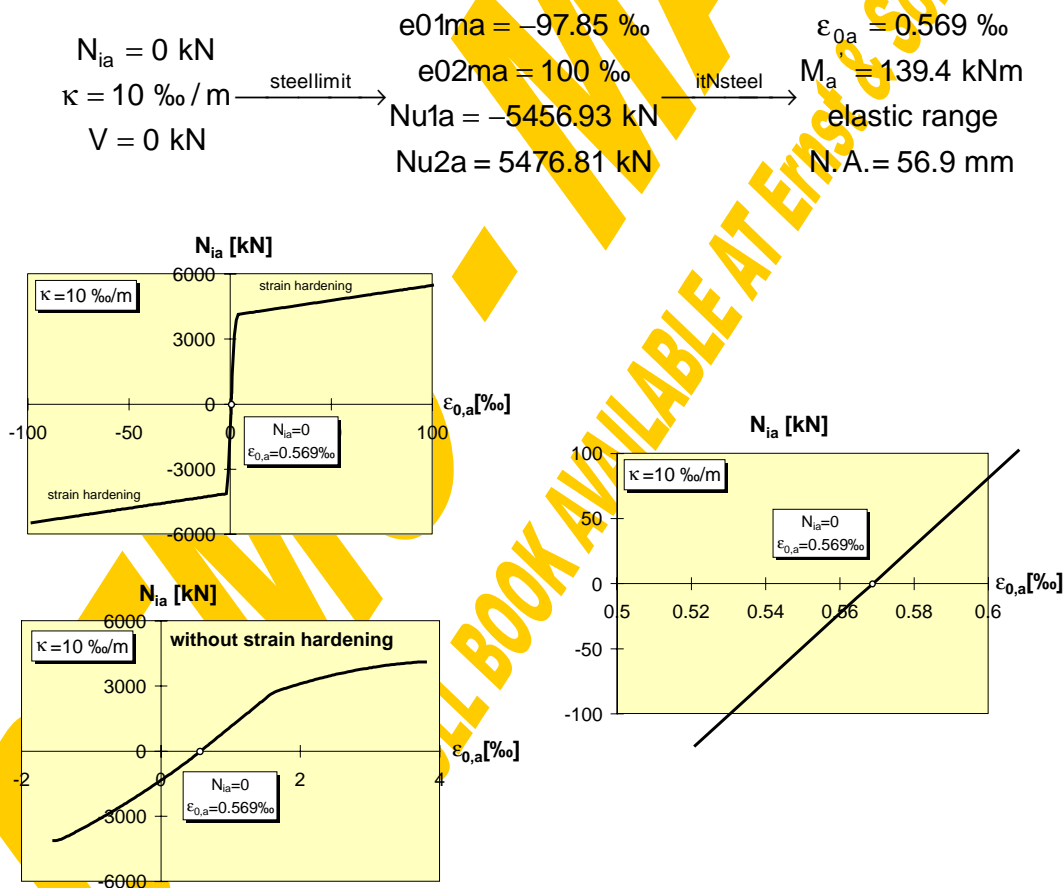


Fig.4-17 Iteration example

Fig.4-17 shows the iteration and the results for the example section. It can clearly be seen that the relatively flat parts of the $N_{ia}-\epsilon_{0a}$ -curve, which result from the strain hardening of the steel elements beyond reaching the design yield strength, dominate this function and therefore drastically slow down the iteration process. However thanks to the quick computers the iteration time anyway keeps really acceptable. Such an iteration plateau could be avoided by using material laws with a flat plateau (without strain hardening).

Apart from the possibility to make interpolations within the $N_{ia}-M_a'$ -curve the described procedure „Nsteeliteration“ e.g. also can be used to iterate the ultimate limit of bending κ_u (when ϵ_u of the first element is reached) or to determine the connection between curvature (κ) and neutral axis (N.A.) or bending moment (M_a') as illustrated in Fig.4-18 for the example section. Of course for the special case that $N_{ia}=0$ the relative bending moment M_a' (related to the datum line) is equal to the absolute one M_a .

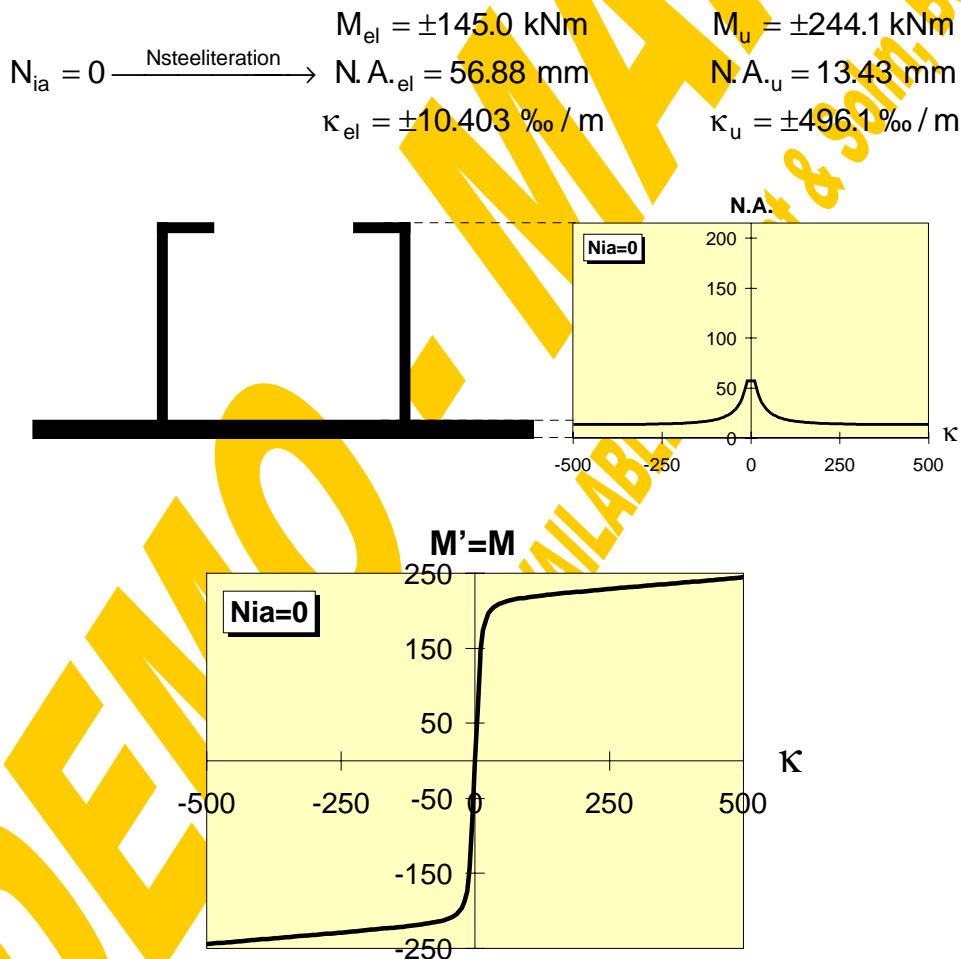
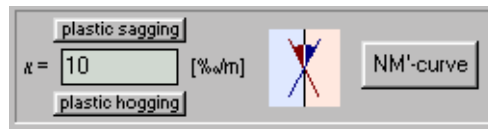


Fig.4-18 Results using the procedure „Nsteeliteration“

4.2.3.4 N-M-relation for a defined curvature (*NMsteel*)



Based on the just described strain iteration the full range between the force limits $Nu1a$ and $Nu2a$ can be analysed for a defined curvature κ (procedure „**NMsteel**“). First the strain and force limits are calculated using the procedure „steellimit“. Then the range between $Nu1a$ and $Nu2a$ is subdivided into 40 parts and for each normal force the corresponding datum strain ϵ_{0a} will be iterated with the procedure „itNsteel“. Afterwards for the found solution the bending moment M_a' and the location of the neutral axis $N.A._a$ are evaluated with the procedure „steelstrain“. Finally the elastic and fully plastic steel section properties are calculated with the procedure „**qwertesteel**“ based on the formulae shown in Fig.4-19.

DEMO - MANU
 FULL BOOK AVAILABLE AT ERNST & SOHN, BERLIN

reference modulus $E_{\text{ref}} = E_{\text{first steel element}}$

elastic neutral axis $ENA = \frac{\sum b_i \cdot h_i \cdot y_{s,i} \cdot \frac{E_i}{E_{\text{ref}}}}{\sum b_i \cdot h_i \cdot \frac{E_i}{E_{\text{ref}}}}$

plastic neutral axis PNA ... itNsteel ($\kappa = \pm\infty$, $N_{ia} = 0$)

Area $A = \sum b_i \cdot h_i$

Shear area $A_{\text{vc}} = \sum_{\text{web elements}} b_i \cdot h_i$

Moment of inertia $I = \sum \left(\frac{b_i \cdot h_i^3}{12} + b_i \cdot h_i \cdot (ENA - y_{s,i})^2 \right) \cdot \frac{E_i}{E_{\text{ref}}}$

upper res.moment $W_o = \frac{I}{y_{\text{max}} - ENA}$

lower res.moment $W_u = \frac{I}{ENA - y_{\text{min}}}$

first yielding y_{el} when $\frac{\frac{E_{\text{ref}}}{E_i} \cdot f_{\text{yv},i}}{|y_i - ENA|} \rightarrow \min$

elastic curvature limit $\kappa_{\text{el}}(N_a = 0, V) = \min \left(\frac{f_{\text{yv}}}{\gamma_a \cdot E_i \cdot |y_{\text{el}} - ENA|} \right)$

elastic limit of bending $M_{\text{el}}(N_a = 0, V) = E_{\text{ref}} \cdot I \cdot \kappa_{\text{el}}$

ideal plastic normal force $N_{\text{pl}} = \sum b_i \cdot h_i \cdot \frac{f_{\text{yv},i}}{\gamma_a}$

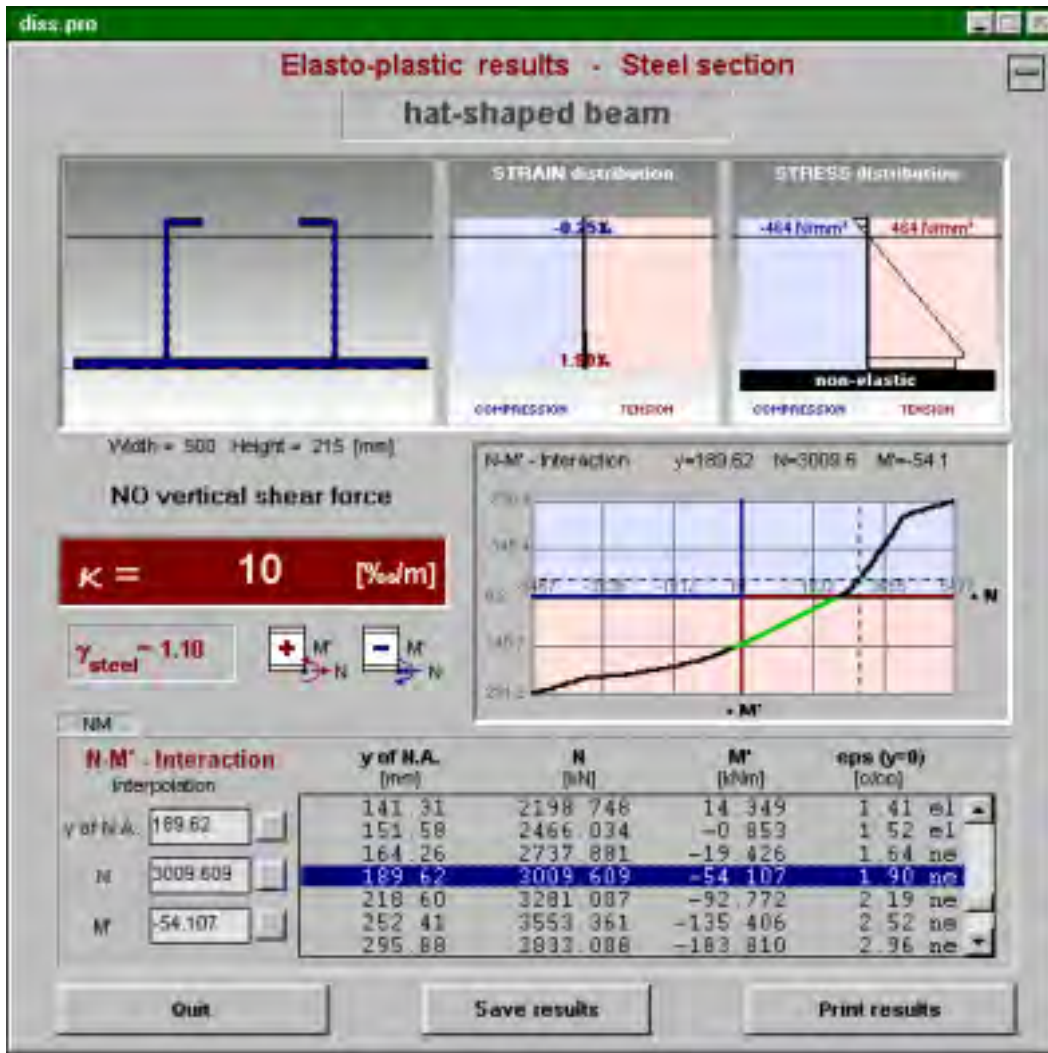
ideal plastic bending moment $M_{\text{pl}} \dots \text{itNsteel} (\kappa = \pm\infty, N_{ia} = 0)$

plastic vertical shear force $V_{\text{pl}} = \sum_{\text{web elements}} b_i \cdot h_i \cdot \frac{f_{\text{yk},i}}{\gamma_a} \cdot \frac{1}{\sqrt{3}}$

(Attention: buckling is not taken into consideration !)

Fig.4-19 Formulae for the calculation of the steel sectional properties (qswertesteel)

Two special buttons have been arranged to enable also a quasi-fully-plastic analysis. When clicking on „plastic sagging“ or „plastic hogging“ the curvature κ will be set equal to $\pm 10^5$ ‰/m and all stress-strain diagrams are modified temporarily in that way, that any strain hardening is cut and an infinite yielding plateau without any limiting strain is provided.



elements

Nr.	Table of elements							
	x [mm]	y [mm]	w [mm]	h [mm]	f _{yk} [N/mm ²]	E [kN/mm ²]	f _u [N/mm ²]	eps _u [‰]
1	50	0	250	15	355	210	510	100
w 2	175	15	10	200	380	210	450	100
3	185	205	45	10	380	210	450	100
11	300	0	250	15	355	210	510	100
w12	415	15	10	200	380	210	450	100
13	370	205	45	10	380	210	450	100

sec.prop.

Location of Neutral Axis (from bottom line):
 E.N.A. = 56.875 [mm]
 P.N.A. (V) = 12.750 [mm]

Elastic Data:	Area = 12400 [mm ²]	Ideal Plastic Data (+ resp. -):
Shear Area A _{vc} = 4000 [mm ²]	Inertia = 6638.2 [cm ⁴]	Normal force (V) = 4113.18 [kN]
upper Resis.Moment = 419.8 [cm ³]	Elastic limit of bending (V) = 145.0 [kNm]	Bend. moment (V) = 216.14 [kNm]
lower Resis.Moment = 1167.2 [cm ³]	elastic limit of kapa (V) = 10.40 [%/m]	Shear force (webs) = 797.79 [kN]

Buckling has to be analysed separately!

Fig.4-20 Window for the presentation of steel results (eps.frm)

In the following the results from calculations for the example section using $\kappa=10\text{‰}$ and $V=0\text{ kN}$ are described. The progress of iteration will be indicated by a flood box. After the termination of the calculation the steel input window will be closed and the window for the presentation of the steel results is shown (Fig.4-20). It comprises the input data (table of elements, safety-factors, ...) an image of the steel section, the actual strain and stress distribution and a table and a graph of the calculated N_{ia} - M_a' -interaction. Those parts of the interaction curve drawn in green represent the elastic range, the non-elastic parts are drawn in black. The interaction table is combined with the possibility for a linear interpolation in view of the neutral axis N.A._a, N_{ia} and M_a' . Clicking on „sec.prop.“ switches to the window including the elastic and ideal plastic section properties calculated according to Fig.4-19.

To make the coherence between neutral axis, normal force and bending moment accessible to the user and therefore to get him the feeling where strengthening of the section would be economic or not special tools have been provided: Clicking on one line within the N_{ia} - M_a' -table will produce the corresponding N.A. within the section image, the strain and stress distribution and a crosshair accentuating the actual location within the interaction curve. This graphical illustration will also be started after a linear interpolation or when following the interaction curve with the computer-mouse while the left mouse-button is pressed.

Using the button „Print results“ will send the following four sheets to your printer: The first sheet (see page 174) contains a drawing of the actual steel section and the analysed range of strain distributions. Unfortunately when taking strain hardening into consideration the decisive strain limits become relatively large (depending on the given ultimate strain values ϵ_u) and therefore the strain diagram with decreasing κ more and more deforms from a parallelogram to a rectangle loosing optical clearness. At the bottom of this first sheet the N_{ia} - M_a' diagram will be displayed. The grey line represents the elastic range, the black one the non-elastic area. At the second sheet the interaction table will be given (see page 175). The elastic or ideal-plastic cross-sectional properties are printed on sheet no.3 (page 176) and finally on sheet no.4 you will find the full input data of the actual section.

To make the results also accessible to other programs they can be saved as a sequential data file with the button „Save results“. That will activate the file management window (Fig.4-4). The default file name is built up by that of the section (*.pro) and the extension „eps“ (elasto-plastic steel). The output file of the example calculation can be found on page 177.

Elasto-plastic results - Steel

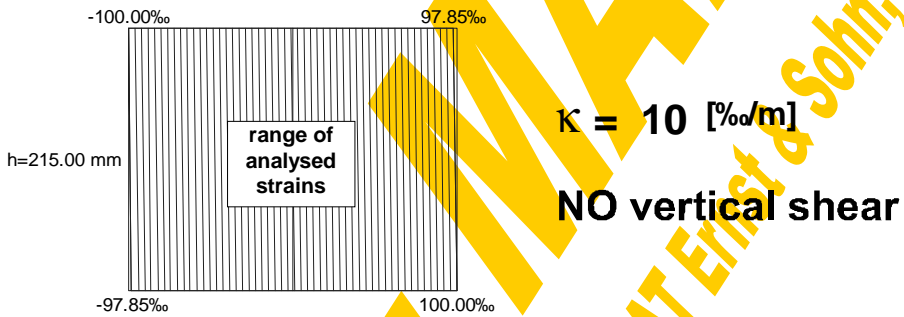
file = c:\ge\dynamic\diss\cobejo\files\DISS.PRO

hat-shaped beam

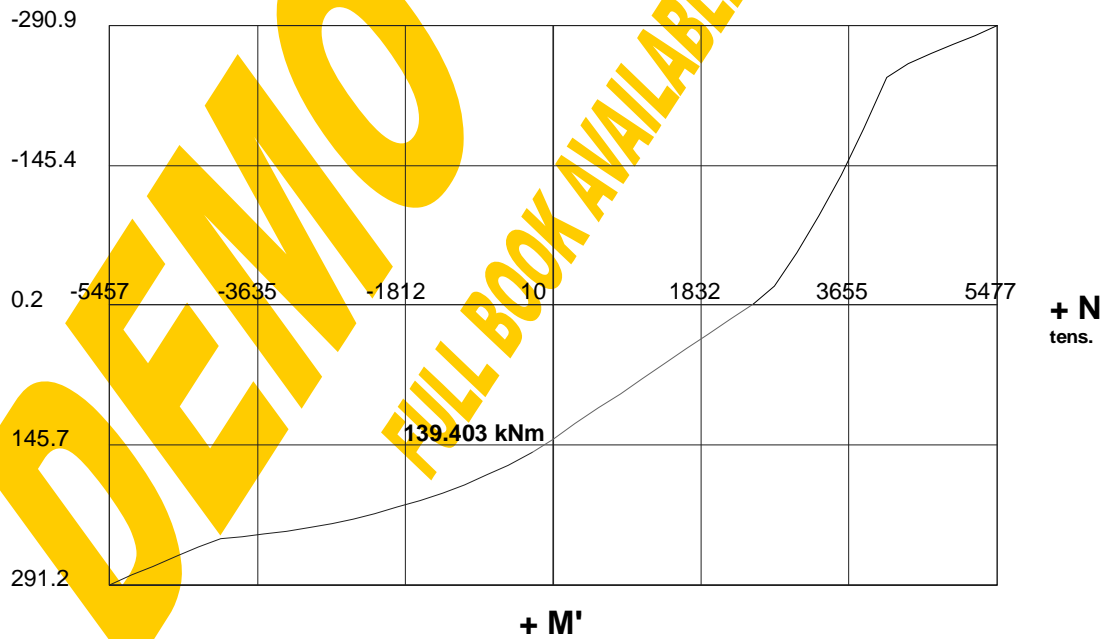


Width = 500 Height = 215 [mm]

Partial safety factor = 1.1



N-M' Interaction [kN,kNm]



N-M' Interaction - Steel

file = c:\ge\dynamic\diss\cobejo\files\DISS.PRO

hat-shaped beam

$$\kappa = 10 \quad [‰ / m]$$

NO vertical shear force

y [mm]	N [kN]	M' [kNm]	e0[‰]	
-9785.00	-5456.930	291.197	-97.850	ne
-7775.59	-5177.552	281.142	-77.756	ne
-5920.74	-4919.665	271.860	-59.207	ne
-3911.33	-4640.286	261.805	-39.113	ne
-1901.91	-4360.908	251.750	-19.019	ne
-146.09	-4086.524	242.884	-1.461	ne
-127.98	-3819.850	240.816	-1.280	ne
-112.28	-3552.793	238.315	-1.123	ne
-96.58	-3275.417	235.276	-0.966	ne
-80.88	-2987.722	231.536	-0.809	ne
-66.39	-2712.999	227.322	-0.664	ne
-53.11	-2453.446	222.704	-0.531	ne
-39.82	-2186.505	217.263	-0.398	ne
-26.54	-1912.176	210.901	-0.265	ne
-13.26	-1630.459	203.520	-0.133	ne
-0.58	-1354.655	195.433	-0.006	ne
11.50	-1085.726	186.707	0.115	ne
23.57	-810.692	176.906	0.236	ne
35.05	-543.753	166.533	0.350	ne
47.12	-252.680	153.568	0.471	ne
56.87	-0.004	139.403	0.569	el
67.65	280.579	123.445	0.676	el
78.52	563.587	107.349	0.785	el
88.78	830.873	92.147	0.888	el
99.05	1098.159	76.945	0.990	el
109.92	1381.168	60.849	1.099	el
120.18	1648.454	45.647	1.202	el
130.44	1915.739	30.445	1.304	el
141.31	2198.748	14.349	1.413	el
151.58	2466.034	-0.853	1.516	el
164.26	2737.881	-19.426	1.643	ne
189.62	3009.609	-54.107	1.896	ne
218.60	3281.087	-92.772	2.186	ne
252.41	3553.361	-135.406	2.524	ne
295.88	3833.088	-183.810	2.959	ne
363.51	4110.935	-237.175	3.635	ne
2116.91	4380.792	-251.439	21.169	ne
4126.33	4660.170	-261.494	41.263	ne
6135.74	4939.548	-271.549	61.357	ne
7990.59	5197.436	-280.831	79.906	ne
10000.00	5476.814	-290.886	100.000	ne

el=elastic

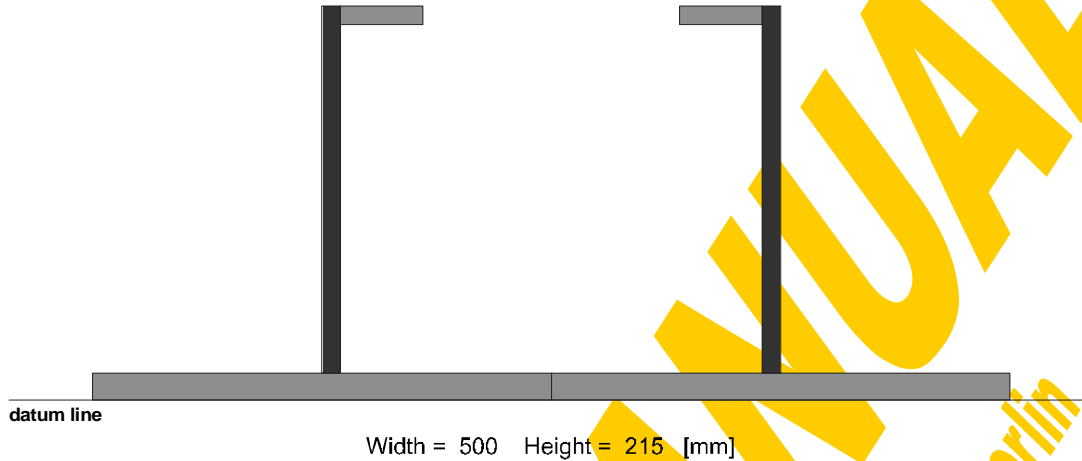
ne=non-elastic

Institute of Steel and Timber Constructions - University of Innsbruck Dipl.-Ing. Gerald Huber

Cross-sectional properties - Steel

file = c:\geldynamic\diss\cobejo\files\DISS.PRO

hat-shaped beam



Vertical distances from bottom line:

Elastic neutral axis :	56.88	[mm]
Plastic neutral axis :	12.75	[mm]
first yielding :	215.00	[mm]

Partial safety factor = 1.1

Elastic data:

Area =	12400.0	[mm ²]
Shear area A _{vc} =	4000.0	[mm ²]
Inertia =	6638.2	[cm ⁴]
upper Resis.Mom. =	419.8	[cm ³]
lower Resis.Mom. =	1167.2	[cm ³]
Elastic limit of bend.=	145.0	[kNm]
elastic limit of kapa =	10.40	[o/oo/m]

Plastic data (+ resp. -):

Normal force =	4113.18	[kN]
Bend. moment =	216.14	[kNm]
Shear force (web-parts)=	797.79	[kN]

Buckling has to be analysed separately !

Elasto-plastic results - steel section

Section: "hat-shaped beam"

kapa [o/oo / m]=,10

interacting vertical shear force [N]=,0

Savety factor steel: ,1.1

Table of elements (No,x,y,w,h,fyk,E/1000,fu,eu,flange=0/web=1) [N,mm]

1	50	0	250	15	355	210	510	0.1	0
2	175	15	10	200	380	210	450	0.1	1
3	185	205	45	10	380	210	450	0.1	0
11	300	0	250	15	355	210	510	0.1	0
12	415	15	10	200	380	210	450	0.1	1
13	370	205	45	10	380	210	450	0.1	0

N-M' Interaction Table (y[mm],N[kN],M'[kNm],e0[o/oo])

-9785.00	-5456.930	291.197	-97.850	non-elastic
-7775.59	-5177.551	281.142	-77.756	non-elastic
-5920.74	-4919.665	271.860	-59.207	non-elastic
-3911.33	-4640.286	261.805	-39.113	non-elastic
-1901.91	-4360.908	251.750	-19.019	non-elastic
-146.09	-4086.523	242.884	-1.461	non-elastic
-127.98	-3819.850	240.816	-1.280	non-elastic
-112.28	-3552.793	238.315	-1.123	non-elastic
-96.58	-3275.417	235.276	-0.966	non-elastic
-80.88	-2987.722	231.536	-0.809	non-elastic
-66.39	-2712.999	227.322	-0.664	non-elastic
-53.11	-2453.446	222.704	-0.531	non-elastic
-39.82	-2186.505	217.263	-0.398	non-elastic
-26.54	-1912.176	210.901	-0.265	non-elastic
-13.26	-1630.458	203.520	-0.133	non-elastic
-0.58	-1354.655	195.433	-0.006	non-elastic
11.50	-1085.726	186.707	0.115	non-elastic
23.57	-810.692	176.906	0.236	non-elastic
35.05	-543.753	166.533	0.351	non-elastic
47.12	-252.680	153.568	0.471	non-elastic
56.87	-0.004	139.403	0.569	elastic
67.65	280.579	123.445	0.677	elastic
78.52	563.587	107.349	0.785	elastic
88.78	830.873	92.147	0.888	elastic
99.05	1098.159	76.945	0.991	elastic
109.92	1381.168	60.849	1.099	elastic
120.18	1648.454	45.647	1.202	elastic
130.44	1915.739	30.445	1.304	elastic
141.31	2198.748	14.349	1.413	elastic
151.58	2466.034	-0.853	1.516	elastic
164.26	2737.881	-19.426	1.643	non-elastic
189.62	3009.609	-54.107	1.896	non-elastic
218.60	3281.087	-92.772	2.186	non-elastic
252.41	3553.361	-135.406	2.524	non-elastic
295.88	3833.088	-183.810	2.959	non-elastic
363.51	4110.935	-237.175	3.635	non-elastic
2116.91	4380.792	-251.439	21.169	non-elastic
4126.33	4660.170	-261.494	41.263	non-elastic
6135.74	4939.548	-271.549	61.357	non-elastic
7990.59	5197.436	-280.831	79.906	non-elastic
10000.00	5476.814	-290.886	100.000	non-elastic

Section properties:reference E-modulus [kN/mm²]:,210

E.N.A.from bottom line [mm]:,56.875

first yielding at [mm]:,215

Area [mm²]:,12400Shear area Avc [mm²]:,4000Inertia [cm⁴]:,6638.224upper Resis.Moment [cm³]:,419.8086lower Resis.Moment [cm³]:,1167.16

El.limit of bending [kNm]:,145.0248

El.limit of kapa [o/oo/m]:,10.4033

Plastic normal force [kN]:,4113.182," without buckling-check"

Plastic shear force (web-parts): [kN],797.7931," without buckling-check"

end

Applying the formulae given in Fig.4-19 this procedure (4.2.3.4) can also be used e.g. to determine the $M_{Rd}-V_{Sd}$ or the $N_{Rd}-V_{Sd}$ interaction of a steel section. In Fig.4-21 the maximum plastic sagging moment of the example section has been evaluated for different values of interacting vertical shear. Fig.4-22 shows the interaction between normal force resistance and actual vertical shear. As described in Fig.4-9 the interaction between normal stresses and vertical shear stresses leads to a fictitious reduction of the stress-strain diagram of the steel web elements.

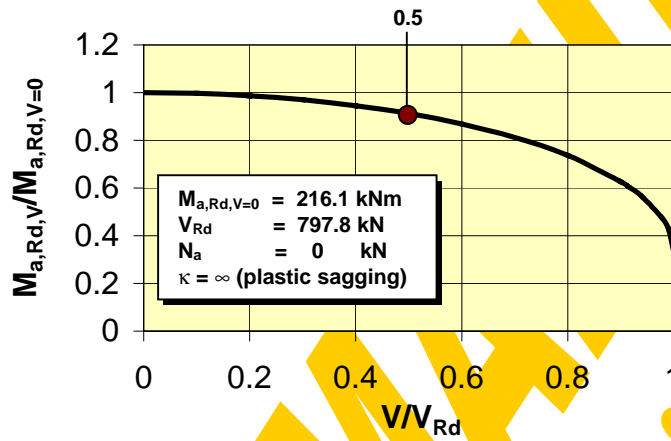


Fig.4-21 Interaction between bending resistance and vertical shear

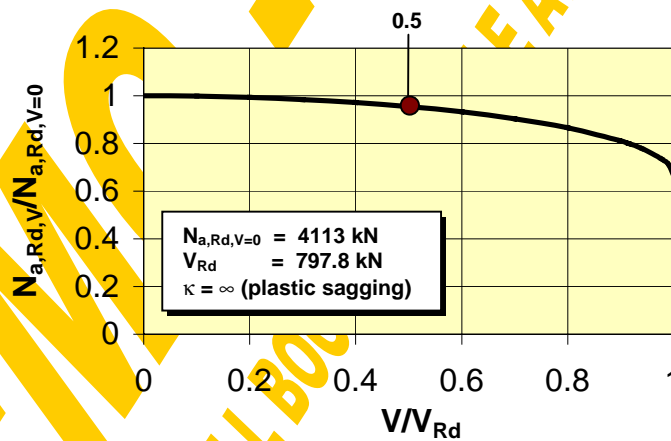


Fig.4-22 Interaction between normal force resistance and vertical shear

4.2.4 Concrete section

4.2.4.1 Section input

The concrete section window, shown in Fig.4-23 and Fig.4-26, first of all enables the input of the reinforced concrete section part consisting of up to 10 rectangular concrete elements and 10 layers of reinforcement. It will be assumed that the overall concrete section is shear-connected to the steel part.

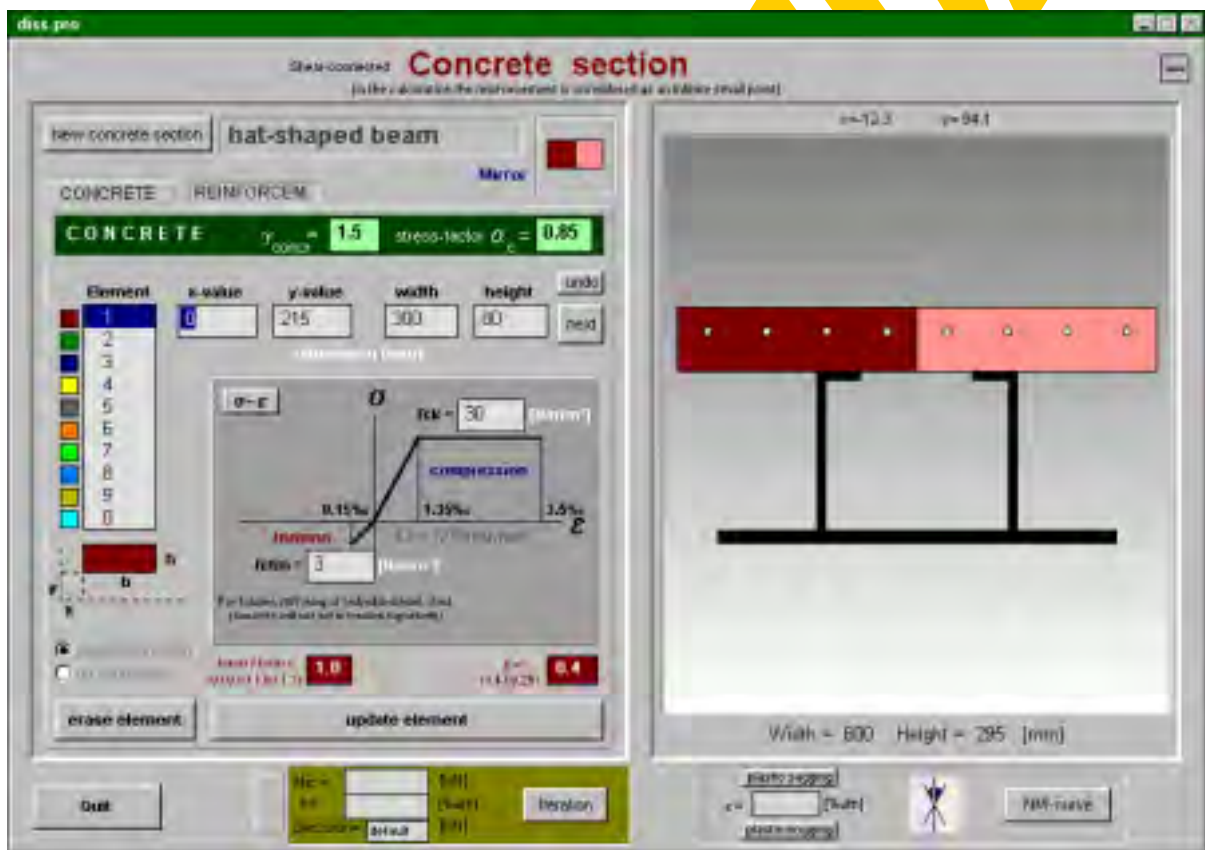


Fig.4-23 Window for the reinforced concrete section part - concrete elements (prc.frm)

First the input window for the 10 concrete elements (button „CONCRETE“) will be opened as illustrated in Fig.4-23. In view of the possibility to mirror the section horizontally the final concrete section may consist of up to 20 concrete elements. The 10 basic elements are marked with different colours. To point out the mirrored elements they are drawn with a more pale colour, what is also stressed in the „Mirror“-box. For each element the coordinates of one corner (x,y) and the width and height (b,h) to the other corner can be defined. Also negative values are accepted, however then the x- and y-coordinates will automatically be re-calculated for the lower left corner. To facilitate the input the coordinates of the actual mouse-position are indicated at the top of the drawing. A single click within the drawing will write the coordinates of the nearest existing element corner (also steel elements are accepted) to the x- and y-boxes. A

double-click is understood as the second corner of the actual element. Therefore the actual element width and height then are calculated as the distance between the given x- and y-values and the nearest element corner from the double-click position. Attention has to be paid that the corners of mirrored elements cannot be caught; they will automatically be transformed to the basic element corner.

Apart from the geometrical properties also the material properties can be defined for each concrete element separately. The stress-strain diagram is based on the following input data: Characteristic compressive strength f_{ck} and mean tensile strength f_{ctm} . Further it depends on the global partial safety factor of concrete $\gamma_{concr}=\gamma_c$ (default=1.5) and the stress factor α_c (default=0.85). The definition of the bi-linear stress-strain diagram for concrete elements used in this program is summarised in Fig.4-24 based on [182]. It can be seen that for the bare concrete **no tensile strength** is taken into consideration. The effective tensile strength $f_{ct,eff}$, which can be gained from the mean value f_{ctm} multiplied by a factor, is only considered for the **tension stiffening effect of the reinforcement** embedded in this concrete element. The strains of cracking, elastic limit and crushing have generally been defined to 0.15, 1.35 and 3.5‰ independently of the concrete grade. The corresponding elastic modulus can be calculated according to the following formula and will be displayed for each element. So to make an elastic calculation the compressive strength f_{ck} of these elements has to be chosen so that a given value of the elastic modulus E_c results from the following relationship.

$$E_c = \frac{\alpha_c \cdot f_{ck}}{\gamma_c \cdot \frac{1.35}{1000}}$$

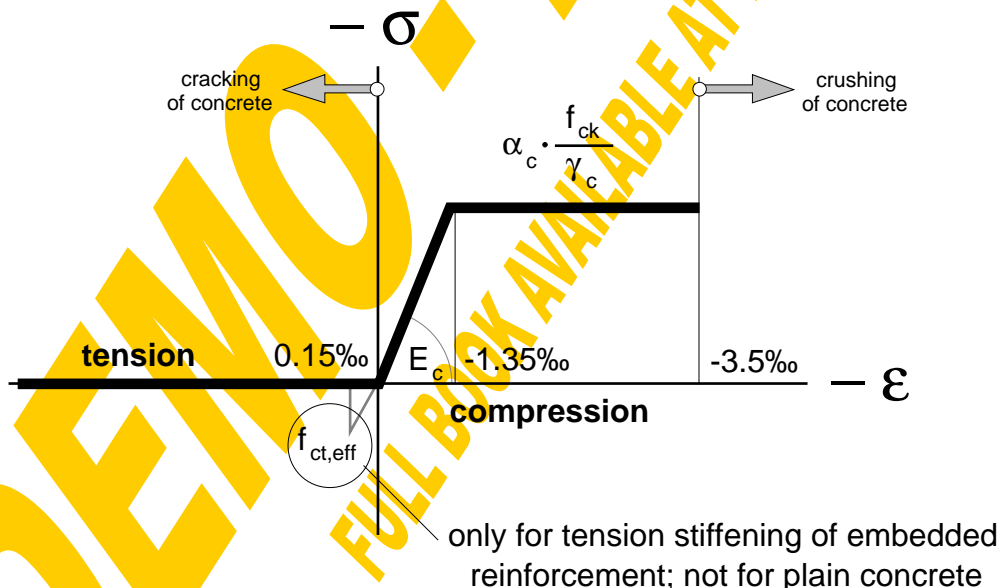


Fig.4-24 Stress-strain diagram of concrete elements

The actual stress-strain diagram of each concrete element can be seen true to scale when clicking on the „ σ - ϵ “-button (Fig.4-25). There will be the possibility to calculate the corresponding stress to a given strain and vice versa by a linear interpolation.

According to [59,109] the contribution of concrete to the overall vertical shear resistance has generally been neglected because it is much smaller than the resistance of the steel section (web elements). This assumption has been made especially in view of conventional composite beams with relatively thin slabs on top of deep steel beams. However also in view of slim floors in the joints (being the decisive locations for shear design) the whole vertical shear force anyway has to be carried by the bare steel connection. Therefore at these decisive points all the vertical shear force yet has to be assigned to the steel webs alone. So this justifies the assumption to ignore the concrete contribution to vertical shear.

The longterm redistribution of forces from the concrete to the reinforcing steel due to creep and shrinkage generally has not been taken into consideration because of its minor influence.

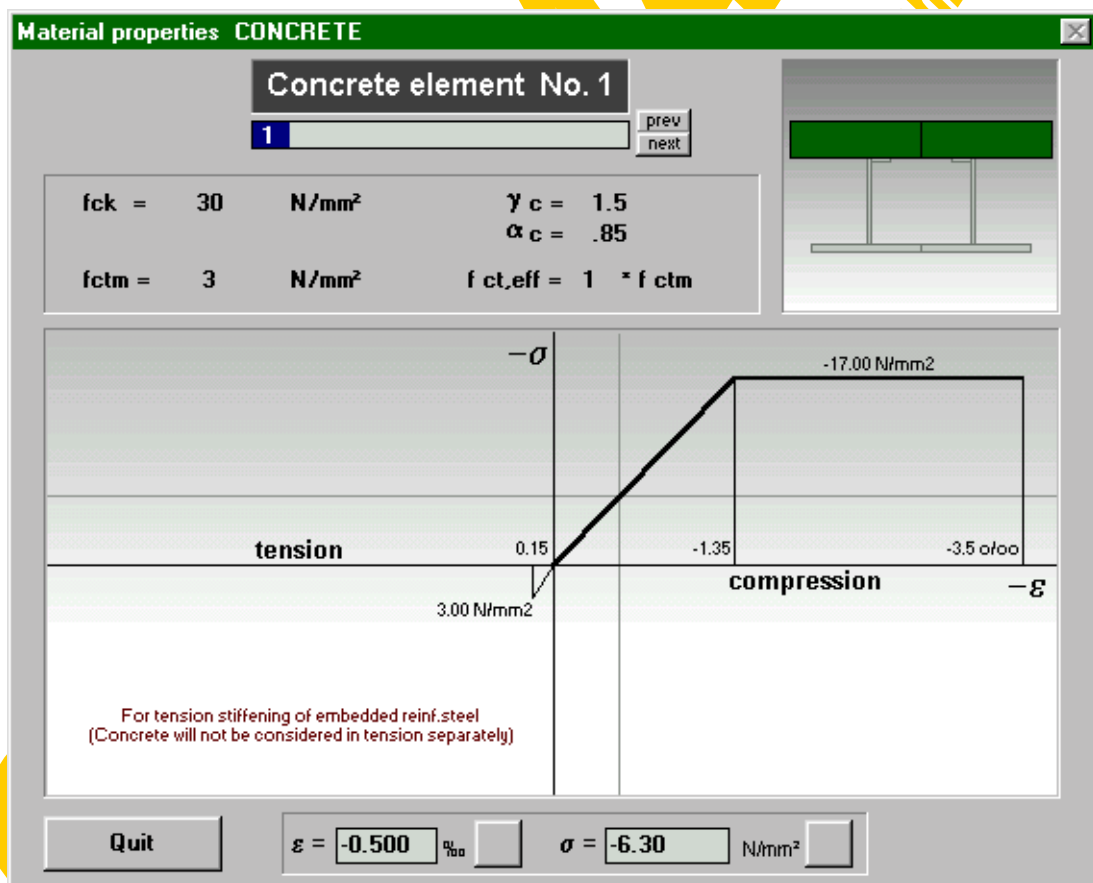


Fig.4-25 Window for the actual stress-strain diagrams of concrete elements (stoffgc.frm)

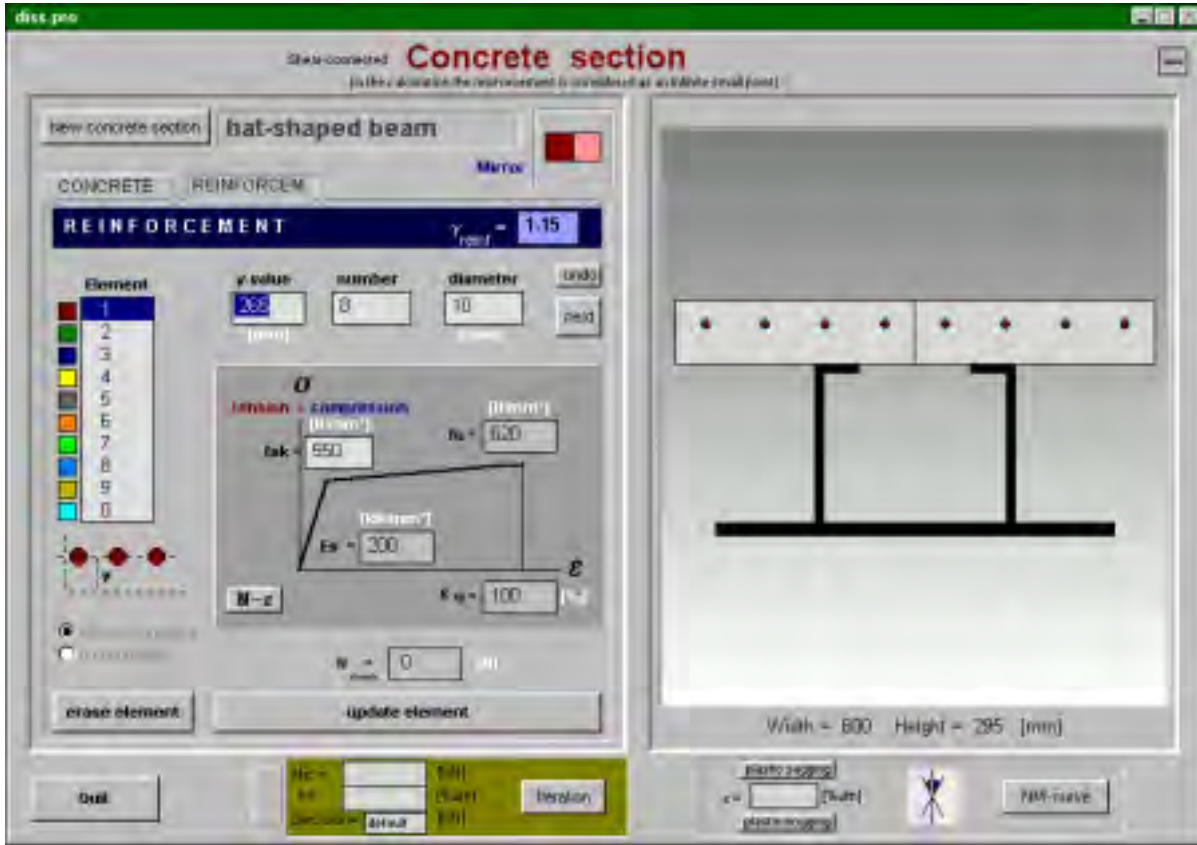


Fig.4-26 Window for the reinforced concrete section part - reinforcement layers (prc.frm)

Clicking on the button „REINFORCEM.“ switches from the concrete input window to that for the reinforcement (Fig.4-26). The 10 layers are marked with different colours. For each layer the y-coordinate has to be defined. To facilitate the input the coordinates of the actual mouse-position are indicated at the top of the drawing. A single click within the drawing will write the y-coordinate of the nearest existing element corner (steel and concrete elements) to the y-box. Further the diameter and number of reinforcing bars at this level have to be given. In the drawing the rebars are shown true to scale however simplifying with an equidistant spacing in horizontal direction (the x-values anyway do not have any meaning for the calculations). Attention has to be paid that the reinforcement in the calculations is regarded to be concentrated at the given y-value. The diameter only is necessary to evaluate the area of reinforcement, the strain distribution within the rebars and therefore their bending stiffness will be neglected.

Apart from the geometrical properties also the material properties can be defined for each reinforcement layer separately. The stress-strain diagram of a bare (unembedded) reinforcing bar is assumed to be symmetrical for tension and compression (Fig.4-27) and is based on the following input data: Young modulus E_s , characteristic yielding strength f_{sk} , ultimate strength f_u and ultimate strain ϵ_u . Further it depends on the global partial safety factor of reinforcement $\gamma_{reinf.} = \gamma_r$ (default=1.15).

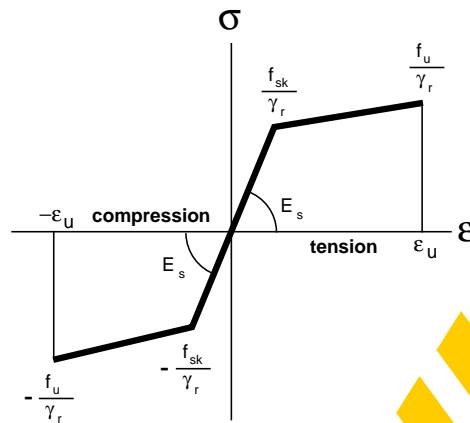


Fig.4-27 Stress-strain diagram of bare unembedded reinforcement

As already mentioned the concrete itself will not be taken into consideration in tension but it significantly contributes to the behaviour of the reinforcement. This strengthening effect of the reinforcement in tension by the concrete between the cracks is called „**tension stiffening effect**“ [72,73,177]. The mechanical background can easily be explained for a reinforced concrete member in pure tension. Until the tensile strength of the weakest concrete cross section is reached the strains of concrete and reinforcement are equal and there are no bond stresses in between. At the state of the first crack in the cracked cross section the full crack force $N=N_1$ has to be carried by the bare reinforcement leading to an increase of strain in comparison to the composite section between the cracks. At the cracked section the concrete strain is zero. Within a transmission length l_t to both sides of the crack due to bond stresses the strain of the reinforcement gradually is reduced and that of the concrete gradually is raised until at the ends of this force transmission the strains of reinforcement and concrete again are equal and the total force $N=N_1$ is shared between these two section parts. Due to the crack the elongation of the member increases in comparison to the uncracked state and can be calculated by integrating the strain distribution over the member length. Increasing the tension force beyond N_1 will lead to the next crack in the second weakest cross section with the same effect of bond stresses and strain distribution within the transmission length. This quick formation of cracks can be continued until the distance between the cracks approximately is equal to the transmission length. From this state on the bond stresses along the half crack distance are too small to activate the tensile strength in the concrete and therefore to initiate new cracks. This occurs at the force limit N_2 . Within the following range of stabilised cracks there are nearly no new cracks and the whole increase of force is taken over by the bare reinforcement. The average transmission length is assumed to be $2/3$ of l_t , so the average crack distance is 2 times $2/3 l_t$. The average steel strain ϵ_{sm} taking into consideration the tension stiffening effect can be got by integrating the strain distribution. It obviously will be smaller than the bare unembedded steel strain. The third bend (N_3) of the embedded force-strain diagram is linked to the yield stress of the reinforcement. Finally it has to be emphasised that the ultimate strain of an embedded rebar is drastically reduced in comparison to that of bare steel. This negative effect gains importance with decreasing degree of

reinforcement. The mechanical principles of tension stiffening are summarised in Fig.4-28 and Fig.4-29.

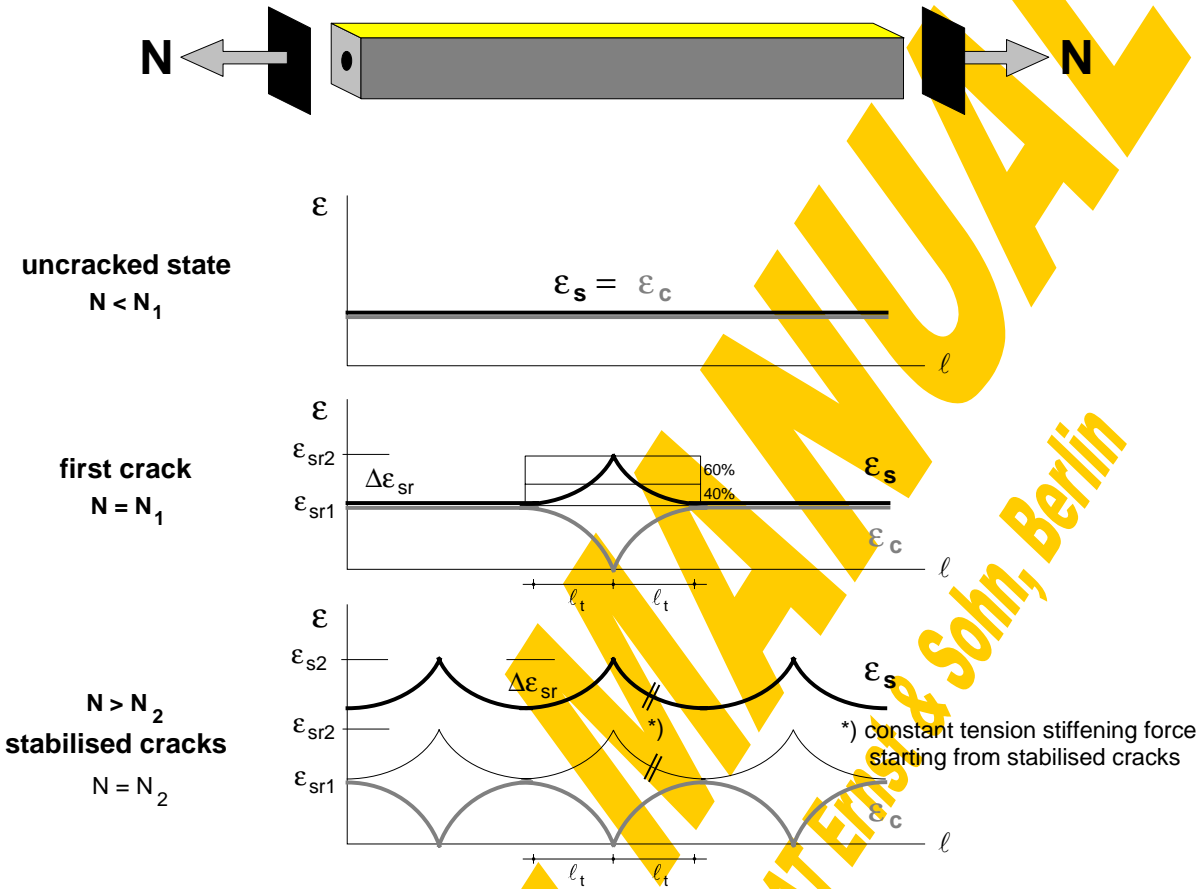


Fig.4-28 Tension stiffening effect in a reinforced concrete tension member

$$l_t \Rightarrow \epsilon_{sm} = \epsilon_{s2} - B \cdot \Delta\epsilon_{sr} \quad B \approx 0.6$$

$$l_{tm} = \frac{2}{3} \cdot l_t \Rightarrow \epsilon_{sm} = \epsilon_{s2} - \frac{2}{3} \cdot B \cdot \Delta\epsilon_{sr} = \epsilon_{s2} - \beta \cdot \Delta\epsilon_{sr} \quad \beta_{\text{short term}} = 0.4$$

ϵ_{sm} ... average steel strain considering tension stiffening
 ϵ_{s2} ... steel strain in the crack (state II)

$$\Delta\epsilon_{sr} = \epsilon_{sr2} - \epsilon_{sr1} = \frac{f_{ct,eff} \cdot A_{ct}}{E_s \cdot A_s}$$

$$\epsilon_{sr1} = \frac{f_{ct,eff}}{E_s} \quad n = \frac{E_s}{E_{c,tension}}$$

$$\epsilon_{sr2} = \frac{N_1}{E_s \cdot A_s} \quad N_1 = f_{ct,eff} \cdot (A_{ct} + n \cdot A_s)$$

Fig.4-29 Mechanical background of tension stiffening

Following the rules given in [62]-Annex L the mathematical model shown in Fig.4-30 and Fig.4-31 has been adopted for the described computer program. Only the strain of the first crack as a minor modification generally has been defined with 0.15‰. As a simplification the relatively small steel area will not be subtracted from the concrete (n instead of $(n-1)$).

$$\begin{aligned} \varepsilon_1 &= \frac{0.15}{1000} \\ N_3 &= A_s \cdot \frac{f_{sk}}{\gamma_r} \\ N_1 &= E_s \cdot A_s \cdot \varepsilon_1 + A_{ct} \cdot f_{ct,eff} \leq N_3 \\ N_0 &\leq N_1 \quad \text{normal force due to shrinkage decreases between } \varepsilon_1 \text{ and } \varepsilon_2 \\ N_2 &= 1.3 \cdot N_1 \leq N_3 \\ \Delta\varepsilon &= \frac{f_{ct,eff} \cdot A_{ct}}{E_s \cdot A_s} \quad \Delta N = E_s \cdot A_s \cdot \beta \cdot \Delta\varepsilon = \beta \cdot f_{ct,eff} \cdot A_{ct} \quad \begin{array}{l} \beta_{\text{short term loading}} = 0.4 \\ \beta_{\text{long term / repeated loading}} = 0.25 \end{array} \\ \varepsilon_2 &= \frac{N_2 - \Delta N}{E_s \cdot A_s} \\ \varepsilon_3 &= \frac{N_3 - \Delta N}{E_s \cdot A_s} = \varepsilon_y - \beta \cdot \Delta\varepsilon \\ N_4 &= A_s \cdot \frac{f_u}{\gamma_r} \\ \varepsilon_4 &= \varepsilon_3 + \delta \cdot \left(1 - \frac{N_1}{N_3}\right) \cdot (\varepsilon_u - \varepsilon_y) \\ \delta &= 0.8 \quad \text{for ductile steel with } \varepsilon_u > 5\% \text{ and } \frac{f_u}{f_{sk}} > 1.08 \end{aligned}$$

Fig.4-30 Modelling of the tension stiffening effect - formulae

When setting the area of concrete in tension (A_{ct}) to zero the formulae given in Fig.4-30 lead directly to the basic stress-strain diagram of the bare reinforcement. Only the ultimate strain ε_4 would be smaller than ε_u . This inconsistency has been corrected in the computer program: if $A_{ct} > 0$ $\varepsilon_4 = \varepsilon_u$, otherwise the formula given in Fig.4-30 is used. Attention has been paid to the following special cases: If N_2 exceeds the yielding force (N_3) in case of a low degree of reinforcement it will be set equal to N_3 . If even the uncracked force in tension (N_1) exceeds the yielding force of the bare reinforcement (N_3) that indicates that the area of reinforcement has been chosen below the **minimum reinforcement**. This fact will be indicated by a warning. However to enable still a further hypothetical calculation N_1 in this case will be set equal to N_3 and ε_4 will be taken equal to ε_u .

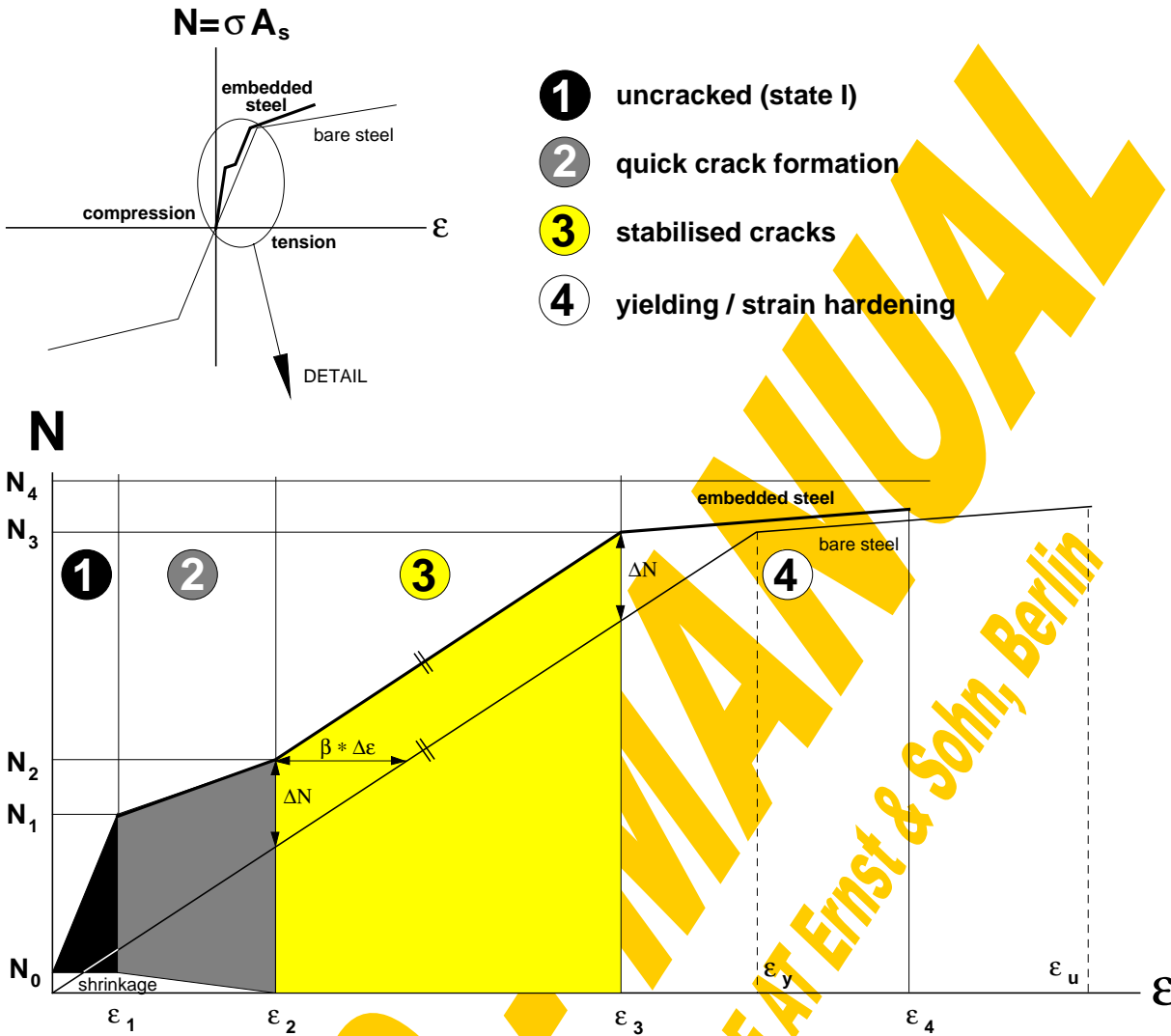


Fig.4-31 Modelling of the tension stiffening effect - graph

Both in the drawings and the tables the resulting normal force explicitly will be set together by the shares of the bare steel, the concrete in tension between the cracks and occasionally also of the shrinkage influence. For the fictitious normal force due to shrinkage an input box has been arranged within the reinforcement window („N_{shrink.}“). Although they influence the response of the reinforcement in tension the β -value as well as the ratio between effective and mean tensile strength of concrete ($f_{ct,eff}/f_{ctm}$) have to be set on the concrete input window, as they are primarily linked to the concrete in tension between the cracks.

Strictly the described procedure only is valid for reinforced concrete members in pure tension. So as a simplification for the computer program the concrete section part in tension and bending has been divided into substituting tension members consisting of the reinforcement layers with surrounding concrete. The resulting tension forces will be taken from the strain-force diagram of the embedded steel for the strain at the reinforcement centre. Concrete in tension is taken into consideration by a modification of the reinforcement behaviour; there will not be calculated a further separate tension

stress-block of the concrete itself. The remaining problem was to define the effective area of concrete contributing in tension (A_{ct}) to the reinforcement bars (see Fig.4-32). For that purpose first a square of $15d_s$ is drawn around each rebar as the maximum contributing concrete area. This value has been taken from [30] where an area of 2 times $7.5d_s$ is specified to influence the crack initiation at the surface. Strictly until the first crack occurs for a bare tension member the whole area of concrete in tension would have to be considered. Due to the slender concrete elements in composite members the relatively high upper limit of $7.5d_s$ anyway very rarely becomes decisive and therefore has been accepted as a compromise. This maximum area of contributing concrete around each rebar has to be reduced if the section borders are reached, if contributing areas of several rebars are overlapping (in that case the distance in between is shared corresponding to the ratio of reinforcement areas) or if it would reach into the compression area. This is the case if the neutral axis lies in between the $7.5d_s$ -radius of a reinforcement layer. Finally in the special case that several reinforcement layers have the same y-value only for that layer with the maximum steel area the tension stiffening effect will be taken into consideration. The other layers at this level then will be calculated as bare steel layers.

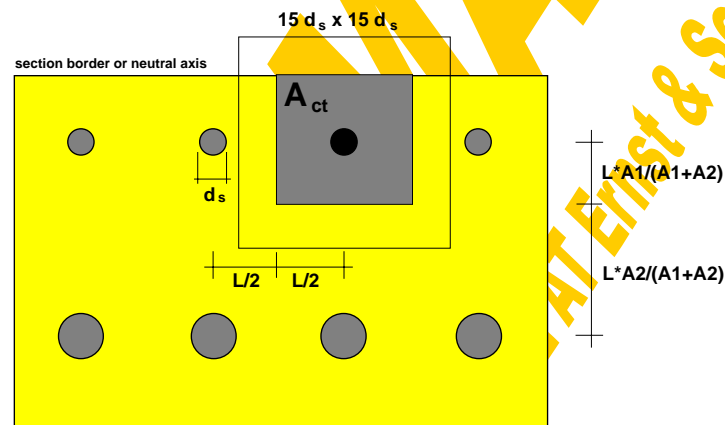


Fig.4-32 Definition of the contributing area of concrete in tension

The actual strain-force diagram of each reinforcement layer can be seen true to scale when clicking on the „N-ε“-button (Fig.4-33). There the actual layer is painted in black, the contributing concrete area in yellow. The boxes for ϵ and N enable a linear interpolation between strains and corresponding forces. Fig.4-33 shows the N- ϵ diagram of the example section using $\gamma_r=1.15$, $\beta=0.4$ and $f_{ct,eff}/f_{ctm}=1$. Fig.4-34 gives the detail without the yielding or strain-hardening part (click on diagram). To take into consideration an eventual reduction of the tension stiffening concrete area (indicated in yellow) if the actual neutral axis reaches into this yellow area in Fig.4-33 a neutral axis input box has been provided.

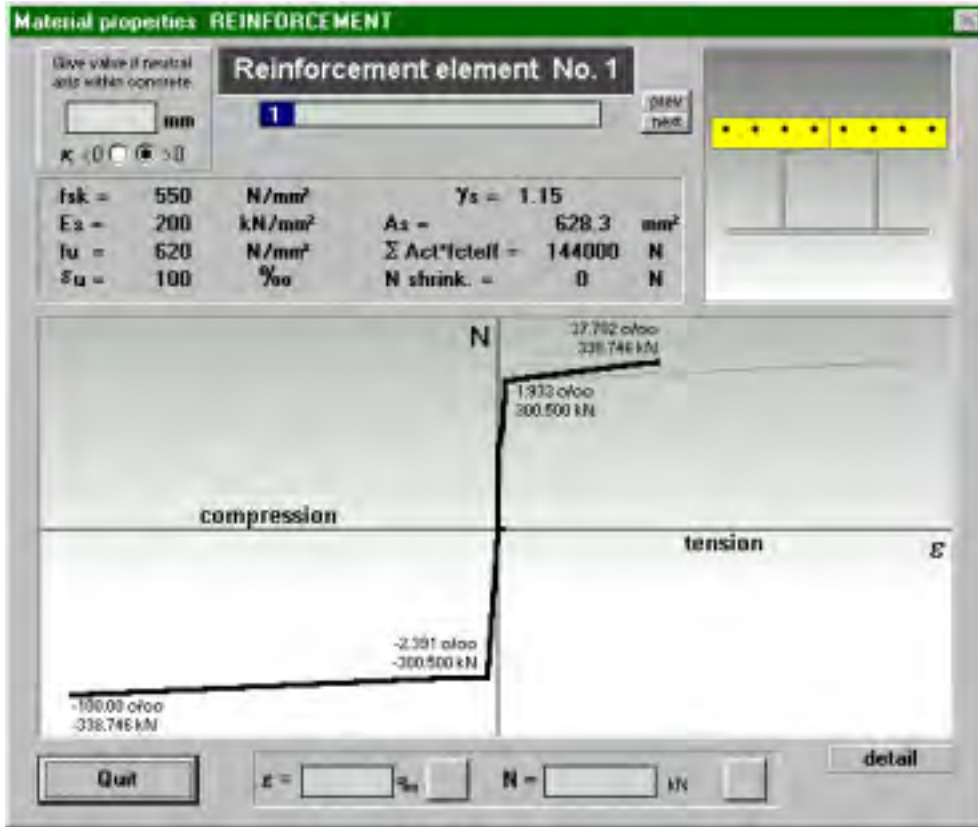


Fig.4-33 Window for the actual strain-force diagrams of rebars (stoffgr.frm)

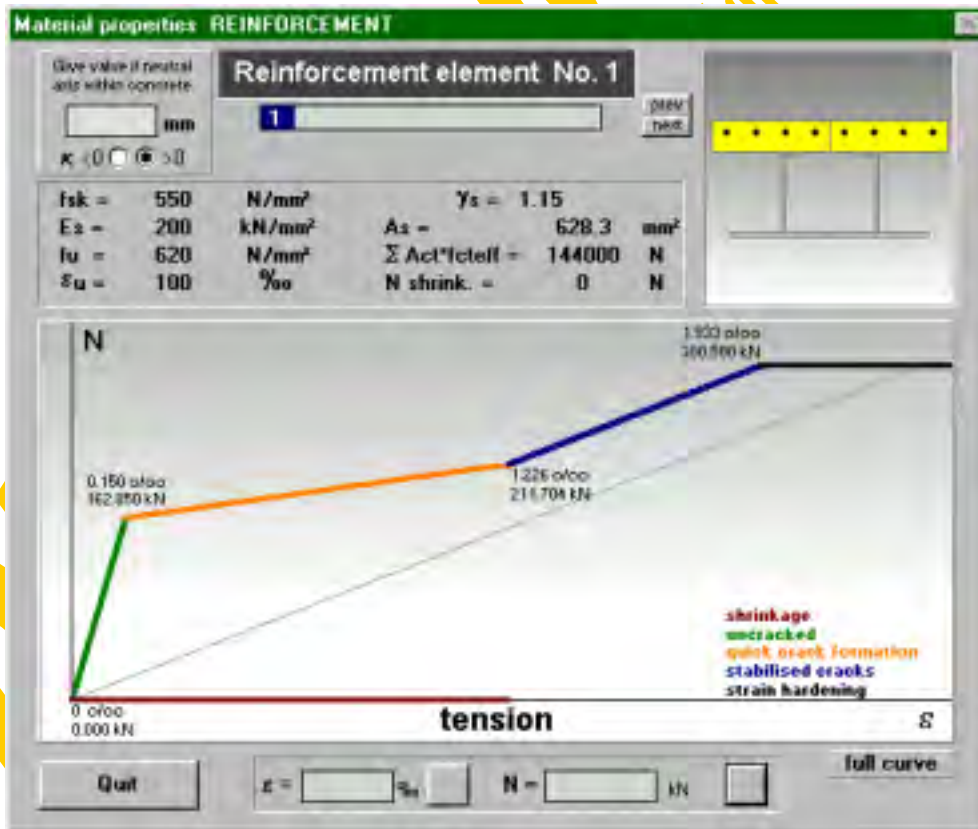


Fig.4-34 Window for the actual strain-force diagrams of rebars (stoffgr.frm)

Before returning from the concrete section window to the section management window or before starting any calculation it will be checked automatically if elements are overlapping and therefore these areas would be calculated more than once. Further after each element input the entire composite cross section automatically will be moved so that the minimum x-value of the entire section is equal to zero.

Based on the so-defined concrete section including geometry and material properties the following three calculations or iterations can be carried out:

- internal forces to a given strain distribution
- strain distribution to a given normal force
- N-M-relation for a defined curvature

4.2.4.2 Internal forces to a given strain distribution (*concstrain*)

$\varepsilon (y=0) =$	2.685	[%]	Calculation
$\kappa =$	10	[%/m]	

The actual linear strain distribution within the reinforced concrete section can be defined by the strain at height of the datum line ($y=0$ =steel bottom) ε_{0c} and the curvature κ as shown in Fig.4-35.

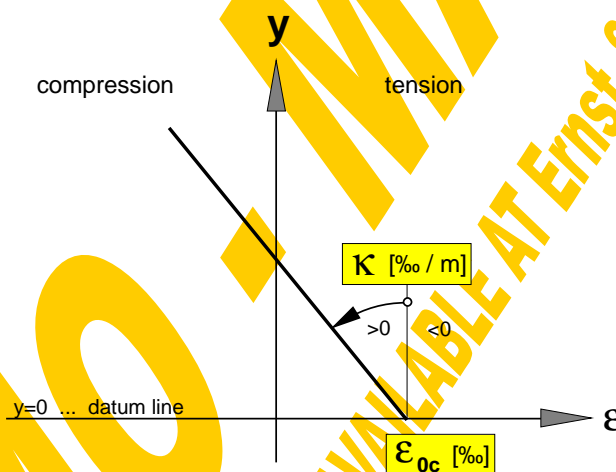


Fig.4-35 Linear strain distribution

Based on that the global procedure „*concstrain*“ calculates the corresponding stresses of each concrete element and the corresponding forces of each reinforcement layer based on the material properties. The following indicator flags are set (Fig.4-36): elastic („el“) means that for a reinforced concrete section all concrete strains are in between -1.35 and 0.15% . For a plain concrete section even no tension ($\varepsilon=0$) will be allowed. Further the yield strain ε_y of all rebars in compression must not be exceeded. The non-elastic flag („ne“) is set if the strain in at least one concrete point exceeds -1.35% in compression or passes 0.15% in tension. Non-elastic will also be indicated if the strain in at least one rebar exceeds ε_y . If the concrete strain in compression reaches -3.5% crushing of concrete („cr“) will be indicated and for the case that the provided reinforcement is less than the minimum reinforcement „beyond ultimate strain“ („**“) is shown for $\varepsilon > \varepsilon_3$.

concrete

- non elastic $0.15\text{‰} (0\text{‰}) < \epsilon$
- elastic $-1.35\text{‰} < \epsilon < 0.15\text{‰} (0\text{‰})$
- non - elastic $-3.5\text{‰} < \epsilon < -1.35\text{‰}$
- crushing of concrete $\epsilon < -3.5\text{‰}$

reinforcement

- non – elastic $\epsilon < -\epsilon_y$
- elastic $-\epsilon_y < \epsilon < 0.15\text{‰}$
- non - elastic $0.15\text{‰} < \epsilon$
- " $>\epsilon_u$ " if $A_s < A_{s,min}$ $\epsilon_3 < \epsilon$

Fig.4-36 Indicator flags

An integration of the stresses and forces over the whole concrete section leads to the normal force N_{ic} (compression positive). Integrating the stresses and forces multiplied by their lever arms to the steel bottom results in the moment M_c' , which of course is related to this datum line $y=0$ as described in [106] (sagging moments positive). Finally also the y -value of the neutral axis (N.A.) is declared.

Fig.4-37 illustrates this basic calculation for the example section leading from strains to stresses and internal forces.

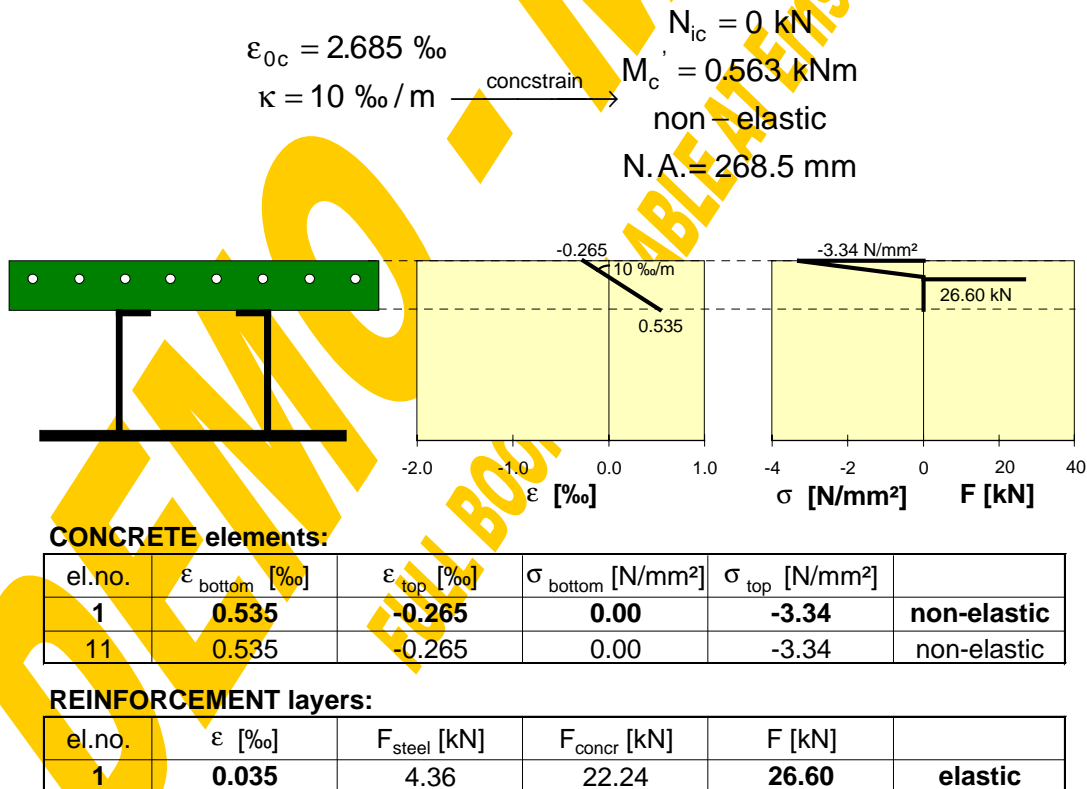


Fig.4-37 Calculation example

4.2.4.3 Strain distribution to a given normal force (*Nconcriteration*)



The global procedure „**Nconcriteration**“ goes the opposite direction iterating the corresponding strain distribution to a given normal force N_{ic} and a given curvature κ . This problem is solved in two steps:

First the ultimate boundaries of datum strains (at $y=0$) depending on the curvature κ and the ultimate strain values ϵ_u of the concrete and reinforcement elements are derived within the procedure „**conclimit**“. Then the yielding datum strain boundaries are calculated. These are the boundaries from where on any parallel movement of the strain distribution would not bring any changes of stresses or forces. Comparing the ultimate strain boundaries with the yielding ones leads to the decisive strain boundaries. The lower and upper ultimate normal force in the reinforced concrete section (depending on the given curvature κ) then can be calculated with the procedure „**concstrain**“ as shown in Fig.4-38.

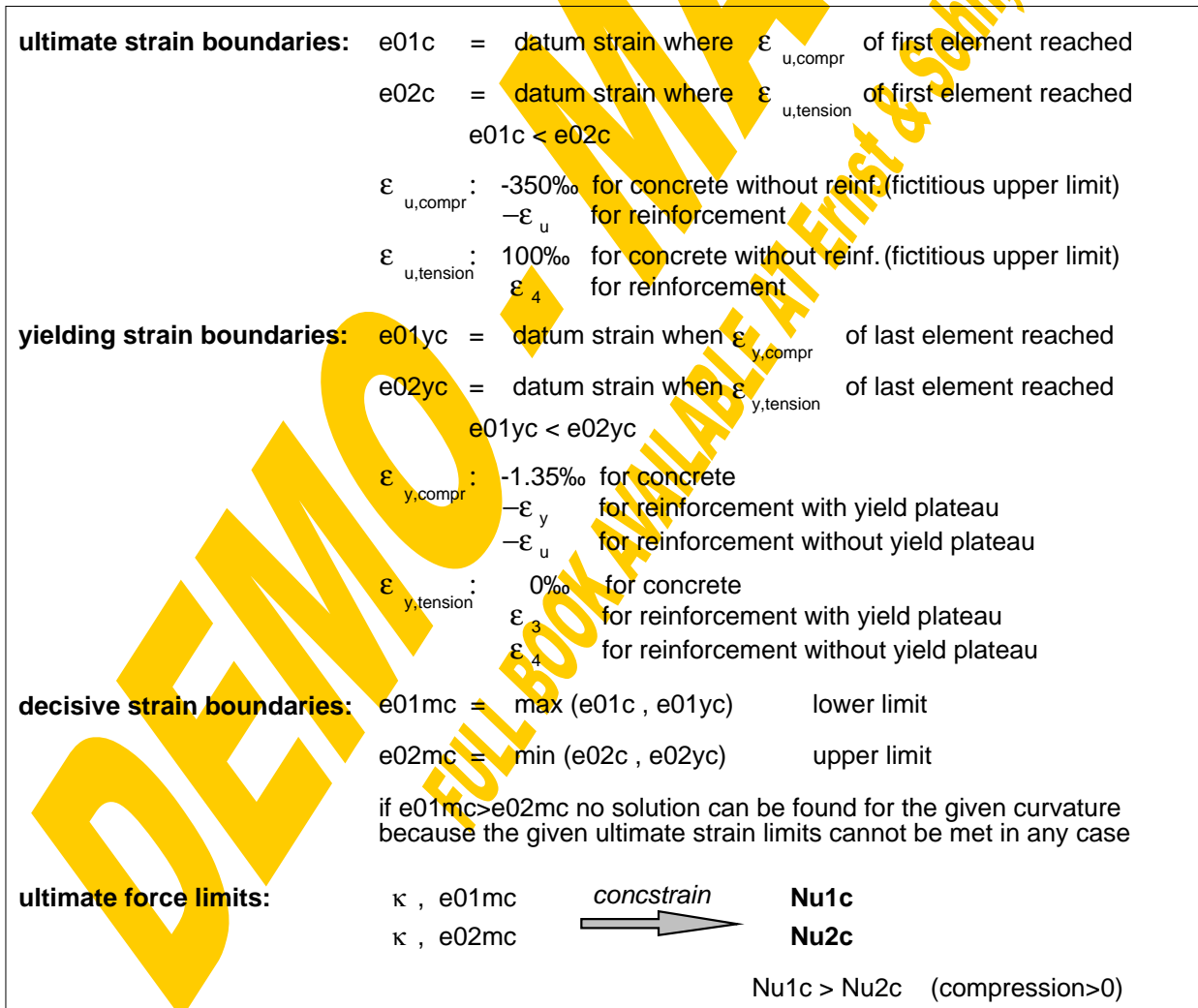


Fig.4-38 Strain boundaries from procedure „conclimit“

In the second step the iteration for the corresponding datum strain in between the decisive strain boundaries will start, if the given normal force N_{ic} lies in between the just calculated limits $Nu1c$ and $Nu2c$. This is done within the procedure „itNconcr“ in the following iterative way:

Starting with the boundaries $e01mc$ and $e02mc$ the actual normal force for the bisection point of these strains is calculated using the procedure „concstrain“. Then the strain boundaries are adapted so that the prescribed normal force lies within these new boundaries. This iteration based on the bisection method is repeated until one of the following criteria is fulfilled: Either the actual normal force attains the prescribed one with a given accuracy or the changes of strains lie below a given tolerance. A stop is also caused if the iteration time exceeds a stop-limit. That would indicate a jump of the normal force despite of a minor change of the datum strain due to the force within the reinforcement in combination with a big curvature. In that case the final solution of ϵ_{0c} is found by an interpolation. A summary of the iteration accuracy criteria can be found at the end of chapter 4.2.

Fig.4-39 shows the iteration and the results for the example section. It can clearly be seen that the relatively flat parts of the $N_{ic}-\epsilon_{0c}$ -curve, which result from the strain hardening of the reinforcement elements beyond the design yield strength, dominate this function and therefore drastically slow down the iteration process. However thanks to the quick computers the iteration time anyway keeps really acceptable. Such an iteration plateau could be avoided by using material laws with a flat plateau (without strain hardening).

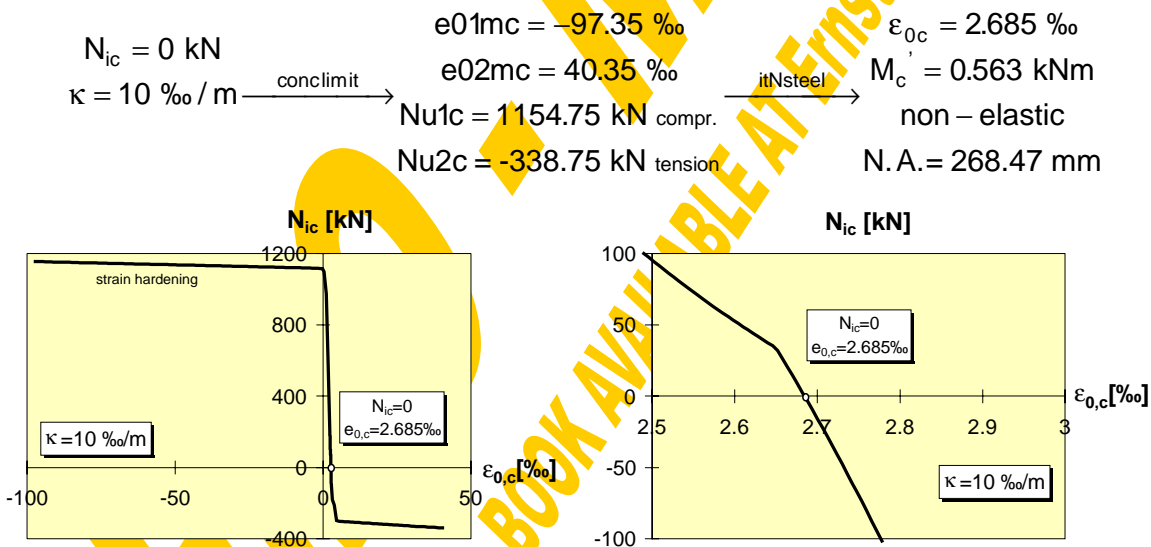


Fig.4-39 Iteration example

Apart from the possibility to make interpolations within the $N_{ic}-M_c'$ -curve the described procedure „Nconcritation“ e.g. also can be used to iterate manually the ultimate limit of bending κ_u (iteration until ϵ_u of the first element is reached) or to determine the coherence between curvature (κ) and neutral axis (N.A.) or bending moment (M_c') as illustrated in Fig.4-40 for the example section. Of course for the special case that $N_{ic}=0$ the relative bending moment M_c' (related to the datum line) is equal to the absolute one M_c .

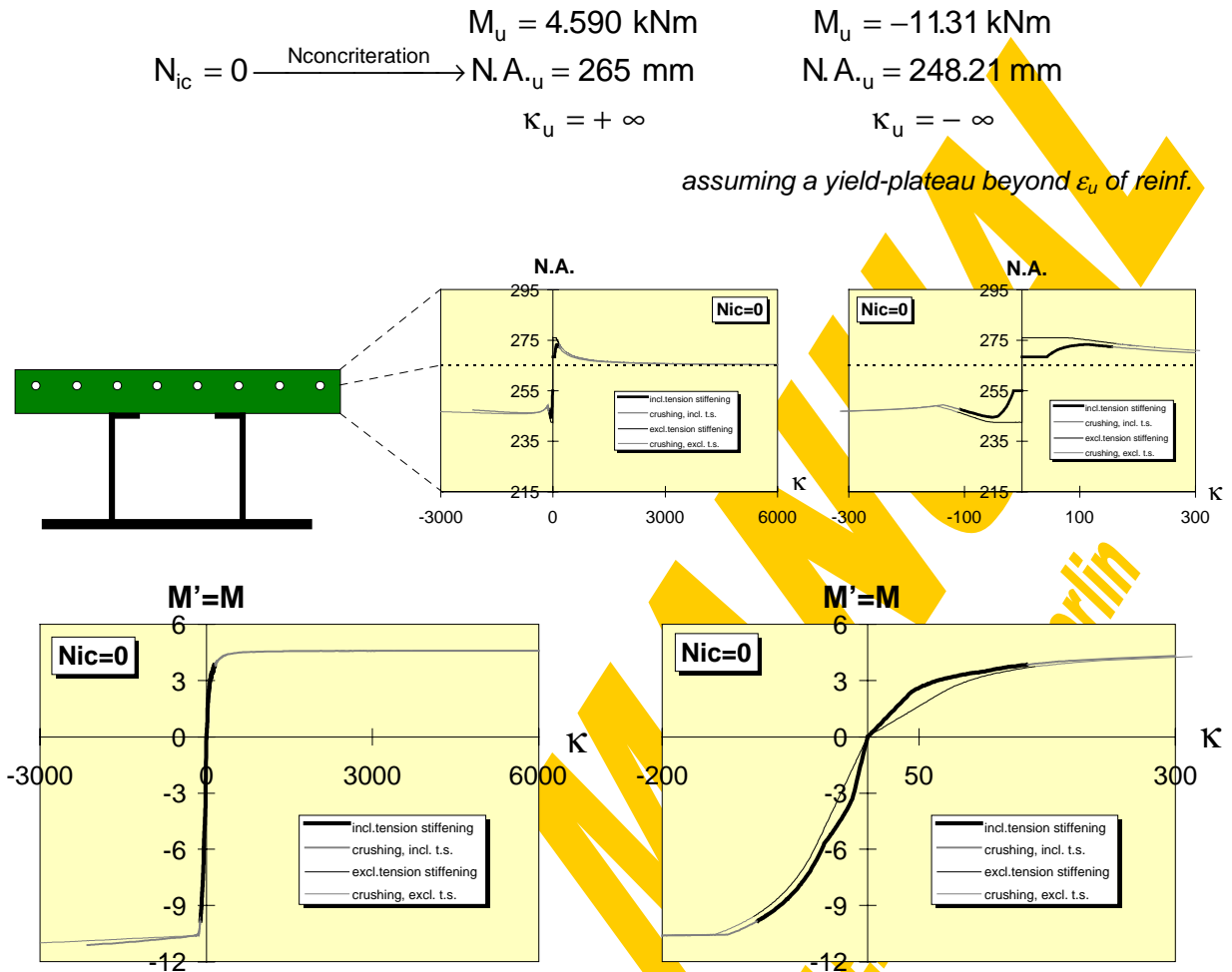


Fig.4-40 Results using the procedure „Nconcriteration“ for further iterations

4.2.4.4 N-M-relation for a defined curvature (NMconcr)



Based on the just described strain iteration the full range between the force limits $Nu1c$ and $Nu2c$ can be analysed for a defined curvature κ (procedure „**NMconcr**“). First the strain and force limits are calculated using the procedure „conclimit“. Then the range between $Nu2c$ and $Nu1c$ is subdivided into 40 parts and for each normal force the corresponding datum strain ϵ_{0c} will be iterated with the procedure „itNconcr“. Afterwards for the found solution the bending moment M_c' and the location of the neutral axis $N.A._c$ are evaluated with the procedure „constrain“. Finally the fully plastic concrete section properties are calculated with the procedure „**qswerteconcr**“ based on the formulae shown in Fig.4-41.

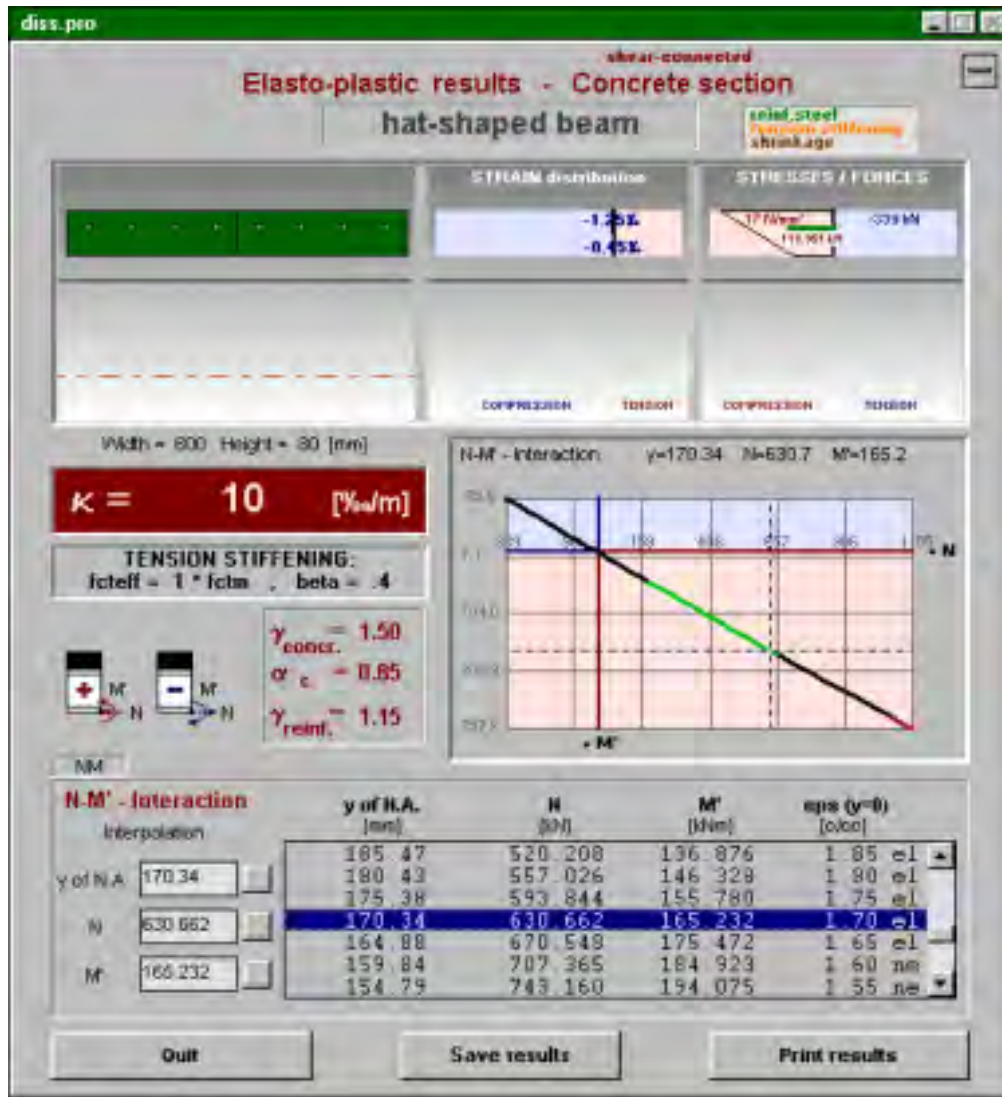
$$\begin{aligned}
 \text{Area concrete } A_c &= \sum_{\text{concrete elements}} b_i \cdot h_i \\
 \text{Area reinforcement } A_r &= \sum_{\text{reinf. layers}} n \cdot \frac{d_i^2 \cdot \pi}{4} \\
 \text{plastic neutral axis PNA ... itNconcr } &(\kappa = \pm\infty, N_{ic} = 0) \\
 \text{ideal plastic normal force } N_{\text{pl,tension}} &= \sum_{\text{reinf.}} \frac{n \cdot d_i^2 \cdot \pi}{4} \cdot \frac{f_{sk}}{\gamma_r} \\
 \text{ideal plastic normal force } N_{\text{pl,compression}} &= \sum_{\text{concr.}} b_i \cdot h_i \cdot \frac{\alpha_c \cdot f_{ck}}{\gamma_c} + \sum_{\text{reinf.}} \frac{n \cdot d_i^2 \cdot \pi}{4} \cdot \frac{f_{sk}}{\gamma_r} \\
 \text{ideal plastic bending moment } M_{\text{pl}} &\dots \text{itNconcr } (\kappa = \pm\infty, N_{ic} = 0)
 \end{aligned}$$

Fig.4-41 Formulae for the calculation of the concrete sectional properties (qswerteconcr)

Two special buttons have been arranged to enable also a quasi-fully-plastic analysis. When clicking on „plastic sagging“ or „plastic hogging“ the curvature κ will be set equal to $\pm 10^5$ ‰/m and all stress-strain diagrams of the reinforcement layers are modified temporarily in that way, that any strain hardening is cut and an infinite yielding plateau without any limiting strain is provided.

In the following the results from calculations for the example section using $\kappa=10$ ‰/m are described. The progress of iteration will be indicated by a flood box. After the termination of the calculation the concrete input window will be closed and the window for the presentation of the concrete results is shown (Fig.4-42). It comprises the input data (table of concrete elements and reinforcement layers, safety-factors, ...) an image of the concrete section, the actual strain and stress distribution and a table and a graph of the calculated N_{ic} - M_c' -interaction. Those parts of the interaction curve drawn in green represent the elastic range, the non-elastic parts are drawn in black, the range of crushing concrete in compression is indicated with a red colour. Where even ε_u is exceeded a white colour is used. The resulting force of each reinforcement layer also in the stress-drawing clearly is set together by the bare steel part (green), the contribution of concrete between the cracks (orange) and the shrinkage influence (brown). The interaction table is combined with the possibility for a linear interpolation in view of the neutral axis N.A._c, N_{ic} and M_c' . Clicking on „sec.prop.“ switches to the window of the ideal plastic section properties calculated according to the formulae shown in Fig.4-41.

To make the coherence between neutral axis, normal force and bending moment accessible to the user and therefore to get him the feeling where strengthening of the section would be economic or not special tools have been provided: Clicking on one line within the N_{ic} - M_c' -table will produce the corresponding N.A. within the section image, the strain and stress distribution and a crosshair accentuating the actual location within the interaction curve. This graphical illustration will also be started after a linear interpolation or when following the interaction curve with the computer-mouse while the left mouse-button is pressed.



elements							
Concrete	x [mm]	y [mm]	w [mm]	h [mm]	fck [N/mm ²]	fctm [N/mm ²]	
1	0	215	300	80	30	3	
11	300	215	300	80	30	3	
Reinforcem.	y [mm]	no.	d [mm]	fsk [N/mm ²]	Es [kN/mm ²]	fu [N/mm ²]	eps u [o/oo]
1	265	8	10	550	200	620	100

sec.prop.			
Area concrete	=	480.00	[cm ²]
Area reinforcement	=	628.32	[mm ²]
plastic neutral axis	=	265.53	[mm]
plast. bending moment	=	4.59	[kNm]
plast. tension force	=	300.50	[kN]
plast. compression force	=	1116.50	[kN]

Fig.4-42 Window for the presentation of concrete results (epc.frm)

Using the button „Print results“ will send the following four sheets to your printer: The first sheet (see page 197) contains a drawing of the actual concrete section and the analysed range of strain distributions. Unfortunately when taking strain hardening into consideration the decisive strain limits become relatively large (depending on the given ultimate strain values ϵ_u) and therefore the strain diagram with decreasing κ more and more deforms from a parallelogram to a rectangle losing optical clearness. At the bottom of this first sheet the N_{ic} - M_c' diagram will be displayed. The thick grey line represents the elastic range, the thick black one the non-elastic area, the range of crushing concrete is drawn with a thin grey line and those areas beyond ϵ_u are indicated with a very thin grey line. At the second sheet the interaction table will be given (see page 198). Only if κ is infinite the ideal-plastic cross-sectional properties are printed on sheet no.3 (page 199) and finally on sheet no.4 you will find the full input data of the actual section.

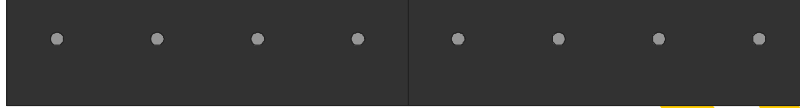
To make the results also accessible to other programs they can be saved as a sequential data file with the button „Save results“. The default file name is built up by that of the section (*.pro) and the extension „epc“ (elasto-plastic concrete). The output file of the example calculation can be found on page 200.

DEMO - MAIN
FULL BOOK AVAILABLE AT Ernst & Sohn, Berlin

Elasto-plastic results - Concrete

file = c:\ge\dynamic\diss\cobejo\files\DISS.PRO

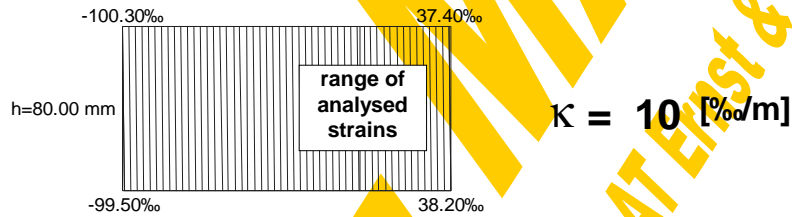
hat-shaped beam



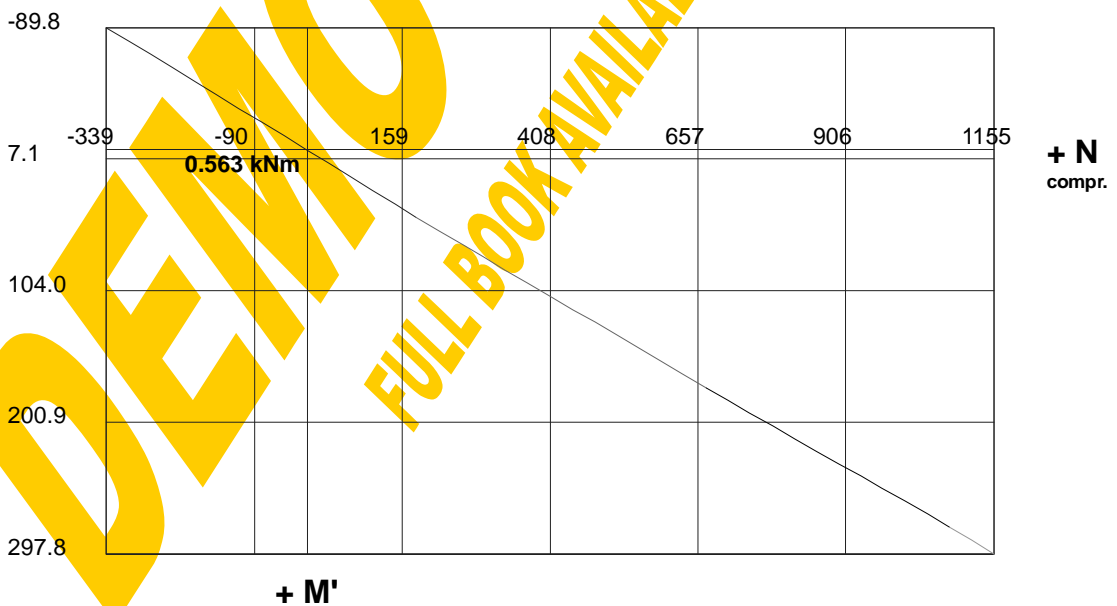
datum line

Width = 600 Height = 80 [mm]

Partial safety factor concrete =	1.5
Stress factor concrete =	.85
Partial safety factor reinforcem. =	1.15
Tension stiffening effect: f_{cteff}/f_{ctm} =	1
Tension stiffening effect: β (short) =	.4



N-M' Interaction [kN,kNm]



N-M' Interaction - Concrete

file = c:\geldynamic\diss\cobejo\files\DISS.PRO

hat-shaped beam $\kappa = 10 \quad [\% / m]$

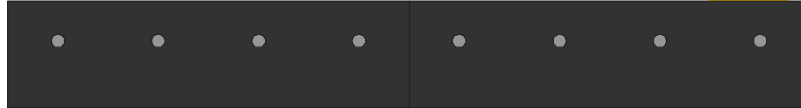
y [mm]	N [kN]	M' [kNm]	e0[o/oo]	
4035.24	-338.746	-89.768	40.352	ne
592.68	-301.937	-80.013	5.927	ne
429.63	-264.476	-70.086	4.296	ne
399.37	-226.454	-60.010	3.994	ne
337.17	-188.802	-50.032	3.372	ne
288.43	-153.242	-40.564	2.884	ne
278.97	-115.112	-30.265	2.790	ne
275.82	-78.675	-20.521	2.758	ne
272.25	-39.353	-9.990	2.722	ne
268.47	0.000	0.563	2.685	ne
264.89	34.372	9.792	2.649	ne
255.23	72.032	20.089	2.552	ne
247.24	108.467	29.957	2.472	ne
239.68	147.427	40.405	2.397	ne
233.38	183.196	49.904	2.334	ne
227.07	221.967	60.104	2.271	el
221.61	257.997	69.496	2.216	el
216.15	296.282	79.388	2.161	el
211.10	333.050	88.829	2.111	el
206.06	369.868	98.281	2.061	el
201.02	406.686	107.733	2.010	el
195.56	446.572	117.972	1.956	el
190.51	483.390	127.424	1.905	el
185.47	520.208	136.876	1.855	el
180.43	557.026	146.328	1.804	el
175.38	593.844	155.780	1.754	el
170.34	630.662	165.232	1.703	el
164.88	670.548	175.472	1.649	el
159.84	707.365	184.923	1.598	ne
154.79	743.160	194.075	1.548	ne
148.91	782.492	204.049	1.489	ne
143.03	819.209	213.281	1.430	ne
136.72	855.647	222.366	1.367	ne
129.58	893.314	231.676	1.296	ne
121.59	930.848	240.877	1.216	ne
112.77	966.730	249.609	1.128	ne
101.00	1005.419	258.993	1.010	ne
83.35	1043.839	268.478	0.834	ne
54.78	1080.174	278.086	0.548	ne
-267.96	1117.652	288.018	-2.680	cr
-9735.00	1154.746	297.848	-97.350	cr

el=elastic ne=non-elastic cr=crushing of concrete **=epsilon > epsilon ultimate

Institute of Steel and Timber Constructions - University of Innsbruck Dipl.-Ing. Gerald Huber

Cross-sectional properties - Concrete

file = c:\ge\dynamic\diss\cobejo\files\DISS.PRO

hat-shaped beam

datum line

Width = 600 Height = 80 [mm]

Partial safety factor concrete =	1.50
Stress factor concrete =	0.85
Partial safety factor reinforcement =	1.15
Area concrete =	480.00 [cm ²]
Area reinforcement =	628.32 [mm ²]
PNA from steel bottom =	265.53 [mm]
Plastic bend.moment =	4.59 [kNm]
Plastic tension force =	300.50 [kN]
Plastic compression force =	1116.50 [kN]

Elasto-plastic results - shear-connected concrete section

Section: "hat-shaped beam"

kapa [o/oo / m]=,10

Savety factor concrete:, 1.5

Stress factor concrete:, 0.85

Savety factor reinf.:, 1.15

Tension stiffening effect : fcteff/fctm =, 1

Tension stiffening effect: beta (short) =, 0.4

Table of concrete elements (No,x,y,w,h,fck,fctm) [N,mm]

1	0	215	300	80	30	3
11	300	215	300	80	30	3

Table of reforcem. elements (No,y,no,d,fy,E/1000,fu,eu,N(shrink.)) [N,mm]

1	265	8	10	550	200	620	0.1	0
---	-----	---	----	-----	-----	-----	-----	---

N-M' Interaction Table (y[mm],N[kN],M'[kNm],e0[o/oo])

4035.24	-338.746	-89.768	40.352	non-elastic
592.68	-301.937	-80.013	5.927	non-elastic
429.63	-264.476	-70.086	4.296	non-elastic
399.37	-226.454	-60.010	3.994	non-elastic
337.17	-188.802	-50.032	3.372	non-elastic
288.43	-153.242	-40.564	2.884	non-elastic
278.97	-115.112	-30.265	2.790	non-elastic
275.82	-78.675	-20.521	2.758	non-elastic
272.25	-39.353	-9.990	2.723	non-elastic
268.47	0.000	0.563	2.685	non-elastic
264.89	34.372	9.792	2.649	non-elastic
255.23	72.032	20.089	2.552	non-elastic
247.24	108.467	29.957	2.472	non-elastic
239.68	147.427	40.405	2.397	non-elastic
233.38	183.196	49.904	2.334	non-elastic
227.07	221.967	60.104	2.271	elastic
221.61	257.997	69.496	2.216	elastic
216.15	296.282	79.388	2.162	elastic
211.10	333.050	88.829	2.111	elastic
206.06	369.868	98.281	2.061	elastic
201.02	406.686	107.733	2.010	elastic
195.56	446.572	117.972	1.956	elastic
190.51	483.390	127.424	1.905	elastic
185.47	520.208	136.876	1.855	elastic
180.43	557.026	146.328	1.804	elastic
175.38	593.844	155.780	1.754	elastic
170.34	630.662	165.232	1.703	elastic
164.88	670.548	175.472	1.649	elastic
159.84	707.365	184.923	1.598	non-elastic
154.79	743.160	194.075	1.548	non-elastic
148.91	782.492	204.049	1.489	non-elastic
143.03	819.209	213.281	1.430	non-elastic
136.72	855.647	222.366	1.367	non-elastic
129.58	893.314	231.677	1.296	non-elastic
121.59	930.848	240.877	1.216	non-elastic
112.77	966.730	249.609	1.128	non-elastic
101.00	1005.419	258.993	1.010	non-elastic
83.35	1043.839	268.478	0.834	non-elastic
54.78	1080.173	278.086	0.548	non-elastic
-267.96	1117.651	288.018	-2.680	crush.of concr.
-9735.00	1154.746	297.848	-97.350	crush.of concr.

Section properties:

Area concrete [cm2]:, 480

Area reforcem. [mm2]:, 628.3185

end

4.2.5 Composite section

4.2.5.1 Section input

The composite cross section has to be built up by the steel section and the concrete section part using the corresponding input windows. Before starting composite calculations it is advisable to save the whole input data using the „File management window“ (start-up window). From there the button „COMPOSITE“ gives a link to the composite calculation window (Fig.4-43).

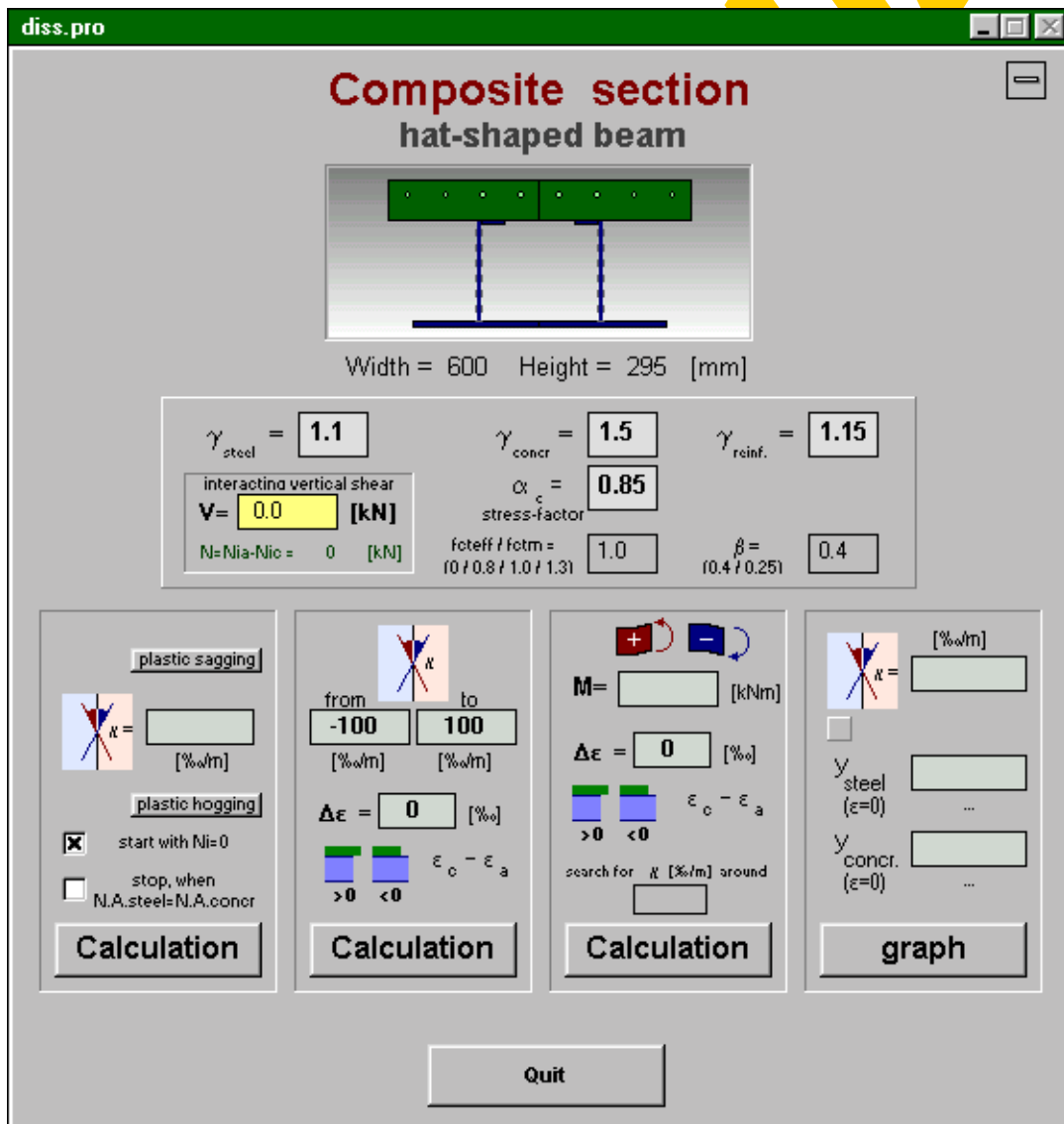


Fig.4-43 Composite calculation window (prcom.frm)

The name of the actual section and a small sketch of it are given together with the main dimensions. Input boxes have been provided to modify the safety-factors γ_a , γ_c , γ_r , the concrete stress factor α_c , the effective tension factor $f_{ct,eff}/f_{ctm}$ and the β -value for the tension stiffening effect. Note: if $f_{ct,eff}/f_{ctm}=0$ no tension stiffening will be taken into consideration, what has been very useful to study the influence of concrete between the

cracks. Further the interacting vertical shear force can be defined, which fully will be assigned to the steel webs (concrete does not contribute to vertical shear). Before any calculation it will be checked automatically if the given shear value does not exceed the design shear resistance of all steel web elements together. Finally also the normal force of the whole composite cross section can be chosen, however for conventional beam calculations N has to be set equal to zero.

4.2.5.2 Theoretical background

The whole program is based on the clear separation of the composite cross section into its two basic section parts: steel and reinforced concrete. So with reference to the principle of equivalence the resulting inner forces and moments of the entire composite section can be set together by those of the section parts as shown in Fig.4-44. As the normal forces and bending moments of the steel and concrete section parts have already been related to a common datum line ($y=0$ =steel bottom) they can simply be added without any further movement.

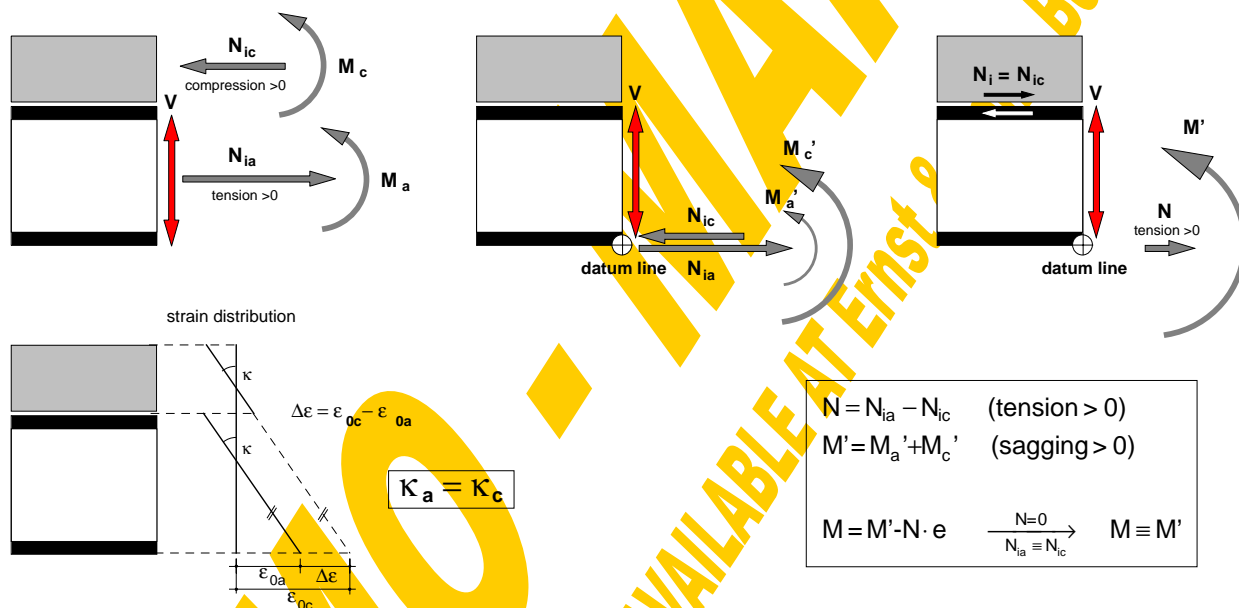
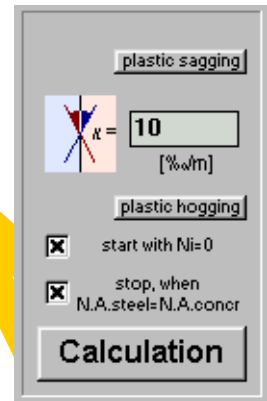


Fig.4-44 Inner forces and moments of section parts and entire composite section

Recall that the vertical shear force will be fully assigned to the web elements of the steel section. There it reduces their resistance with respect to additional normal stresses due to normal forces and bending moments.

Based on this theoretical background the following iterations can be carried out using the subroutines already described in detail in the previous chapters:

- N_i - M -relation for a defined curvature
- N_i - M - κ -relation for a defined strain jump at the steel-concrete interface
- Given M and strain jump at the interface (cross sectional design)
- Forces and moments to a given strain distribution

4.2.5.3 N_i - M -relation for a defined curvature (NMcomp)

Analogous to the iteration of the N_{ia} - M_a' - or N_{ic} - M_c' -curves the relation between the (internal) horizontal shear force in the dowel interface ($N_i=N_{ic}$) and the entire bending moment of the composite section (M') can be derived. Assuming the standard case (entire normal force $N=0$) the condition $N_{ia}\equiv N_{ic}$ must be fulfilled along the whole curve and $M'\equiv M$. As $M'=M_a'+M_c'$ ($N_{ia}\equiv N_{ic}$) the N_i - M -curve can simply be obtained by adding the N_{ia} - M_a' - and the N_{ic} - M_c' -curves.

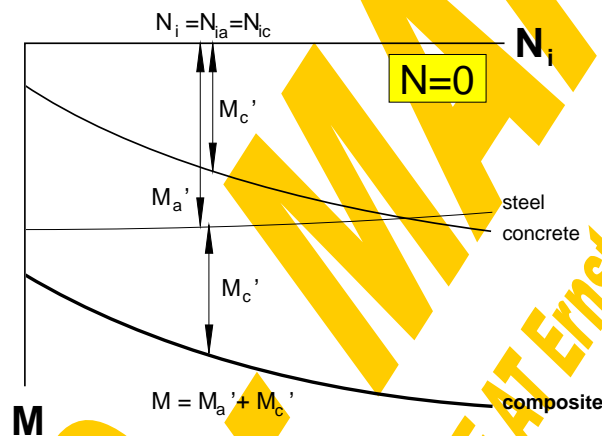


Fig.4-45 Determination of the relationship between N_i and M

An input box has been arranged to prescribe a curvature κ . To ensure a result $N_i \neq 0$ the curvature κ must be within the limits -0.005 ‰/m and $+0.005$ ‰/m. Again the buttons „plastic sagging“ and „plastic hogging“ allow for a quasi-plastic calculation with $\kappa = \pm 10^5$ ‰/m and temporarily modified fully plastic stress-strain diagrams. The progress of the iteration is shown by a flood box and a comment line. Any calculation can be interrupted by pressing the „STOP“-button.

The determination of this N_i - M relationship is carried out within the global procedure „**NMcomp**“ which is subdivided into the following six calculation steps:

- 1.) The procedure „steellimit“ is used to determine the **strain and force limits** of the **steel** section part for the given curvature κ .
- 2.) The procedure „conclimit“ is used to determine the **strain and force limits** of the **concrete** section part for the given curvature κ .
- 3.) In the third step the **starting strains** e_{0a} and e_{0c} of the section parts have to be calculated. The status of the option button „start with $N_i=0$ “ (active or passive) determines the decisive starting point of the interaction curve in view of N_i .

3.1.) Conventionally („start with $N_i=0$ “ is active) the interaction curve starts with $N_i=0$ (no horizontal shear force in dowel layer). Making use of the procedure „itNsteel“ gives the corresponding steel strain e_{0a} for $N_{ia}=N$ (so normally $N_{ia}=0$). The concrete strain e_{0c} for $N_{ic}=0$ will be iterated using the procedure „itNconcr“.

3.2.) To analyse the full range of possible shear forces between the steel and concrete section parts also that part of the curve „before“ reaching $N_i=0$ could be of interest. So if the option button „start with $N_i=0$ “ is passive an additional calculation has to be carried out to evaluate the state of minimum shear connection: According to the definition that increasing interaction (at least at the beginning) means approach of the neutral axes of the section parts the state „before“ reaching $N_i=0$ clearly can be defined where the neutral axes are even farther than at the state $N_i=0$. So based on the strains e_{0a} and e_{0c} a decisive starting value $N_{i,start}$ can be derived as shown in Fig.4-46 using the limiting normal forces of the section parts Nu_{1a} , Nu_{2a} , Nu_{1c} and Nu_{2c} (according to points 1.) and 2.).

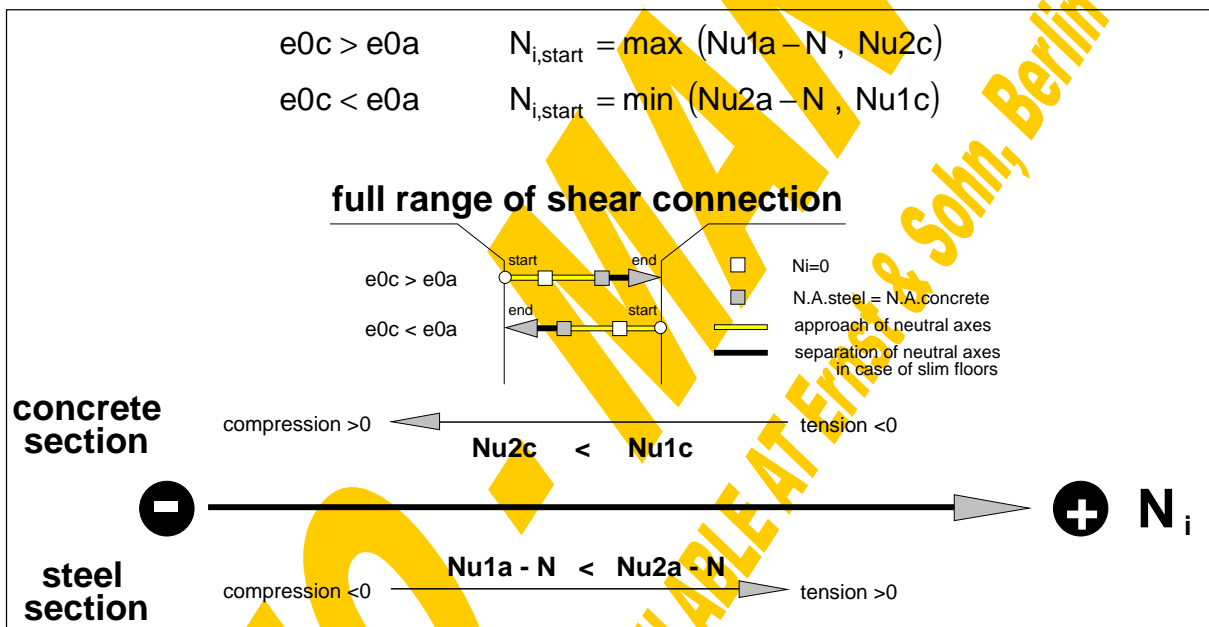


Fig.4-46 Derivation of the full range of shear connection

Based on that the decisive starting strain values of the steel and concrete section can be found: e_{0a} results from the procedure „itNsteel“ for $N_{ia}=N_{i,start}+N$ and e_{0c} results from the procedure „itNconcr“ for $N_{ic}=N_{i,start}$.

4.) The next step concerns the **end strain values** of the section parts (e_{0ga} , e_{0gc}). Again it can be decided by an option button (active or passive status of “Stop, when N.A.steel=N.A.concr”) whether the interaction curve should stop, where the neutral axes of steel and concrete are congruent, or if the full possible range of inner shear forces should be exhausted.

4.1.) For that case that the full possible range should be analysed (option button passive) the weaker section part determines the upper limit of the internal shear forces $N_{i,end}$. The following formulae can directly be derived from Fig.4-46, where it can be seen that the neutral axes of steel and concrete are approaching each other between the start of interaction and the congruence of the neutral axes and that they

are again separating beyond their congruence until the end of interaction is reached due to the limiting normal force of the weaker section part.

$$e_{0c} > e_{0a} \quad N_{i,end} = \min (Nu_{2a} - N, Nu_{1c})$$

$$e_{0c} < e_{0a} \quad N_{i,end} = \max (Nu_{1a} - N, Nu_{2c})$$

The decisive end strain of the steel section e_{0ga} then results from the procedure „itNsteel“ for $N_{ia}=N_{i,end}+N$ and that of concrete e_{0gc} results from the procedure „itNconcr“ for $N_{ic}=N_{i,end}$.

4.2.) If the option button „stop when N.A.steel=N.A.concr“ is active it will be checked first, if congruence of the neutral axes really would occur before reaching $N_{i,end}$ according to point 4.1.). So this stop-criterion only will become decisive if the following conditions are fulfilled:

$$(e_{0a} < e_{0c} \quad \text{and} \quad e_{0ga} > e_{0gc}) \quad \text{or}$$

$$(e_{0a} > e_{0c} \quad \text{and} \quad e_{0ga} < e_{0gc})$$

Generally this will not occur for cross sections where the concrete plate completely is located above the steel section in combination with a relatively large curvature κ . However for slim-floors (where steel and concrete elements are sharing the same y-range) this criterion in any case will have to be taken into consideration.

The iteration for that decisive N_i , where the neutral axes of the steel and concrete section are congruent, then will be carried out according to the bisection method between the limits $N_{i,start}$ (point 3.) and $N_{i,end}$ (point 4.1.). At each iteration step of N_i the corresponding normal force in the steel section can be calculated according to $N_{ia}=N_i+N$ and that of the concrete section $N_{ic}=N_i$. Based on that the appropriate strains e_{p01a} and e_{p01c} can be determined with the procedures „itNsteel“ and „itNconcr“. The accuracy limits have been defined pursuant to a sensitivity study, as the iteration loops and therefore their deviations here are interconnected. The iteration will be stopped if the difference between the steel and concrete neutral axes falls short of an accuracy limit or if the iteration steps become smaller than a given tolerance. For the summary of prescribed tolerances reference is made to the end of chapter 4.2.

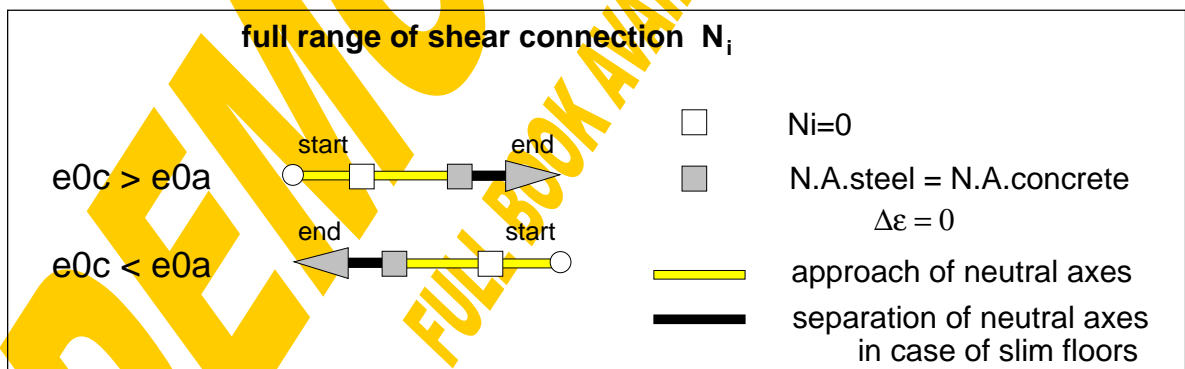


Fig.4-47 Full range of shear connection

In Fig.4-47 it is repeated that the full range of shear connection N_i indeed may exceed the limits of $N_i=0$ and equality of neutral axes. Also beyond these limits the equilibrium condition $N=N_{ia}-N_{ic}$ is fulfilled for the composite cross section. Therefore

these parts of the interaction curve will not to be excluded in the global analysis. Their mechanical meaning and occurrence will have to be studied there. The point of congruent neutral axes clearly separates the areas of approaching and separating tendency of the two neutral axes (steel and concrete). Therefore at this point the strain jump $\Delta\varepsilon$ in the shear interface changes its sign. As $\Delta\varepsilon$ gives the slope of the slip curve that directly is linked to a maximum or minimum of slip (see Fig.4-48).

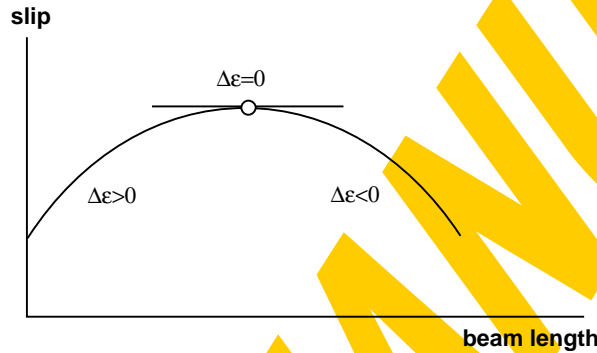
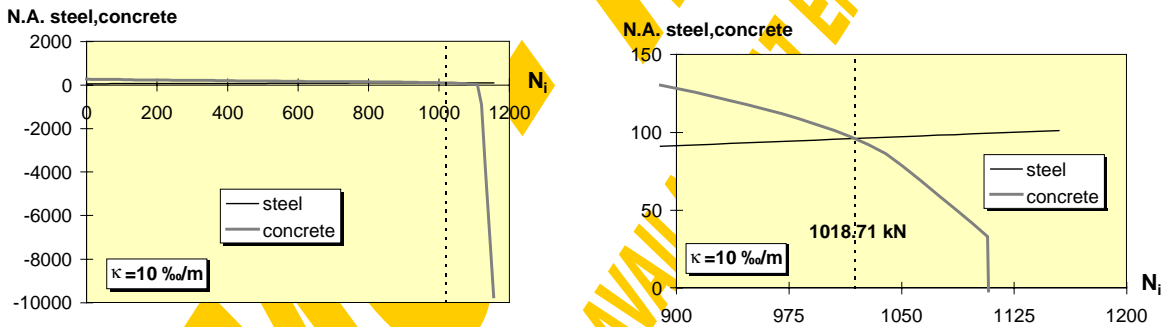


Fig.4-48 Slip-curve

Fig.4-49 shows the described iteration to find that inner horizontal shear force N_i , where the neutral axes of the steel and concrete section parts are equal.



Sensitivity study for necessary provisional iteration tolerances

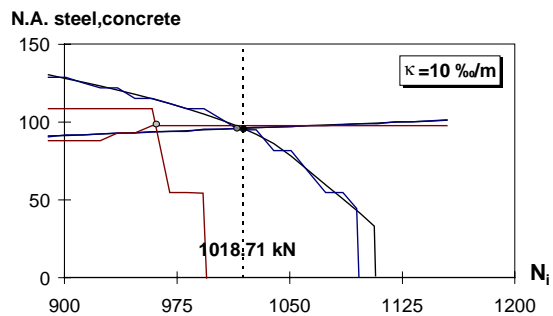


Fig.4-49 Iteration of congruent neutral axes for the example section

- 5.) Knowing the limiting inner shear forces $N_{i,start}$ and $N_{i,end}$ this range is subdivided into 40 parts. Based on the procedure „itNsteel“ the corresponding bending moment M_a' and the location of the neutral axis $N.A._a$ are iterated for each $N_{ia}=N_i+N$.
- 6.) For the same N_i -values ($N_{ic}=N_i=N_{ia}-N$) also the corresponding bending moment M_c' and $N.A._c$ are determined with the routine „itNconcr“. According to Fig.4-45 the bending moment of the entire composite section then can be set together by the moment of the steel and that of the concrete section ($M'=M_a'+M_c'$) for the same inner shear force N_i ($N=0 \Rightarrow M \equiv M'$). The cross section conditions are treated in the following hierarchic order: elastic, non-elastic, crushing of concrete, beyond ϵ_u . So if the stresses in both the steel and the concrete section are still within the elastic range for that interaction point „elastic“ will be given. If „non-elastic“ has been registered at least for one point the section will be treated as such kind and so on. Finally the error of the inner shear force after termination of the iteration will be reported: $dev = |N_{ia} - N - N_{ic}|$

Fig.4-50 shows, how the M - N_i -curve of the entire composite example section is set together adding up steel and concrete as described in Fig.4-45. It can clearly be seen that the range of possible inner shear forces is dominated by the force limits of the concrete plate being the weaker section part both in tension and compression. The isolated decisive part of shear interaction for the example section can be seen in Fig.4-51 for the given curvature $\kappa=10\text{‰}/\text{m}$.

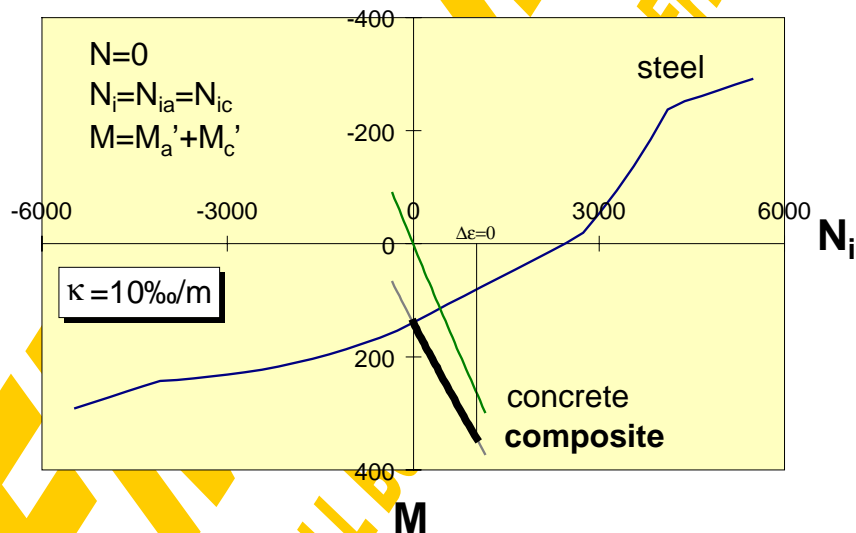


Fig.4-50 N_i - M -interaction of example section (full range)

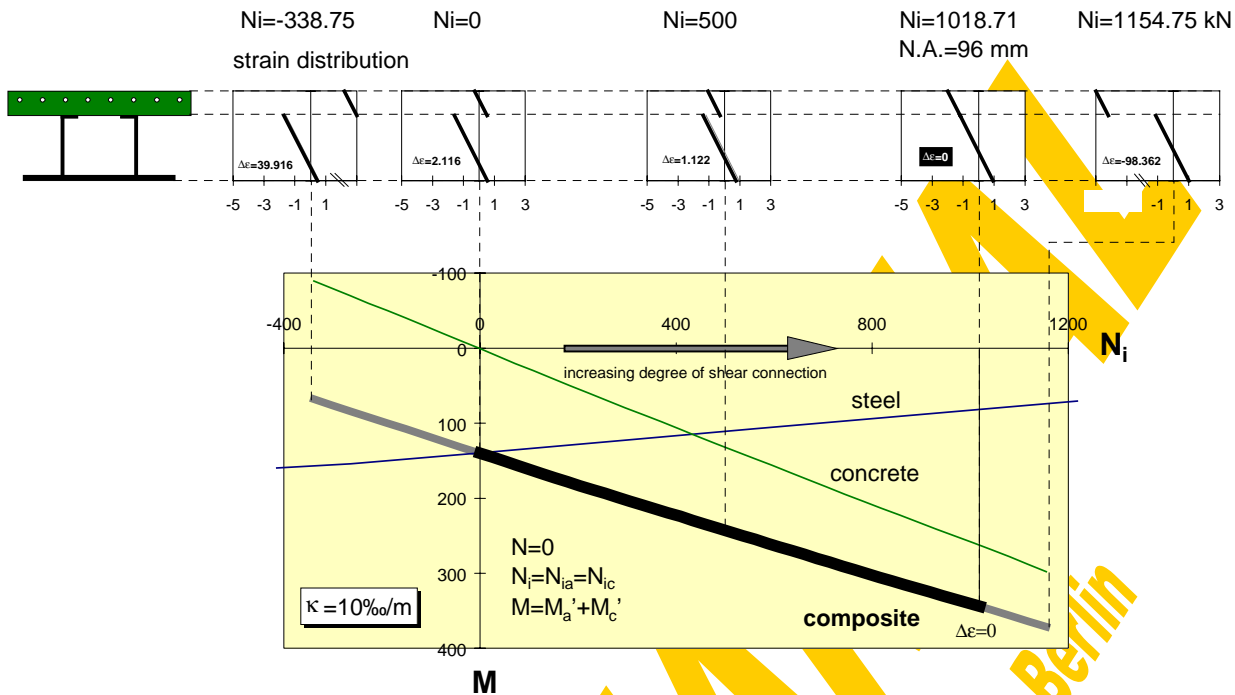


Fig.4-51 Ni-M-interaction of example section (detail)

Finally also the elastic and fully-plastic composite cross sectional properties are determined with the procedure „*qswertecomp*“ according to the formulae given in Fig.4-52:

Attention has to be paid to the following fact: The formulae given in Fig.4-52 have been derived assuming that the concrete in tension (until $f_{ct,eff}$ is reached) behaves with the same elastic modulus as in compression. As in all iterations concrete stresses in tension have explicitly been neglected and have fully been assigned to the reinforcement (tension stiffening) the iteration results within the elastic range might differ slightly from those theoretical ones according to the formulae in Fig.4-52.

In the following the calculation results are described for the example section using $\kappa = 10 \text{ ‰/m}$ and $V = 0 \text{ kN}$. After termination of the iteration the composite calculation window is closed and the window for the presentation of the gained results is shown (Fig.4-53).

reference module $E_{ref} = E_{\text{first steel element}}$

full fictitious area $A_f = \sum_{\text{steel, concrete, reinf.}} A_i \cdot \frac{E_i}{E_{ref}}$

ideal plastic normal force $N_{pl,tension} = \sum_{\text{steel}} A_i \cdot \frac{f_{yv}}{\gamma_a} + \sum_{\text{reinf.}} A_i \cdot \frac{f_{sk}}{\gamma_r}$

ideal plastic normal force $N_{pl,compression} = \sum_{\text{steel}} A_i \cdot \frac{f_{yv}}{\gamma_a} + \sum_{\text{reinf.}} A_i \cdot \frac{f_{sk}}{\gamma_r} + \sum_{\text{concrete}} A_i \cdot \frac{\alpha_c \cdot f_{ck}}{\gamma_c}$

plastic vertical shear force $V_{pl} = \sum_{\text{steel web elements}} A_i \cdot \frac{f_{yk,i}}{\gamma_a} \cdot \frac{1}{\sqrt{3}}$

elastic neutral axis $ENA = \frac{\sum_{\text{steel,concr,reinf.}} A_i \cdot y_{s,i} \cdot \frac{E_i}{E_{ref}}}{A_f}$

fictitious inertia $I_f = \sum_{\text{steel,concr.}} \frac{b_i \cdot h_i^3}{12} \cdot \frac{E_i}{E_{ref}} + \sum_{\text{steel,concr,reinf.}} A_i \cdot (y_{s,i} - ENA)^2 \cdot \frac{E_i}{E_{ref}}$

upper fict. res.moment $W_o = \frac{I_f}{ENA - y_{max}}$

lower fict. res.moment $W_u = \frac{I_f}{ENA - y_{min}}$

elastic curvature limit $\kappa_{el}(N=0, V) = \min \left(\begin{array}{l} \overbrace{\frac{f_{yv,i}}{\gamma_a \cdot E_i \cdot |y_i - ENA|}}^{\text{steel}} , \overbrace{\frac{1.35}{1000 \cdot |y_i - ENA|}}^{\text{concr.compr.}} \\ \overbrace{\frac{\gamma_c \cdot 1.35 \cdot f_{ct,eff,i}}{\alpha_c \cdot 1000 \cdot |y_i - ENA| \cdot f_{ck,i}}}_{\text{concr.tension}} , \overbrace{\frac{f_{sk,i}}{\gamma_r \cdot E_i \cdot |y_i - ENA|}}^{\text{reinforcement}} \end{array} \right)$

elastic limit of bending $M_{el}(N=0, V) = \kappa_{el} \cdot E_{ref} \cdot I_f$

Fig.4-52 Formulae for the calculation of the composite sectional properties (qswertcomp)

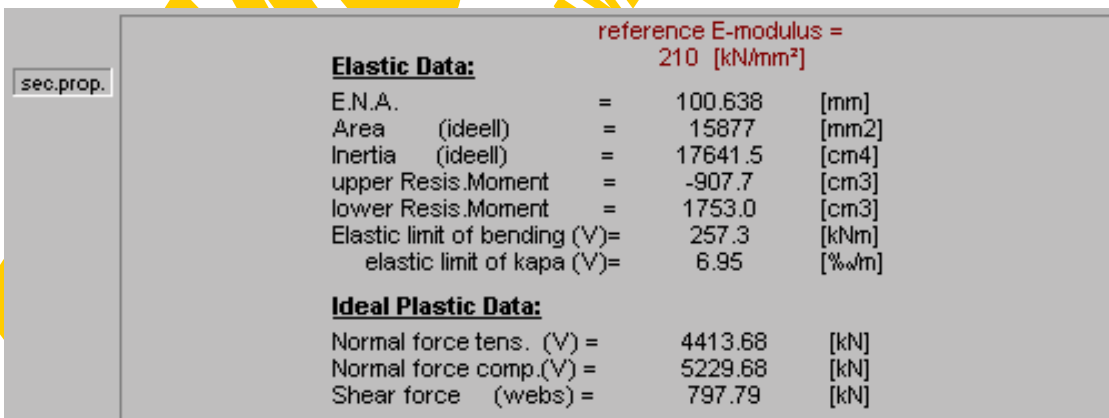
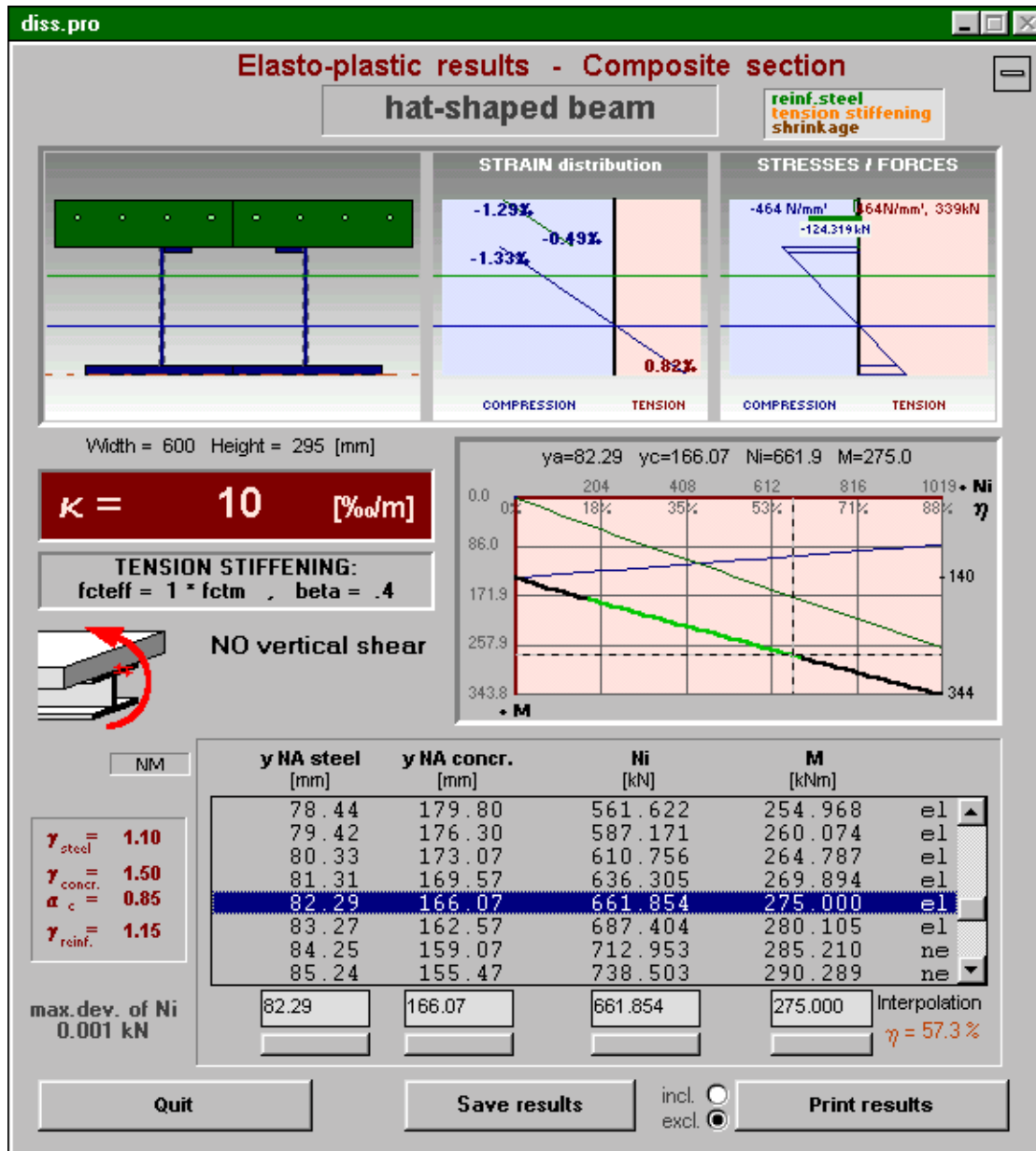


Fig.4-53 Window for the presentation of composite results (ep.frm)

It comprises the input data, an image of the composite section, the actual strains, stresses and forces (bare reinforcement in green, concrete action between the cracks in orange and shrinkage influence in brown) and a table and a graph of the calculated N_i - M' -interaction. There the final composite interaction curve is drawn with a thick line, the contribution of the steel section part is indicated by a thin blue and that of the reinforced concrete part by a thin green line. Those parts of the composite interaction curve drawn in light green represent the elastic range, the non-elastic parts are drawn in black, crushing of concrete is indicated with a red colour and those parts, where even ϵ_u is exceeded in case of a too small reinforcement area, are drawn in white. Further for the horizontal N_i -axis also the corresponding η -values are given, representing the degree of shear connection. η has been defined as the ratio between the actual inner shear force and the maximum possible shear force $N_{i,end}$ related to the weaker section part and the given curvature (acc. to chapter 4.2.5.3_{4.1}):

$$\eta = \frac{N_i}{N_{i,end}(\kappa)}$$

So for ideal plastic stress-strain diagrams of each element $N_{i,end}(\kappa)$ is equal to the ideal plastic normal force of the weaker section part. Finally also the minimum and maximum bending moments are given in the diagram. The interaction table is combined with the possibility of a linear interpolation in view of the neutral axes $N.A._a$, $N.A._c$, N_i and M' . Clicking on „sec.prop.“ switches to the window including the elastic and ideal (perfectly) plastic sectional properties calculated according to Fig.4-52.

To make the coherence between neutral axes, internal shear force and bending moment accessible to the user and therefore to get him the feeling where strengthening of the section parts would be economic or not special tools have been provided: Clicking on one row of the N_i - M' -table will produce the corresponding $N.A._a$ and $N.A._c$ within the section image, the strain, stress and force distribution and a reticule accentuating the actual location within the interaction curve. This graphical illustration will also be started after a linear interpolation or when following the interaction curve with the computer-mouse while the left mouse-button is pressed.

Using the button „Print results“ will send the following four sheets to your printer: The first sheet contains a drawing of the actual composite section and the analysed range of strain distributions. At the bottom of this first sheet the N_i - M' diagram will be displayed. The actual condition of the cross section in view of elasticity is indicated with different line styles. At the second sheet the interaction table will be given. The elastic and ideal-plastic cross-sectional properties are printed on sheet no.3 and finally on sheet no.4 you will find the full input data of the actual section.

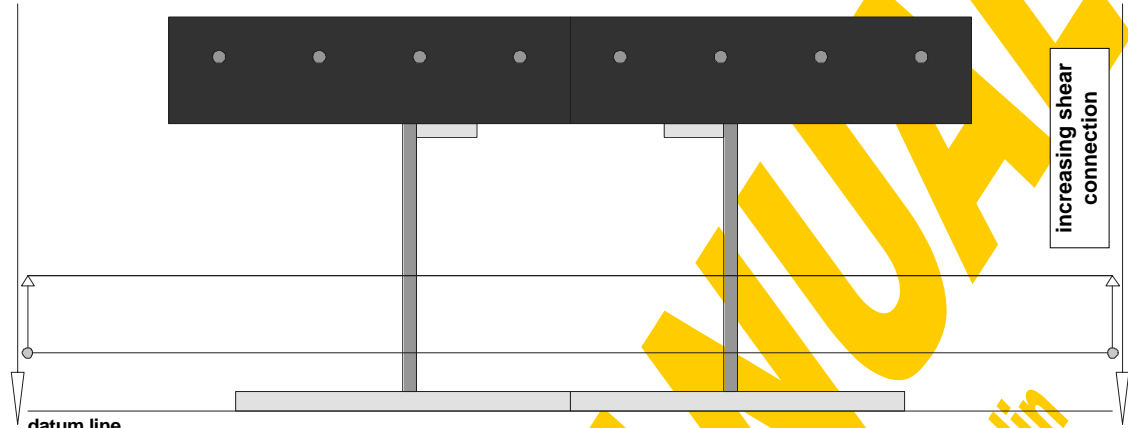
To make the results also accessible to other programs they can be saved as a sequential data file with the button „Save results“. The default file name is built up by that of the section (*.pro) and the extension „ep1“ (elasto-plastic composite - first calculation block).

On the pages 212,213 and 214 you can find the print-outs of the example section for the full interaction range. The corresponding output file can be seen on page 215. The pages 216,217 and 218 give the results for the limited interaction range between $N_i=0$ and the congruence of the neutral axes representing a detail of the full curve.

Elasto-plastic results - COMPOSITE

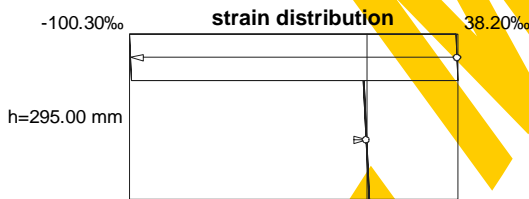
file = c:\geldynamic\diss\cobejo\files\DISS.PRO

hat-shaped beam



Width = 600 Height = 295 [mm]

- Partial safety factor steel = 1.1
- Partial safety factor concrete = 1.5
- Stress factor concrete = .85
- Partial safety factor reinforcem. = 1.15
- Tension stiffening effect: f_{cteff}/f_{ctm} = 1
- Tension stiffening effect: beta (short) = .4

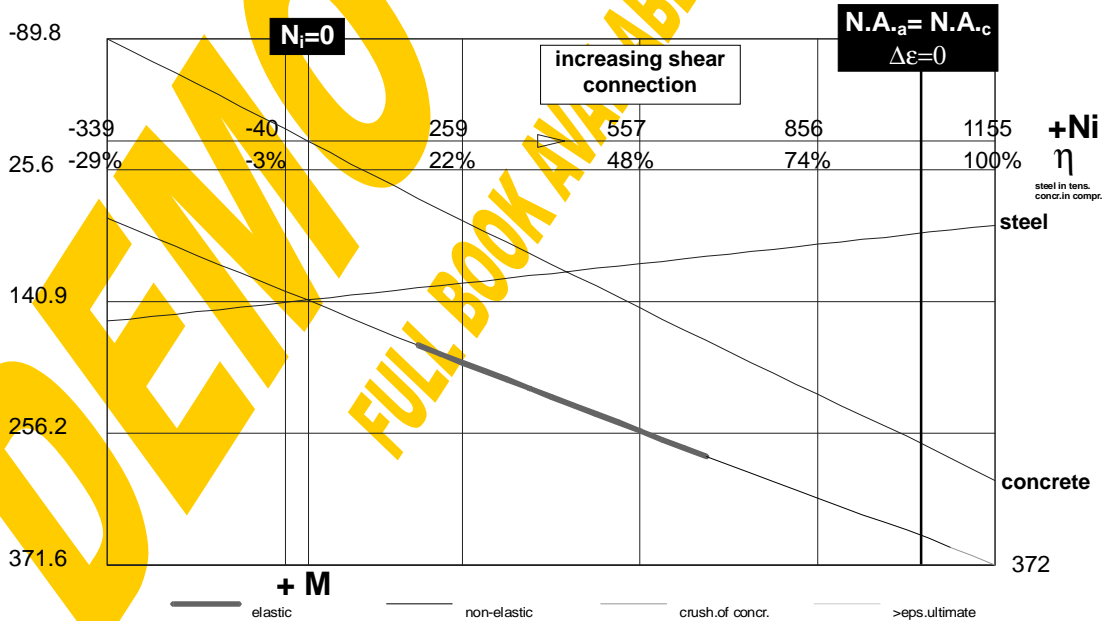


$K = 10$ [‰/m]

$N = 0.00$ [kN]

$V = 0.00$ [kN]

Ni-M Interaction [kN,kNm] sagg.mom.



Ni-M Interaction - COMPOSITE

file = c:\geldynamic\diss\cobejo\files\DISS.PRO

hat-shaped beam

$$\kappa = 10 \quad [‰ / m]$$

max.deviation of Ni= 0.001 kN

NO normal force

NO vertical shear force

ya [mm]	yc [mm]	Ni [kN]	M [kNm]	e0a [‰]	e0c [‰]	
43.66	4035.24	-338.746	68.062	0.437	40.352	ne
45.16	580.70	-301.809	76.076	0.452	5.807	ne
46.67	429.32	-264.096	84.173	0.467	4.293	ne
48.18	398.90	-225.858	92.298	0.482	3.989	ne
49.61	337.71	-189.046	100.043	0.496	3.377	ne
51.05	287.90	-151.795	107.863	0.510	2.879	ne
52.48	278.92	-114.454	115.823	0.525	2.789	ne
53.91	275.68	-77.113	123.686	0.539	2.757	ne
55.35	272.29	-39.771	131.562	0.553	2.723	ne
56.78	268.71	-2.430	139.452	0.568	2.687	ne
58.22	264.74	34.912	147.358	0.582	2.647	ne
59.65	255.18	72.253	155.442	0.596	2.552	ne
61.08	247.01	109.595	163.430	0.611	2.470	ne
62.52	239.77	146.936	171.319	0.625	2.398	ne
63.95	233.19	184.277	179.112	0.640	2.332	ne
65.39	227.13	221.619	186.811	0.654	2.271	el
66.82	221.47	258.960	194.420	0.668	2.215	el
68.25	216.14	296.302	201.943	0.683	2.161	el
69.69	211.02	333.643	209.408	0.697	2.110	el
71.12	205.91	370.984	216.870	0.711	2.059	el
72.56	200.79	408.326	224.333	0.726	2.008	el
73.99	195.68	445.667	231.795	0.740	1.957	el
75.42	190.56	483.009	239.258	0.754	1.906	el
76.86	185.45	520.350	246.720	0.769	1.855	el
78.29	180.34	557.691	254.183	0.783	1.803	el
79.73	175.22	595.033	261.645	0.797	1.752	el
81.16	170.11	632.374	269.108	0.812	1.701	el
82.59	164.99	669.716	276.571	0.826	1.650	el
84.03	159.88	707.057	284.033	0.840	1.599	ne
85.46	154.61	744.398	291.456	0.855	1.546	ne
86.90	149.03	781.740	298.800	0.869	1.490	ne
88.33	143.05	819.081	306.066	0.883	1.430	ne
89.76	136.58	856.423	313.252	0.898	1.366	ne
91.20	129.49	893.764	320.357	0.912	1.295	ne
92.63	121.54	931.105	327.385	0.926	1.215	ne
94.07	112.31	968.447	334.348	0.941	1.123	ne
95.50	100.87	1005.789	341.281	0.955	1.009	ne
96.93	83.82	1043.130	348.371	0.969	0.838	ne
98.37	54.54	1080.471	356.116	0.984	0.545	ne
99.80	-309.15	1117.813	363.888	0.998	-3.091	cr
101.22	-9735.00	1154.746	371.574	1.012	-97.350	cr

el=elastic ne=non-elastic cr=crushing of concrete **=epsilon > epsilon ultimate

Nia = Ni (Normal force in steel part; tension > 0)

Nic = Ni (Normal force in concrete part; compression > 0)

Ni (Horizontal shear force in dowel layer)

Ni max = 1154.746 [kN]**M max = 371.574 [kNm]**

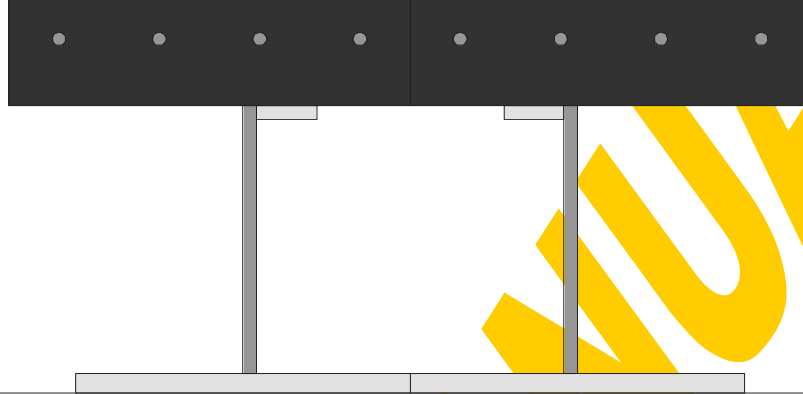
steel in tension, concrete in compression

Ni start = ultimate**Ni limit = ultimate**

Institute of Steel and Timber Constructions - University of Innsbruck Dipl.-Ing. Gerald Huber

Cross-sectional properties - COMPOSITE

file = c:\geldynamic\diss\cobejo\files\DISS.PRO

hat-shaped beam

datum line

Width = 600 Height = 295 [mm]

Elastic data:

Reference E-modulus =	210	[kN/mm ²]
Elastic neutral axis :	100.64	[mm]
Area =	15876.7	[mm ²]
Inertia =	17641.5	[cm ⁴]
upper Resis.Mom. =	-907.7	[cm ³]
lower Resis.Mom. =	1753.0	[cm ³]
Elastic limit of bend.=	257.3	[kNm]
Elastic limit of kapa =	6.95	[o/oo/m]

EI=37047 kNm²**Ideal Plastic data:**

Normal force tension =	4413.68	[kN]
Normal force compression =	5229.68	[kN]
Shear force (web-parts)=	797.79	[kN]
Buckling has to be analysed separately !		

Elasto-plastic results - composite section - kappa

Section: "hat-shaped beam"
 kappa [o/oo / m]=,10
 Savety factor steel: ,1.1
 Savety factor concrete: ,1.5
 Stress factor concrete: ,0.85
 Savety factor reinf.: ,1.15
 Tension stiffening effect : fcteff/fctm =,1
 Tension stiffening effect: beta (short) =,0.4
 SAGGING moment

NO normal force in composite section (Nia=Nic)

Table of steel elements (No,x,y,w,h,fyk,E/1000,fu,eu,flange=0/web=1) [N,mm]

1	50	0	250	15	355	210	510	0.1	0
2	175	15	10	200	380	210	450	0.1	1
3	185	205	45	10	380	210	450	0.1	0
11	300	0	250	15	355	210	510	0.1	0
12	415	15	10	200	380	210	450	0.1	1
13	370	205	45	10	380	210	450	0.1	0

Table of concrete elements (No,x,y,w,h,fck,fctm) [N,mm]

1	0	215	300	80	30	3
11	300	215	300	80	30	3

Table of reinforcem. elements (No,y,no,d,fy,E/1000,fu,eu,N(shrink.)) [N,mm]

1	265	8	10	550	200	620	0.1	0
---	-----	---	----	-----	-----	-----	-----	---

Ni-M Interaction Table (ya[mm],yc[mm],Ni[kN],M[kNm],e0a[o/oo],e0c[o/oo])

Ni start = ultimate		Ni limit = ultimate							
43.66	4035.24	-338.746	68.062	0.437	40.352	non-elastic			
45.16	580.70	-301.809	76.076	0.452	5.807	non-elastic			
46.67	429.32	-264.096	84.173	0.467	4.293	non-elastic			
48.18	398.90	-225.858	92.298	0.482	3.989	non-elastic			
49.61	337.71	-189.046	100.043	0.496	3.377	non-elastic			
51.05	287.90	-151.795	107.863	0.511	2.879	non-elastic			
52.48	278.92	-114.454	115.823	0.525	2.789	non-elastic			
53.91	275.68	-77.113	123.686	0.539	2.757	non-elastic			
55.35	272.29	-39.771	131.562	0.554	2.723	non-elastic			
56.78	268.71	-2.430	139.452	0.568	2.687	non-elastic			
58.22	264.74	34.912	147.358	0.582	2.647	non-elastic			
59.65	255.18	72.253	155.442	0.597	2.552	non-elastic			
61.08	247.01	109.595	163.430	0.611	2.470	non-elastic			
62.52	239.77	146.936	171.319	0.625	2.398	non-elastic			
63.95	233.19	184.277	179.112	0.640	2.332	non-elastic			
65.39	227.13	221.619	186.811	0.654	2.271	elastic			
66.82	221.47	258.960	194.420	0.668	2.215	elastic			
68.25	216.14	296.302	201.943	0.683	2.161	elastic			
69.69	211.02	333.643	209.408	0.697	2.110	elastic			
71.12	205.91	370.984	216.870	0.711	2.059	elastic			
72.56	200.79	408.326	224.333	0.726	2.008	elastic			
73.99	195.68	445.667	231.795	0.740	1.957	elastic			
75.42	190.56	483.009	239.258	0.754	1.906	elastic			
76.86	185.45	520.350	246.720	0.769	1.855	elastic			
78.29	180.34	557.691	254.183	0.783	1.803	elastic			
79.73	175.22	595.033	261.646	0.797	1.752	elastic			
81.16	170.11	632.374	269.108	0.812	1.701	elastic			
82.59	164.99	669.716	276.571	0.826	1.650	elastic			
84.03	159.88	707.057	284.033	0.840	1.599	non-elastic			
85.46	154.61	744.398	291.456	0.855	1.546	non-elastic			
86.90	149.03	781.740	298.800	0.869	1.490	non-elastic			
88.33	143.05	819.081	306.066	0.883	1.431	non-elastic			
89.76	136.58	856.423	313.252	0.898	1.366	non-elastic			
91.20	129.49	893.764	320.358	0.912	1.295	non-elastic			
92.63	121.54	931.105	327.386	0.926	1.215	non-elastic			
94.07	112.31	968.447	334.348	0.941	1.123	non-elastic			
95.50	100.87	1005.789	341.281	0.955	1.009	non-elastic			
96.93	83.82	1043.130	348.371	0.969	0.838	non-elastic			
98.37	54.54	1080.471	356.116	0.984	0.545	non-elastic			
99.80	-309.15	1117.813	363.888	0.998	-3.092	crush.of concr.			
101.22	-9735.00	1154.746	371.574	1.012	-97.350	crush.of concr.			

max.deviation of Ni [kN], 0.00147

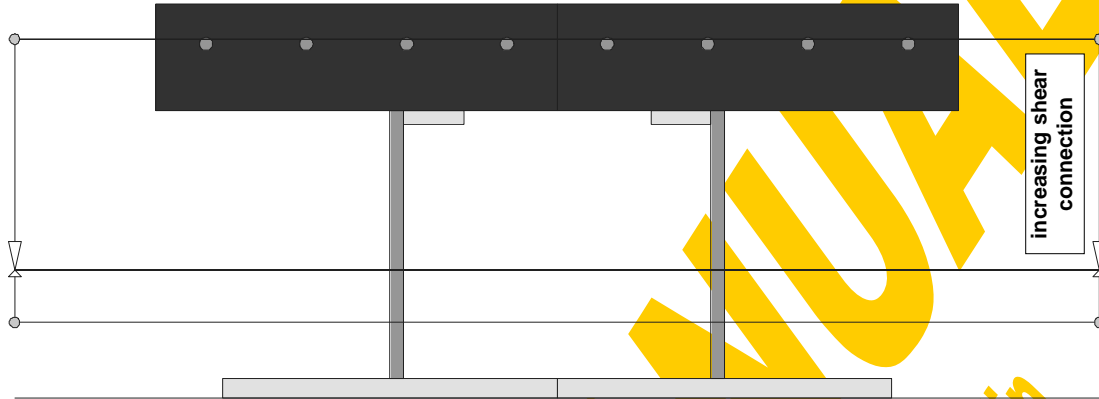
Section properties:

reference E-modulus [kN/mm²]:,210
 E.N.A.from bottom line [mm]:,100.6376
 Area (ideall) [mm²]:,15876.71
 Inertia (ideall) [cm⁴]:,17641.47
 upper Resis.Moment (ideall) [cm³]:,-907.659
 lower Resis.Moment (ideall) [cm³]:,1752.97
 El.limit of bending [kNm]:,257.3213
 El.limit of kapa [o/oo/m]:,6.9458
 Plastic normal force tension [kN]:,4413.682
 Plastic normal force compr. [kN]:,5229.682, "without buckling-check"
 Plastic shear force (web-parts): [kN],797.7931, "without buckling-check"
 end

Elasto-plastic results - COMPOSITE

file = c:\geldynamic\diss\cobejo\files\DISS.PRO

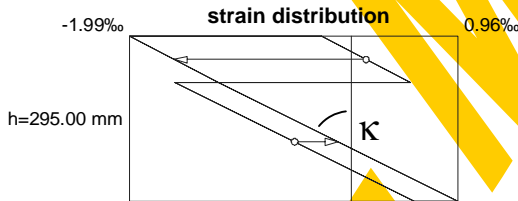
hat-shaped beam



datum line

Width = 600 Height = 295 [mm]

Partial safety factor steel =	1.1
Partial safety factor concrete =	1.5
Stress factor concrete =	.85
Partial safety factor reinforcem. =	1.15
Tension stiffening effect: f_{cteff}/f_{ctm} =	1
Tension stiffening effect: beta (short) =	.4



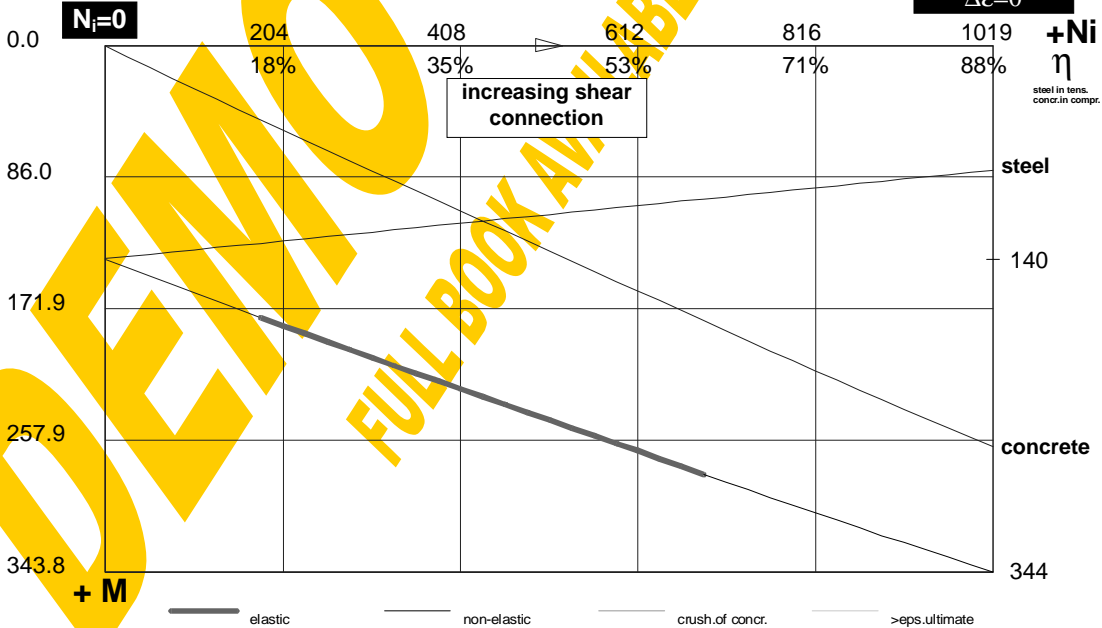
$K = 10$ [‰/m]

$N = 0.00$ [kN]

$V = 0.00$ [kN]

Ni-M Interaction [kN,kNm] sagg.mom.

$N.A._s = N.A._c$
 $\Delta\epsilon = 0$



Ni-M Interaction - COMPOSITE

file = c:\geldynamic\diss\cobejo\files\DISS.PRO

hat-shaped beam

$$\kappa = 10 \quad [\% / m]$$

max.deviation of Ni= 0.001 kN



NO normal force				NO vertical shear force		
ya [mm]	yc [mm]	Ni [kN]	M [kNm]	e0a [o/oo]	e0c [o/oo]	
56.88	268.47	0.000	139.965	0.569	2.685	ne
57.84	265.93	25.085	145.272	0.578	2.659	ne
58.82	260.50	50.634	150.773	0.588	2.605	ne
59.80	254.26	76.184	156.288	0.598	2.543	ne
60.78	248.64	101.733	161.757	0.608	2.486	ne
61.76	243.49	127.283	167.179	0.618	2.435	ne
62.74	238.69	152.832	172.556	0.627	2.387	ne
63.73	234.20	178.381	177.888	0.637	2.342	ne
64.71	229.95	203.931	183.175	0.647	2.299	el
65.69	225.91	229.480	188.420	0.657	2.259	el
66.67	222.05	255.029	193.623	0.667	2.220	el
67.65	218.35	280.579	198.786	0.676	2.183	el
68.63	214.79	306.128	203.909	0.686	2.148	el
69.61	211.29	331.678	209.015	0.696	2.113	el
70.59	207.79	357.227	214.121	0.706	2.078	el
71.57	204.29	382.776	219.227	0.716	2.043	el
72.56	200.79	408.326	224.333	0.726	2.008	el
73.54	197.30	433.875	229.439	0.735	1.973	el
74.52	193.80	459.424	234.545	0.745	1.938	el
75.50	190.30	484.974	239.651	0.755	1.903	el
76.48	186.80	510.523	244.757	0.765	1.868	el
77.46	183.30	536.073	249.862	0.775	1.833	el
78.44	179.80	561.622	254.968	0.784	1.798	el
79.42	176.30	587.171	260.074	0.794	1.763	el
80.33	173.07	610.756	264.787	0.803	1.731	el
81.31	169.57	636.305	269.894	0.813	1.696	el
82.29	166.07	661.854	275.000	0.823	1.661	el
83.27	162.57	687.404	280.105	0.833	1.626	el
84.25	159.07	712.953	285.210	0.843	1.591	ne
85.24	155.47	738.503	290.289	0.852	1.555	ne
86.22	151.72	764.052	295.331	0.862	1.517	ne
87.20	147.80	789.601	300.337	0.872	1.478	ne
88.18	143.70	815.151	305.306	0.882	1.437	ne
89.16	139.37	840.700	310.236	0.892	1.394	ne
90.14	134.78	866.250	315.130	0.901	1.348	ne
91.12	129.88	891.799	319.985	0.911	1.299	ne
92.10	124.59	917.348	324.805	0.921	1.246	ne
93.08	118.79	942.897	329.590	0.931	1.188	ne
94.07	112.31	968.447	334.348	0.941	1.123	ne
95.05	104.83	993.996	339.090	0.950	1.048	ne
96.02	95.71	1019.423	343.827	0.960	0.957	ne

el=elastic ne=non-elastic cr=crushing of concrete **=epsilon > epsilon ultimate

Nia = Ni (Normal force in steel part; tension > 0)
 Nic = Ni (Normal force in concrete part; compression > 0)
 Ni (Horizontal shear force in dowel layer)

Ni max = 1019.423 [kN]
M max = 343.827 [kNm]
 steel in tension, concrete in compression

Ni start = 0 **Ni limit = N.A. (steel=concrete)**

Elasto-plastic results - composite section - kappa

Section:,"hhat-shaped beam
 kappa [o/oo / m]=,10
 Savety factor steel:.,1.1
 Savety factor concrete:.,1.5
 Stress factor concrete:.,0.85
 Savety factor reinf.:.,1.15
 Tension stiffening effect : fcteff/fctm =,1
 Tension stiffening effect: beta (short) =,0.4
 SAGGING moment

NO normal force in composite section (Nia=Nic)

Table of steel elements (No,x,y,w,h,fyk,E/1000,fu,eu,flange=0/web=1) [N,mm]

1	50	0	250	15	355	210	510	0.1	0
2	175	15	10	200	380	210	450	0.1	1
3	185	205	45	10	380	210	450	0.1	0
11	300	0	250	15	355	210	510	0.1	0
12	415	15	10	200	380	210	450	0.1	1
13	370	205	45	10	380	210	450	0.1	0

Table of concrete elements (No,x,y,w,h,fck,fctm) [N,mm]

1	0	215	300	80	30	3
11	300	215	300	80	30	3

Table of reforcem. elements (No,y,no,d,fy,E/1000,fu,eu,N(shrink.)) [N,mm]

1	265	8	10	550	200	620	0.1	0
---	-----	---	----	-----	-----	-----	-----	---

Ni-M Interaction Table (ya[mm],yc[mm],Ni[kN],M[kNm],e0a[o/oo],e0c[o/oo])

Ni start = 0 , Ni limit = N.A. (steel=concrete)

56.88	268.47	0.000	139.965	0.569	2.685	non-elastic
57.84	265.93	25.085	145.272	0.578	2.659	non-elastic
58.82	260.50	50.634	150.773	0.588	2.605	non-elastic
59.80	254.26	76.184	156.288	0.598	2.543	non-elastic
60.78	248.64	101.733	161.757	0.608	2.486	non-elastic
61.76	243.49	127.283	167.180	0.618	2.435	non-elastic
62.74	238.69	152.832	172.556	0.627	2.387	non-elastic
63.73	234.20	178.381	177.888	0.637	2.342	non-elastic
64.71	229.95	203.931	183.175	0.647	2.300	elastic
65.69	225.91	229.480	188.420	0.657	2.259	elastic
66.67	222.05	255.030	193.623	0.667	2.221	elastic
67.65	218.35	280.579	198.786	0.677	2.184	elastic
68.63	214.79	306.128	203.909	0.686	2.148	elastic
69.61	211.29	331.678	209.015	0.696	2.113	elastic
70.59	207.79	357.227	214.121	0.706	2.078	elastic
71.57	204.29	382.776	219.227	0.716	2.043	elastic
72.56	200.79	408.326	224.333	0.726	2.008	elastic
73.54	197.30	433.875	229.439	0.735	1.973	elastic
74.52	193.80	459.425	234.545	0.745	1.938	elastic
75.50	190.30	484.974	239.651	0.755	1.903	elastic
76.48	186.80	510.523	244.757	0.765	1.868	elastic
77.46	183.30	536.073	249.863	0.775	1.833	elastic
78.44	179.80	561.622	254.968	0.784	1.798	elastic
79.42	176.30	587.171	260.074	0.794	1.763	elastic
80.33	173.07	610.756	264.788	0.803	1.731	elastic
81.31	169.57	636.305	269.894	0.813	1.696	elastic
82.29	166.07	661.854	275.000	0.823	1.661	elastic
83.27	162.57	687.404	280.105	0.833	1.626	elastic
84.25	159.07	712.953	285.210	0.843	1.591	non-elastic
85.24	155.47	738.503	290.289	0.852	1.555	non-elastic
86.22	151.72	764.052	295.331	0.862	1.517	non-elastic
87.20	147.80	789.601	300.337	0.872	1.478	non-elastic
88.18	143.70	815.151	305.306	0.882	1.437	non-elastic
89.16	139.37	840.700	310.236	0.892	1.394	non-elastic
90.14	134.78	866.250	315.130	0.901	1.348	non-elastic
91.12	129.88	891.799	319.985	0.911	1.299	non-elastic
92.10	124.59	917.348	324.805	0.921	1.246	non-elastic
93.08	118.79	942.897	329.590	0.931	1.188	non-elastic
94.07	112.31	968.447	334.348	0.941	1.123	non-elastic
95.05	104.83	993.996	339.090	0.951	1.048	non-elastic
96.02	95.71	1019.423	343.827	0.960	0.957	non-elastic

max.deviation of Ni [kN], 0.0009375

Section properties:

reference E-modulus [kN/mm²]:,210
 E.N.A.from bottom line [mm]:,100.6376
 Area (ideell) [mm²]:,15876.71
 Inertia (ideell) [cm4]:,17641.47
 upper Resis.Moment (ideell) [cm3]:,-907.659
 lower Resis.Moment (ideell) [cm3]:,1752.97
 El.limit of bending [kNm]:,257.3213
 El.limit of kappa [o/oo/m]:,6.9458
 Plastic normal force tension [kN]:,4413.682
 Plastic normal force compr. [kN]:,5229.682, "without buckling-check"
 Plastic shear force (web-parts): [kN],797.7931, "without buckling-check"
 end

This first calculation block within the composite calculation window can also be used to determine the M_{Rd} - V_{sd} interaction curve of a composite section. In Fig.4-54 the maximum plastic sagging moment resistance of the example section has been evaluated for different values of interacting vertical shear. The decreasing moment resistance with increasing vertical shear comes from the fictitious reduction of the stress-strain diagram of the steel web elements due to the simultaneously acting shear stress.

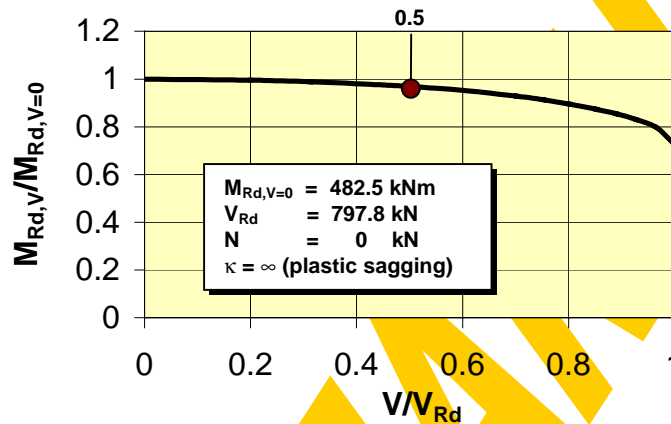


Fig.4-54 Interaction between bending resistance and vertical shear

Apart from that the N_i - M -interaction curve is required for the derivation of the fully-plastic **moment envelope** according to the theory of partial shear connection [121][59,109,Annex E.3], which can be interpreted as the extension of the plastic analysis of frames to that of the shear interface. Excluding a stability failure and requiring a fully-plastic **redistribution** of horizontal shear forces along the shear interface the moment envelope e.g. for a single span beam can be gained directly from the **plastic sagging Ni-M-interaction** ($\kappa=+\infty$) with two separate plastic neutral axes – one for the steel part and one for the concrete part. Due to the redistribution of shear forces the available shear capacity at each beam location can be calculated as the sum of the shear capacities from the beam end to this point. So assuming e.g. an equidistant dowel spacing the shear design resistance T_{Rd} [kN/m] will be constant along the beam axis and therefore the design shear force for each location ℓ can be calculated according to the formula:

$$N_i = \sum_{\text{dowels}} N_{i,Rd} = T_{Rd} \cdot \ell + N_{Rd,\text{end anchorage}}$$

From that it follows that $\ell = (N_i - N_{Rd,e.a.}) / T_{Rd}$ what directly can be applied on the interaction diagram as shown in Fig.4-55 for the example section ($V=0$). There dowels providing an end-anchorage of $N_i=200$ kN have been supposed in combination with punched shear connectors along the whole beam providing $T_{Rd}=711$ kN/m. The final moment envelope is set together by the M - ℓ -interaction curve depending on the beam span L . So the actual moment diagram must not exceed the plastic moment envelope ($M_{Sd} \leq M_{Rd}$) (Fig.4-56). Recall that this design method only is valid assuming a ductile shear interface allowing for plastic redistribution of horizontal shear forces.

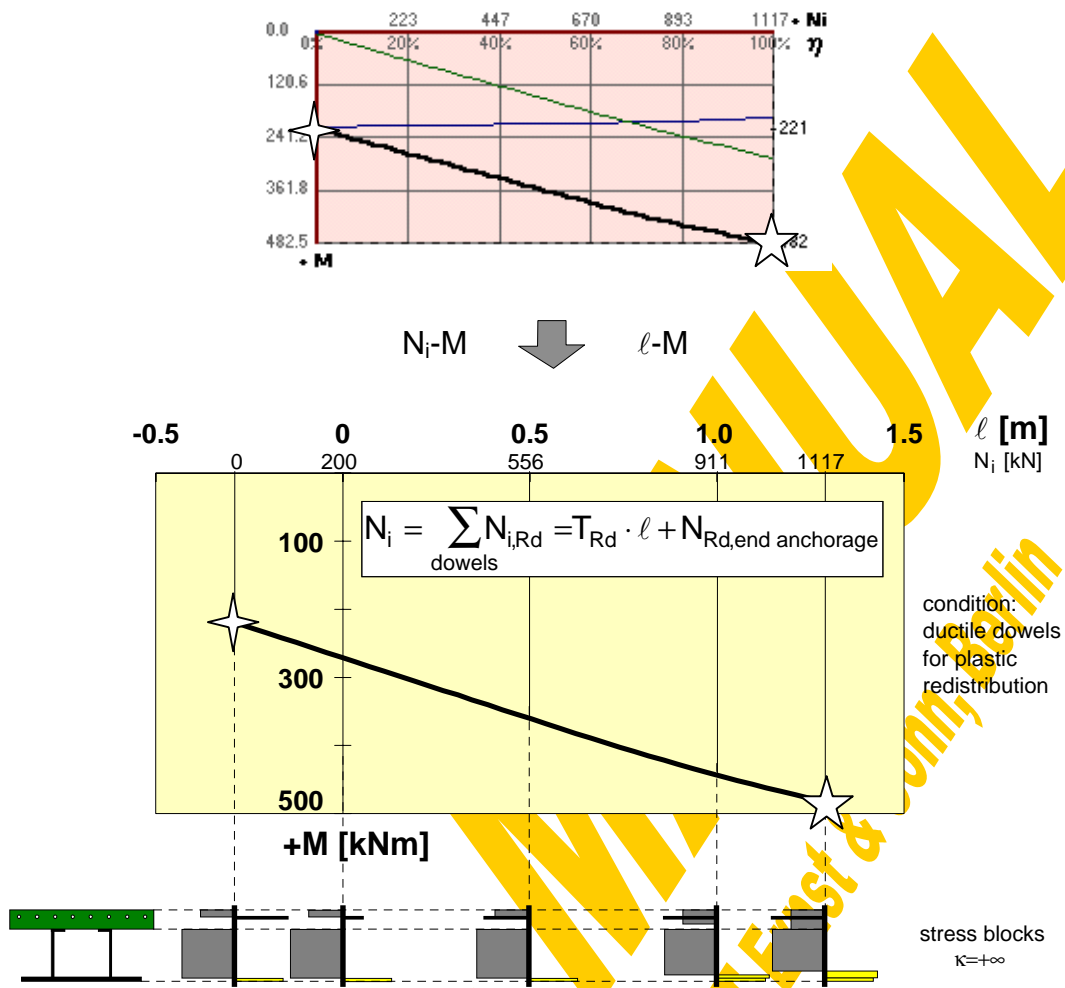


Fig.4-55 Moment envelope gained from plastic sagging N_i - M -curve

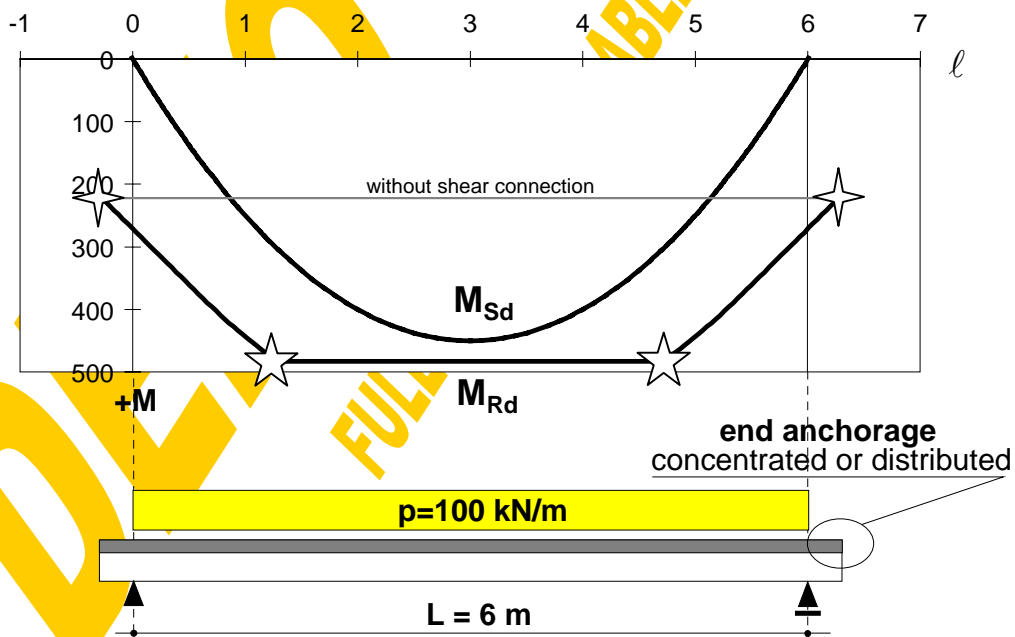


Fig.4-56 Design ($M_{Sd} \leq M_{Rd}$) for example section

The design of continuous composite beams is based on the same principles. In the following the calculation will be demonstrated for the example section for a symmetrical two-span beam loaded with eight single loads (Fig.4-57).

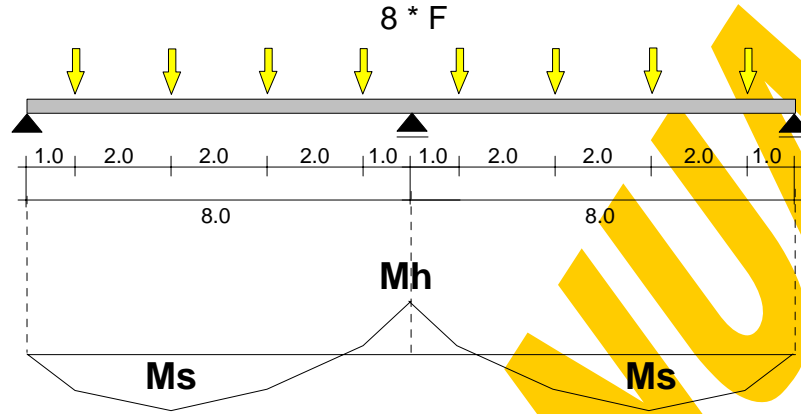


Fig.4-57 Two-span continuous beam

To be able to show the principles of calculation the shear capacity of the connector here will be assumed to be $T_{Rd}=100 \text{ kN/m}$. Hence the shear capacity within the sagging moment area is $N_{is}=3[\text{m}]\cdot 100[\text{kN/m}]=300 \text{ kN}$. As shown in Fig.4-58 the corresponding partial bending moment resistance M_s can be gained from the plastic sagging N_i - M -diagram. The remaining shear capacity for activating the composite section in hogging is $N_{ih}=(8-2\cdot 3)[\text{m}]\cdot 100[\text{kN/m}]=200 \text{ kN}$. The appropriate partial bending moment resistance M_h is taken from the plastic hogging N_i - M -diagram (Fig.4-58).

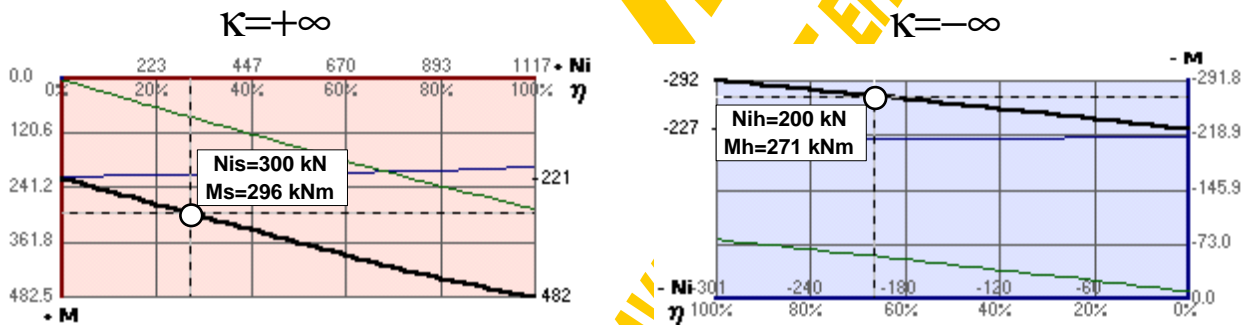


Fig.4-58 N_i - M -diagram for plastic sagging and plastic hogging

Based on the theory of plastic design with plastic hinges in the sagging and hogging moment area the capable forces F can be calculated as:

$$F_{pl,Rd} = \frac{M_s + M_h \cdot \frac{3}{8}}{4} = 99.4 \text{ kN}$$

Here it should be emphasised that according to the present state of EC4 [59,109] partial shear connection ($\eta < 100\%$) is not allowed within the hogging moment area in contradiction to the given example ($\eta_{hog}=66\%$).

As described before the plastic design of composite beams with ductile shear connectors is based on the knowledge about the design resistance T_{Rd} of the shear connectors. Going the opposite direction the resistance of the dowels can be gained not only from push-out- but also from four-point bending tests as shown in Fig.4-59. This evaluation method is given in [59,109,Annex E.2] for composite slabs but of course can also be applied to composite beams. It has successfully been used for the characterisation of punched shear connectors as described in detail in chapter 2.3.3.2.

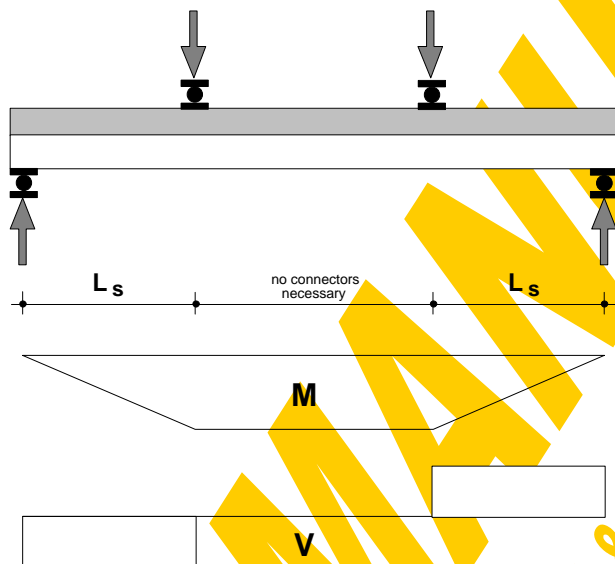


Fig.4-59 Four-point bending test for shear resistance of connectors

To enable a test evaluation in view of the shear interface the other possible types of failure like bending and shear resistance of the whole cross section have to be excluded by an appropriate shear length L_s . From the test the bending moment resistance $M_{R,test}$ due to the applied forces and the dead load caused by failure of the connectors can be derived. The corresponding Ni-M-curve for the tested cross section has to be calculated for the measured geometrical and material properties for $\kappa=+\infty$. Fig.4-60 shows the derivation of $T_{R,test}$ from $M_{R,test}$. Obviously from this kind of tests only the plastic resistance value of the connectors can be determined in contrast to the much cheaper push-out tests, which even give the full force-slip curve. However it has become common practice to confirm the results from the push-out-tests by a final beam test.

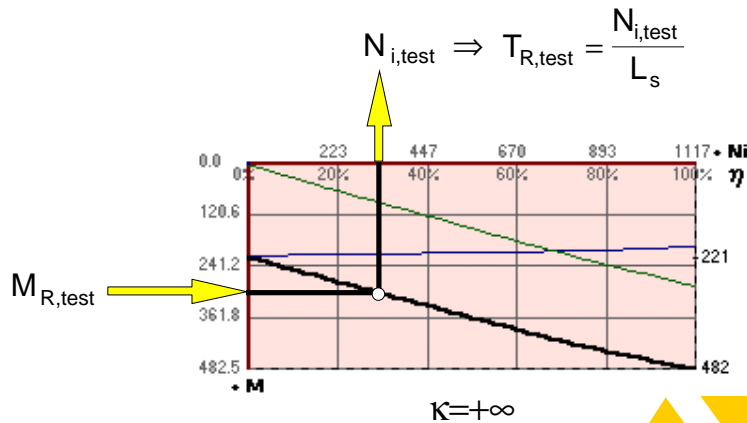
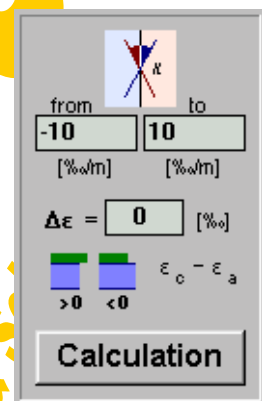


Fig.4-60 Evaluation of four-point bending test

4.2.5.4 N_i - M - κ -relation for a defined strain jump at the steel-concrete interface (DEcomp)



This second calculation block within the composite calculation window is quite similar to the first one, however here the strain jump $\Delta\varepsilon$ is defined and the curvature κ will be varied within given boundaries („from“ - „to“, 40 subdivisions). Ignoring the longer iteration time the solution for each κ -value can be gained using the first calculation block and an interpolation for the given $\Delta\varepsilon$ (this has been done for check calculations). So the second calculation block is simply a further iteration loop within that the first calculation block is repeated.

As illustrated in Fig.4-44 $\Delta\varepsilon$ means the jump within the cross sectional strain distribution between the steel and the concrete section part at the shear interface. The integration of $\Delta\varepsilon$ along the beam axis leads to the slip, or vice versa $\Delta\varepsilon$ represents the slope of the slip-curve (Fig.4-48). $\Delta\varepsilon=0$ along the entire composite beam would mean an infinitely stiff shear-interaction without slip.

For the procedure „DEcomp“ this strain jump has to be given as well as the vertical shear force V and the normal force N of the whole composite section. The curvature κ then will be varied between the specified limits and the solution for each of these κ -values will be recorded for the final presentation of the κ - N_i - M -curves. If $\kappa_{from}=\kappa_{to}$ the iteration will only be performed for this one specified κ -value. Further it has to be repeated that for $\kappa \approx 0$ no interaction between steel and concrete will be found and therefore $|\kappa| < 0.005 \text{ ‰/m}$ will be modified to $\kappa = \kappa + 0.01 \text{ ‰/m}$.

The corresponding strain distribution, where $\Delta\varepsilon$, V and N are fulfilled for the specified curvature κ , is iterated in the following steps. The progress of the iteration is shown by a flood box and a comment line. The calculation can be interrupted by pressing the „STOP“-button.

- 1.) The procedure „steellimit“ is used to determine the **strain and force limits** of the **steel** section part for the given curvature κ .
- 2.) The procedure „conclimit“ is used to determine the **strain and force limits** of the **concrete** section part for the given curvature κ .
- 3.) In the third step the lower and upper limiting inner shear forces are calculated, where the weaker section parts reach their resistance. According to Fig.4-46 it follows that:

$$N_{i,1} = \max (Nu1a - N , Nu2c)$$

$$N_{i,2} = \min (Nu2a - N , Nu1c)$$

- 4.) Using the procedures „itNsteel“ and „itNconcr“ the corresponding datum strains then are determined for these force limits:

$$N_{ia} = N_{i,1} + N \xrightarrow{\text{itNsteel}} e0a$$

$$N_{ia} = N_{i,2} + N \xrightarrow{\text{itNsteel}} e0ga$$

$$N_{ic} = N_{i,1} \xrightarrow{\text{itNconcr}} e0c$$

$$N_{ic} = N_{i,2} \xrightarrow{\text{itNconcr}} e0gc$$

- 5.) If one of the so-found strain limits of the steel section ($e0a, e0ga$) reaches the yielding limits ($e01ya$ or $e02ya$ acc. to point 1.) it has to be extended for this yield-plateau as shown at the bottom of Fig.4-61.

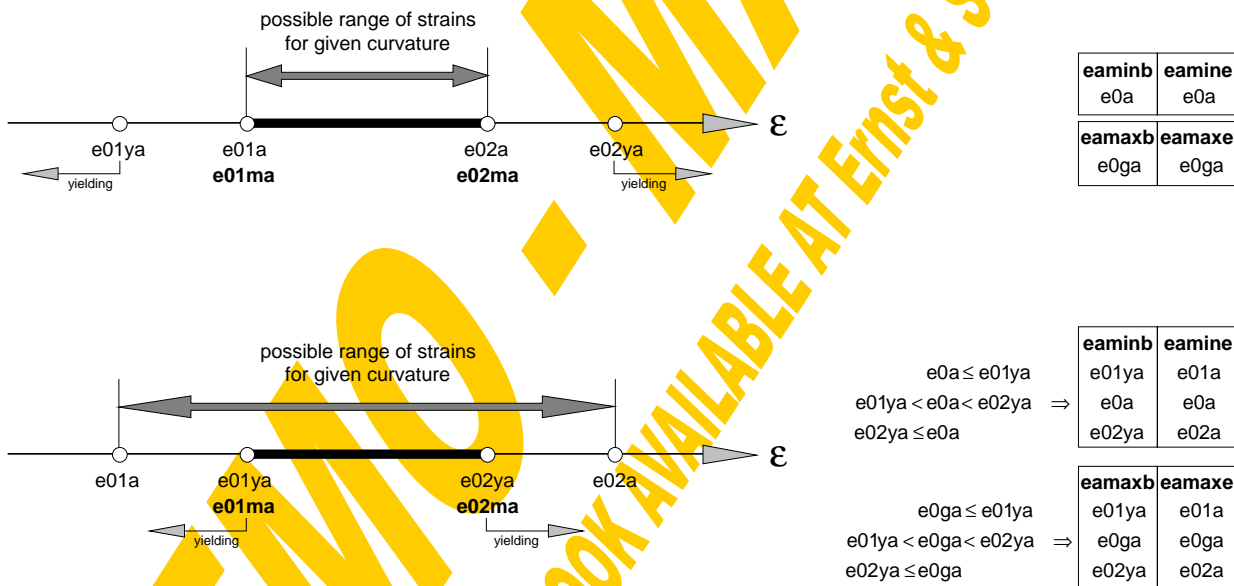


Fig.4-61 Consideration of the yielding plateau

The same philosophy has been applied to the concrete section. For that purpose the index „a“ for steel would have to be changed to „c“ for concrete in Fig.4-61. The possible range of $\Delta\epsilon$ for the given curvature lies between the limits ($eamine - eaminb$) and ($eamaxe - eamaxb$).

- 6.) If the given value of $\Delta\epsilon$ lies in this possible range of $\Delta\epsilon$ a solution can be found within the following iteration according to the bisection method:

- The datum steel strain $e0a$ is iterated between $eaminb$ and $eamaxb$

- For each e_{0a} and the given κ the normal force N_{ia} in the steel section can be found with the procedure „steelstrain“
- $N_{ic}=N_{ia}-N$ follows from the entire equilibrium. „itNconcr“ is used to iterate the corresponding datum strain e_{0c} to the given N_{ic} and κ .
- The actual value of $\Delta\varepsilon$ is equal to $(e_{0c}-e_{0a})$ and will be compared with the given one. Then the iteration is continued with a new assumption for e_{0a} until one of the following criteria is fulfilled: $\Delta\varepsilon$ reaches an appropriate accuracy, the change of e_{0a} is smaller than a given tolerance or the stop-button is pressed.

Then these six calculation steps are repeated for the next κ -value. Fig.4-62 shows the described iteration of e_{0a} ($=\varepsilon_{0,steel}$) for the example section to fulfill $\Delta\varepsilon=0$, $V=0$ and $N=0$ for $\kappa=10\text{‰}/\text{m}$.

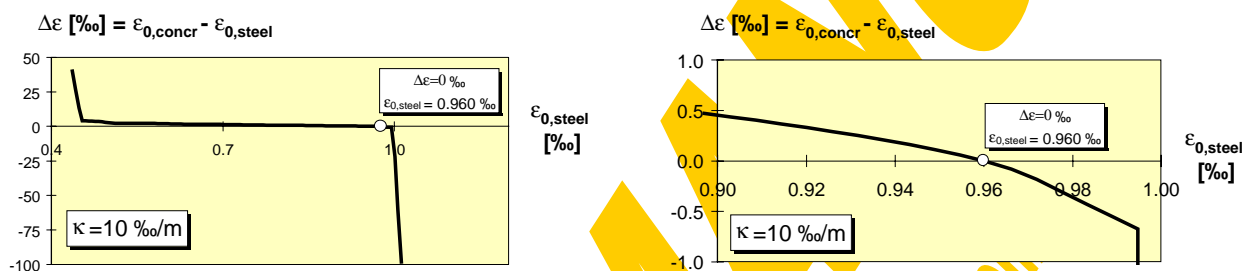


Fig.4-62 Iteration of strain distribution to given $\Delta\varepsilon$

The results for the given range of curvature then are presented in the window shown in Fig.4-63. It comprises some input data, a sketch of the analysed composite cross section and three graphs and a table showing the coherence between κ , N_i and M . The cross sectional condition is indicated by different colours: elastic in green, non-elastic in black, crushing of concrete in red and that part beyond ε_u in white. In Fig.4-63 it can be seen very clearly the influence of the tension stiffening effect for $\kappa < 0$, where the reinforcement is in tension. From the M - κ -curve the actual secant bending stiffness can even be taken for the non-elastic parts according to the formula

$$E \cdot I \text{ [kNm}^2\text{]} = \frac{M \text{ [kNm]} \cdot 1000}{\kappa \text{ [‰/m]}}$$

For the example section in the sagging moment area it can be calculated that $EI_{ini} = 240584/6.5 = 37013 \text{ kNm}^2$. This value can directly be compared with that given on page 214. Here differences might occur due to the different calculation philosophies in view of concrete in tension: For the elastic section properties concrete in tension is taken into consideration with the same Young's modulus as in compression whereas in all iterations the effect of concrete in tension fully has been assigned to the reinforcement (tension stiffening effect).

Finally there have been provided input boxes for linear interpolations between κ , N_i and M . Furthermore also the recorded maximum errors of N_i and $\Delta\varepsilon$ due to the iterations are given. Using the button „Print results“ will send the following four sheets to your printer: The first sheet (see page 228) contains a drawing of the actual composite

section and the input data (safety factors, $\Delta\varepsilon$, N , V). At the bottom of this first sheet the N_i - κ diagram will be displayed. The drawing style of the curve depends on the status of the composite section in view of elasticity and is given in a legend. At the second sheet (page 229) you will find the M' - κ - and the M' - N_i -curve. Attention has to be paid that $M = M' - N \cdot e$ for $N \neq 0$ - or vice versa: for $N = 0$: $M = M'$. Sheet no.3 (page 230) contains the κ - N_i - M' -table and on sheet no.4 you will find the full input data of the analysed section. To make the results also accessible to other programs they can be saved as a sequential data file with the button „Save results“. The default file name is built up by that of the section (*.pro) and the extension „ep2“ (elasto-plastic composite - second calculation block). The output file of the example calculation can be found on page 231.

*Remark: Attention has to be paid to the following fact: The colour of each line segment depends on the section state (elastic, non-elastic,...) at its **endpoint** and therefore its accuracy depends on the curve resolution. So to get detailed information about the section state, especially for steep curves, it is necessary to refine the curve scale within the interesting area.*

DEMO

FULL BOOK AVAILABLE AT ERNST & SOHN, BERLIN

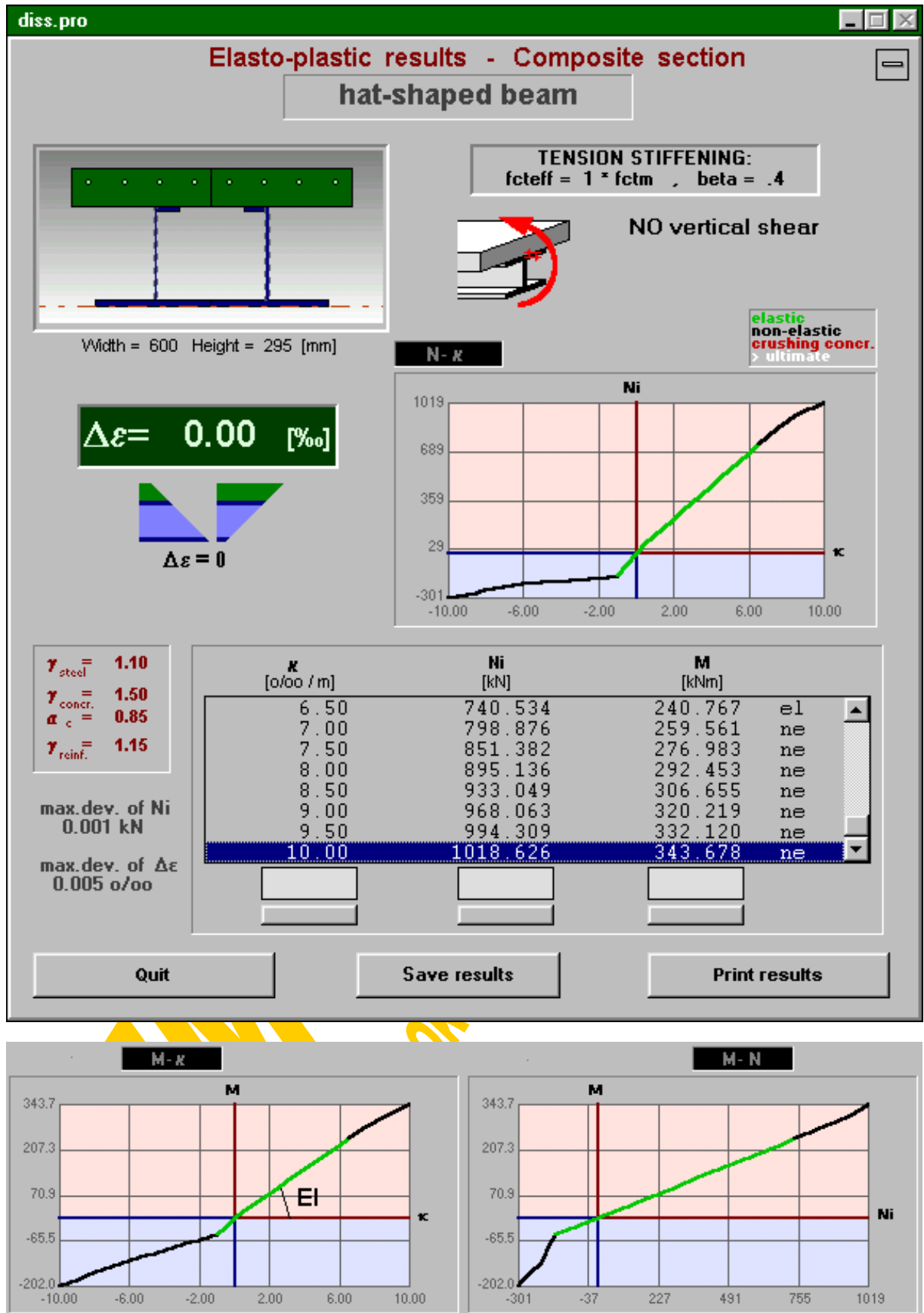


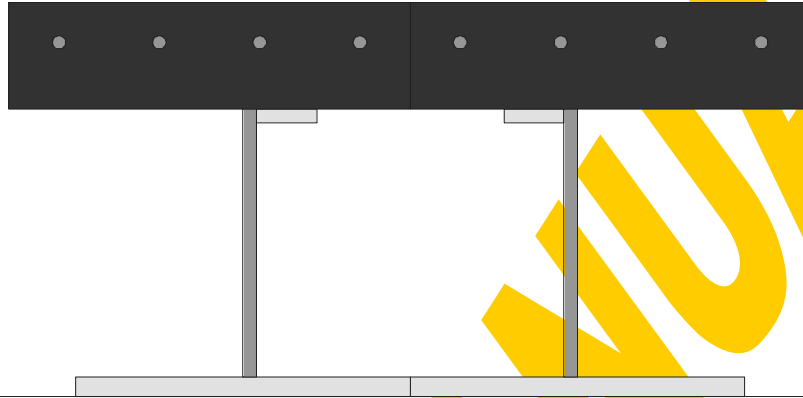
Fig.4-63 Window for the presentation of composite results (ep_de.frm)

Institute of Steel and Timber Constructions - University of Innsbruck Dipl.-Ing. Gerald Huber

Elasto-plastic results - COMPOSITE

file = c:\geldynamic\diss\cobejo\files\DISS.PRO

hat-shaped beam



datum line

Width = 600 Height = 295 [mm]

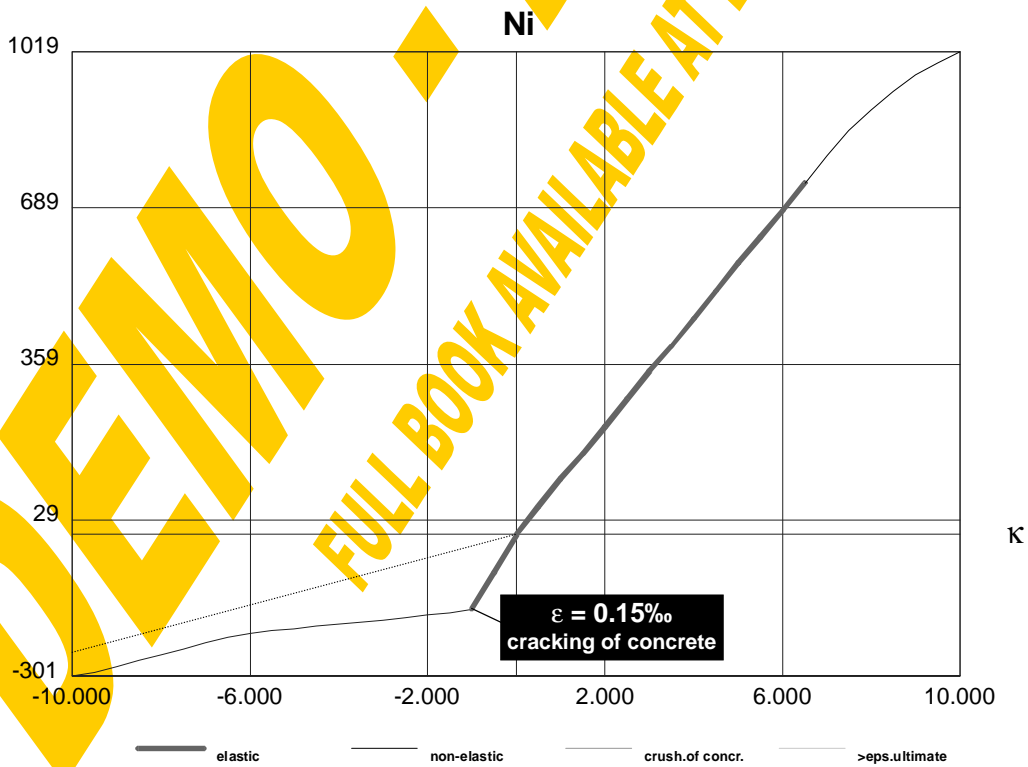
Partial safety factor steel =	1.1
Partial safety factor concrete =	1.5
Stress factor concrete =	.85
Partial safety factor reinforcem. =	1.15
Tension stiffening effect: f_{cteff}/f_{ctm} =	1
Tension stiffening effect: beta (short) =	.4

$\Delta\varepsilon = 0.00$ [‰]

$N = 0.00$ [kN]

$V = 0.00$ [kN]

Ni-kappa-Curve [kN,o/oo]

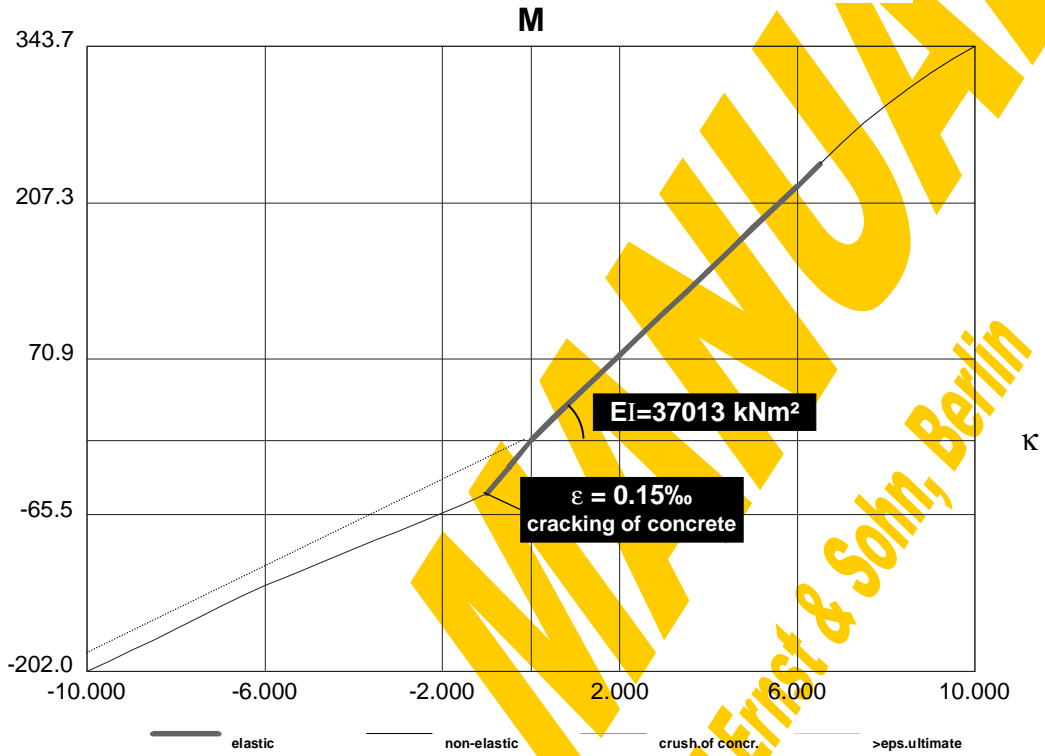


Elasto-plastic results - COMPOSITE

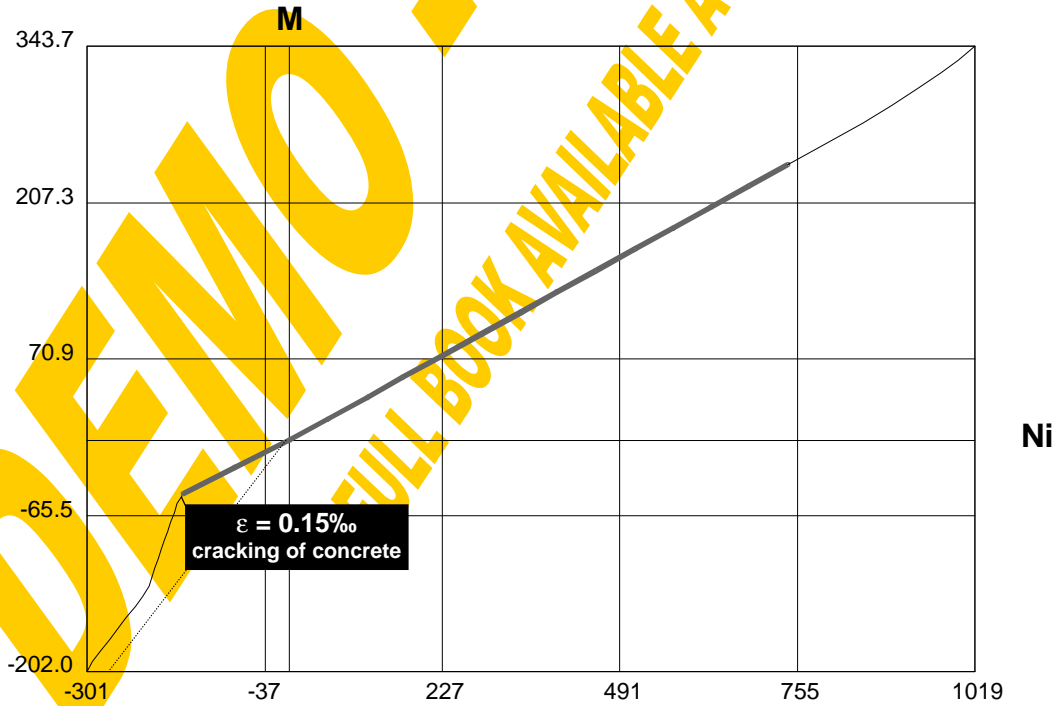
file = c:\geldynamic\diss\cobejo\files\DISS.PRO

hat-shaped beam

M-kappa-Curve [kNm,o/oo]



M-Ni-Curve [kNm,kN]



Institute of Steel and Timber Constructions - University of Innsbruck Dipl.-Ing. Gerald Huber

kappa-Ni-M Table - COMPOSITE

file = c:\geldynamic\diss\cobejo\files\DISS.PRO

hat-shaped beam $\Delta\varepsilon = 0.00$ [‰]

max.deviation of Ni = 0.001kN

max.deviation of delta epsilon = 0.005 o/oo

NO normal force

NO vertical shear force

kappa [o/oo]	Ni [kN]	M [kNm]	
-10.00	-300.535	-201.952	ne
-9.50	-291.959	-193.196	ne
-9.00	-279.939	-183.725	ne
-8.50	-267.496	-174.165	ne
-8.00	-254.533	-164.497	ne
-7.50	-242.486	-155.019	ne
-7.00	-229.364	-145.318	ne
-6.50	-217.683	-135.917	ne
-6.00	-208.941	-127.127	ne
-5.50	-204.562	-119.246	ne
-5.00	-199.820	-111.289	ne
-4.50	-195.089	-103.334	ne
-4.00	-190.703	-95.451	ne
-3.50	-185.965	-87.495	ne
-3.00	-181.229	-79.539	ne
-2.50	-176.489	-71.583	ne
-2.00	-171.744	-63.625	ne
-1.50	-167.370	-55.744	ne
-1.00	-157.892	-46.801	ne
-0.50	-82.053	-24.047	el
0.01	-0.375	0.061	el
0.50	57.958	18.719	el
1.00	116.308	37.517	el
1.50	168.810	55.146	el
2.00	227.146	73.940	el
2.50	285.489	92.737	el
3.00	343.828	111.532	el
3.50	396.329	129.160	el
4.00	454.676	147.957	el
4.50	513.006	166.751	el
5.00	571.346	185.546	el
5.50	626.777	203.761	el
6.00	682.198	221.973	el
6.50	740.534	240.767	el
7.00	798.876	259.561	ne
7.50	851.382	276.983	ne
8.00	895.136	292.453	ne
8.50	933.049	306.655	ne
9.00	968.063	320.219	ne
9.50	994.309	332.120	ne
10.00	1018.626	343.678	ne

el=elastic ne=non-elastic cr=crushing of concrete **=epsilon > epsilon ultimate

Nic = Ni (Normal force in concrete part; compression > 0)**Nia = Ni (Normal force in steel part; tension > 0)****Ni (Shear force in dowel layer)**

Elasto-plastic results - composite section - delta epsilon

Section: "hat-shaped beam"

DELTA EPSILON [o/oo]: 0

Savety factor steel: 1.1

Savety factor concrete: 1.5

Stress factor concrete: 0.85

Savety factor reinf.: 1.15

Tension stiffening effect : fcteff/fctm =, 1

Tension stiffening effect: beta (short) =, 0.4

NO normal force in composite section (Nia=Nic)

Table of steel elements (No,x,y,w,h,fyk,E/1000,fu,eu,flange=0/web=1) [N,mm]

1	50	0	250	15	355	210	510	0.1	0
2	175	15	10	200	380	210	450	0.1	1
3	185	205	45	10	380	210	450	0.1	0
11	300	0	250	15	355	210	510	0.1	0
12	415	15	10	200	380	210	450	0.1	1
13	370	205	45	10	380	210	450	0.1	0

Table of concrete elements (No,x,y,w,h,fck,fctm) [N,mm]

1	0	215	300	80	30	3			
11	300	215	300	80	30	3			

Table of reforcem. elements (No,y,no,d,fy,E/1000,fu,eu,N(shrink.)) [N,mm]

1	265	8	10	550	200	620	0.1	0
---	-----	---	----	-----	-----	-----	-----	---

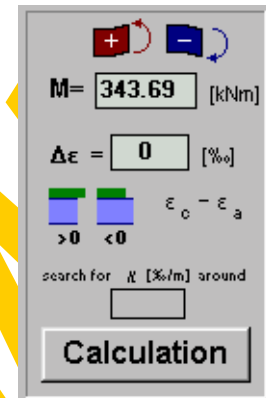
kappa-Ni-M Table (kappa[o/oo / m],Ni[kN],M[kNm])

-10.0	-300.54	-201.95	non-elastic
-9.5	-291.96	-193.20	non-elastic
-9.0	-279.94	-183.72	non-elastic
-8.5	-267.50	-174.16	non-elastic
-8.0	-254.53	-164.50	non-elastic
-7.5	-242.49	-155.02	non-elastic
-7.0	-229.36	-145.32	non-elastic
-6.5	-217.68	-135.92	non-elastic
-6.0	-208.94	-127.13	non-elastic
-5.5	-204.56	-119.25	non-elastic
-5.0	-199.82	-111.29	non-elastic
-4.5	-195.09	-103.33	non-elastic
-4.0	-190.70	-95.45	non-elastic
-3.5	-185.96	-87.49	non-elastic
-3.0	-181.23	-79.54	non-elastic
-2.5	-176.49	-71.58	non-elastic
-2.0	-171.74	-63.62	non-elastic
-1.5	-167.37	-55.74	non-elastic
-1.0	-157.89	-46.80	non-elastic
-0.5	-82.05	-24.05	elastic
0.0	-0.38	0.06	elastic
0.5	57.96	18.72	elastic
1.0	116.31	37.52	elastic
1.5	168.81	55.15	elastic
2.0	227.15	73.94	elastic
2.5	285.49	92.74	elastic
3.0	343.83	111.53	elastic
3.5	396.33	129.16	elastic
4.0	454.68	147.96	elastic
4.5	513.01	166.75	elastic
5.0	571.35	185.55	elastic
5.5	626.78	203.76	elastic
6.0	682.20	221.97	elastic
6.5	740.53	240.77	elastic
7.0	798.88	259.56	non-elastic
7.5	851.38	276.98	non-elastic
8.0	895.14	292.45	non-elastic
8.5	933.05	306.66	non-elastic
9.0	968.06	320.22	non-elastic
9.5	994.31	332.12	non-elastic
10.0	1018.63	343.68	non-elastic

max.deviation of Ni [kN], 0.00149

max.deviation of delta eps [o/oo], 0.00468

end



4.2.5.5 Given M and strain jump at the interface (cross sectional design) (QSNWcomp)

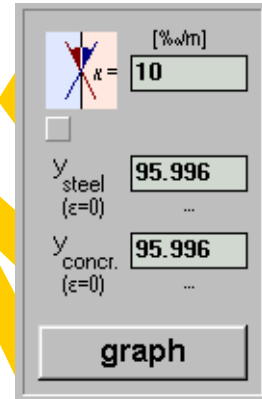
Additionally to $\Delta\varepsilon$, V and N in this third calculation block also the overall bending moment M has to be defined. Within the iterative procedure „**QSNWcomp**“ the corresponding strain distribution (κ , ε_{0a} , ε_{0c}) will be determined. Strictly this could also be done by analysing the corresponding range of κ with the second calculation block and making an interpolation for the searched M . So this calculation block is built up by the second one (\equiv procedure „**QSNWcomp_sub**“) repeated within a further additional iteration loop, where κ is varied. The calculation can be subdivided into the following four steps:

- 1.) Any **starting value** for the curvature κ has to be determined, where a solution for the given $\Delta\varepsilon$, V and N can be found. Obviously the iteration can drastically be speeded up by giving an approximated κ_{start} , known from the global analysis or from the second calculation block. If no value is given for κ it will be set +0.1‰ for $\Delta\varepsilon > 0$ or -0.1‰ for $\Delta\varepsilon < 0$.
- 2.) Using the procedure „QSNWcomp_sub“ it will be checked, if a solution can be found for κ_{start} fulfilling $\Delta\varepsilon$, V and N . There are three possibilities:
 - 2.1.) The corresponding moment M_{start} to the given curvature κ_{start} approximately is equal to the given value M and therefore the solution is already found.
 - 2.2.) It is possible to find a solution for κ_{start} but $M_{\text{start}} \neq M$ and therefore the calculation has to be continued with step 3.
 - 2.3.) No solution can be found for the estimated κ_{start} and therefore a new value has to be assumed. Step by step the starting curvature will be modified in the following way until a starting solution can be found:

$$\kappa_{\text{start}} = \kappa_{\text{start}} \pm (0.2, 0.4, 0.6, 0.8, 1.0, 2, 4, 6, 8, 10, 20, 40, 60, 80, 100, 200, 400, 600, 800, 1000)\% / \text{m}$$

- 3.) Based on κ_{start} any curvature κ_{end} at the **opposite side of the solution** has to be determined. For that purpose κ -values are examined using the procedure „QSNWcomp_sub“ (step by step more far away from κ_{start}) until a curvature is found, which fulfils the following conditions:
 - a) a solution can be found meeting the given $\Delta\varepsilon$, V and N
 - b) the corresponding M_{end} has to lie at the opposite side of M_{start} in view of the given bending moment M , because as the relation of M - κ is continuous and monotonous

4.2.5.6 Forces and moments to a given strain distribution



In contrast to the three calculation blocks described before this fourth one does not consist of interlaced iteration loops but calculates the inner forces and moments based on a given linear strain distribution (κ , ϵ_{0a} or y_{steel} , ϵ_{0c} or y_{concr} as shown in Fig.4-65) and the material laws of the several steel, concrete and reinforcement elements. Of course the remaining properties in view of longitudinal stresses depend on the existence of a vertical shear force V and the safety factors.

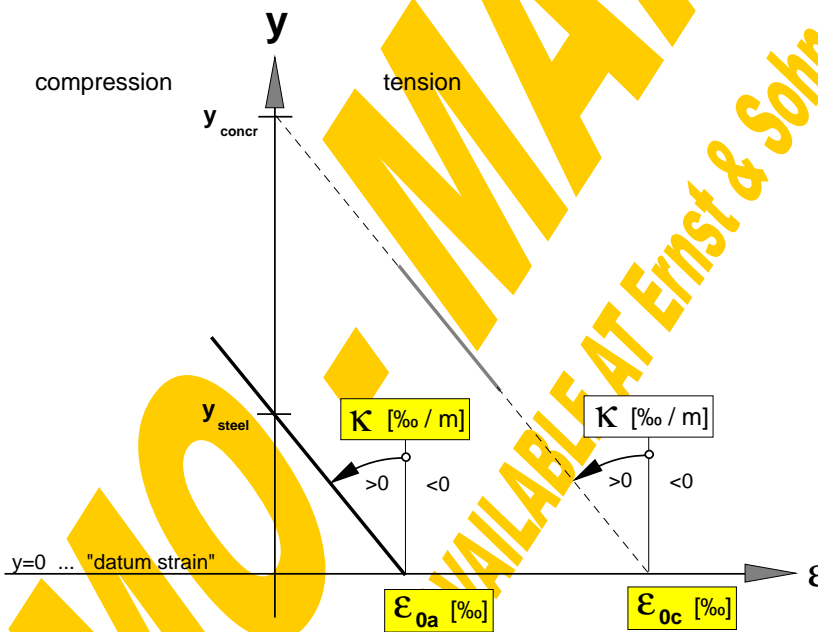


Fig.4-65 Linear strain distribution

This calculation is directly based on the basic stress-strain relations and does not call for any iterative solutions. Therefore it proved to be very useful for checks of the several iteration results. Further use was made of it to analyse several cross sections of test specimens, where the strain distribution has been measured with strain gauges.

The calculation can be subdivided into the following three steps:

- 1.) The inner normal force of the steel section N_{ia} , the bending moment M_a' and the status in view of elasticity are determined with the procedure „steelstrain“ based on the given κ and ϵ_{0a} .

- 2.) The inner normal force of the concrete section N_{ic} , the bending moment M_c' and the status in view of elasticity are determined with the procedure „constrain“ based on the given κ and ϵ_{0c} .
- 3.) Finally the composite section is set together adding up the section parts steel and concrete based on the principles given in Fig.4-44.

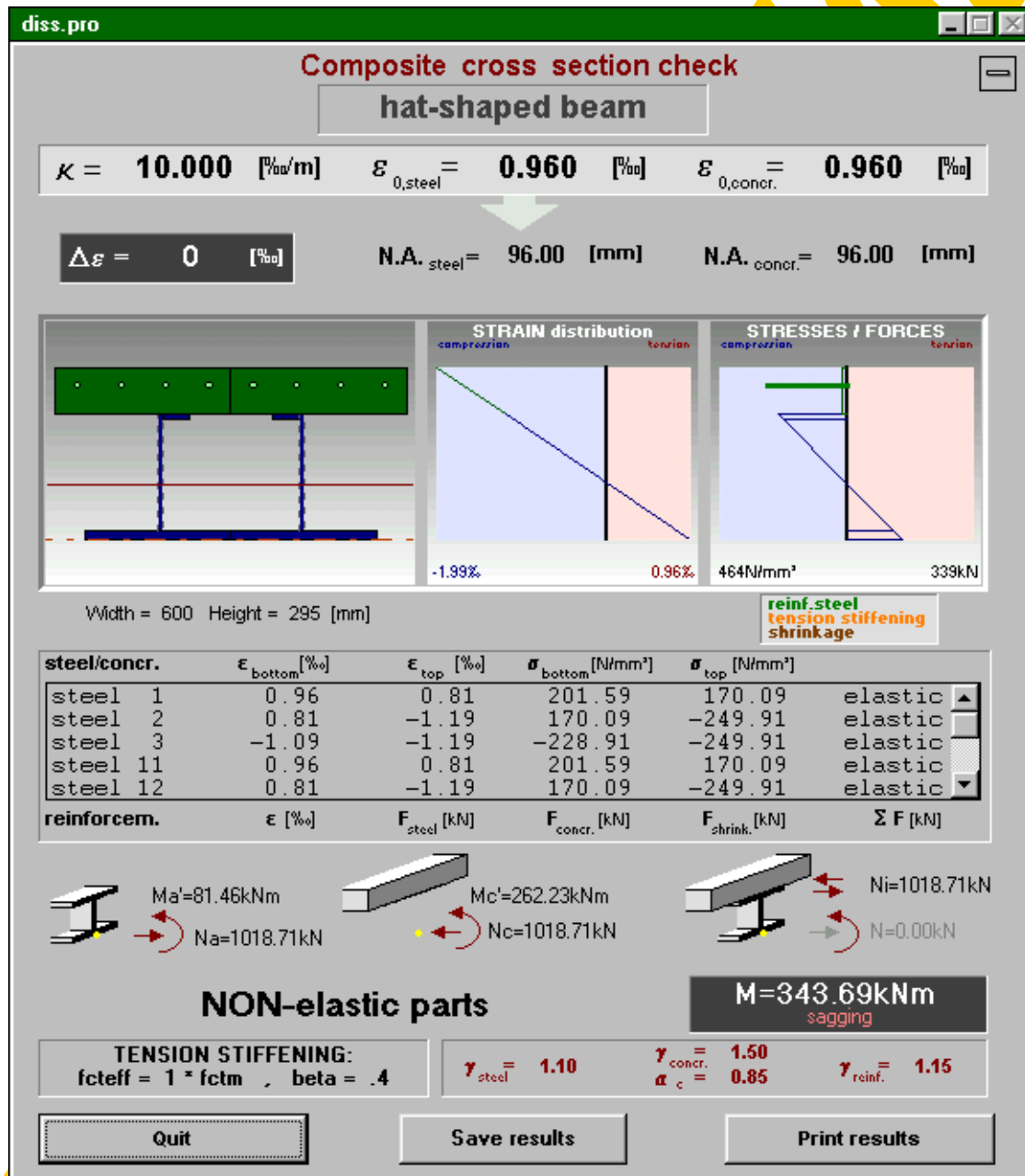


Fig.4-66 Window for the presentation of composite results (ep_qsnw.frm)

The results then are presented within the window shown in Fig.4-66. It contains the input data (κ , ϵ_{0a} , ϵ_{0c}), from which $\Delta\epsilon$ and the neutral axes of steel and concrete are derived. Further a sketch of the analysed composite section including the neutral axes, the chosen strain distribution and the resulting stress distribution are given. Pressing

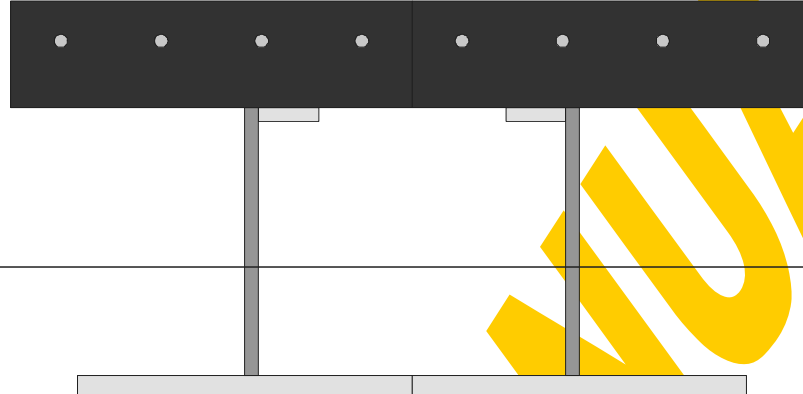
the left mouse button and moving the mouse within the section sketch, the strain or the stress graphs will produce a reticule and shows the corresponding x -, y -, ε - and σ -values. This enables then to pick special values from the graphs. In the centre of the presentation window you can find a table, where the strains and stresses of each element are listed. Concerning the reinforcement the resulting force explicitly is set together by the parts of bare steel, contribution of the concrete between the cracks and shrinkage. Clicking on an element within the table will high-lighten it in the section graphic as well as in the strain and stress distribution. At the bottom the inner normal forces and bending moments of the section parts are given as well as those of the entire composite section set together by steel and concrete. The arrows of the forces and moments automatically are drawn corresponding to their sign pointing to the effective direction. The sketch of the composite section set together by an I-shaped steel beam and an upper concrete plate only is symbolical.

With the „Print“-button the following three sheets can be printed: The first sheet comprises a sketch of the composite section, the input data (κ , ε_{0a} , ε_{0c}) and the inner forces and moments of the section parts as well as those of the entire composite section (see page 237). On the second sheet (page 238) the strain and stress distribution is given both as graphs and as a table. The third sheet again gives the whole input data of the composite cross section. To make the results also accessible to other programs they can be saved as a sequential data file with the button „Save results“. The default file name is built up by that of the section (*.pro) and the extension „ep3“ (elasto-plastic composite - third calculation block). The output file of the example calculation can be found on page 239.

COMPOSITE cross section check

file = c:\geldynamic\diss\cobejo\files\DISS.PRO

hat-shaped beam



N.A. concrete

N.A. steel

datum line

Width = 600 Height = 295 [mm]

Partial safety factor steel =	1.1
Partial safety factor concrete =	1.5
Stress factor concrete =	.85
Partial safety factor reinforcem. =	1.15
Tension stiffening effect: f_{cteff}/f_{ctm} =	1
Tension stiffening effect: beta (short) =	.4

= INPUT

$\kappa = 10.000 \text{ } \mu\text{m/m}$

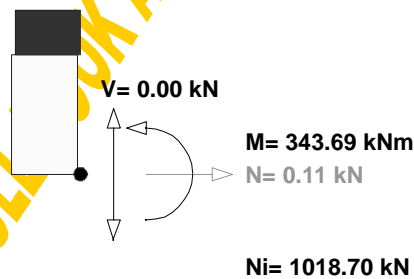
$\epsilon_{0,steel} = 0.960 \text{ } \text{‰}$

$\epsilon_{0,concr} = 0.960 \text{ } \text{‰}$

Internal forces - Steel and concrete parts separately



Internal forces - Composite cross section



M= 343.69 kNm

N= 0.11 kN

V= 0.00 kN

sagging area

NON-elastic parts

COMPOSITE cross section check

file = c:\geldynamic\diss\cobejo\files\DISS.PRO

hat-shaped beam

$\kappa = 10.000 \text{ ‰/m}$

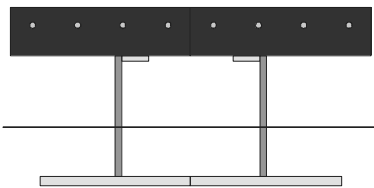
$\epsilon_{0,steel} = 0.960 \text{ ‰}$

$\epsilon_{0,concr} = 0.960 \text{ ‰}$

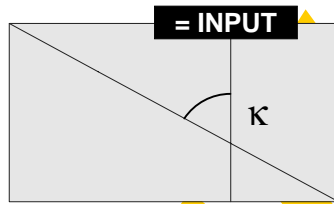
$\Delta\epsilon = 0.000 \text{ ‰}$

$N.A._{steel} = 96.00 \text{ mm}$

$N.A._{concr} = 96.00 \text{ mm}$



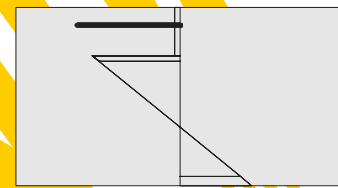
Width= 600 Height= 295 [mm]



-1.99‰

strains

0.96‰



463.64 N/mm²

stresses/forces

338.75 kN

Table of strains and stresses / forces

		strains [o/oo]		stresses [N/mm ²]		forces [kN]	
STEEL							
No		eps bottom	eps top	sigma bottom	sigma top		
1		0.960	0.810	201.60	170.10		
w 2		0.810	-1.190	170.10	-249.90		elastic
3		-1.090	-1.190	-228.90	-249.90		elastic
11		0.960	0.810	201.60	170.10		elastic
w 12		0.810	-1.190	170.10	-249.90		elastic
13		-1.090	-1.190	-228.90	-249.90		elastic
CONCRETE							
No		eps bottom	eps top	sigma bottom	sigma top		
1		-1.190	-1.990	-14.99	-17.00		non-elastic
11		-1.190	-1.990	-14.99	-17.00		non-elastic
REINFORCEMENT							
No		eps		F steel	F concr	F shrink	sum(F)
1		-1.690		-212.37	0.00	0.00	-212.37

Composite cross section check

Section: hat-shaped beam
 kappa [o/oo / m]= 10
 EPS steel (y=0) [o/oo]= 0.95996
 EPS concr (y=0) [o/oo]= 0.95996
 delta eps [o/oo]= 0
 Neutral axis steel [mm]= 96
 Neutral axis concr [mm]= 96
 Savety factor steel: 1.1
 Savety factor concrete: 1.5
 Stress factor concrete: 0.85
 Savety factor reinf.: 1.15
 Tension stiffening effect : fcteff/fctm = 1
 Tension stiffening effect: beta (short) = 0.4
 Vertical shear force in steel part [kN]= 0
 Normal force in steel part (tension>0) [kN]= 1018.711
 Normal force in concr part (compr.>0) [kN]= 1018.71
 Normal force in composite (tension>0) [kN]= 0.0005
 Horizontal shear force in dowel layer [kN]= 1018.71
 Bend.moment in steel part (at y=0) (sagg>0) [kNm]= 81.46352
 Bend.moment in concr part (at y=0) (sagg>0) [kNm]= 262.23
 Bend.moment in composite (at y=0) (sagg>0) [kNm]= 343.6935
 SAGGING area
 NON-elastic parts

Table of steel elements (No,x,y,w,h,fyk,E/1000,fu,eu,flange=0/web=1) [N,mm]

1	50	0	250	15	355	210	510	0.1	0
2	175	15	10	200	380	210	450	0.1	1
3	185	205	45	10	380	210	450	0.1	0
11	300	0	250	15	355	210	510	0.1	0
12	415	15	10	200	380	210	450	0.1	1
13	370	205	45	10	380	210	450	0.1	0

Table of concrete elements (No,x,y,w,h,fck,fctm) [N,mm]

1	0	215	300	80	30	3
11	300	215	300	80	30	3

Table of reforcem. elements (No,y,no,d,fy,E/1000,fu,eu,N(shrink.)) [N,mm]

1	265	8	10	550	200	620	0.1	0
---	-----	---	----	-----	-----	-----	-----	---

Table of strains and stresses**steel elements (No,eps bottom,eps top,sigma bottom,sigma top,0=el/1=non-el) (eps[o/oo],sigma[N/mm2])**

1	0.95996	0.80996	201.5916	170.0916	0
2	0.80996	-1.19004	170.0916	-249.9084	0
3	-1.09004	-1.19004	-228.9084	-249.9084	0
11	0.95996	0.80996	201.5916	170.0916	0
12	0.80996	-1.19004	170.0916	-249.9084	0
13	-1.09004	-1.19004	-228.9084	-249.9084	0

concrete elements (No,eps bottom,eps top,sigma bottom,sigma top,0=el/1=non-el/2=crush) (eps[o/oo],sigma[N/mm2])

1	-1.19004	-1.99004	-14.98569	-17	1
11	-1.19004	-1.99004	-14.98569	-17	1

reinforcement elements (No,eps,Fsteel,Fconcr,Fshrink,sum(F)) (eps[o/oo],F[kN])

1	-1.69004	-212.3767	0	0	-212.3767
---	----------	-----------	---	---	-----------

end

The described calculation has also been used to study the influence of the tension stiffening effect on the course of the internal horizontal shear force N_i and the entire bending moment M along the whole range of possible curvatures κ for the example section, prescribing $\Delta\varepsilon=0$, $V=0$ and $N=0$ (see Fig.4-67).

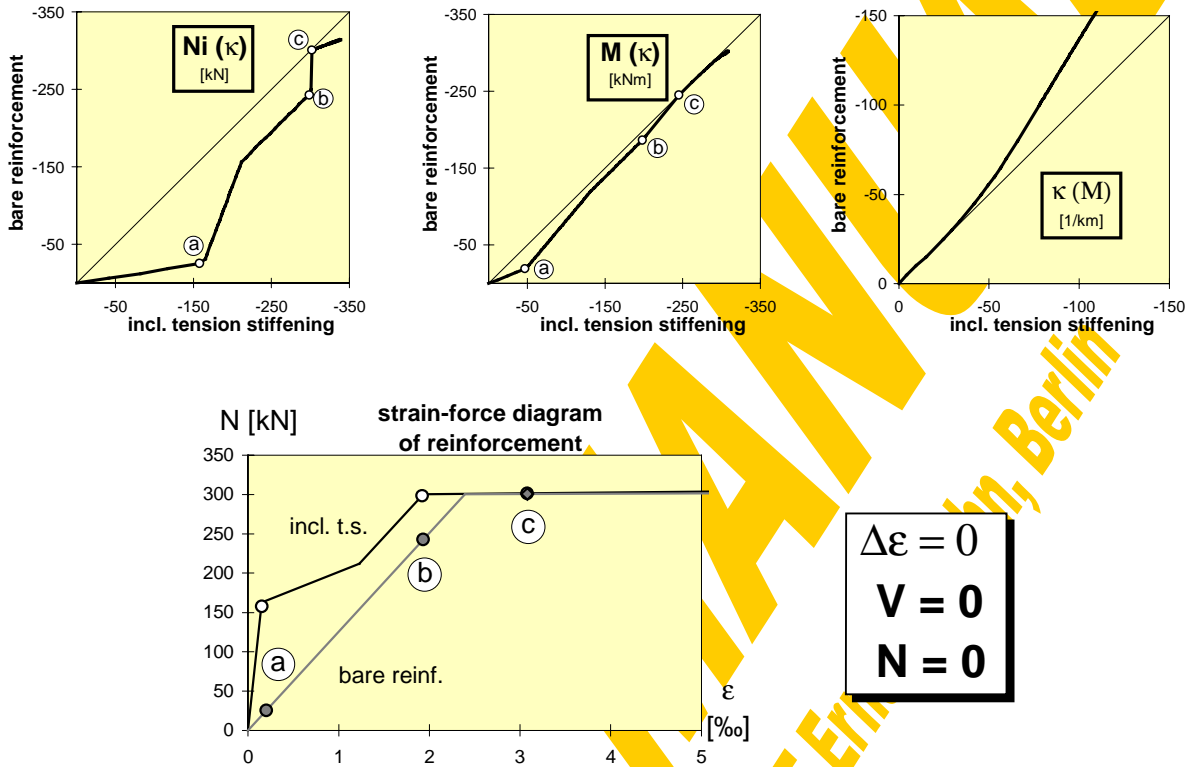


Fig.4-67 Influence of the tension stiffening effect

Furthermore this calculation block can directly be used to determine the N-M interaction curve for the design of composite columns:

For that purpose κ has to be set equal to $+\infty$ and then N and M' have to be determined for a varying location of neutral axes $y_{steel}=y_{concrete}$. The common y values should start with zero and end, where $N=0$ (due to the different behaviour of concrete in tension and compression this occurs for $y>h_c/2$). Each M' (related to the bottom datum line) then has to be converted to the centre line ($y=h_c/2$) using the formula

$$= M' + N \cdot \frac{h_c}{2}$$

In Fig.4-68 this calculation has been done for the example section defined in [101]. The comparison between the curves shows perfect agreement.

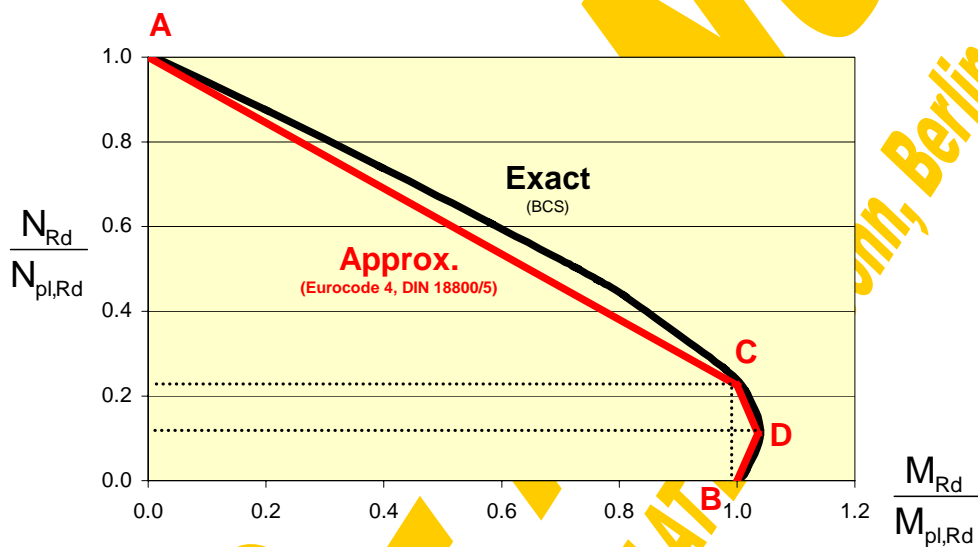
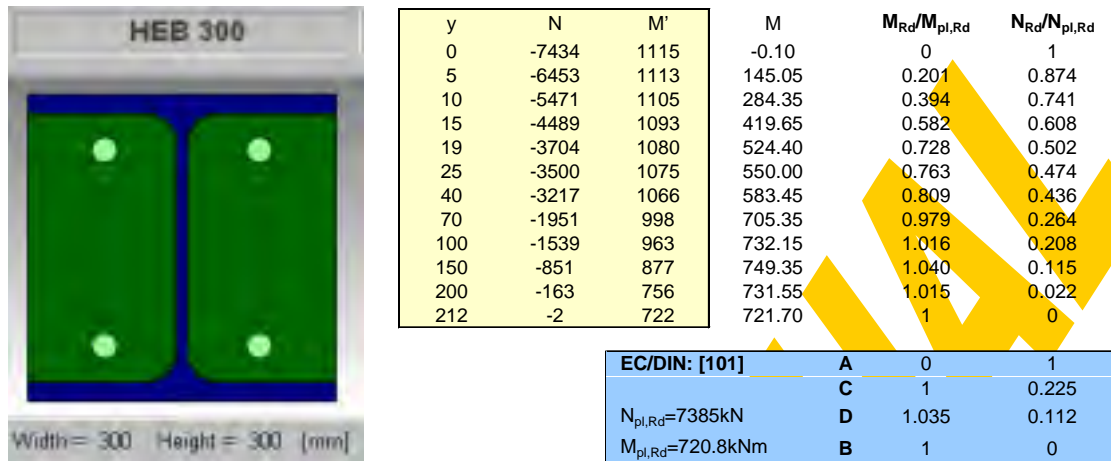


Fig.4-68 N-M interaction curve for composite column design

4.2.5.7 Summary

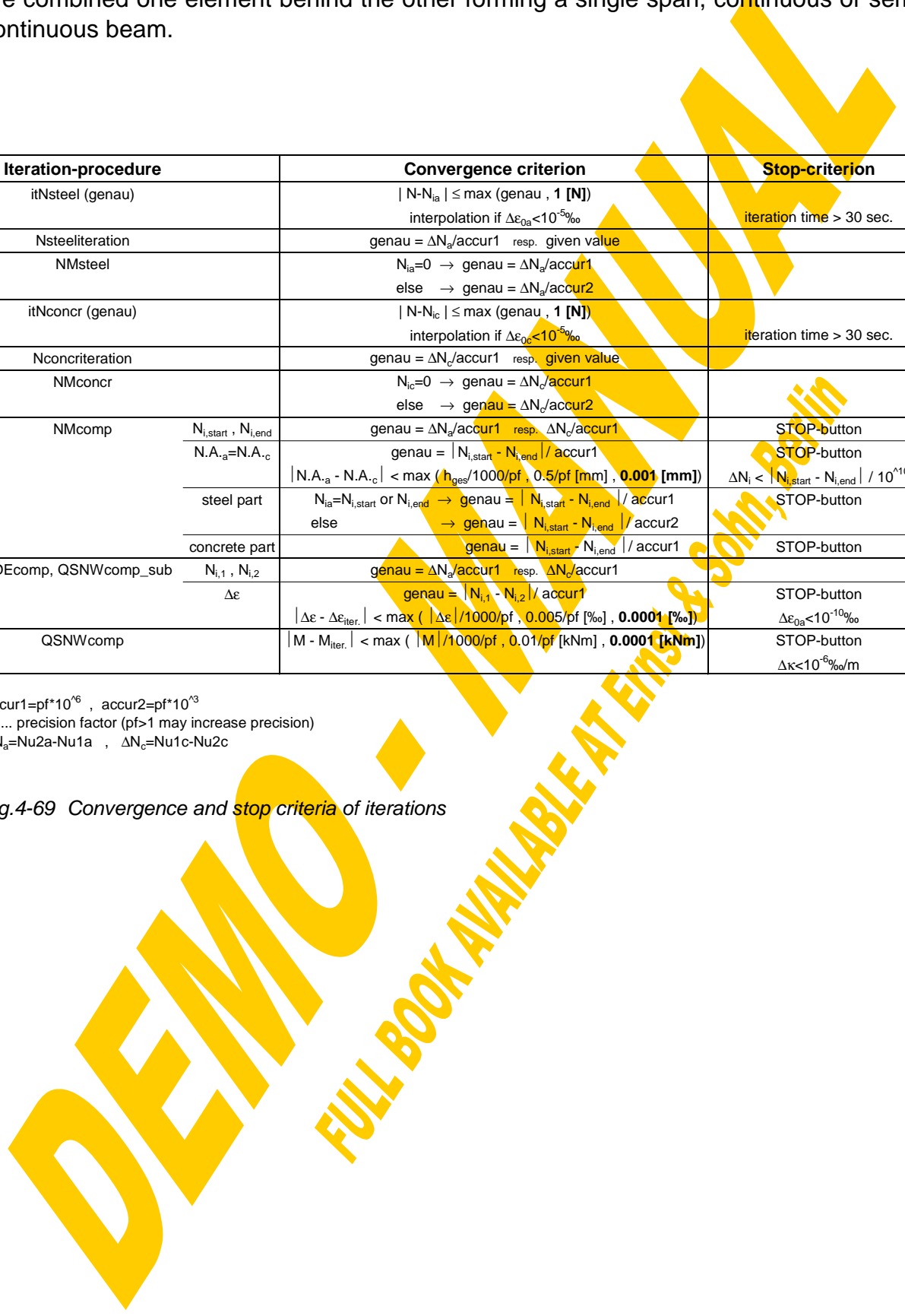
Within the composite calculation window there are four different types of cross section analyses. The first calculation block is used to determine the relation between inner horizontal shear force and bending moment for a given curvature. This calculation is repeated within a further iteration loop for the second calculation block, where a given $\Delta\epsilon$ shall be met for a variety of κ -values. And finally for the third iteration block a further iteration loop has been added to find that special strain distribution, where both $\Delta\epsilon$ and a given bending moment M are met. The fourth block represents the bare calculation of stresses from a given strain distribution, finally leading to inner forces and moments by integrating the stresses over the whole section. In Fig.4-69 the convergence and stop criteria of all used iterations are summarised. They have been defined as a compromise between accuracy and iteration time. For those cases of interlaced iteration loops sensitivity studies have been carried out. All these considerations serve as the

fundamental background for the global analysis, where finite beam elements and joints are combined one element behind the other forming a single span, continuous or semi-continuous beam.

Iteration-procedure		Convergence criterion	Stop-criterion
itNsteel (genau)		$ N - N_{ia} \leq \max(\text{genau}, 1 \text{ [N]})$ interpolation if $\Delta\epsilon_{0a} < 10^{-5}\%$	iteration time > 30 sec.
Nsteeliteration		genau = $\Delta N_a / \text{accur1}$ resp. given value	
NMsteel		$N_{ia} = 0 \rightarrow \text{genau} = \Delta N_a / \text{accur1}$ else $\rightarrow \text{genau} = \Delta N_a / \text{accur2}$	
itNconcr (genau)		$ N - N_{ic} \leq \max(\text{genau}, 1 \text{ [N]})$ interpolation if $\Delta\epsilon_{0c} < 10^{-5}\%$	iteration time > 30 sec.
Nconcriteration		genau = $\Delta N_c / \text{accur1}$ resp. given value	
NMconcr		$N_{ic} = 0 \rightarrow \text{genau} = \Delta N_c / \text{accur1}$ else $\rightarrow \text{genau} = \Delta N_c / \text{accur2}$	
NMcomp	$N_{i,\text{start}}, N_{i,\text{end}}$	genau = $\Delta N_a / \text{accur1}$ resp. $\Delta N_c / \text{accur1}$	STOP-button
	$N.A._a = N.A._c$	genau = $ N_{i,\text{start}} - N_{i,\text{end}} / \text{accur1}$	STOP-button
	steel part	$ N.A._a - N.A._c < \max(h_{\text{ges}}/1000/\text{pf}, 0.5/\text{pf} \text{ [mm]}, \mathbf{0.001 \text{ [mm]}})$ $N_{ia} = N_{i,\text{start}} \text{ or } N_{i,\text{end}} \rightarrow \text{genau} = N_{i,\text{start}} - N_{i,\text{end}} / \text{accur1}$ else $\rightarrow \text{genau} = N_{i,\text{start}} - N_{i,\text{end}} / \text{accur2}$	$\Delta N_i < N_{i,\text{start}} - N_{i,\text{end}} / 10^{10}$ STOP-button
	concrete part	genau = $ N_{i,\text{start}} - N_{i,\text{end}} / \text{accur1}$	STOP-button
DEcomp, QSNWcomp_sub	$N_{i,1}, N_{i,2}$	genau = $\Delta N_a / \text{accur1}$ resp. $\Delta N_c / \text{accur1}$	
	$\Delta\epsilon$	genau = $ N_{i,1} - N_{i,2} / \text{accur1}$ $ \Delta\epsilon - \Delta\epsilon_{\text{iter.}} < \max(\Delta\epsilon /1000/\text{pf}, 0.005/\text{pf} \text{ [%]}, \mathbf{0.0001 \text{ [%]}})$	STOP-button $\Delta\epsilon_{0a} < 10^{-10}\%$
QSNWcomp		$ M - M_{\text{iter.}} < \max(M /1000/\text{pf}, 0.01/\text{pf} \text{ [kNm]}, \mathbf{0.0001 \text{ [kNm]}})$	STOP-button $\Delta\kappa < 10^{-6}\%/m$

accur1 = $\text{pf} * 10^{-6}$, accur2 = $\text{pf} * 10^{-3}$
 pf ... precision factor (pf > 1 may increase precision)
 $\Delta N_a = N_{u2a} - N_{u1a}$, $\Delta N_c = N_{u1c} - N_{u2c}$

Fig.4-69 Convergence and stop criteria of iterations



4.3 Joint Characterisation

The sophisticated theoretical background in view of joint representation has already been described in detail in chapter 3. So the following introduction is primarily intended to practical users of the computer program CoBeJo. Some general repetitions therefore are deliberate.

4.3.1 Introduction

4.3.1.1 General

Conventionally joints (beam-to-column, beam-to-beam and beam splices) have been treated either as nominally pinned without any strength or stiffness (simple joints) or as fully rigid with full strength (continuous joints); this has been due to incomplete knowledge on joint's moment-rotation behaviour and due to a lack on modelling. In reality both assumptions only represent the limiting cases of the real moment-rotation behaviour of joints. The verification of these assumptions can lead to uneconomical joint detailing as well as to a wrong assessment of the actual structural behaviour in terms of stiffness, resistance and deflections. A modern approach is to develop efficient joint types first and then to take their realistic behaviour into consideration within the frame analysis. An accurate representation of the joint behaviour forms the basis for a correct and safe structural design, where the available joint properties have to be compared with the requirements from the structure at serviceability and ultimate limit states.

Recognition of the importance of integrating the joint behaviour into the global frame analysis in conjunction with modern methods of analysis has resulted in a tremendous number of research activities all over the world aimed at innovation in design. The co-operation and exchange of experience between experts all over Europe in recent years has now enabled a high level of knowledge to be available [36,40,49,87,94,176].

The following concerns the design of steel and composite beam-to-column joints for continuous and semi-continuous framing. However the concept applies similarly to beam-to-beam joints and beam splices. Moment-resisting joints have to transfer moments and forces between members with an adequate margin of safety. Their behaviour obviously influences the distribution of forces within the structure. Therefore the list of the usual construction elements, namely beams, slabs and columns, has to be extended to include the joints. An overall account of the joint's behaviour would need to recognise its three-dimensional nature. However the presence of stiff continuous floor slabs usually allows neglect of out-of-plane and torsional deformations of the joint. In comparison with the obsolete assumptions of joints being hinges or complete restraints with emphasis on resistance, the modern approach requires the following actions in view of the joints:

Representation (German: Modellbildung):

- **Characterisation**, determination of the (non-linear) moment-rotation curves; at least the determination of the corresponding key values (initial rotational stiffness, upper moment resistance and rotation capacity)
- Classification, a possible but not obligatory tool for simplification of modelling providing boundary conditions defining the limits for the use of conventional types of joint modelling (nominally rigid or nominally pinned)
- Idealisation, the conversion of non-linear moment-rotation curves into simplified ones
- **Modelling**, the reproduction of the joint behaviour within the structural analysis.

4.3.1.2 Joint characterisation (German: Knotencharakterisierung)

This chapter describes how to derive the M - ϕ -curves, reflecting the joint behaviour and being the necessary input data for the joint models. The general background for any joint model comprises three separate curves: one for the left hand connection, one for the right hand connection and one for the column web panel in shear. Only later (during the modelling process) the M - ϕ -characteristic of the shear panel may be shared into a left and right hand side part and then may be assigned to combined springs representing the connection and the shear together.

There are three possibilities of joint characterisation: the experimental one using full-scale joint tests, the numerical one based on finite element calculations and the analytical one, which will be treated now more in detail; this is because it is the only practical approach for every-day design.

Component method

An analytical description of the behaviour of a joint has to cover all sources of deformabilities, local plastifications, plastic redistribution of forces within the joint itself and local instabilities. Due to the multitude of influencing parameters, a macroscopic inspection of the complex joint by subdividing it into components has proved to be most appropriate. In comparison with the finite element method, these components, which can be modelled by translational springs with non-linear force-deformation response, are exposed to internal forces and not to stresses. The procedure can be expressed in three steps:

- Identification of the contributing components,
- Characterisation of the components (determination of their structural properties)
- Assembly of the component properties or curves to those of the joint.

Component identification

According to EC3 [60] a (basic) component of a joint is a specific part of a joint that makes – dependent on the type of loading – an identified contribution to one or more of its structural properties. When identifying the contributing components within a joint one can distinguish between components loaded in tension (or bending), compression and shear. Apart from the type of loading one can distinguish between components linked to the connecting elements and those linked to load-introduction into the column web panel (both are included in the “connection”) and the component “column web panel in

shear". The nodal subdivision for the most general case of a composite beam-to-column joint leads to a sophisticated component model (spring model), see Fig.4-70. There, the interplay of the several components is modelled in a very realistic way. Any composite joints (beam-to-column, beam-to-beam or beam splice), even steel joints can be derived as being only special cases of this general model. The sophisticated component model leads to a complex interplay of components and therefore to iterations within the joint characterisation itself. The solution of these iterations is the objective of the computer program herein.

To avoid such iterations in the codes [49,60] simplifications concerning the component interplay have been adopted resulting in a simplified component model (spring model), see Fig.4-70.

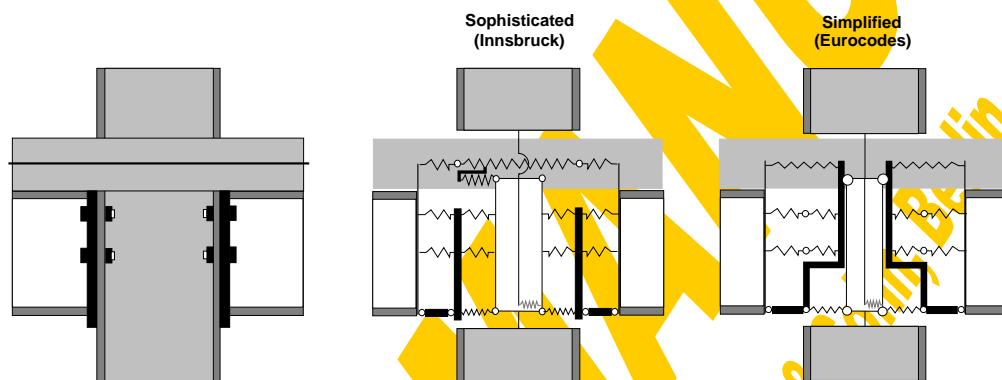


Fig.4-70 Sophisticated and simplified component models (spring models)

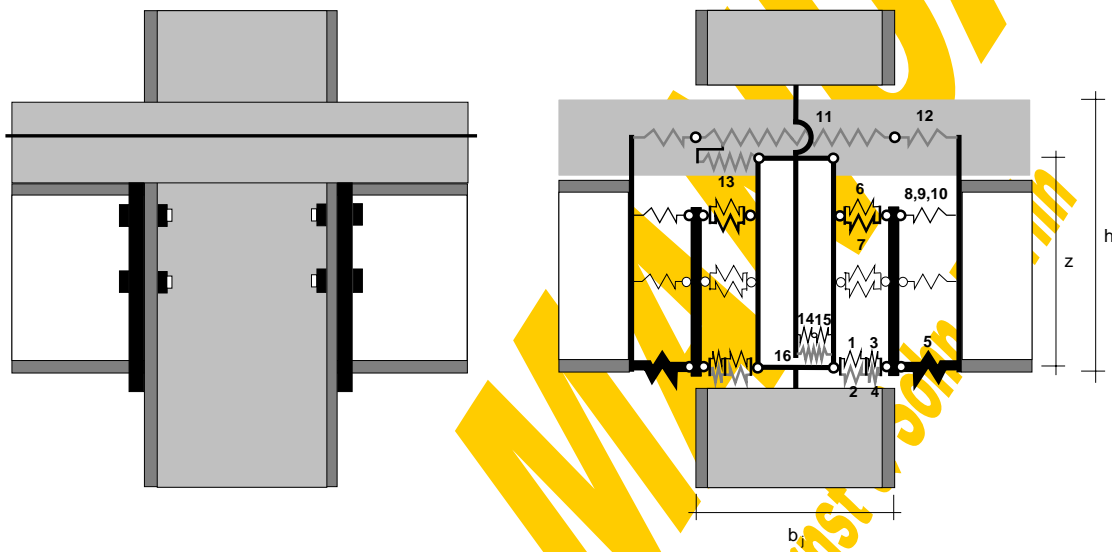
Through familiarity with the component model, which represents the interplay of all deformation influences, the principles of economic joint construction with respect to stiffness, resistance, failure modes and ductility can be logically derived. Assuming a specific component with a given resistance and deformation capacity, it is self-evident that by increasing its lever arm the joint's moment resistance increases whilst the rotation capacity decreases. Providing resistance in the compression region far beyond the resistance of the tension region is uneconomic. Similarly strengthening the connecting elements will not make the joint capable of sustaining more load, if failure is already dominated by the column web in tension, compression or shear. It also can be recognised immediately that it makes no sense to combine a relatively weak and ductile slab reinforcement with a stiff and brittle steelwork connection. These examples give ideas on how to use the component model directly for a qualitative assessment of the joint's response. Generally, the most efficient joint is that, for which, due to plastic redistribution within the joints itself, all components are used up to their plastic resistance and which provides a further yield plateau for redistribution of moments within the whole frame system.

Component characterisation

The component model is based on known force-deformation curves of the individual contributing components, which have to be derived within the component characterisation (derivation of the components' key values or even the full curves). Again this can be done at different levels of accuracy using different tools, such as

component tests (experimental approach), finite element simulations (numerical approach) or analytical mechanical models.

In order to describe the complex component response by easily understandable mechanical models the components given in Fig.4-70 are subdivided into basic joint components leading to the refined component model shown in Fig.4-71. So for example the load-introduction into an encased column web panel is split into the contribution due to the steel section and that due to the concrete encasement.



No.	component
1	interior steel web panel
2	concrete encasement
3	exterior steel web panel (column flange+local effects)
4	effect of concrete encasement on exterior spring
5	beam flange (local effects), contact plate, end plate
6	steel web panel incl. part of flange, fillet radius
7	stiffener in tension
8	column flange in bending (stiffened)
9	end plate in bending, beam web in tension
10	bolts in tension
11	reinforcement (within panel) in tension
12	slip of composite beam (due to incomplete interaction)
13	redirection of unbalanced forces
14	steel web panel in shear
15	steel web panel in bending
16	concrete encasement in shear

Fig.4-71 Refined component model

Sophisticated mechanical models describing the basic components' response have been developed at several research centres and validated against component test results and numerical simulations. With the help of comprehensive parameter studies the sophisticated and relatively complex formulae describing the stiffness, resistance and deformation capacity of each basic component can be reduced to easy-to-handle formats. Such simplified formulae are integrated into the codes [49,60].

Component assembly

The transfer from the force-deformation curves of the individual basic joint components to the moment-rotation curves representing the connection or the shear panel has to be done based on the component model fulfilling the requirements of compatibility and equilibrium. Doing so it is assured that the joint model behaves exactly in the same way than the complex component model with respect to applied moments. Depending on the intended level of accuracy the assembly can be done for the main rotational key values only (initial rotational stiffness, upper moment resistance, rotation capacity) or for the full shape of the resulting $M-\phi$ curves.

As already mentioned the assembly of the sophisticated component model leads to iteration loops due to the complex interplay of components. These iterations are solved by the “joint characterisation” module of the computer program CoBeJo.

For simplification iterations can be avoided by using the simplified component model used in the Eurocodes, where the sum of all basic component springs can be derived by adding them step by step acting parallel or in series. However also in that case the “joint characterisation” module of the CoBeJo package proves to be a valuable tool to assemble the overall non-linear spring curves (and not only the initial elastic lines) step by step parallel or in series.

4.3.1.3 Joint classification (German: Knotenklassifikation)

After the joint response in terms of $M-\phi$ -curves has been derived with the help of the joint characterisation the engineer working in practice has now the possibility either to reproduce the so-gained joint behaviour in the global frame analysis using an advanced joint model or, simplifying, to determine whether already a conventional joint model (nominally pinned or nominally rigid) is able to reproduce the frame response with sufficient accuracy. Such a decision can be made with the help of a joint classification.

In view of the drastic increase of frame software capability the use of advanced joint models (as described in 4.3.1.5) will become more and more natural and therefore the need for a classification tool to fall back on conventional joint modelling will have less and less importance. Therefore the author proposes to get familiar now with the new concept of joint modelling reproducing the realistic joint $M-\phi$ -behaviour with (non-linear) springs and to refrain from the old-fashioned approach to regard joints either as nominally pinned or nominally rigid. Consequently, the joint classification is no more of interest.

When still aiming at conventional rigid or hinged joint models the joint characteristics in view of stiffness, strength and rotation capacity have to be compared to classification boundaries [36,49,60]. Depending on the method of global analysis either all or only one of the classification checks becomes decisive [49,60](Table J.2). So e.g. when using elastic-plastic global analysis a simple joint model (hinged) may be used in the case that the joint provides sufficient rotation capacity. In contrast to what is given in the code [60] its stiffness and strength are of minor importance in view of a safe design. A continuous joint model in elastic-plastic global analysis may be used if the joint can be classified to be quasi-rigid and to have full strength. Regardless of that the main problem is the definition of such classification boundaries for stiffness, strength and

ductility based on accuracy criteria for ULS (ultimate limit state) or SLS (serviceability limit state), which should generally be valid for any kind of frame configuration.

4.3.1.4 Curve idealisation (German: Kurvenidealisation)

Depending on the available software either the full non-linear shape of all joint-curves discussed until now or multi-linear simplifications of them can be assigned to the respective joint springs of the joint model. Fig.4-72 shows curve idealisations proposed in EC3 [60]. It is evident that the required input as well as the capability required from the software both increase if high accuracy is intended.

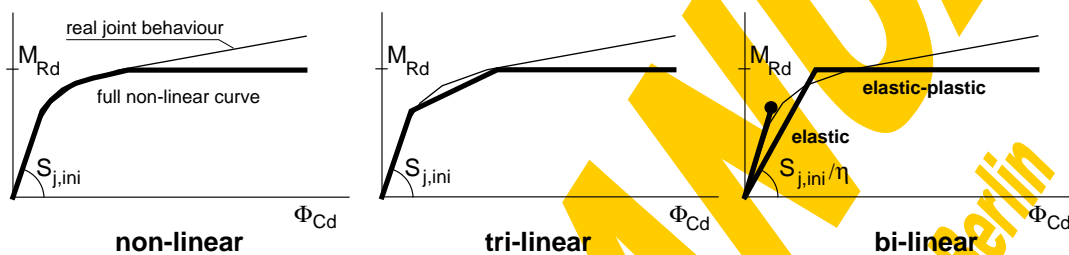


Fig.4-72 Possibilities of curve idealisation

The actual moment-rotation response of joints usually is described by means of a non-linear curve. However, the use of such non-linear curves requires sophisticated frame analysis programs. In order to enable a (more simple) linear calculation, e.g. an elastic global frame analysis (this is still the current practice in most European countries), the non-linear curve may be simplified by straight lines. As a conservative assumption each curve lying below the non-linear curve in general may be used in the frame analysis. For example a tri-linear curve is shown in Fig.4-72. The most simple curve is a bi-linear one. In order to use a bi-linear curve which provides the most efficient solutions, comparative studies were performed to calibrate an idealised joint stiffness S_j^* . The idealised joint stiffness S_j^* is constant for all values of applied moments smaller than the design moment resistance of the joint. The revised Annex J of EC3 gives guidelines on how to derive such a simplified bi-linear curve: The idealised joint stiffness S_j^* can be calculated by dividing the initial joint stiffness $S_{j,ini}$ with a stiffness modification factor η : $S_j^* = S_{j,ini} / \eta$.

The stiffness modification factor η depends on the type of joint (welded, bolted end-plate, bolted flange cleats, contact plate composite joint) and on the joint configuration (beam-to-column or other) and varies between 1.5, 2 and 3.5. Of course, if the applied moment does not exceed the values of $M_{j,elastic}$ ($2/3 M_{j,Rd}$), a reduction of the initial stiffness $S_{j,ini}$ is not required.

4.3.1.5 Joint modelling (German: Knotenmodellierung)

Linked to the joint characteristics there are three types of joint modelling which are closely linked to the method of global analysis and to the classification of the joint: A continuous joint ensures full rotational continuity, a semi-continuous joint ensures only partial rotational continuity and a simple joint prevents any rotational continuity between the connected members (Fig.4-73).

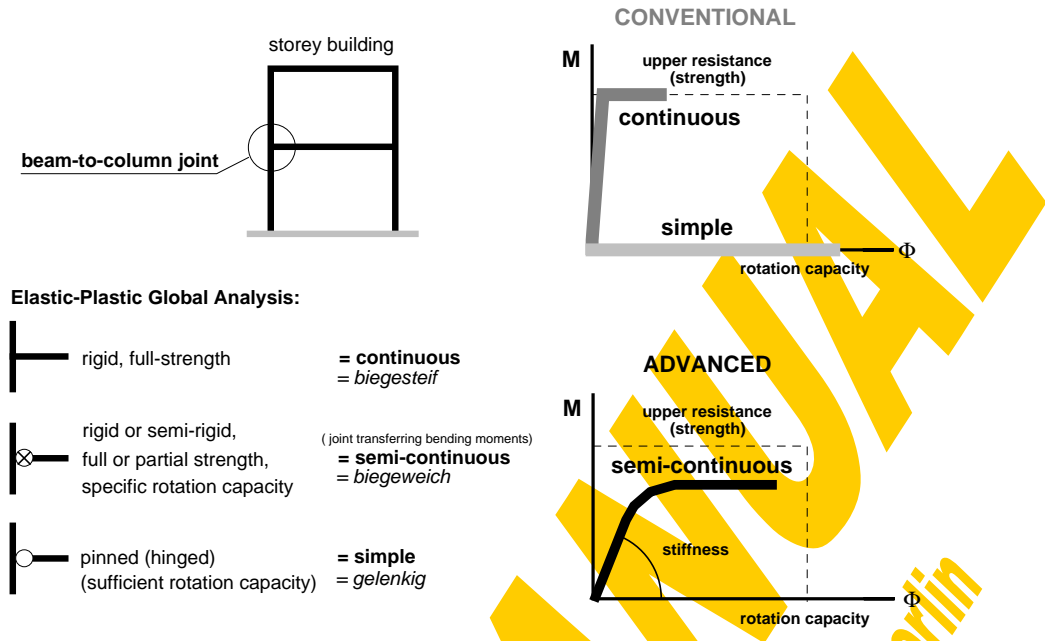


Fig.4-73 Joint modelling – conventional and advanced

It is true that the conventional simplifications of simple or continuous framing result in the advantage of a simple calculation. However as reality lies in between these extreme boundaries, in the age of rapid development of hardware and software it is appropriate to replace the conventional calculation methods by more realistic ones with the joints as additional members with finite dimensions. Depending on the required accuracy several possibilities of joint modelling for global structural analysis can be applied.

Joint modelling reflecting the actual behaviour

Within a joint two separate sources of deformation have to be distinguished – those due to the connection (load-introduction into the column through the connecting elements) and those due to the shear panel (column web panel in shear due to moment imbalance between the left and right hand sides). To reflect actual joint behaviour a cruciform joint configuration has to be modelled by two separate $M_L-\phi_L$ -curves representing the left and the right connection and one additional $M_S-\phi_S$ -curve (which can be derived from a $V-\gamma$ relationship) for the shear panel, see Fig.4-74.

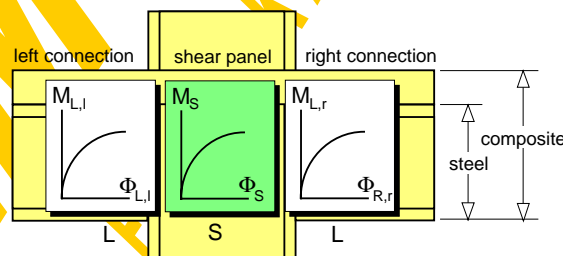


Fig.4-74 Joint modelling reflecting the actual behaviour

To reflect actual joint behaviour a single-sided joint has to be modelled by two separate $M-\phi$ -curves, one for the connection and one for the shear. Fig.4-75 illustrates

equally good possibilities of joint modelling reflecting the actual behaviour by so-called finite joint models.

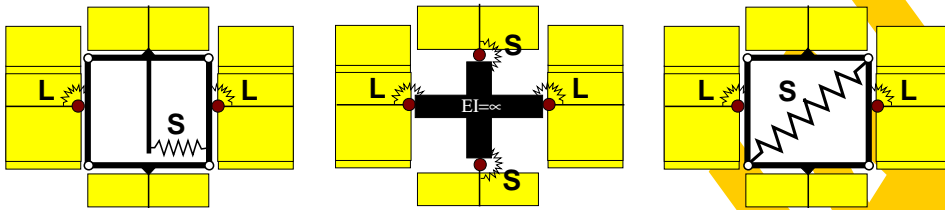


Fig.4-75 Application of joint modelling reflecting actual behaviour by finite joint models

Simplified joint modelling

For sake of simplicity a simplified joint model has been introduced in EC3 [60] for every-day design, where the nodal zone is no longer taken into account with finite dimensions. The aim is to represent the overall joint behaviour in one single rotational spring for each joint. Therefore simplifications are introduced as described below.

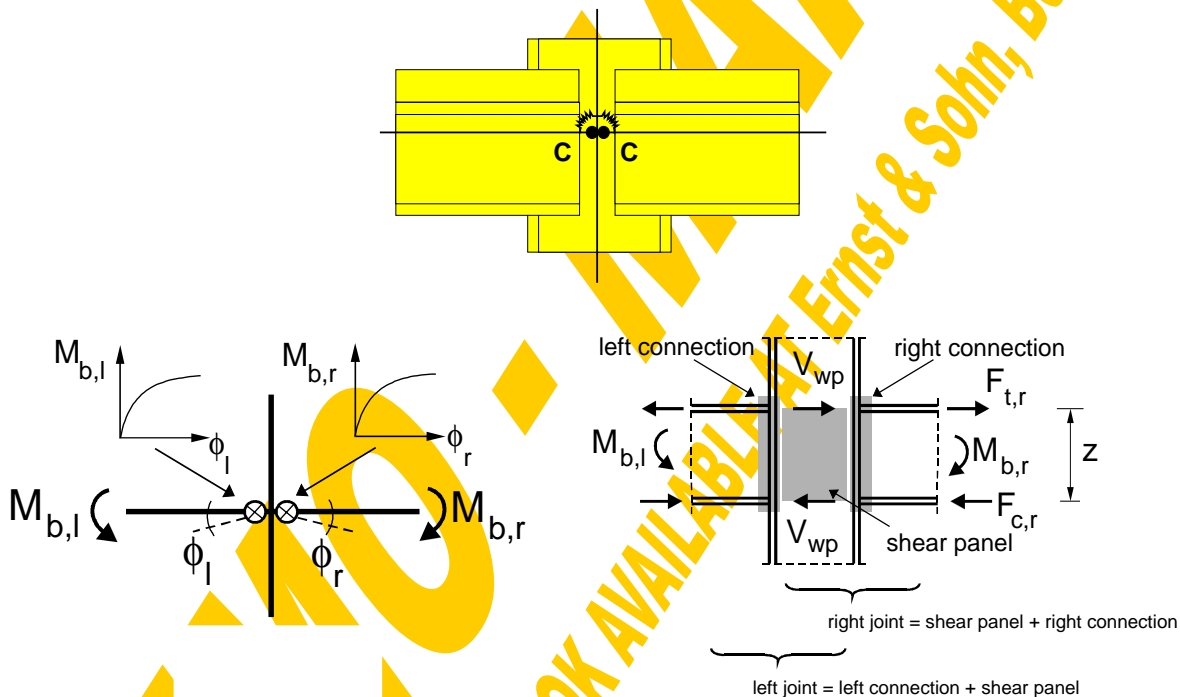


Fig.4-76 Modelling the web panel and the connections as combined rotational springs

The load-deformation ($V-\gamma$) curve of the column web panel in shear has to be converted into a moment-rotation ($M_s-\phi_s$) curve, using the lever arm z . However, the actual shear force V_{wp} in the column web panel is not equal to the "local" tension and compression forces within the connection ($F_c = F_t = M/z$, see Fig.4-76 and Fig.3-82), due to the "global" shear forces acting in the column. For the simplified modelling according to EC3 this effect is neglected. In case of a single-sided beam-to-column joint configuration, both the curve representing the web panel in shear and that for the connection are added in series to one combined $M-\phi$ -curve for the joint, see Fig.4-77. In case of a double-sided joint configuration, two separate but interacting joints may be

modelled. Each of these joints takes into account the behaviour of the column web panel as well as the behaviour of the relevant connection, see Fig.4-76. Thus, the web deformation would be taken into account twice but a so-called transformation factor β can be introduced to consider the actual loading of the shear panel in relation to the loading of the individual joints. The validity and accuracy of this procedure is demonstrated in [89].

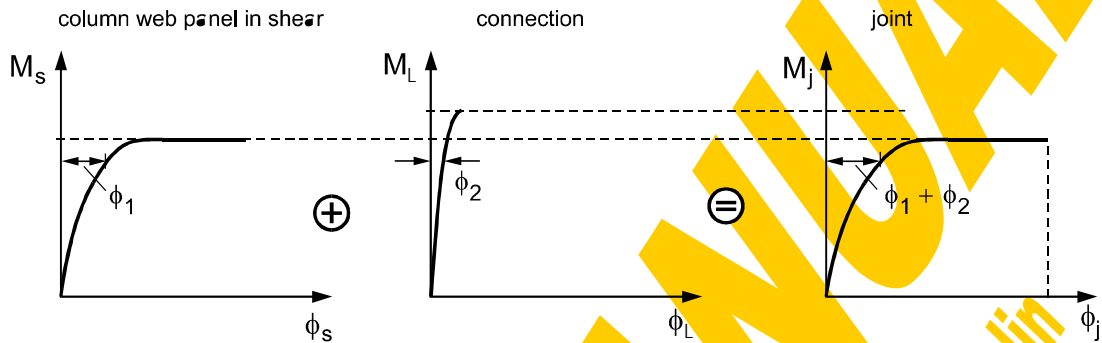


Fig.4-77 Derivation of a combined rotational spring for the simplified modelling

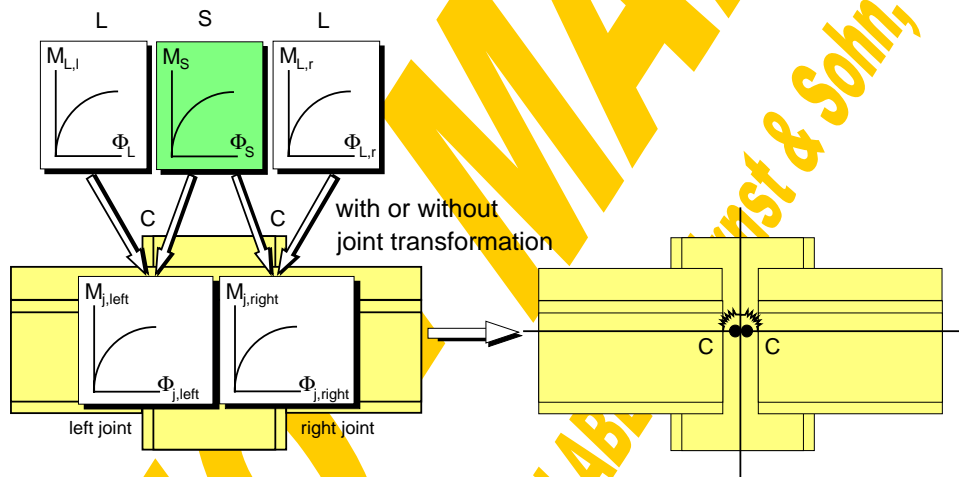


Fig.4-78 Application of simplified joint modelling by a concentrated joint model

The second difference between the models reflecting actual behaviour and the simplified models concerns the location of the rotational springs. In finite joint models the connection springs are arranged at the edges of the finite joint area, as shown in Fig.4-75. In the simplified joint model the combined joint springs for shear and connections are located at the beam-to-column axes intersection point, see Fig.4-76. It is obvious that the acting bending moment usually increases from the joint edge to the axis intersection point. The consideration of the larger value for the applied moment therefore leads to a more conservative design. On the other hand the flexibility of the extended beam and column stubs within the finite joint area adds an extra rotation to the joints leading to an overestimation of the global frame deformation. This simplification is the same as that, made in the conventional design where simple or continuous modelling is used. The influence of both effects becomes more important with increasing joint dimensions in comparison to the beam span and column height.

These effects can be compensated by a so-called "spring transformation" described in detail in chapter 3.9, which leads to additional refining terms within the formulae characterising the joint properties.

Substituting stub method

If the software for frame analysis does not support rotational springs as used for both finite and concentrated joint models they may be substituted by equivalent beam stubs with appropriate bending stiffness. The derivation of the equivalent stub stiffness is shown in Fig.4-79 assuming a constant bending moment along the stub. Thus less deviation to the actual behaviour is achieved if the stub is short.

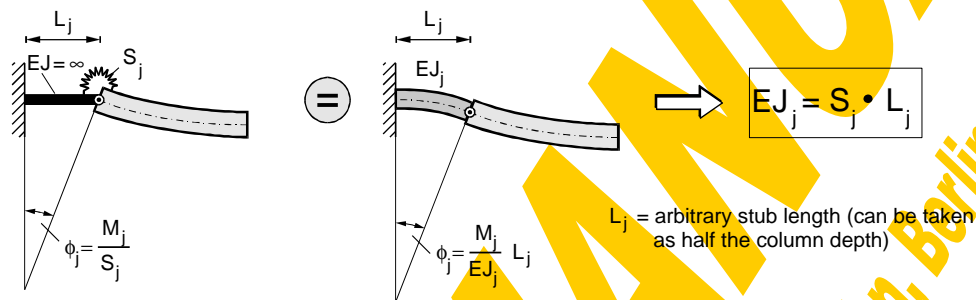


Fig.4-79 Equivalent stub instead of rotational spring

4.3.1.6 Summary

So far joints have been simplified by treating them either as fully continuous or as pinned in structural analysis. Joint detailing had to be adapted to these rough calculation assumptions, which could be expensive. Nowadays there is the opportunity to follow the opposite but much more efficient way: Economic joint types are developed first to ease construction and then their realistic behaviour is determined and taken into account within the global frame analysis. Thus, due to knowledge on joint representation and powerful software the working expenditure shifts from the construction to the cheaper calculation process. It is shown in Fig.4-80, how the moment-rotation behaviour of joints can be represented in structural analysis in a practical way.

It has been described briefly how to derive the joint's response (M - ϕ -curves), which forms the necessary input data for the frame calculation, focusing on the analytical approach – the so-called component method. Both, sophisticated models as well as the simplifications used in Annex J to Eurocode 3 and the intended corresponding Annex to Eurocode 4 have been discussed. However any new design method which involves even minor changes to existing practice will only be adopted if genuine and significant benefits can be demonstrated, justifying the increase of design efforts. Such benefits from semi-continuous frame design can be: A reduction of beam dimension in comparison to hinged girders and therefore a reduction of cladding costs and easier integration of services; and in comparison with continuous construction a remarkable reduction of construction and erection costs. Naturally these benefits gain importance

for unbraced frames. Furthermore it is important to be conscious that the acceptance of this new philosophy will be improved by providing design guidelines and every-day design aids like manuals, tables and software.

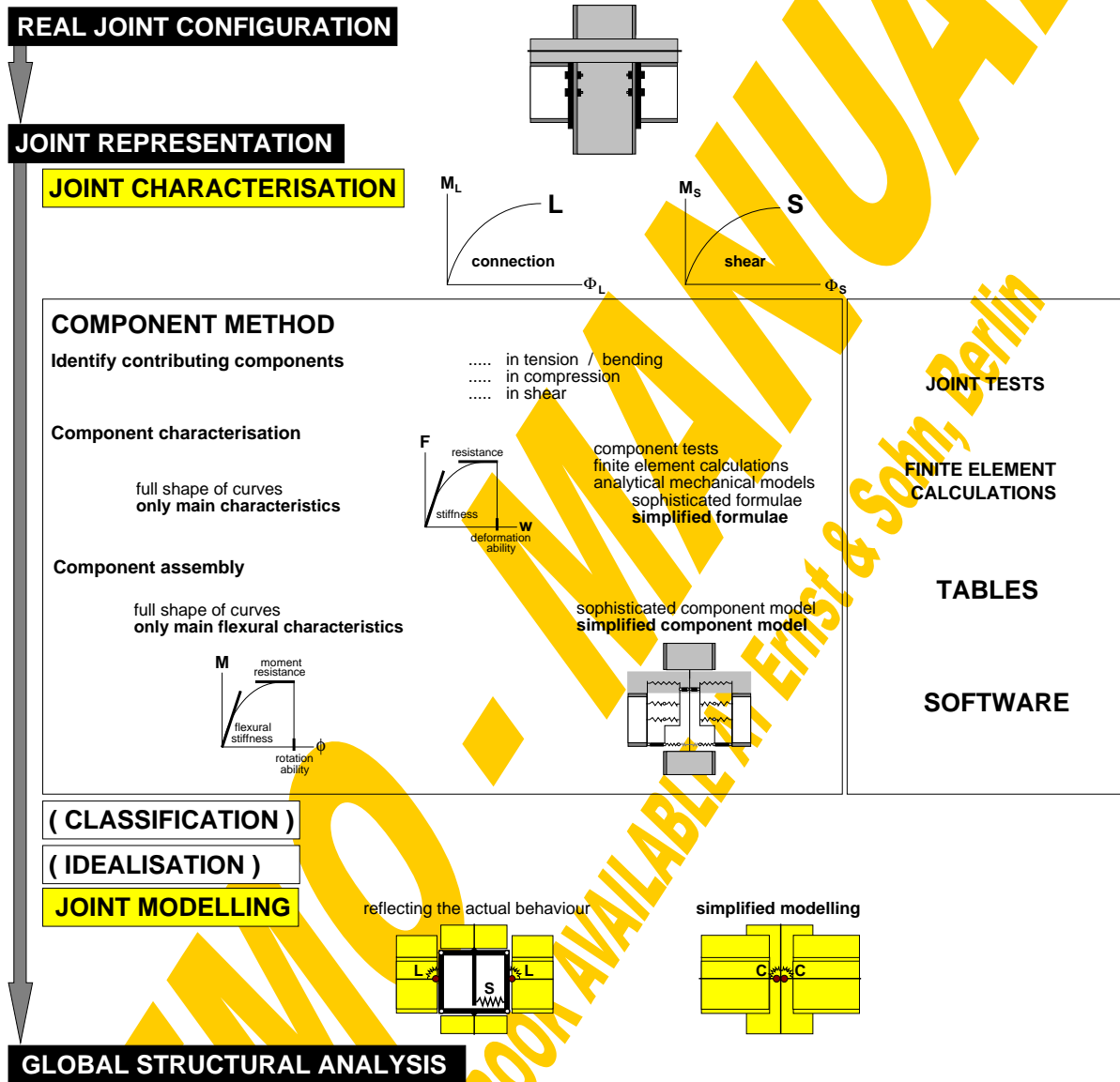


Fig.4-80 Practical procedure of joint representation in structural analysis

4.3.2 General

The module “Joint characterisation” of the CoBeJo-program package is a design aid, providing the joint curves on the basis of the analytical component method approach (Fig.4-81). It is assumed that the force-deformation behaviour of all contributing components in terms of F-w-curves is already known (from mechanical models, component tests, FE-calculations). The computer program iteratively assembles all these component curves fulfilling equilibrium and compatibility.

The reasons not to rely on an existing FEM program but to develop such a self-standing joint module have been:

- the high demands on pre- and post-processing especially adjusted to the joint characterisation problem
- the independence of such little disseminated and expensive programs
- the plan to integrate this iterative assembly procedure into the Module Bank Program [118] where the component characterisation is already done automatically based on mechanical models

This joint characterisation module should serve as a tool both for scientists and advanced practitioners to “play” with different joint configurations and so to improve acceptance of the new joint representation philosophy. Therefore special attention has been directed to a clear graphical display of the gained results and also to the coherence between individual component characteristics and the joint response. Differently to FEM-programs the solution of this non-linear spring assembly problem in the CoBeJo-Joint-module is solved iteratively with an energy criterion step by step considering the load history and not using a step by step modified stiffness matrix.

The main task of the CoBeJo-Joint-module is the full assembly of non-linear translational component springs to an overall joint response including post limit effects of the contributing components as well as failure of individual components. In the future this tool should give the following possibilities to researchers:

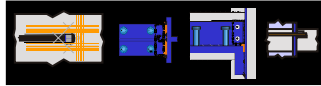
- Comparison between different assembly methods due to different component models (see Fig.4-70)
- Comparison between the full spring assembly and the assembly in view of the key values stiffness and strength only
- Check of curve idealisation methods
- Influence of overstrength effects of single components on the overall joint behaviour (especially in view of rotation capacity for different failure modes)
- Study of failure modes
- Investigations in view of available rotation capacity

Within the scope of this work the assembly has only been realised for symmetrically loaded joints ($\beta=0=1-M_{\text{left}}/M_{\text{right}}$). Later on also fully unbalanced joints ($\beta=1$) should be covered. Further it is assumed that the joint configuration in view of contributing components and their behaviour is symmetrical and that the joint is subjected to hogging bending only.

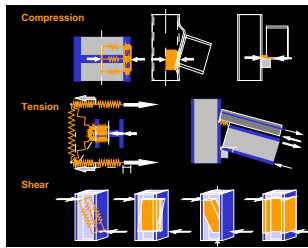
The general structure of the module can be taken from Fig.4-82.

Joint Characterisation
based on the Component Method

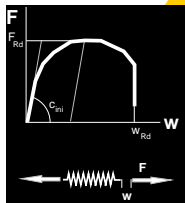
Joint Configuration



Component Identification

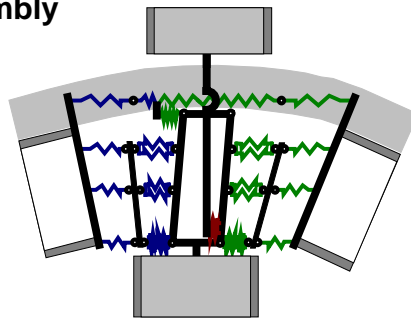


Component Characterisation



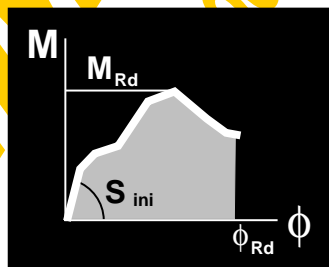
e.g. based on analytical mechanical models

Component Assembly



iteratively fulfilling equilibrium and compatibility

Joint Response



Module Bank Program

**CoBeJo
Joint**

Fig.4-81 Joint characterisation using CoBeJo-Joint

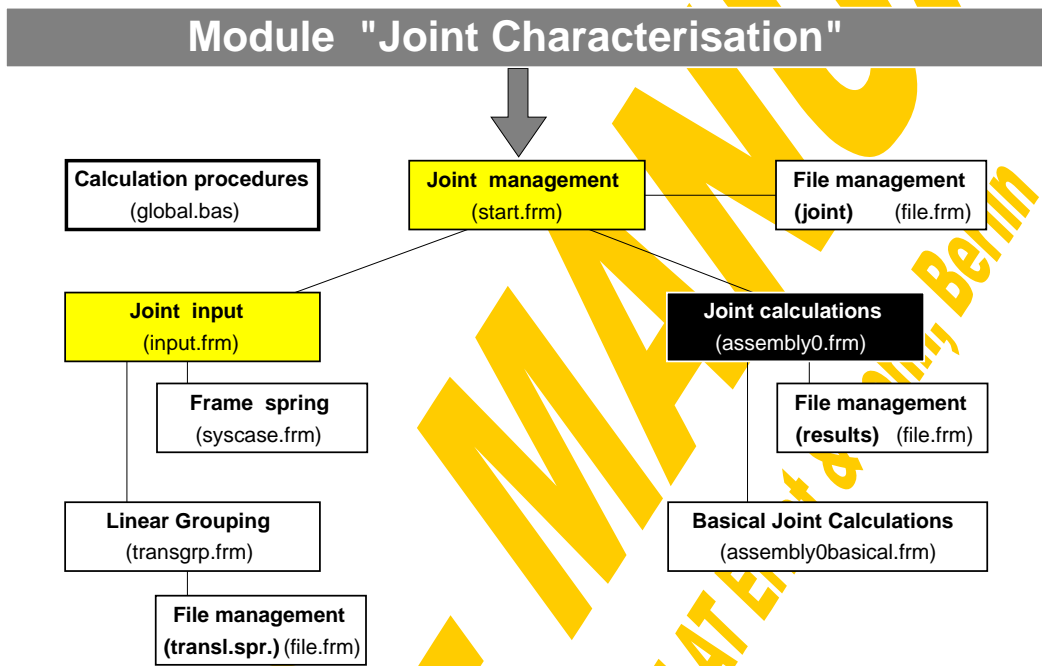


Fig.4-82 Structure of the module "Joint Characterisation"

4.3.3 Joint management

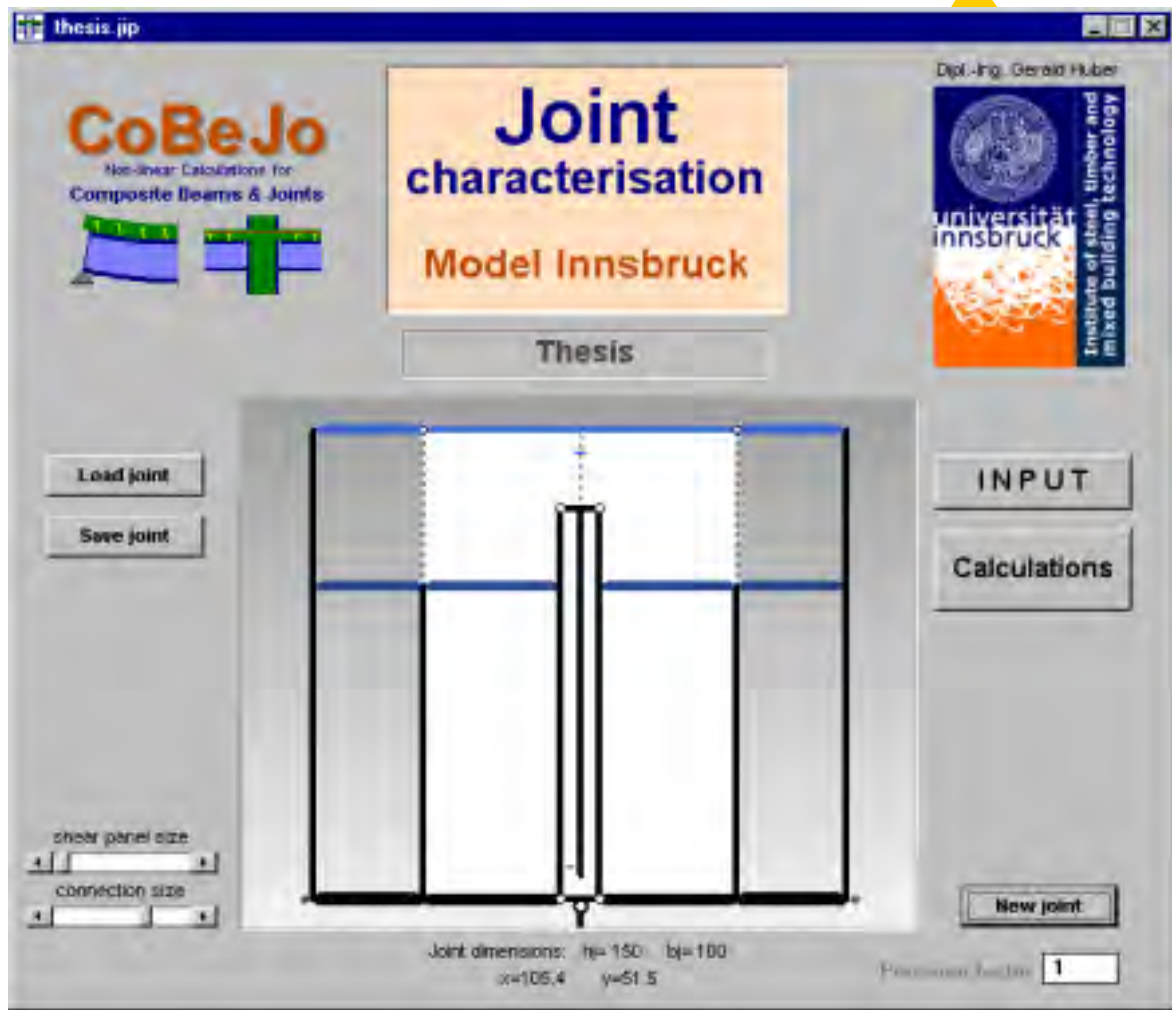


Fig.4-83 Start-up window of the module "Joint Characterisation" (start.frm)

Fig.4-83 shows the start-up window of the module "Joint Characterisation". It serves for the file-management of joint data and gives the link to the windows for the joint input and the joint calculation (assembly for $\beta=0$: balanced joint loading). A special joint configuration (see Fig.4-84) consisting of one steelwork row in tension and one layer of slab reinforcement in tension has been chosen for the following examples.

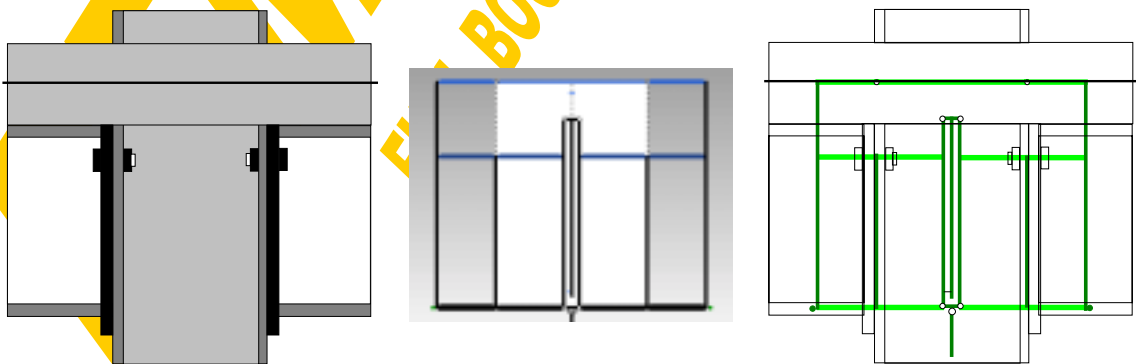


Fig.4-84 Example joint configuration

An image box in the centre of the start-up window shows the actual joint configuration as a symbolic sketch (Fig.4-85). The white area marks the joint area. Stiff separation bars are drawn at the boundaries to the adjacent beams (sb1) and in view of the steelwork rows between the connecting elements and the elements subjected to load introduction into the web panel (sb2). The bars sb2 are located directly at the joint edges (white area), the bars sb1 and therefore also the area of the connecting elements for illustrative reasons fictitiously is extended into the beam area (in reality the distance between the bars sb1 and sb2 is zero). With the scroll bar "connection size" this illustrative ratio between the fictitious size of the connecting elements and the joint width can be adjusted between 1/60 and 1/2. An analogous illustration method has been chosen for the web panel in shear. Strictly the components subjected to load introduction into the web panel and those of the web panel in shear (in case of moment imbalance) are sharing the same area within the joint. To avoid any misleading overlap of component springs the joint width (white area) fictitiously is shared between the load introduction and the shear components. Again the illustration ratio between the shear panel size and the joint width can be adjusted between 2/10 and 2/1.1 with the scroll bar "shear panel size". As described in detail in chapter 3.4 the following components may be identified within a joint configuration:

<i>Component</i>		<i>basic components acc. to Fig.4-71</i>
A	Web panel in compression	1,2,3,4
B	Beam flange in compression	5
C	Web panel in tension	6,7
D	Connecting elements in tension	8,9,10
E	Reinforcement within the <i>full</i> column depth in tension	11
F	Redirection of unbalanced forces	13a-g
G	Slip between steel beam and slab at the column front	12
H	Shear influence	14,15,16
Sys	Flexibility of the adjacent columns or the frame system	

Each of these components symbolically is drawn as a horizontal bar at the height of its relevant lever arm. The drawing width of the bars represents the stiffness ratio between the several components and the colour of the bars represents their strength: light blue means relatively low strength, black means relatively high strength. (The system spring Sys is not considered for these illustrative ratios.) This should ease a first check of the given joint data. The described joint module of CoBeJo enables the input of up to 5 rows of steelwork connections (springs C,D) and 2 layers of reinforcement (springs E,F,G). Finally the coupling height between the joint as a whole and any adjacent beam member has to be defined for a semi-continuous global beam analysis with beam and joint elements placed one behind the other (this module will follow in the future).

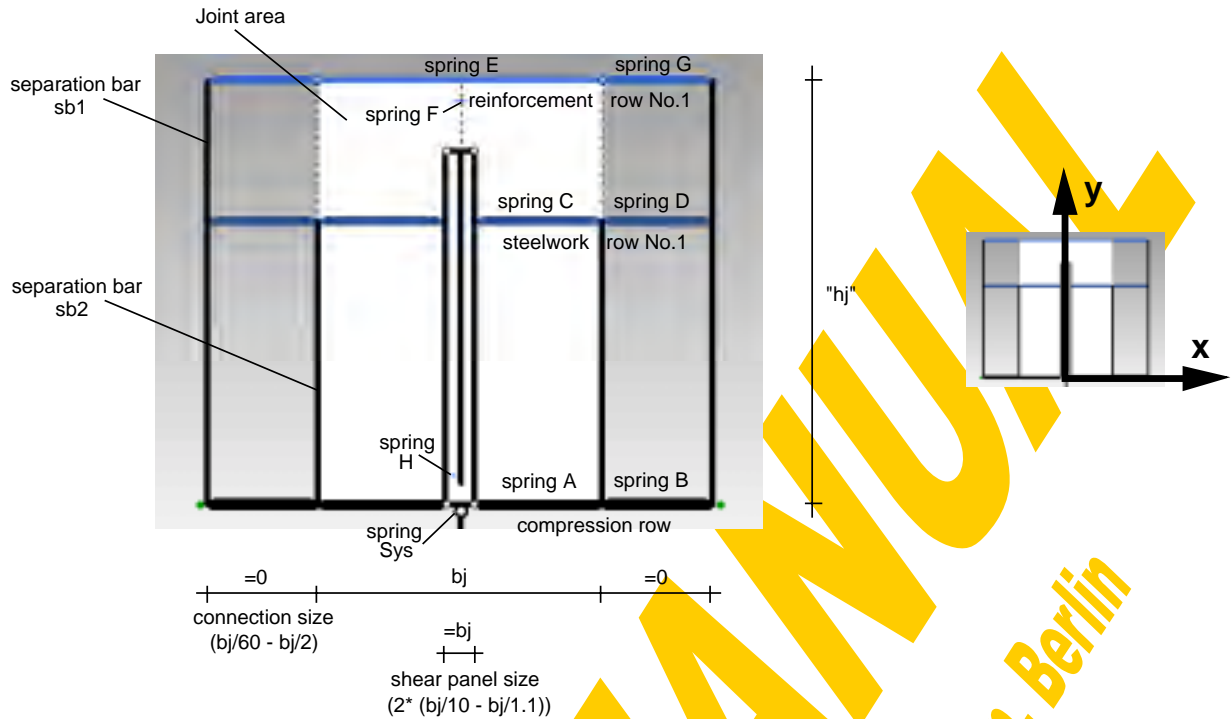


Fig.4-85 Joint configuration sketch

All joint data including joint name, joint-ID, joint width, height of coupling point and all identified components with their force-deformation behaviour and relevant lever arms are saved to a file with the default-extension “*.jip”. The input file of the example joint can be seen on page 263. Clicking on the “Load joint” or “Save joint” buttons activates the window for the file management (Fig.4-86). Apart from the possibility to load or save joint data buttons are provided for a small variety of disk manipulations like “Create Directory”, “Remove Directory”, “Rename File”, “Copy File” and “Delete File”.

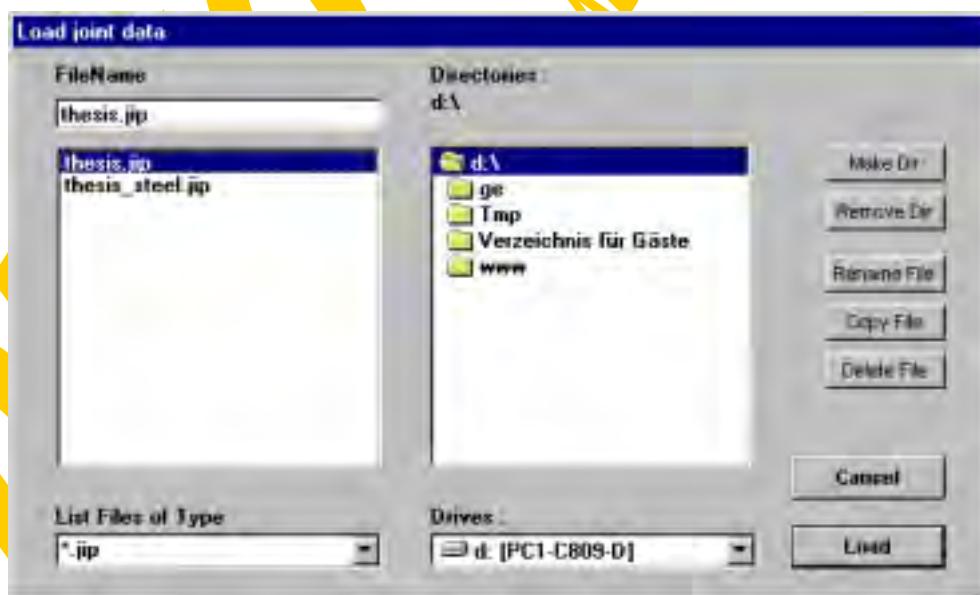


Fig.4-86 File management (file.frm)

Before saving, before calculating and after loading a joint configuration an automatic joint check will be done with a final message box summarising all noticed errors and warnings. In the following an enumeration of the checked data is given:

error checks (in case of errors no calculation will be allowed):

- complete compression row (springs A+B)?
- at least one complete tension row (springs C+D or E+F)?
- existing incomplete tension row?
- slip spring given for both reinforcement rows or for none?
- defined shear spring?

warning checks (in case of warnings a further calculation is possible):

- slip spring defined for reinforcement row (otherwise slip value has to be given)?
- lever arm of reinforcement rows higher than that of steelwork connections?
- comparison between joint height and effective lever arm of shear panel?
- defined system spring (otherwise it will automatically be set infinitely stiff)?

It was generally tried to keep the program self-explaining, anyway also the other possible operations within the start-up window at least should be mentioned here. A special text field is reserved for a joint name and the button "New joint" deletes the actual joint input. While moving the mouse pointer over the joint sketch the actual position (width, height) is indicated.

Finally it should not be forgotten to mention the precision factor, which as default value is set equal to one. Generally all accuracy pre-settings within the iteration loops have been defined as a compromise between precision and calculation time. For each iteration result at the end the final error will be declared. So if this indicated error should exceed the desired limits the accuracy might be improved by raising this precision factor.

The button "Joint input" or "Calculations" will close the start-up window and open that for the joint input or the joint calculation, which will be described in detail in the following chapters.

Input file: thesis.jip

Joint data		dimensions: kN, mm
Thesis		keyword
Joint-ID	990319183637	joint name
Check-indicator	1	identification for coherence between input and result files
joint width	100	indicates successful joint check
Coupling point y=	0	b_j
		height of coupling point to beam elements

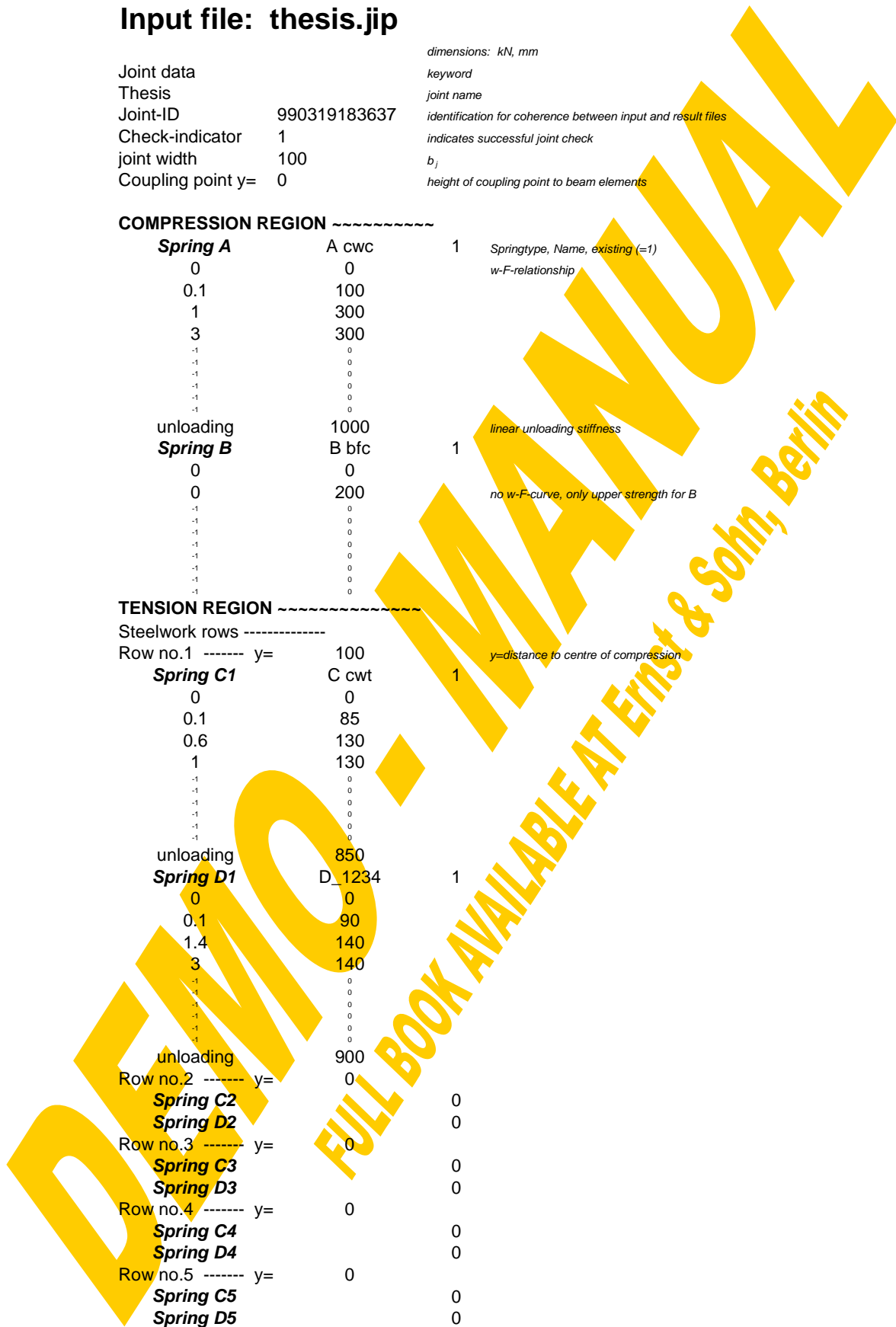
COMPRESSION REGION ~~~~~

Spring A	A cwc	1	Springtype, Name, existing (=1)
0	0		w-F-relationship
0.1	100		
1	300		
3	300		
-1	0		
-1	0		
-1	0		
-1	0		
-1	0		
unloading	1000		linear unloading stiffness
Spring B	B bfc	1	
0	0		no w-F-curve, only upper strength for B
0	200		
-1	0		
-1	0		
-1	0		
-1	0		
-1	0		
-1	0		
-1	0		

TENSION REGION ~~~~~

Steelwork rows -----

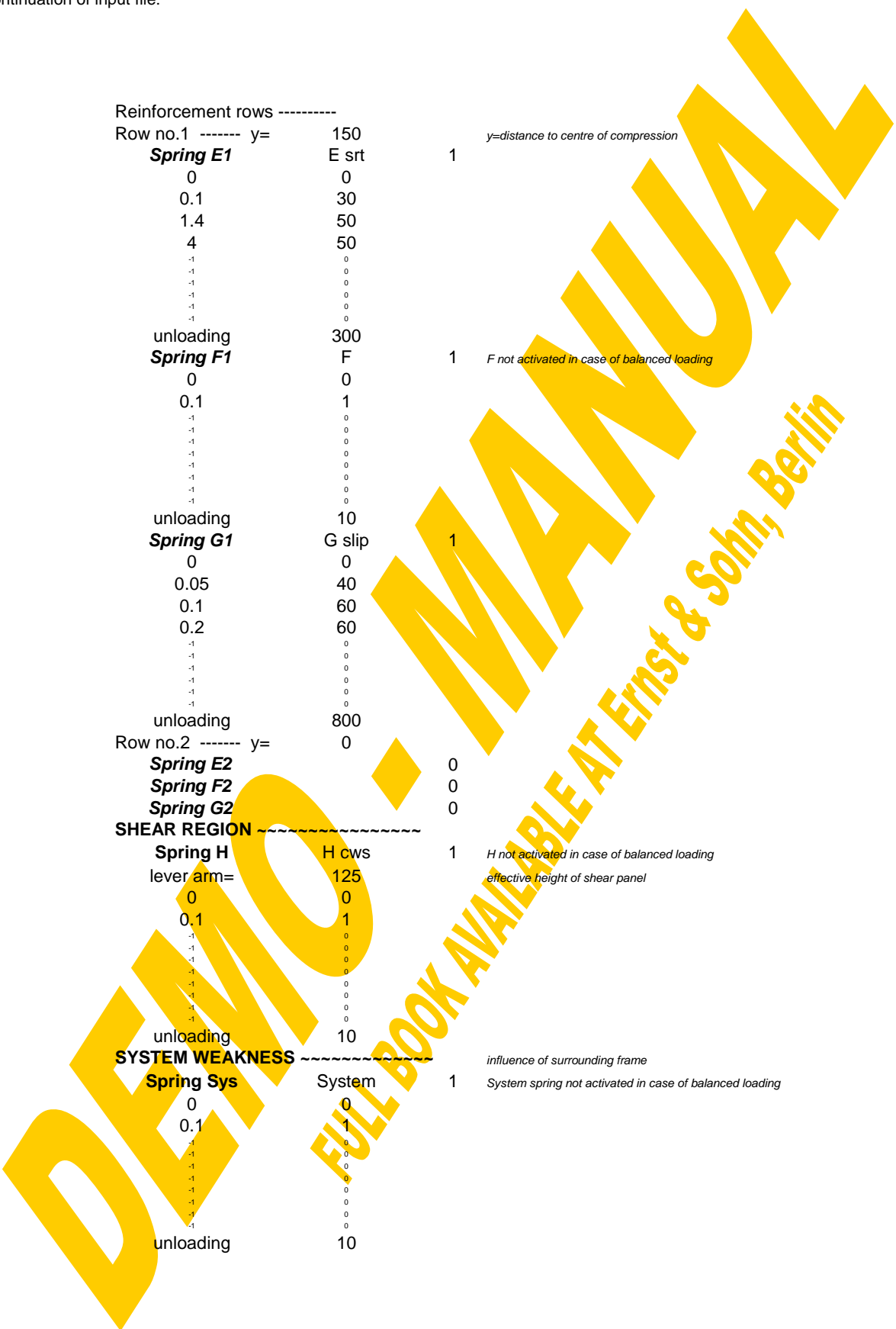
Row no.1 ----- y=	100		y=distance to centre of compression
Spring C1	C cwt	1	
0	0		
0.1	85		
0.6	130		
1	130		
-1	0		
-1	0		
-1	0		
-1	0		
-1	0		
unloading	850		
Spring D1	D_1234	1	
0	0		
0.1	90		
1.4	140		
3	140		
-1	0		
-1	0		
-1	0		
-1	0		
-1	0		
unloading	900		
Row no.2 ----- y=	0		
Spring C2		0	
Spring D2		0	
Row no.3 ----- y=	0		
Spring C3		0	
Spring D3		0	
Row no.4 ----- y=	0		
Spring C4		0	
Spring D4		0	
Row no.5 ----- y=	0		
Spring C5		0	
Spring D5		0	



Continuation of input file:

```

Reinforcement rows -----
Row no.1 ----- y=      150      y=distance to centre of compression
Spring E1      E srt      1
  0              0
  0.1            30
  1.4            50
  4              50
  -1             0
  -1             0
  -1             0
  -1             0
  -1             0
  unloading      300
Spring F1      F          1      F not activated in case of balanced loading
  0              0
  0.1            1
  -1             0
  -1             0
  -1             0
  -1             0
  -1             0
  -1             0
  -1             0
  unloading      10
Spring G1      G slip    1
  0              0
  0.05           40
  0.1            60
  0.2            60
  -1             0
  -1             0
  -1             0
  -1             0
  -1             0
  unloading      800
Row no.2 ----- y=      0
Spring E2      0
Spring F2      0
Spring G2      0
SHEAR REGION -----
Spring H      H cws      1      H not activated in case of balanced loading
lever arm=      125      effective height of shear panel
  0              0
  0.1            1
  -1             0
  -1             0
  -1             0
  -1             0
  -1             0
  -1             0
  -1             0
  unloading      10
SYSTEM WEAKNESS -----
Spring Sys    System     1      influence of surrounding frame
  0              0
  0.1            1
  -1             0
  -1             0
  -1             0
  -1             0
  -1             0
  -1             0
  -1             0
  -1             0
  unloading      10
  
```



4.3.4 Joint input

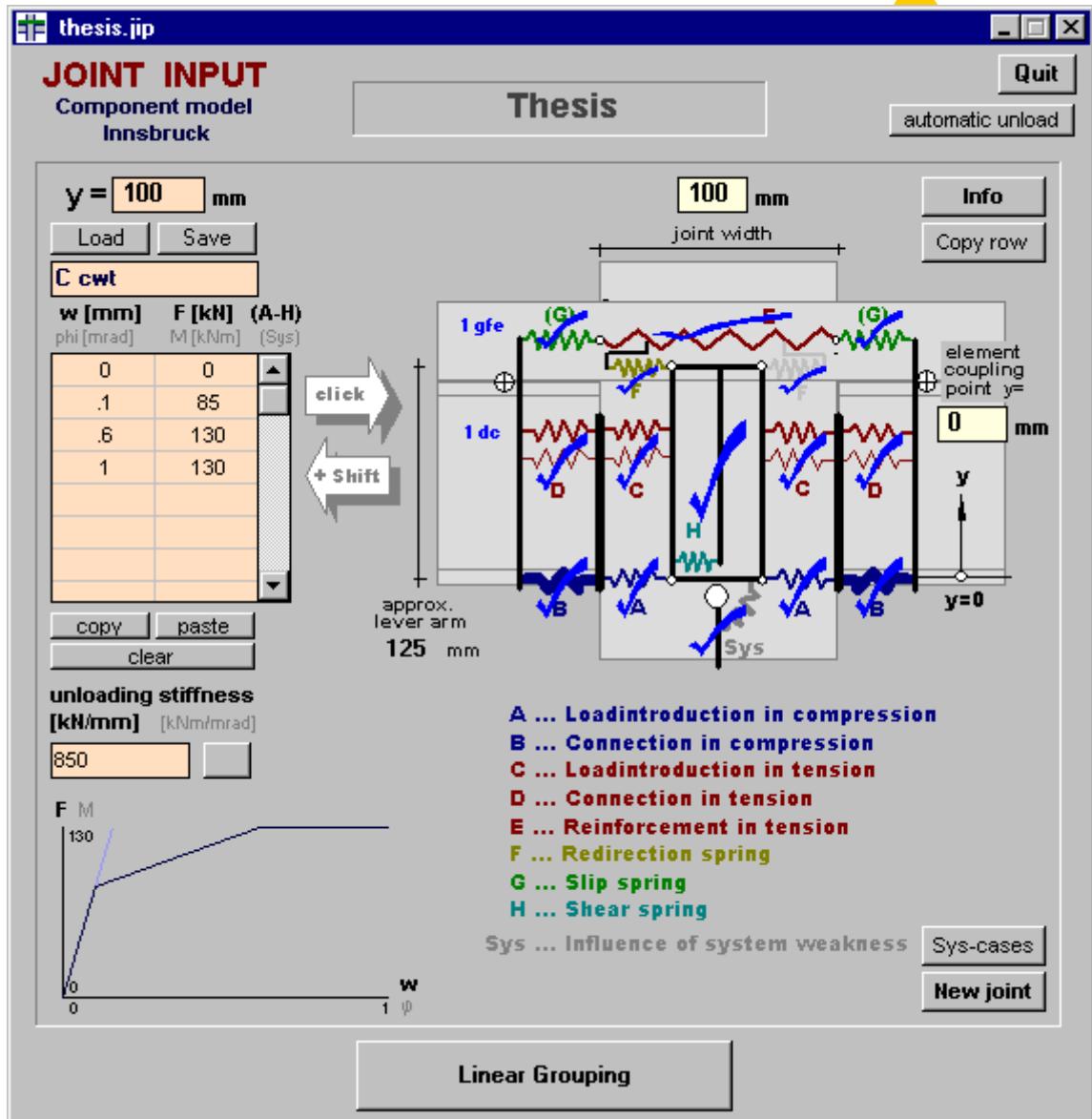


Fig.4-87 Window for the input of the joint configuration data (input.frm)

The window shown in Fig.4-87 enables the input of the joint configuration data. The following self-explaining options are available: definition of a joint name by a text box, with "New joint" all actual data can be deleted to start with a new joint configuration and the "Quit"-button closes the input window and leads back to the start-up window.

The "info"-button provides the user with some general information about the meaning of the component springs A-H and Sys:

- A Web panel in compression
- B Beam flange in compression (infinitely stiff, limited resistance, see Fig.4-88)
- C Web panel in tension
- D Connecting elements in tension (beam flange and endplate in bending, bolts in tension,...)

- E Reinforcement within the *full* column depth in tension (pay attention: the spring E spans over the whole joint width b_j and not only over $b_j/2$)
- F Redirection of unbalanced forces (only acting in compression; therefore only on less heavily loaded side). The spring characteristic itself is independent of the load ratio left/right (see Fig.3-12: spring $13=F$ for fully unbalanced situation $\mu=1\approx\beta$)
- G Slip between steel beam and slab at column front.
For an isolated joint characterisation an assumption has to be made for the w-F characteristic of this slip spring representing the weakness of the horizontal shear joint between the steel beam and the concrete slab outside of the joint area itself. F is equal to the internal shear force N_i (see 4.2.5) and w is the corresponding slip value, both at the beam end (=joint edge). So this w-F characteristic of spring G would have to be derived by a sophisticated or simplified beam calculation considering incomplete shear interaction (see 1.4.5 and Fig.3-13). Strictly there is an interaction between the beam and the joint response and therefore only an overall semi-continuous beam-including-joint analysis would give really realistic results. Such a tool will be provided by the third CoBeJo module "Global Analysis" (see Fig.4-1) combining beam and joint elements. There the slip will be derived as the difference of the displacements between beam and slab along the whole beam span. This slip value then will be taken for the corresponding joint characterisation ignoring any defined w-F-relationship. So only for such an overall analysis no slip response G has to be entered.
- H Shear influence. Strictly depending on the actual lever arm z, which here is assumed to be constant during joint moment increase. The correct lever arm could be derived from

$$z = \frac{M}{F_{\text{compression}}} = \frac{M}{\sum F_{\text{tension}}}$$

- Sys Flexibility of the adjacent columns. For a bare joint analysis this system spring has to be set infinitely stiff.
For really detailed information on the individual components it is referred to chapter 3.4 herein.

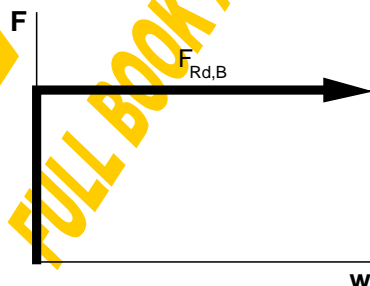


Fig.4-88 Response of compression spring B

Now the definition of the joint input data will be described: Both for joint sketches true to scale and for a final integration of joint elements into semi-continuous beam

calculations (planned for the future) the joint width b_j [mm] has to be entered. For the later assembly of joint and beam elements the vertical distance between the coupling point and the compression row has to be given as “element coupling point” [mm].

Then the data of each identified component A-H has to be defined, including the lever arm, the force-deformation response and the unloading stiffness. (For further calculations in the case of balanced loading ($\beta=0$) the components F,H and Sys have no influence on the results as they would only contribute in the case of moment imbalance. Despite at least some fictitious data have to be entered to enable a successful joint check.) Pay attention: if the overall $M-\phi$ behaviour should be studied at the design level already the $F-w$ curves of the contributing components should be given on the design level including safety-factors. Reversely giving characteristic component curves results in characteristic joint curves and giving actual component curves (e.g. from test results) leads to actual joint curves.

Fig.4-89 shows the corresponding tools for this component input within the joint input window.

The screenshot shows a software interface for entering component data. It includes the following elements:

- Lever arm:** A text input field with the value "100" and the unit "mm".
- Name:** A text input field containing "C cwt".
- w-F response:** A table with columns for deformation (w [mm]), force (F [kN]), rotation (phi [mrad]), and moment (M [kNm]). The first three rows contain data: (0, 0), (.1, 85), and (.6, 130). The fourth row shows (1, 130). The remaining rows are empty.
- Unloading stiffness:** A text input field with the value "850" and the unit "kN/mm".

Fig.4-89 Component spring data

Except for the compression row (components A and B) and the shear spring H the lever arm of the actual component has to be defined being the vertical distance to the centre of compression (positive value). Then a name may be defined for the actual component, followed by the input of the force(F [kN])-deformation(w [mm]) response by the help of a grid box with up to ten rows (so the non-linear shape of a component's w - F -curve is restricted to a polygon with at maximum ten nodes). (By way of exception for the compression spring B not a polygon but only an upper strength value has to be entered; the response of spring B will then be set infinitely rigid with a ductile plastic plateau at the given strength limit; see Fig.4-88.)

Within a spring data check it will be inspected if the following principles are fulfilled:

- the w-F-curve must start with $w=0 / F=0$
- at least one further w/F-point has to be given
- the w-values must be increasing from one row to the next (monotonous curve)
- the F-values must be positive

With the button “Save” the actual w-F-curve can be stored to a spring file (*.spr) in the format shown in Fig.4-90. So the w-F-curve of the actual component may either be entered directly value by value or such a saved spring curve can be loaded. The “Load” and “Save” buttons will activate a file management window quite similar to that for the handling of joint files shown in Fig.4-86. Further there is the possibility to use the MS Windows Clipboard for a data exchange to other applications (e.g. MS Excel). For that purpose the buttons “Copy” and “Paste” have been provided. Concerning both the load and paste command it will be checked automatically if the new curve starts with $w=0/F=0$ and in the case of very long numbers eventually some digits behind the comma may be cut. With “Clear” the whole w-F-curve can be deleted. Concerning the manual input of values within the w-F-grid the following actions are possible: the desired grid element may be chosen using the cursor buttons or the mouse, then the value has to be defined using the number keys and the dot “.” as decimal separator. Enter leads you to the next grid box. With the delete button on your keyboard all marked grid elements will be reset. A single mouse click on a grid element activates the overwrite mode, whereas a double click enables to modify an already entered grid value, e.g. using the backspace key.

Finally the unloading stiffness [kN/mm] has to be defined, which normally is equal to the initial (elastic) stiffness of the curve (this can be done automatically using the button beside the input box).

To ease checking of the actual input values a true to scale sketch of the w-F-curve will be drawn below the input boxes. An automatic refresh is performed after each input modification. The unloading stiffness is visualised by a light blue line through the origin.

Spring file: c.spr

C	cwt	Spring name
0	0	w-values [mm] , F-values [kN]
0.1	85	
0.6	130	
1	130	

Fig.4-90 Spring file *.spr

After all data of a contributing component has been entered this information just has to be assigned to such a component by a single mouse click on the relevant area within the component model sketch (Fig.4-91). For the tension springs C,D,E,F,G additionally also a row number has to be given. A hook and a different mouse pointer then are indicating a successfully defined component. As any joint is assumed to have a symmetrical component configuration both components (left and right side) are defined

with only one click on one of both sides. By assigning an empty w-F-box to a component this component will be removed.

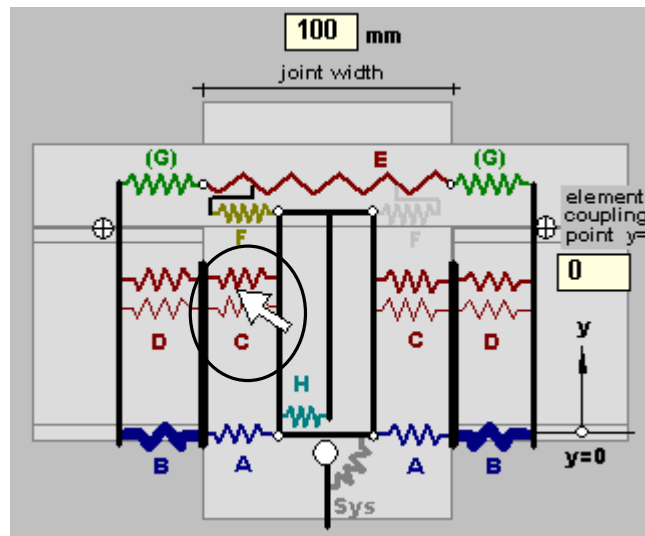


Fig.4-91 Component assignment by a single mouse click

As the w-F-values of the shear spring H have to be converted into ϕ -M-values an estimated lever arm z has to be entered ($\phi = w/z$, $M = F \cdot z$). Strictly the lever arm of the shear panel changes during load increase and therefore also the shear response strictly would have to be adopted to that, however this normally minor influence will be neglected.

As mentioned before with a mouse click the data within the input boxes (lever arm, spring name, w-F grid and unloading stiffness) will be assigned to one of the components. Pressing "SHIFT" while clicking on a component (Fig.4-91) causes the reverse: the stored data of the relevant component is copied to the data boxes. This can be used for component checking, copying or for modifications of the component response or the lever arms. Pay attention to the fact that the component actually only will be modified after the modified data has again been assigned to it with a single mouse click on the same component (without shift button). Completed tension rows can be copied with the "Copy row" button. "Automatic unload" adjusts the unloading stiffness of all actually stored components to their initial stiffness.

The system spring Sys has a special meaning not directly related to the joint behaviour itself. Therefore it is only of interest for a semi-continuous beam calculation using an assembly of beam and joint elements. This spring takes into consideration all flexibilities coming from the columns or even the frame system adjacent to the joint. So for a bare joint calculation this stiffness has to be set infinite (will be done automatically if no ϕ -M-values are defined). The ϕ [mrad]-M[kNm] response either can be entered directly using the input grid (also M values must be monotonous) or use can be made of a special calculation window shown in Fig.4-92. Three types of column support conditions are available. By giving the necessary values h_a , h_b , EI_a and EI_b the corresponding system stiffness S will automatically be calculated. "Accept"ing this stiffness will add a ϕ -M row to the input grid of Fig.4-89 ($\phi = 1 \text{ rad}$, $M = S \cdot \phi$) and assign this

data automatically to the system component in Fig.4-91. If $S=0$ the stiffness will be set infinite.

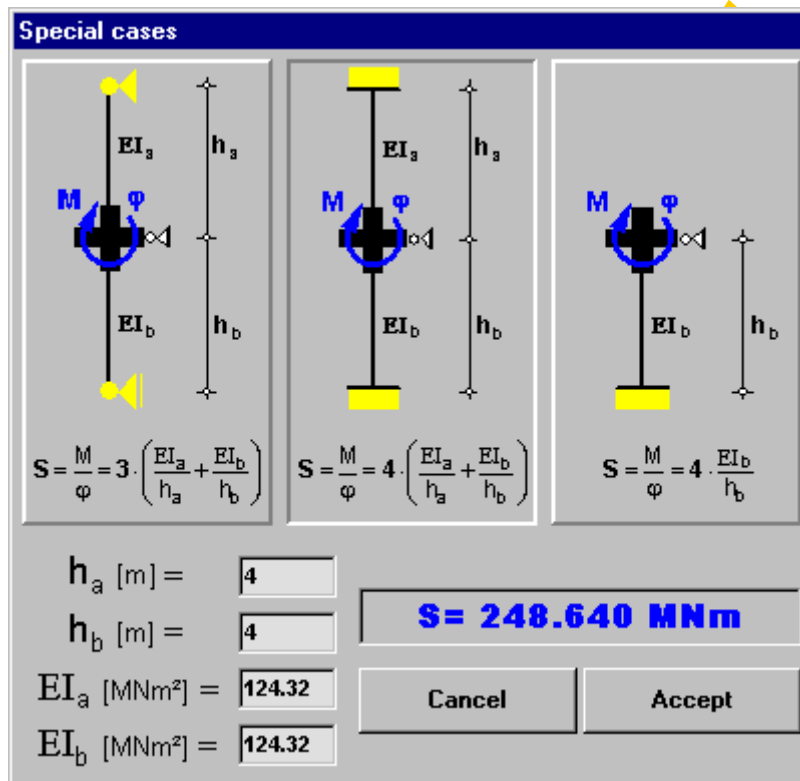


Fig.4-92 Calculation window for the system stiffness (syscase.frm)

It should not be forgotten to mention that by saving a joint in the start-up window (Fig.4-83) it will get a unique joint-ID (identification number), representing the exact saving time. This enables a clear assignment between joint data files and result files later on. For that reason the actual joint-ID gained by saving or loading a joint configuration will be lost again if the joint data is already slightly modified with the help of the input window.

Finally there remains the button "Linear grouping" which closes the input window and leads to the window for linear grouping of translational springs.

4.3.5 Linear Grouping

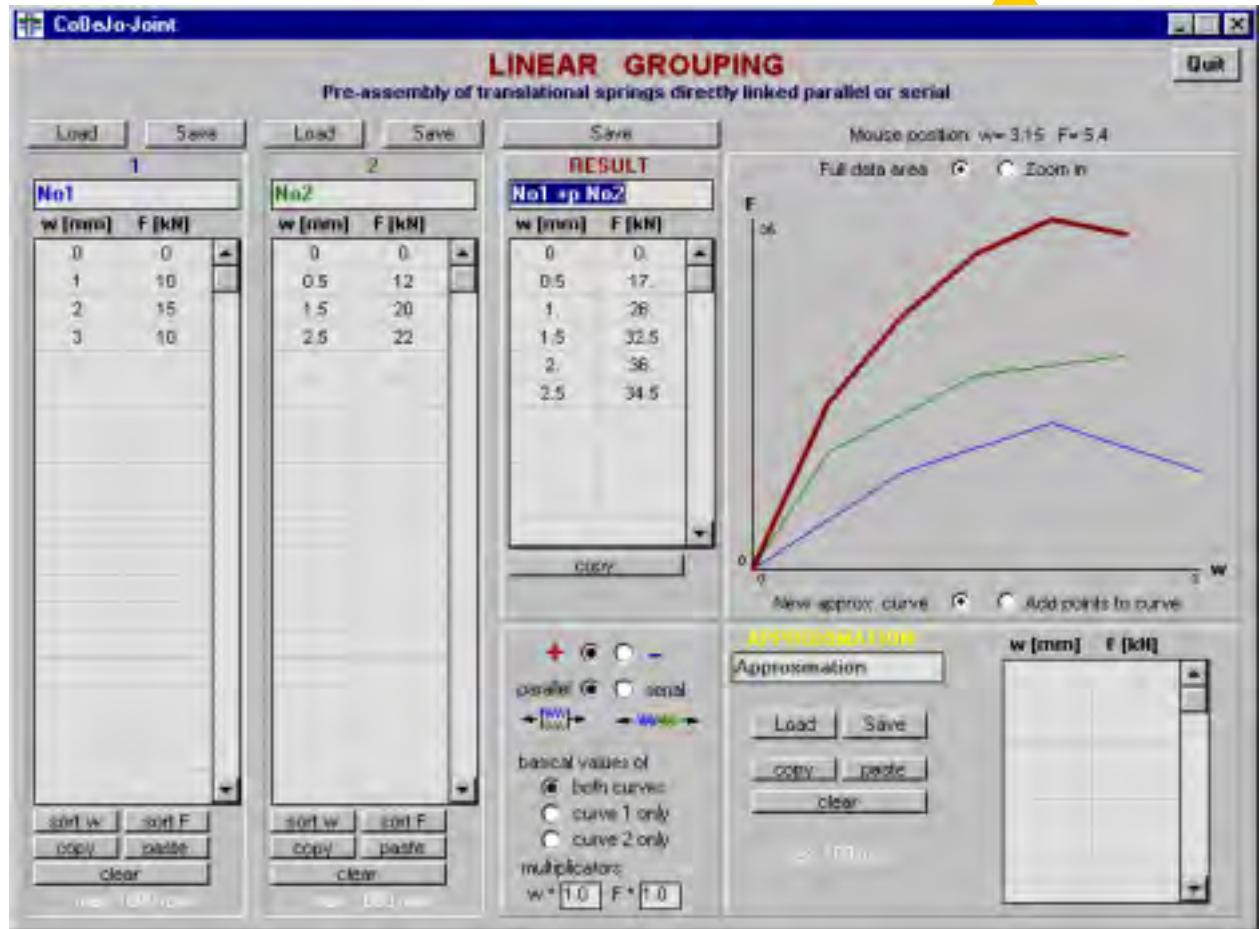


Fig.4-93 Window for the linear grouping (=assembly of translational springs) (transgrp.frm)

With the help of the linear grouping window (Fig.4-93) translational springs directly acting parallel or serial can be assembled. This can be used either as a completely separate tool apart from any joint investigations to add any curves (not only w-F curves) vertically or horizontally or to evaluate average values of two curves (as will be described later) or it is used directly as a kind of pre-assembly (pre-calculation) in view of the joint input. Remember e.g. that the component A is set together by the basic components 1,2,3,4 in direct parallel or serial interplay (acc. to Fig.4-71). The linear grouping tool is also available as a self-standing program.

First of all the principles of parallel and serial spring assembly should be given (see also chapter 3.7.1 herein). The definition of parallel spring interplay is the equal deformation of both springs ($w=w_1=w_2$), the corresponding forces of the two springs (F_1, F_2) have to be added to gain the overall force. So the w-values are regarded as common "basic values". In graphical sense the two w-F-curves are added in vertical direction. Therefore the stiffness and resistance of the parallel spring group exceeds that of both individual springs and is mainly influenced by the stronger one. When reaching the failure of one spring the bearing capacity of the parallel group drops to the resistance of the other spring and therefore the minimum deformation value of the

participating components has to be taken for the deformation capacity of the group. The definition of serial spring interplay is the equal force of both springs ($F=F_1=F_2$), the corresponding deformations of the two springs (w_1, w_2) have to be added. So the F -values are regarded as common “basic values”. In graphical sense the two w - F -curves are added in horizontal direction. Therefore the stiffness of the group is even smaller than the minimum of both components, the resistance is that of the weaker spring but – as a positive effect – the deformation capacity increases (Fig.4-94).

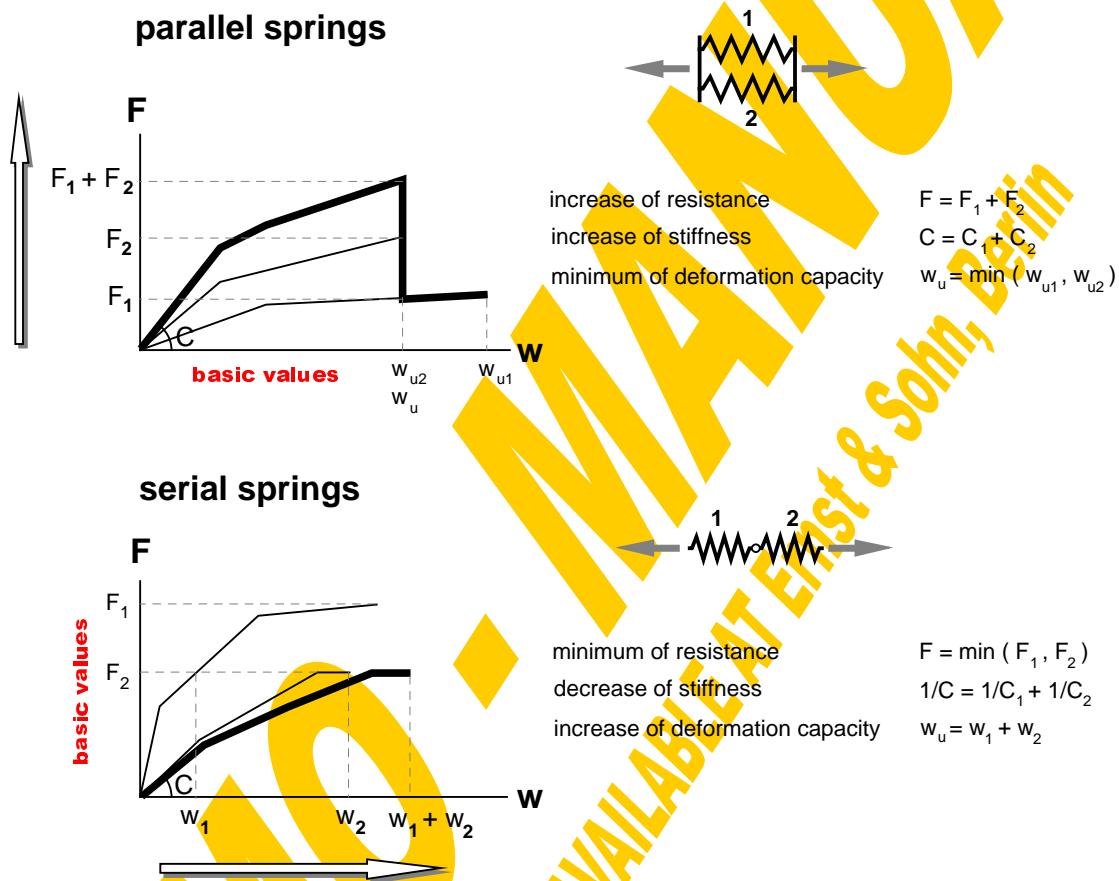


Fig.4-94 Assembly of translational spring groups (linear grouping)

It is obvious that spring curves can only be added within a common area of basic values (within a common w -range for parallel grouping or within a common F -range for serial grouping). Furthermore special attention has to be paid to curves with a falling branch (increase of basic values followed by a drastic decrease = post-limit effect) as shown in Fig.4-95 for the case of a serial spring sequence. In that case the assembly has to be done in two steps: The decisive curve of the weaker spring will be split into two parts – the increasing and the decreasing one. Then first the increasing parts of both curves have to be added, afterwards the decreasing part of the weaker spring will be added to the decreasing (unloading) line of the stronger spring. Normally the unloading stiffness is equal to the initial stiffness.

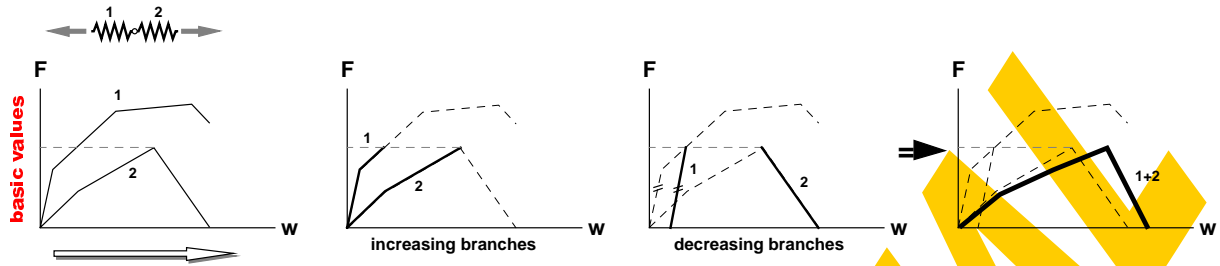


Fig.4-95 Serial spring assembly with decreasing branch

After these general considerations the handling of the “transgrp”-module will now be described. First of all two spring curves (w-F) have to be defined using the input boxes shown in Fig.4-96. A textbox is reserved to a spring name. A grid of at maximum 1000 rows allows the input of the w-F-relationship. The large row number has been chosen in view of an evaluation of test curves. The handling of the grid element is the same as already described in 4.3.4 (Fig.4-89) with the possibilities of a manual input, loading and saving of curves and the use of the MS windows clipboard with the copy and paste buttons. As the basic curve values (w for a parallel assembly and F for a serial assembly) have to increase monotonously (at least within the increasing branch of the curve) for a correct calculation, it might be of help (especially in view of test curves) to re-sort them by w or by F using the buttons “sort w” or “sort F”. A true to scale graphical check of the entered curves can be done with the button “Draw”. The first spring curve is drawn in blue colour, the second one is drawn in green.

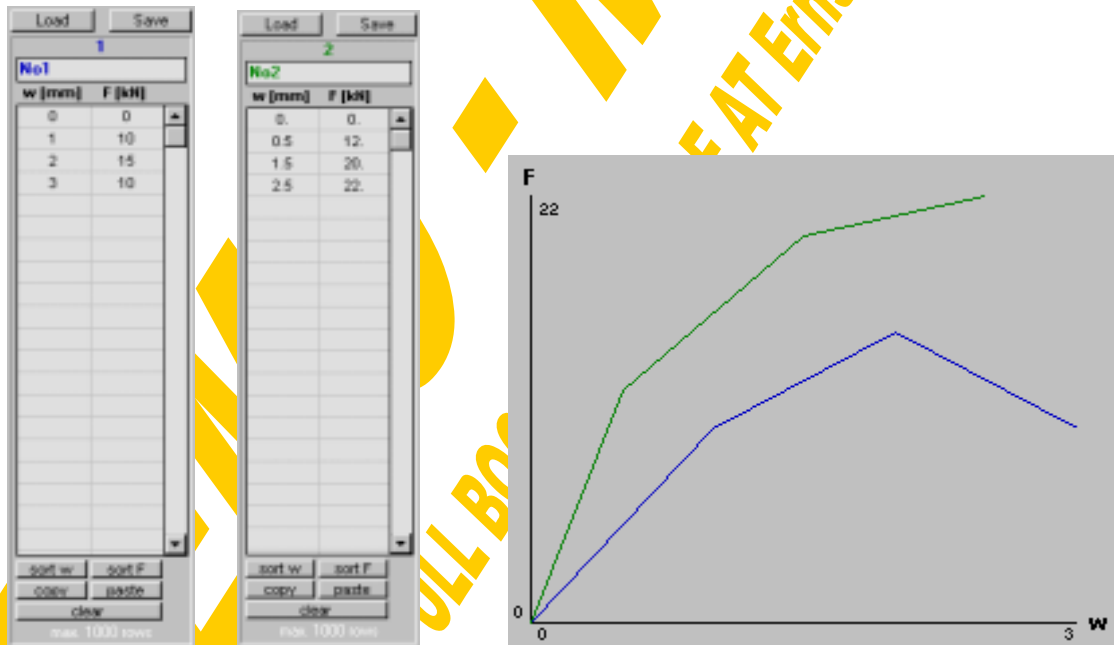


Fig.4-96 Spring curves – input data and graph

Then the user has to decide which calculation method should be used for the given curves. There are the following possibilities (Fig.4-97):

- spring no.2 can be added to (“+”) or subtracted from (“-”) spring no.1
- the assembly can be done parallel or serial

- the basic values can be taken step by step from both curves (to consider all bends of the resulting curve) or only those of spring no.1 or spring no.2 can be considered; this second possibility has been provided in view of the evaluation of test curves with a plenty of curve points and therefore already only a small increase of the basic values from row to row.
- finally there is the possibility to multiply the resulting curve values with a w- and F-multiplier; normally both of these will have to be set equal to one, however a multiplier of 0.5 enables to determine average curves as shown in Fig.4-98.

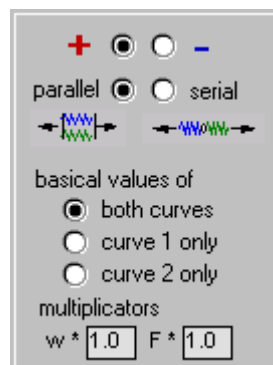


Fig.4-97 Determination of calculation method

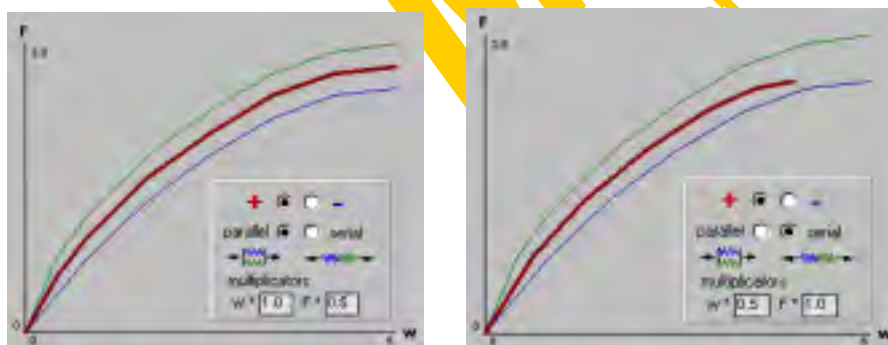


Fig.4-98 Average curves using the linear grouping module

Now the calculation itself can be started with the button "Calculation". First the existence of a common basic data field (common w-range for parallel assembly or common F-range for serial assembly) will be checked, followed by a check if the basic values (w for parallel assembly and F for serial assembly) are increasing monotonously. If a value decrease is observed there are two possibilities: If the decrease is bigger than one percent of the maximum range (drastic decrease=post-limit effect) the curve is split into an increasing and a decreasing branch as shown in Fig.4-95. Then the unloading stiffness of the stronger spring has to be entered (initial stiffness given as default). This unloading branch will then automatically be integrated into the value table of the respective spring and the graph. In the case of a minor decrease this may be tolerated

by the user giving some acceptable monotony-limit (especially for test curves alternatively to a curve re-sort).

After a successful calculation the result panel shown in Fig.4-99 will appear including the spring name, a grid element with at maximum 2000 rows showing the calculated curve values (which cannot be edited any more) and a graph, where the result curve is drawn in red. The values of the resulting curve can be copied to the clipboard with "Copy" or saved to a file with "Save". Moving the mouse over the graph shows the actual mouse position in view of w and F . After clicking on "Zoom in" the corners of a zoom window within the actual graph can be chosen (two single clicks on the diagonal zoom window edge points). The option button "Full data area" reproduced the maximum data field again.

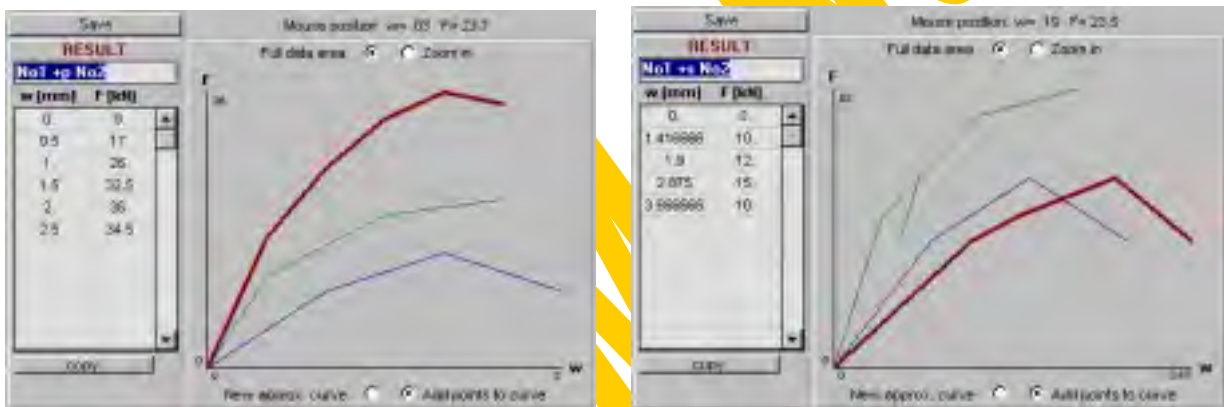


Fig.4-99 Result panel for parallel and serial grouping

Sometimes it might be of interest to approximate a resulting curve with a plenty of bends by a polygon. So a graphic approximation tool has been provided shown in Fig.4-100. The w - F values of such an approximation curve may either be entered into a special grid box or the corresponding values to the actual mouse position within the result graph can be added to the value table with a simple mouse click. After two rows of the approximation curve are entered this curve will automatically be drawn in the graph (starting in yellow for the first ten rows and then continuing in white colour). With a double mouse click or by clicking on "New approx.curve" the whole approximation curve can be deleted. As described for the other spring curves also the approximation curve can be saved, loaded, copied or pasted.

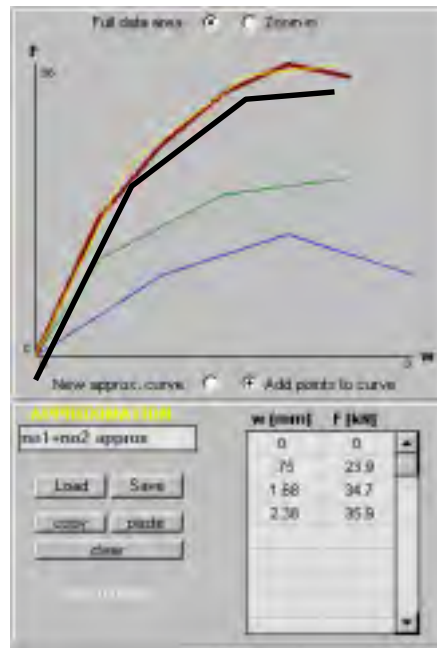


Fig.4-100 Curve approximation by a polygon

Summarising this tool for the assembly of translational springs acting together parallel or serial can even directly be used for the full spring assembly (fulfilling equilibrium and compatibility) when applying the simplified Eurocode component model (Fig.4-101). For that purpose the individual components simply have to be added step by step, taking into consideration their relevant lever arms: First the effective behaviour of the tension rows has to be determined adding C1+D1, D2+D2 and E/2+G in series (E/2 means the curve of the overall E-spring, where the w-values are divided by 2 to take into consideration the left and right influence). Then these *effective* tension rows have to be converted from w-F curves to ϕ -M curves bringing in the lever arms: for each of the rows the w-values have to be divided by z_i and the F-values must be multiplied with z_i ($\phi=w/z$, $M=Fz$). Afterwards all these M- ϕ curves representing the individual tension rows have to be added parallel leading to an *equivalent* overall tension behaviour in terms of M- ϕ . Using the formulae given in [60] or the equivalent counterpart below at least an initial equivalent lever arm z_{eq} can be calculated.

$$z_{eq} = \frac{M}{\sum F_{tension}} = \frac{M}{F_{compression}}$$

Now it has to be checked if the strength of the compression spring B is high enough to activate all these tension forces (equivalent rotational tension spring and converted rotational compression spring B with lever arm z_{eq} in series). Finally also the translational compression spring A has to be converted into a rotational one with the lever arm z_{eq} and added in series to the previous result. In case of full moment imbalance ($\beta=1$) the behaviour of the shear panel H has to be added in series too. As this spring assembly according to the simplified Eurocode component model has not

been of further interest within the scope of this work so far no automated procedure has been provided for that step-by-step assembly.

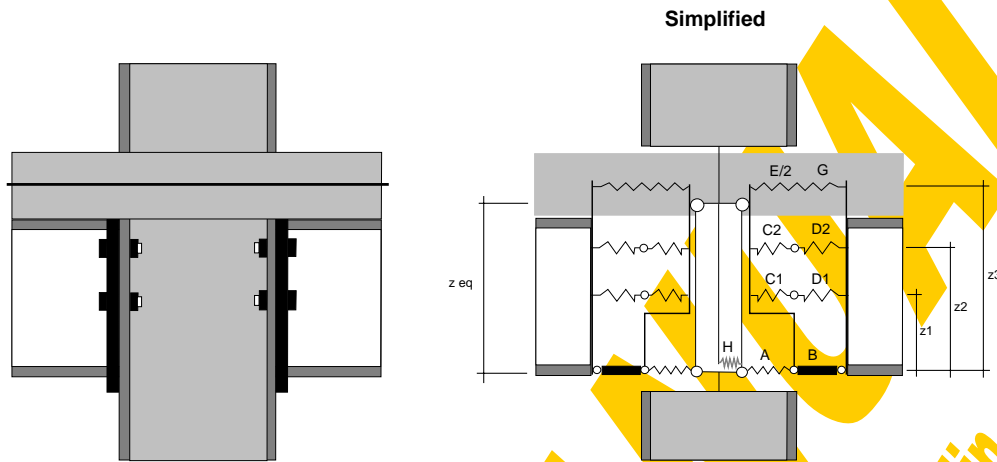


Fig.4-101 Simplified component model (Eurocodes)

The step-by-step linear grouping method should also be used to determine analytically the full rotational joint response of joint configurations without any steelwork row in tension (so-called boltless joints or contact-plate joints, see Fig.4-102). Such an analytical assembly method has the advantage of perfect accuracy in comparison to the iterative assembly (see chapter 4.3.7) leading to some deviations.

The analytical assembly of the contributing components for such a boltless joint has to be done in the following way: First the w-F-curve of the spring E has to be shared into a left and right hand side part leading to a spring E/2 ($w_{E/2}=w_E/2$, $F_{E/2}=F$). Then the w-F-curves of the springs E/2, G, A and B have to be added in series step by step (eventually considering decreasing branches). The resulting w-F curve has to be converted into a ϕ -M curve using the following formulae:

$$\phi = \frac{w}{z} \quad M = F \cdot z$$

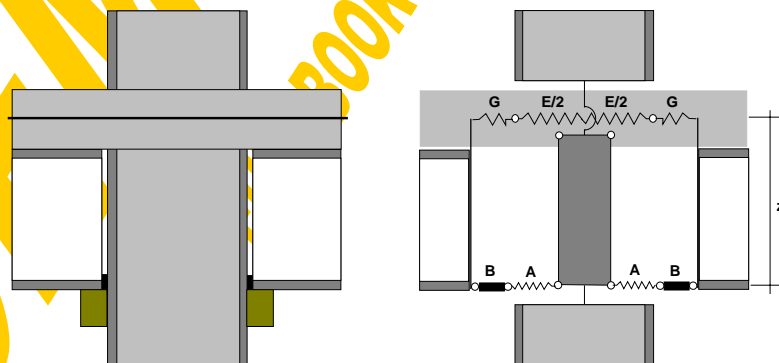


Fig.4-102 Linear grouping step-by-step for boltless joints

An analogous linear step-by-step assembly can be applied to stiffened (by stiffeners or column concrete encasement) joints with only steelwork connections and no slab reinforcement (Fig.4-103): Springs D1 and D2 are added parallel taking into consideration the respective lever arms, then spring B and finally spring A are added serial using the equivalent lever arm z_{eq} .

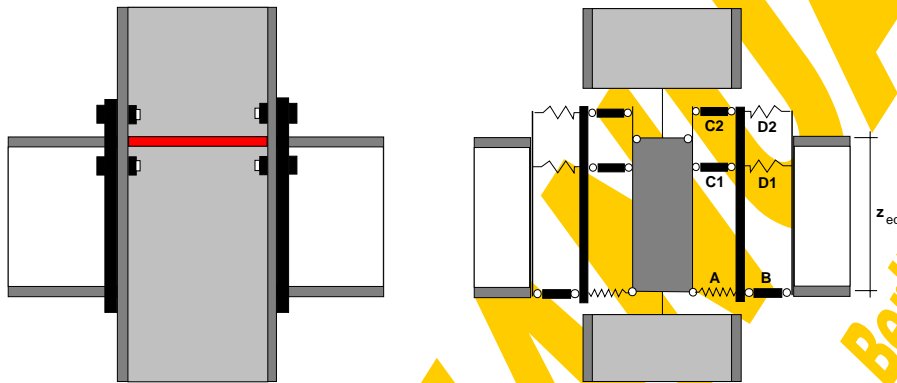


Fig.4-103 Linear grouping step-by-step for stiffened steelwork joints

Finally the button "Quit" closes the linear grouping window again and leads back to the joint input window (Fig.4-87).

DEMO -

FULL BOOK AVAILABLE AT ERNST & SOHN, BERLIN

4.3.6 Basic joint calculations

Clicking on “Calculations” within the start-up window (Fig.4-83) opens the main calculation window (Fig.4-126). However to explain the mechanical and mathematical background of the joint calculations it seems to be more favourable to start here with the “basic calculations” (button) offered by the window shown in Fig.4-104. Furthermore this proceeding is better in line with the historical development of the CoBeJo-Joint module.

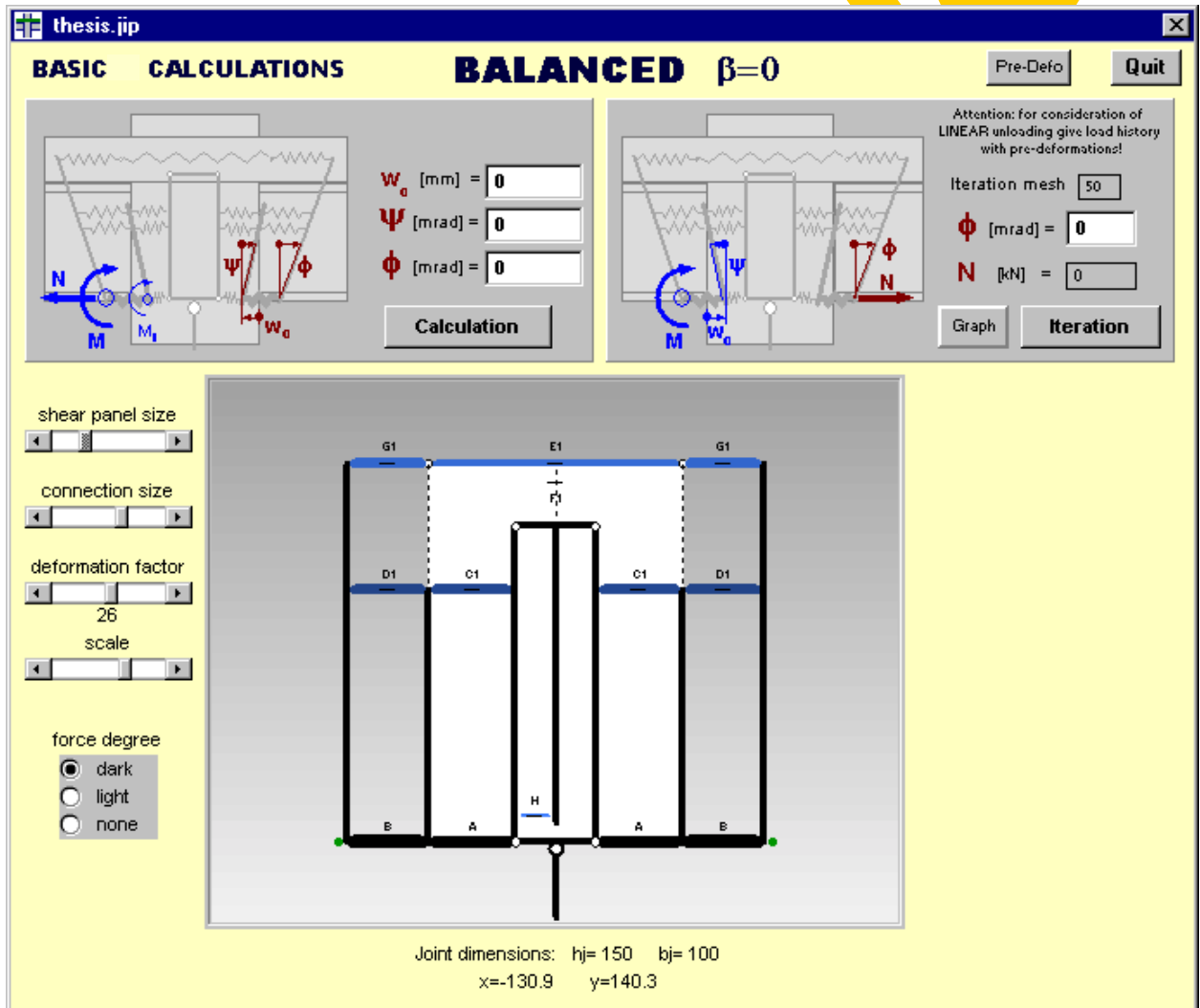


Fig.4-104 Basic joint calculation window (assembly0basical.frm)

When entering the calculation windows the springs E and G will be added in series automatically (G+E+G) as a kind of pre-assembly according to the principles given in the chapter of “linear grouping” (4.3.5), if necessary taking into consideration that decreasing branches of one spring have to be added with the respective unloading line of the other spring. If no spring G has been defined a specific slip value gained from a previous beam calculation considering incomplete shear interaction has to be entered. So in this case w_G will be equal to this specified slip value independently of the actual force in the reinforcement layer according to a w-F characteristic shown in Fig.4-105.

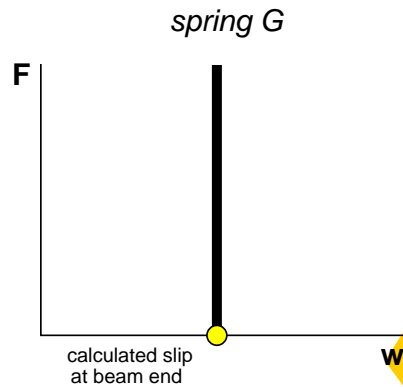


Fig.4-105 w - F characteristic of missing G spring

4.3.6.1 Fundamental calculation (“basic0”)

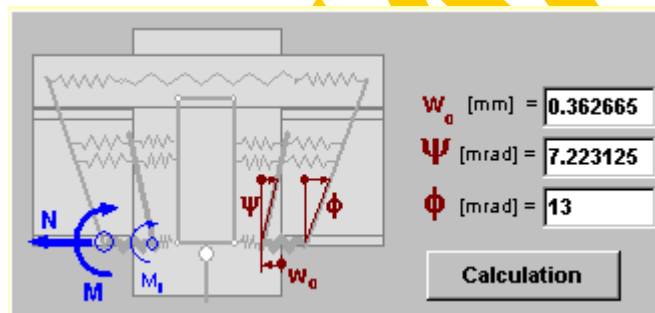


Fig.4-106 Fundamental calculation window

Fig.4-106 shows the fundamental calculation window being a part of Fig.4-104. Three fundamental joint deformation values have to be entered defining a unique (symmetrical) joint deformation state:

- w_0 is the deformation of the compression row (dent into the column web panel)
- Ψ is the rotation of the column front centre line (loadintroduction, separation bar sb2, see Fig.4-85)
- ϕ is the real joint rotation including the rotation of the loadintroduction Ψ and the additional rotation due to the weakness of the connecting elements ϑ (see Fig.3-42).

For the herein assumption of a balanced loading configuration ($\beta=0=1-M_{\text{left}}/M_{\text{right}}$) these joint deformations will appear symmetrically also at the left hand side of the joint. With the “calculation” button the following fundamental calculation will be launched (basic0 in global.bas):

Individual spring deformations

Knowing the values w_0 , Ψ and ϕ the individual deformations of all identified springs can be calculated out of the compatibility conditions:

$$\begin{aligned} w_A &= w_0 \\ w_B &= 0 \\ w_{C_i} &= \Psi \cdot y_i - w_0 \\ w_{D_i} &= (\phi - \Psi) \cdot y_i \\ w_{E+2G_k} &= 2 \cdot (\phi \cdot y_k - w_0) \end{aligned}$$

Corresponding spring forces

With that information the corresponding forces of the individual translational springs A, C_i, D_i, E_k, G_k can be determined from the relevant w - F -curve as shown in Fig.4-107 (using the global routine interpolation). If the deformation is less than zero the force is zero and an indicator flag “invalid force sign” will be set (compression spring in tension or tension spring in compression). If the deformation is bigger than w_{\max} (the maximum w -value of the spring) the corresponding force again is zero and the indicator flag “spring failure” is set.

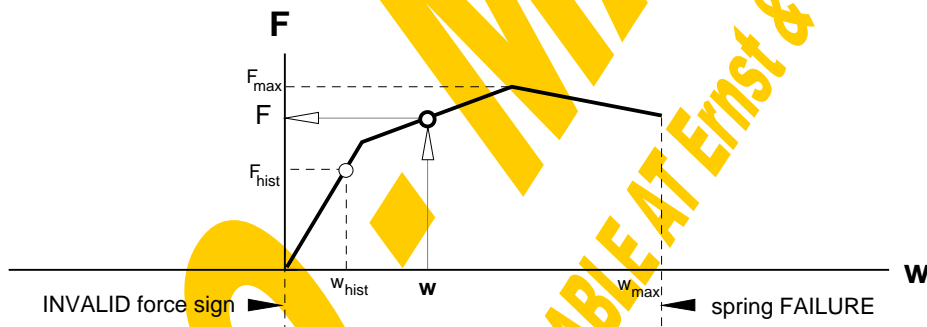


Fig.4-107 Interpolation of the corresponding force to a given spring deformation

In view of a progressive load history it is possible that the deformation of a spring decreases again although ϕ is increasing. Such a decrease of w causes a linear unloading instead of going back the w - F curve directly. To take into consideration such effects there has been provided the button “pre-defo” to enter recent w - F -points (w_{hist} , F_{hist}) of all contributing springs representing a decisive previous step of a load history (pressing “shift” and “pre-defo” will reset the pre-deformations). So within the interpolation routine it will be checked for each spring if the previous (maximum) deformation value is exceeded by the actual deformation or not. If the actual one (w) is bigger then the previous one (w_{hist}) the interpolation is performed according to Fig.4-107. Otherwise instead of a curve interpolation the corresponding force will be calculated using the unloading stiffness of the respective spring (see Fig.4-108). If w_{\max} has been exceeded once during the load history the force of this spring from then on will always be set zero, because such a spring rupture cannot be repaired again.

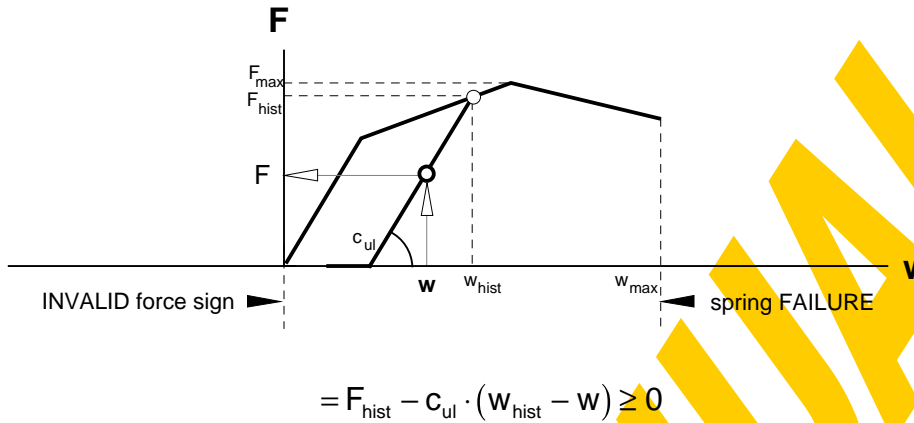


Fig.4-108 Interpolation considering the load history

Force degrees

To get a feeling about the percentage of use of the identified components at the actual deformation state the corresponding force degrees (F/F_{max}) are calculated.

Equilibrium conditions

From the condition $\Sigma H=0$ (horizontal forces) the remaining force in spring B can be calculated with the help of cut 1 (see Fig.4-109). Further the internal moment $M_{internal}$ can be gained with cut 1. Cut 2 leads to the normal force N_{joint} and the moment M_{joint} .

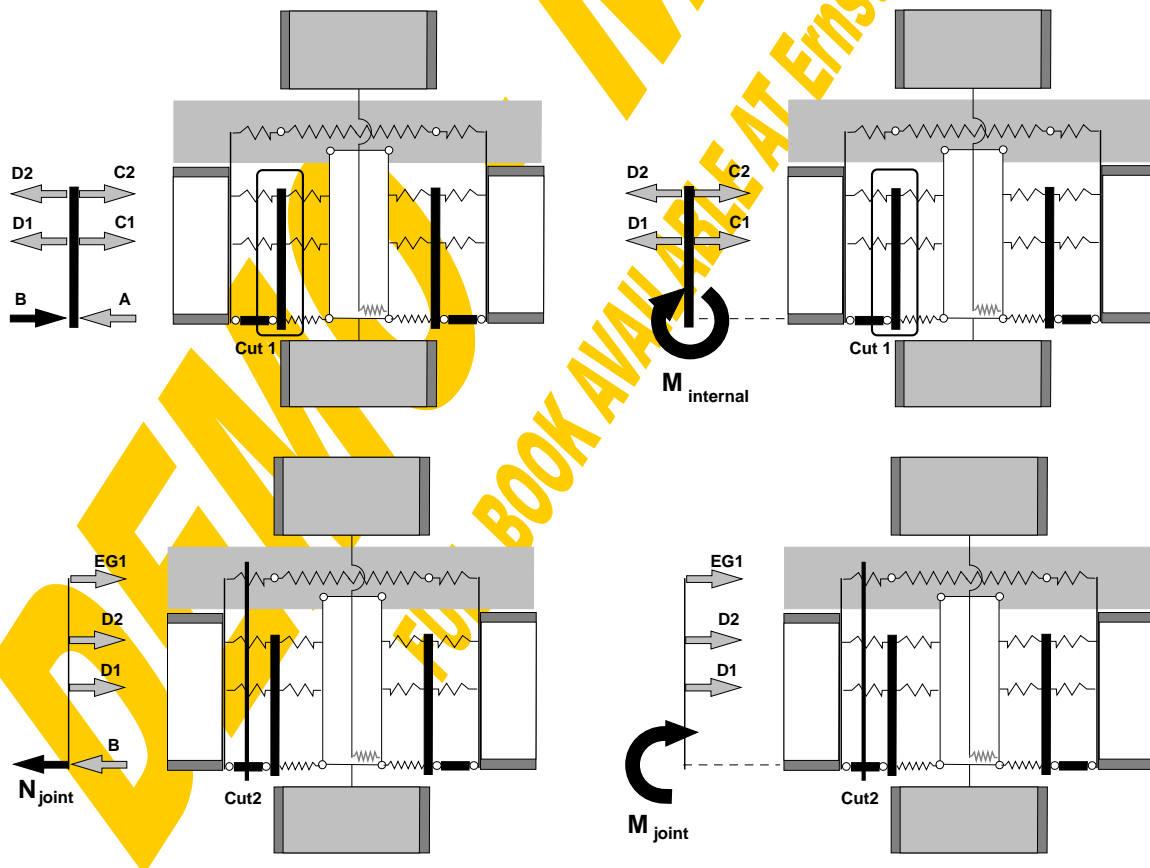


Fig.4-109 Internal forces from equilibrium conditions

Presentation of results

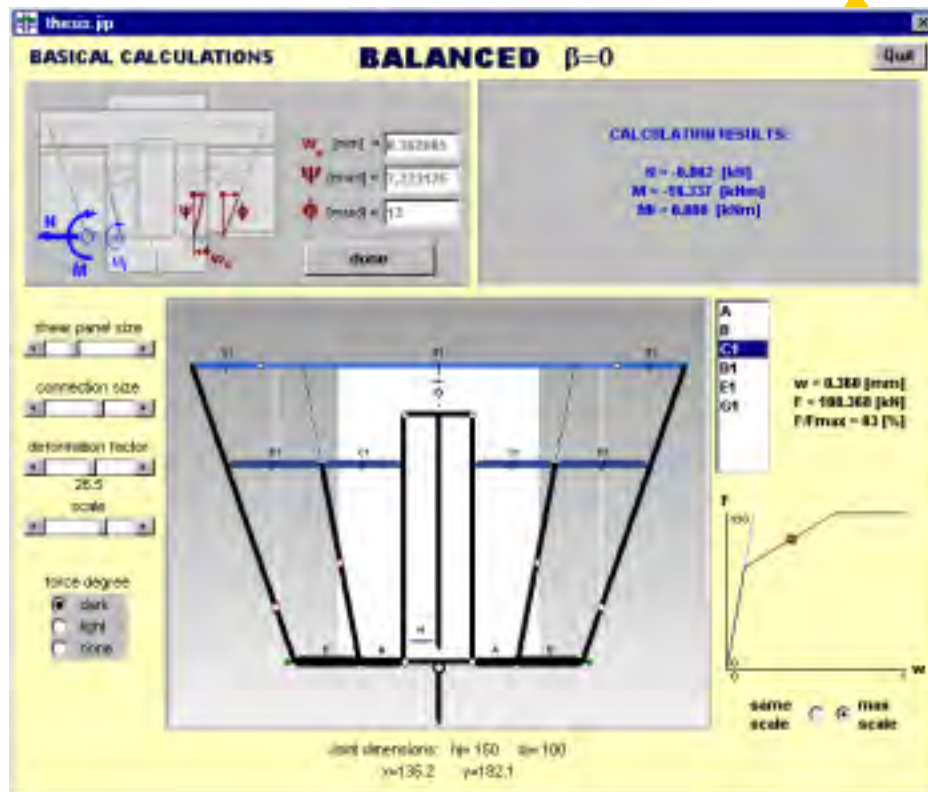


Fig.4-110 Resulting window from fundamental calculation

After these calculations have been carried out the results corresponding to the chosen deformation state (w_0, Ψ, ϕ) are presented in a window like Fig.4-110 comprising the following information:

- The primary results are the actual normal force $N_{\text{joint}}=N$ and the bending moment $M_{\text{joint}}=M$ at the joint edge as well as the internal bending Moment $M_{\text{internal}}=M_i$ presented in Fig.4-111. From the general assumption of upper tension rows and a compression row at the lowest level it follows that M_{joint} is always negative (hogging bending).

CALCULATION RESULTS:

$N = -0.002$ [kN]
 $M = -18.337$ [kNm]
 $M_i = 0.000$ [kNm]

Fig.4-111 Primary results from the fundamental calculation

- The graphical illustration of the deformed joint is given in Fig.4-112. Additionally to the joint graph already explained in chapter 4.3.3 (Fig.4-85) also the short names of all contributing components are given as well as the respective “degrees of forces” in the form of small lines in the middle of each component spring. A horizontal line means that there is no force acting in a spring (0%) and a vertical line indicates that the maximum force in a spring is reached (100%). A wrong force sign within a

component (compression spring in tension or tension spring in compression) is expressed by a thick horizontal line, a thick vertical line indicates a spring failure. These force degrees should improve the first optical assessment of the joint response. With three option buttons (dark, light, none) the format of these force degrees can be selected. Apart from the possibilities to manipulate the illustration size of the shear panel and that of the connection the deformation factor can be defined between 0 and 50 and the scale of the overall joint graph can be chosen between 0.1 and 1 using the respective scroll bars. Furthermore the rotation centres of the two separation bars sb1 and sb2 (acc. to Fig.4-85) are drawn as red circles. Moving the mouse over the joint graph gives the actual mouse pointer coordinates.

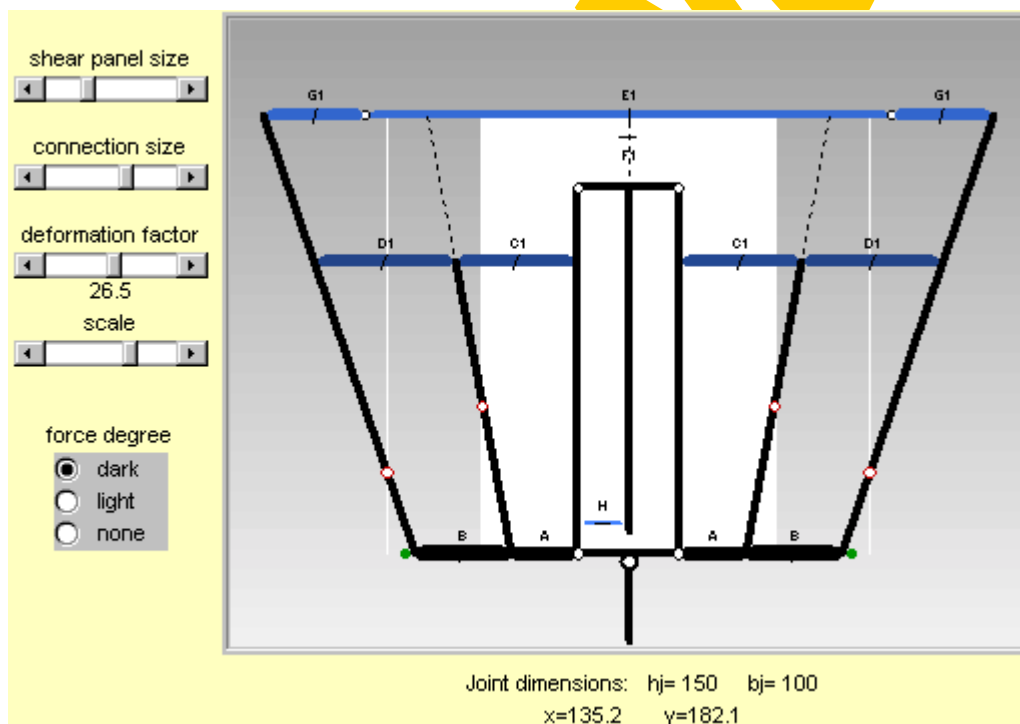


Fig.4-112 Graph of the joint response

- A third area within the result window (Fig.4-110) is dedicated to the individual spring results (see Fig.4-113). Clicking on the table which lists all identified components shows their actual deformation w , the force F , the degree of force F/F_{\max} and a graph of the w - F curve including the actual point as a red circle. Following the principles given in Fig.4-107 and Fig.4-108 the actual point must not always lie on the curve itself. With the option buttons "same scale" or "max scale" it can be chosen if the w - F curves of all components should be drawn in the same scale for a better direct comparison or if for each spring curve the maximum possible scale should be used.

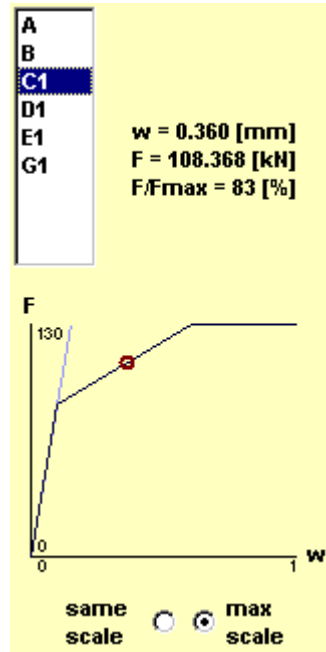


Fig.4-113 Individual spring response

With “Done” in Fig.4-110 the result presentation can be finished to start a new calculation.

4.3.6.2 Fundamental graphs

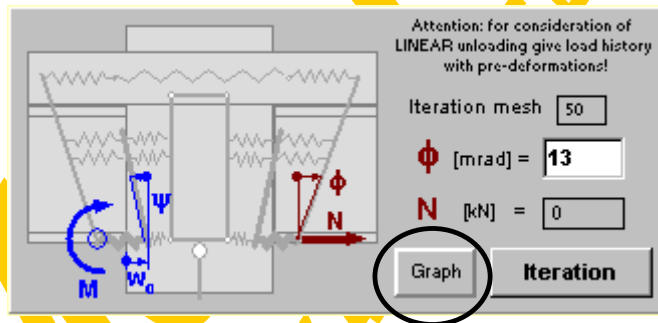


Fig.4-114 Fundamental graph and iteration window

Clicking on the button “Graph” produces a quasi three dimensional diagram (vertical layers in different colours) for N , M_i or M over a variable field of w_0 and Ψ for a specified joint rotation ϕ and a given normal force N (zero as default). This graphs then may serve for visual calculation checks, the discovery of iteration solutions (see next chapter) and to get a principle idea about the joint behaviour when varying deformation parameters.

The resolution of the graph depends on the value given as “Iteration mesh” (increasing mesh point number means increasing resolution). If the calculation time due to a high resolution is too long the “Stop” button can be used for an interruption. First of all the user will be asked for a graph type and the desired w_0 - and Ψ -range to be displayed.

The following types of 3D-layer graphs are available (Fig.4-115):

- type 0 internal moment M_i as third axis
- type 1 difference between actual and given (Fig.4-114) normal force as third axis ($dN=N_{\text{joint}}-N_{\text{given}}$)
For the graph types 0,1,6 the colour of a rectangular graph element (resolution point) depends on the third axis value of its lower left corner. The colour palette covers the range from dark red over light red to light blue and dark blue indicating high positive, low positive, low negative and high negative values.
- type 2 a combination of M_i and dN is drawn: for positive dN values the corresponding M_i values are drawn using the above given colour palette. In case of negative dN a yellow colour is used in the case of a positive M_i and a light yellow indicates a negative M_i value.
- type 3 analogous to type 2 exchanging dN against M_i
- type 4 analogous to type 2 and type 3, however those data areas are drawn in grey, where an "invalid force sign" has been identified
- type 5 analogous to type 2 and type 3, however those data areas are drawn in grey, where an "invalid force sign" has been identified
- type 6 joint moment M as third axis
- type 7 all areas where an "invalid force sign" is recognised are drawn in red, those where a "spring failure" occurs are drawn in blue and the remaining "regular" area is drawn in green.

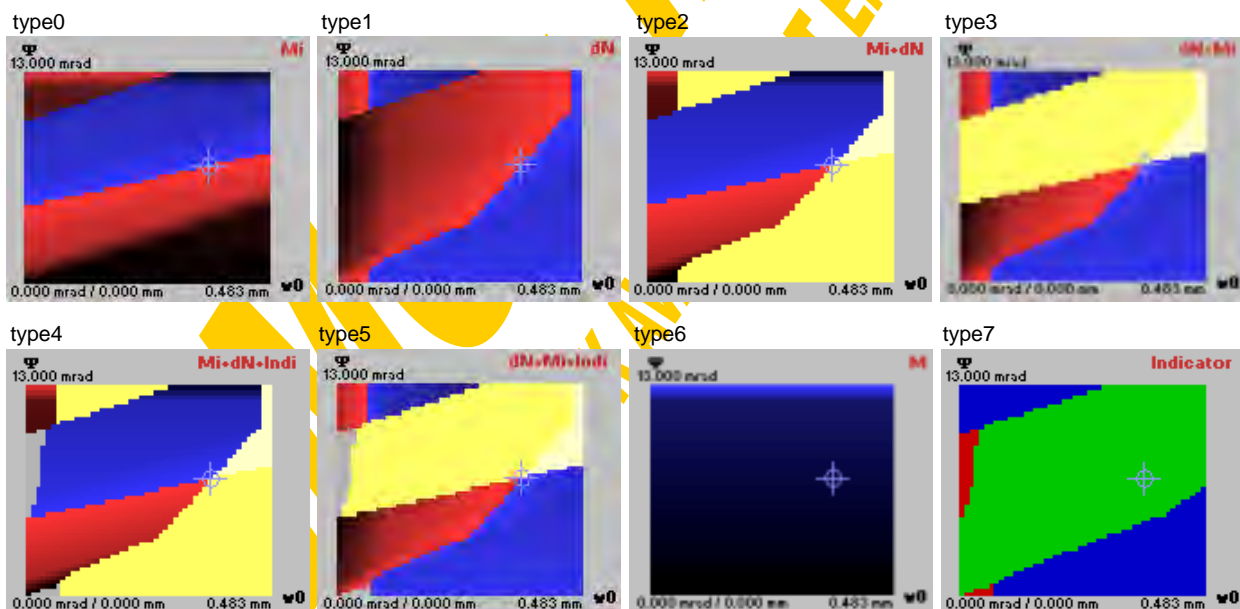


Fig.4-115 3D layer-graph types

Fig.4-116 shows a comparison between the 3D layer graphs of CoBeJo-Joint and the corresponding 3D shape models drawn with the help of MS Excel.

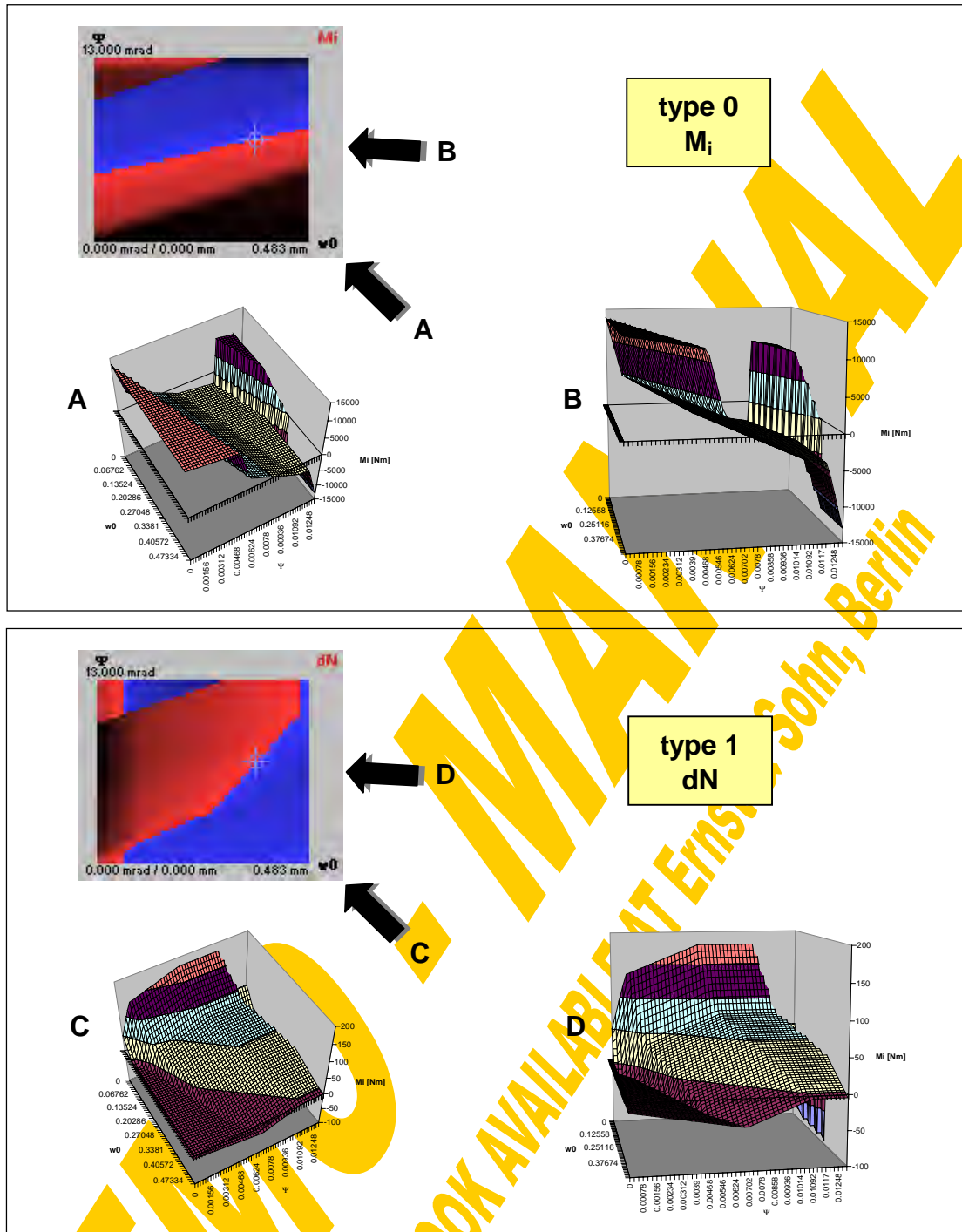


Fig.4-116 3D diagrams – layer graphs and shape models

The maximum available w_0 - and Ψ -range is determined within reasonable limits:

- w_0 may vary between zero and w_{0max} . For that purpose $F_{t,max}$ is calculated as the sum of all strength values of the steelwork tension springs and the reinforcement springs

$$t_{max} = \sum_i F_{max,C_i} + \sum_k \min(F_{max,E_k}, F_{max,G_k})$$

If this is higher than the maximum strength of spring A ($F_{t,max} > F_{max,A}$) the spring A itself probably will cause the joint failure and therefore $w_{0max} = w_{max,A}$ (to increase iteration speed a plastic strength plateau (if existing) of spring A can be reduced to only 5% if its length in view of w). If $F_{t,max} < F_{max,A}$ the corresponding deformation of spring A will be taken as w_{0max} (see Fig.4-117). Finally the so-gained w_{0max} is multiplied with 1.05 to include also such iterative solutions where $w_0 \equiv w_{0max}$.

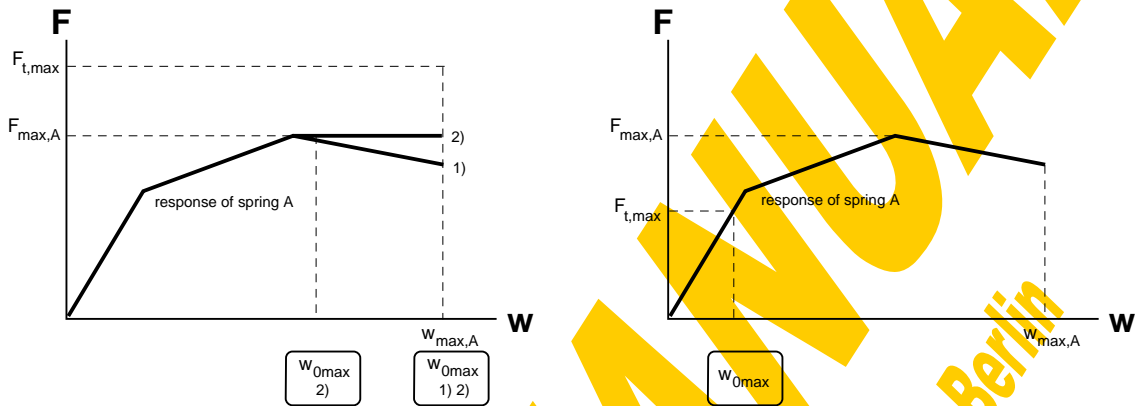


Fig.4-117 Definition of w_{0max}

- Ψ may vary between zero and ϕ .

The user may decide either to display this maximum w_0 - and Ψ -range or to pick out a part of it by entering the graph limits.

As default graph type 4 (see Fig.4-118) will be displayed within the maximum w_0 - and Ψ -range. This type of graph easily helps to identify iteration solutions (see 4.3.6.3). Such solutions are located at the intersection of red, blue and yellow colour (per definition above these are the points where $M_i=0$ and $dN=0$, so fulfilling equilibrium). If ϕ and N input did not change since a previous iteration (4.3.6.3) the stored iteration results (w_0 - Ψ combinations) will be indicated in the graph with a light blue crosshair.

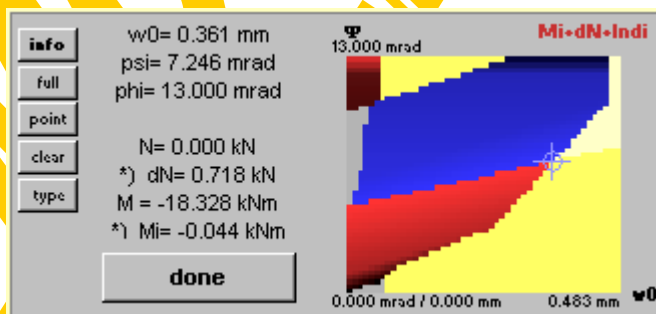


Fig.4-118 Graphical results

The following actions can be carried out with the help of the graphical result window: The "info" button gives an overview of the following possibilities. Moving the mouse pointer over the 3D layer graph will show the corresponding fundamental calculation results (see 4.3.6.1) as well as the deformed joint for the actual deformation state w_0 - Ψ - ϕ . A double click on the mouse even gives all details to the actual joint

deformation state (Fig.4-110). With a mouse click while pressing the shift-key a zoom window can be defined. The button “full” refreshes the original w_0 - Ψ -range again. Specific w_0 - Ψ -points (max.20) can be accentuated on the graph with the “point” button. “Clear” erases all these points again. The graph type according to Fig.4-115 can be change with “Type”.

Clicking on the right mouse button enables to pick a first and then a second point of a sectional cut through the 3D layer graph as shown in Fig.4-119. Instead of defining these cutting points visually they may also be defined by values with the help of an input box which opens when pressing shift and the right mouse button simultaneously. A single mouse click interrupts the definition of a second zoom window corner or a second cutting point.

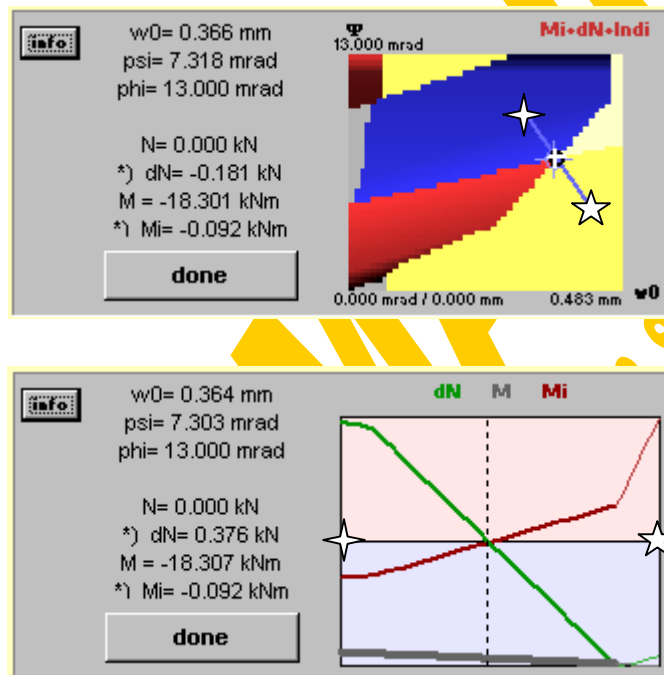


Fig.4-119 Sectional view of 3D graph

Within the sectional graph the dN -course is drawn as a green polygon, the joint moment M is drawn in grey and the internal moment M_i is drawn in red. The resolution of these curves depends again on the chosen “iteration mesh” in Fig.4-114. The red diagram background indicates the positive data area, the blue background indicates the negative one. All three polygons are drawn with a thin line if a spring failure or an invalid force sign has been observed, otherwise a thick line is used. The iteration (4.3.6.3) will determine such w_0 - Ψ - ϕ -combinations, where M_i and dN are zero simultaneously (successful equilibrium within the joint) as shown for the example calculation in Fig.4-119. Attention has to be paid if the curves are passing the zero level in a nearly perpendicular way, because this indicates a spring failure and therefore no real solution or equilibrium.

Again also with the sectional graph some mouse actions are possible: Moving the mouse pointer over the graph will show the corresponding (dashed line) fundamental calculation results (see 4.3.6.1) as well as the deformed joint for the actual deformation state w_0 - Ψ - ϕ . A double click on the mouse even gives all details to the actual joint

deformation state (Fig.4-110). Clicking on the right mouse button will accentuate the actual point within the 3D layer graph (Fig.4-119-top), where a single mouse click leads back to the sectional view again. With “Done” in Fig.4-119-bottom the sectional graph is closed and the 3D layer graph displayed again (Fig.4-118).

With the button “Done” in Fig.4-118 the graphical presentation finally can be finished to start new calculations (Fig.4-104).

4.3.6.3 Fundamental iteration

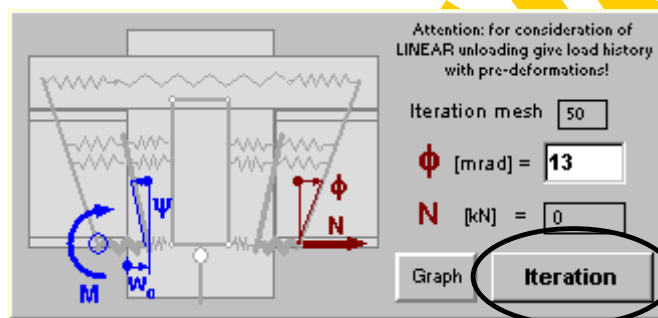


Fig.4-120 Fundamental graph and iteration window

The complex fundamental iteration procedure itself is based on two sub-iterations which should be explained now as a starting point.

$M_i=0$ iteration (“iteration_psi”)

For a given w_0 and ϕ that special corresponding Ψ will be determined (within the boundaries Ψ_a and Ψ_b) where the internal moment M_i is equal to zero (internal joint equilibrium). This iterative procedure is based on the bisection method described in Fig.4-16. So starting with the boundaries Ψ_a and Ψ_b and afterwards also for their bisection point the corresponding internal joint moments M_i is calculated using the fundamental procedure “basic0” described in chapter 4.3.6.1. Knowing these three M_i -values belonging to the three Ψ -values (w_0 and ϕ defined) the Ψ -boundaries are adapted so that the $M_i=0$ intersection again lies in between the new Ψ -boundaries. This halving of the Ψ -boundaries is repeated until one of the following criteria is fulfilled: Either $M_i \approx 0$ with a given accuracy (1 Nm / precision factor=1) or the iteration time exceeds a stop limit (10 seconds) or the change of Ψ lies below a stop limit (0.001 mrad). If in the last case a less severe accuracy limit (100 Nm / precision factor=1) is met this will be accepted anyway as a solution. Otherwise this indicates a drastic jump of M_i due to a spring failure and therefore no solution to be found.

The course of M_i depending on Ψ for a defined w_0 and ϕ can easily be determined as a vertical sectional cut through the 3D layer graph.

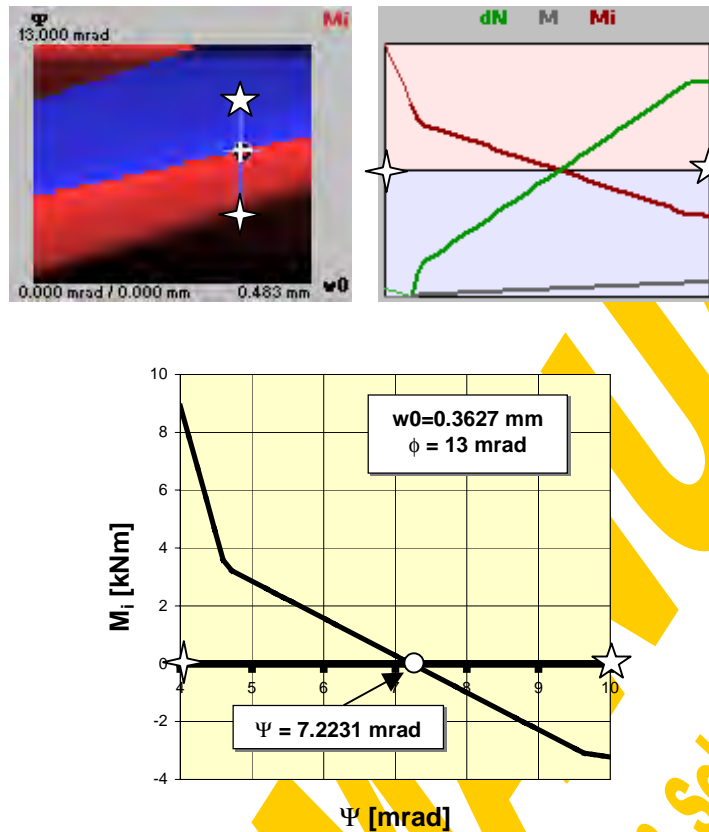


Fig.4-121 Iteration example

dN=0 iteration (“iteration_w0”)

For a given ϕ that special corresponding w_0 (depending on Ψ) will be determined (within the boundaries w_{0a} and w_{0b}) where the error of the normal force $dN=N_{\text{joint}}-N_{\text{given}}$ is equal to zero (external joint equilibrium). While varying w_0 also Ψ will be changed (within the boundaries Ψ_a and Ψ_b) according to the procedure “iteration_psi” to fulfil the condition $M_i=0$ (internal joint equilibrium) simultaneously. So “iteration_w0” is an iteration loop covering “iteration_psi” as a sub-iteration.

First it will be checked for the given boundary w_{0a} if by applying “iteration_psi” at all any Ψ can found fulfilling $M_i=0$. If yes then the corresponding dN_a will be stored. Otherwise Ψ_a is decreased in steps of $(\Psi_b - \Psi_a)/10$ (minimum value is zero), Ψ_b is increased in steps of $(\Psi_b - \Psi_a)/10$ (maximum value is ϕ) and w_{0a} is increased in steps of $(w_{0b} - w_{0a}) / (\text{iteration mesh})$. Then this check is repeated.

An analogous procedure is done for w_{0b} : It will be checked for the given boundary w_{0b} if by applying “iteration_psi” at all any Ψ can found fulfilling $M_i=0$. If yes, then the corresponding dN_b will be stored. Otherwise Ψ_a is decreased in steps of $(\Psi_b - \Psi_a)/10$ (minimum value is zero), Ψ_b is increased in steps of $(\Psi_b - \Psi_a)/10$ (maximum value is ϕ) and w_{0b} is decreased in steps of $(w_{0b} - w_{0a}) / (\text{iteration mesh})$. Then this check is repeated.

Having found the corresponding dN -values (dN_a and dN_b) to the given w_0 -boundaries (w_{0a} and w_{0b}) under the condition that $M_i=0$, the iteration can be started now applying the bisection method: For the bisection point w_{0ab} in between the actual boundaries w_{0a} and w_{0b} that corresponding dN_{ab} is determined with the help of the sub-iteration "iteration_psi", where $M_i \approx 0$. Knowing these three dN -values belonging to the three w_0 -values (respective Ψ -values to each w_0 ; fixed ϕ) the w_0 -boundaries are adapted so that the $dN=0$ intersection again lies in between these new w_0 -boundaries. This halving of the boundaries is repeated until one of the following criteria is fulfilled: Either $dN \approx 0$ with a given accuracy (5 N / precision factor=1) or the iteration time exceeds a stop limit (10 seconds) or the change of w_0 lies below a stop limit (0.01 μm). If in the last case a less severe accuracy limit (500 N / precision factor=1) is met this will be accepted as a solution anyway. Otherwise this indicates a drastic jump of dN due to a spring failure and therefore no solution to be found.

If "iteration_psi" could not find any Ψ_{ab} -solution that indicates that either a spring failure or even more than only one Ψ -solution fulfilling $M_i=0$ lies in between the mesh points Ψ_a - Ψ_b (in the second case a mesh refinement is recommended). Such problems will be stated by a message box. To clarify such iteration problems the graphical tools provided in 4.3.6.2 proved to be really helpful.

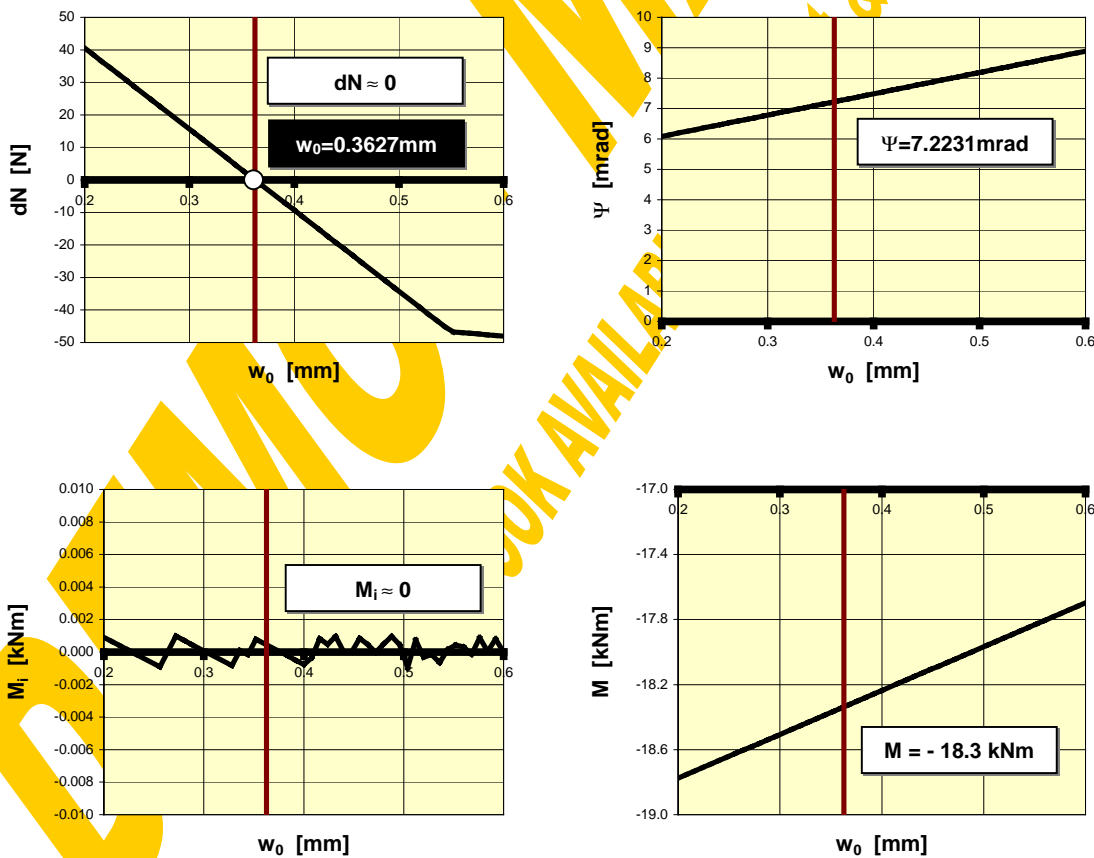


Fig.4-122 Iteration example

Fundamental iteration procedure

An iterative procedure to find all deformation states of the joint (w_0 and Ψ to a given ϕ) fulfilling internal and external equilibrium ($M_i=0, dN=0$) is launched pressing the button “iteration” in Fig.4-115. The iteration for w_0 - Ψ -solutions to such a given ϕ is done in the following steps (a time consuming iteration may be interrupted by a “Stop” button).

Calculation of data field

In a first step a mesh will be put over the maximum considerable range of w_0 and Ψ . The mesh width depends on the chosen value for the “iteration mesh” (Fig.4-115) defining the number of subdivisions for both axes w_0 and Ψ (therefore doubling the iteration mesh factor quadruples the iteration time!). Then for each mesh node (w_0, Ψ, ϕ) the check values M_i and dN in view of a successful joint equilibrium are determined with the help of the fundamental joint calculation “basic0” (chapter 4.3.6.1). This procedure is quite similar to that for the fundamental graphs (4.3.6.2):

In an external loop w_0 will be varied between zero and w_{0max} (as defined in 4.3.6.2), an internal loop changes Ψ between zero and ϕ . To increase the iteration speed before starting any fundamental joint calculation it will be checked, if the actual combination of w_0 and Ψ makes sense at all and if not, this mesh node gets the flag “no solution” immediately without further calculations. As illustrated in Fig.4-123 a wise lower limit of Ψ for a given w_0 can be defined where at least the highest steelwork row is subjected to tension and not to compression. A wise upper limit of Ψ for a given w_0 is reached, where all C-springs are ruptured.

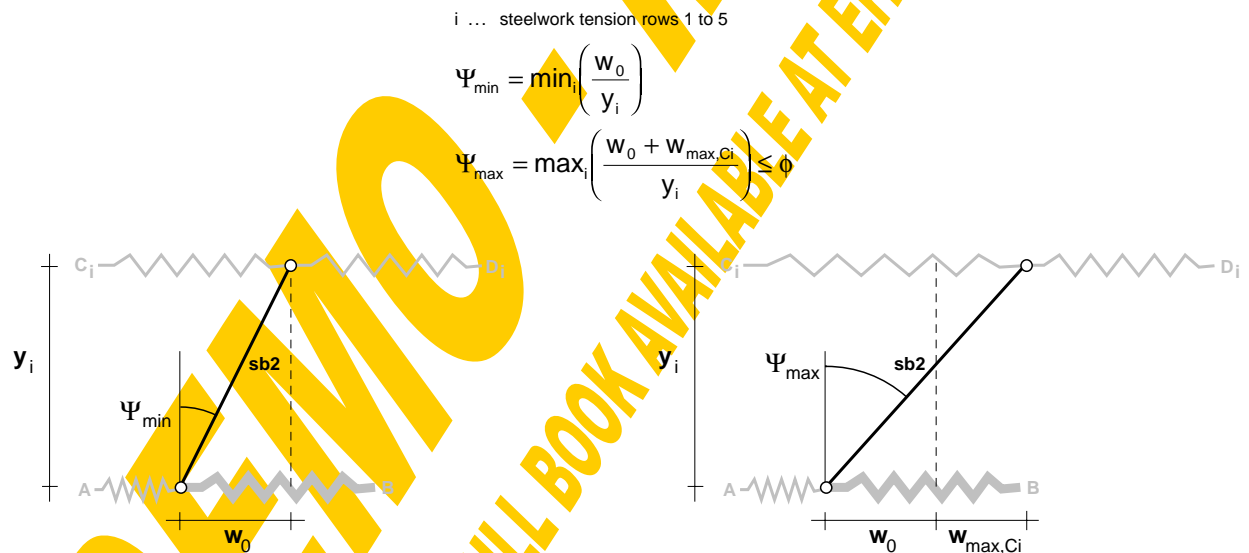


Fig.4-123 Limits of Ψ to a given w_0

Search for solutions

After such a data field of M_i and dN over w_0 and Ψ has been calculated the w_0 - and Ψ loops are passed through again and for any mesh rectangle (Fig.4-124) it will be checked, if a solution within these mesh limits is possible at all. An indication for a

possible solution is that M_i of at least one corner has a different sign than that at the other corners (for a boltless joint without any steelwork connection no separation bar 2 exists, therefore $M_i=0$ for any Ψ and therefore this criterion will always be fulfilled). Simultaneously to the previous criterion also dN of at least one corner has to have a different sign than that at the other corners (or dN must be equal zero in at least one corner). For those mesh rectangles fulfilling both criteria a detailed search for a solution will be launched starting the procedure "iteration_w0" (described above). In the case that a solution really could be found and despite an eventual broadening of the Ψ -boundaries by "iteration_w0" this solution (w_0, Ψ) still lies in between the investigated mesh rectangle (otherwise this solution will be found again during the iteration for another rectangle and therefore should not be stored twice) the found values w_0 and Ψ are stored as a solution. Then the search for other deformation states fulfilling equilibrium will be continued. Attention has to be paid to the fact that due to the described iteration method at maximum one solution per mesh rectangle will be found. So depending on the actual joint configuration the requirements on the iteration mesh vary. As a compromise between iteration time and reliability of the results an iteration mesh value between 50 and 100 is recommended. In special cases of critical points, where solutions are really close together the fundamental graphs (see chapter 4.3.6.2) using the zoom option are helpful.

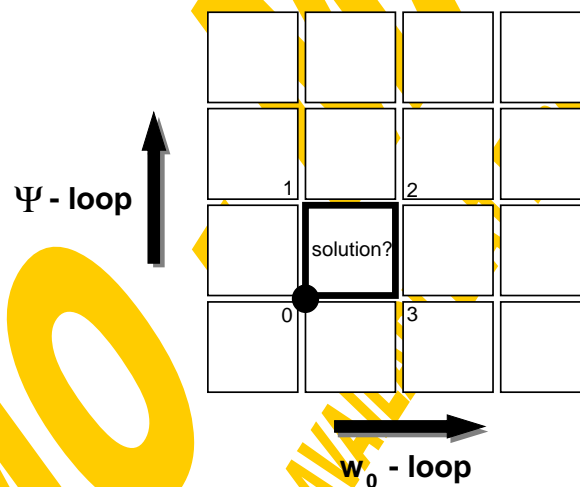


Fig.4-124 Search for solutions within iteration mesh rectangles

Presentation of solutions

At maximum 20 different solutions are stored during the search for solutions. A table summarising the gained w_0 - Ψ combinations for the given ϕ and N will be displayed (see Fig.4-125). A single click on such a solution will copy the exact w_0, Ψ, ϕ values to the fundamental calculation window (Fig.4-106), a double click will directly start the fundamental calculation for this w_0 - Ψ - ϕ combination ending up with the detailed joint and component results (Fig.4-110). With the button "done" the solution table can be closed again to continue with new iterations, graphs or fundamental calculations.

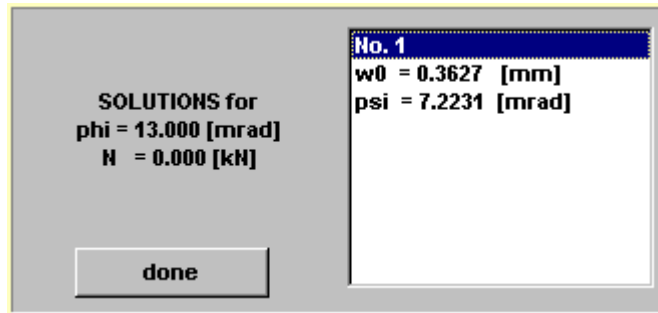


Fig.4-125 Solution table from fundamental iteration

4.3.6.4 Summary

All these basic calculations evaluating the detailed joint response and the corresponding individual spring actions for a specific joint deformation state (w_0, Ψ, ϕ) proved to be a helpful tool during the development of the program in view of check calculations. Beyond that they can be used by an experienced user to get familiar with principles of joint detailing and failure modes. As the program has been built up starting with these basic calculations the explanation of the mechanical and mathematical background of joint iterations seemed to be much easier in that order. For the everyday use of the CoBeJo-Joint module the “basic calculations” will rarely be used directly, however they are the basis of the following main calculations.

4.3.7 Main joint calculations

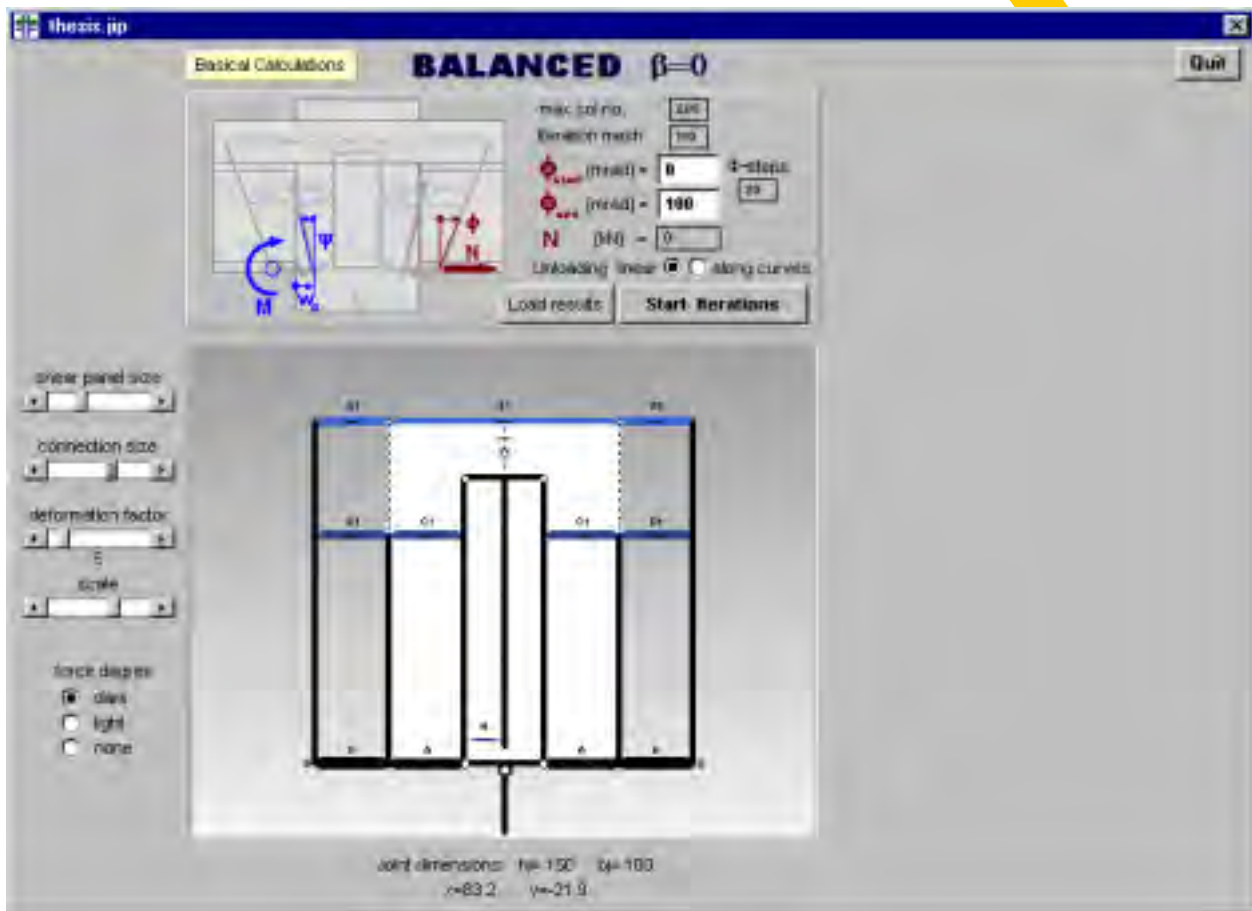


Fig.4-126 Main joint calculation window (assembly0.frm)

The objective of the main joint calculation (Fig.4-126) is the derivation of an $M-\phi$ curve representing the relation between the applied joint moment M (hogging) and the corresponding joint rotation ϕ . This is done by an assembly of all non-linear translational component springs considering post limit effects (also decreasing branches) and even failure of individual components. Obviously in view of such non-linearities the load history plays a significant role and therefore the calculation is performed rotation-controlled gradually increasing the joint rotation ϕ step by step from zero to any upper limit. So within a loop increasing ϕ there will be a “fundamental iteration”(see 4.3.6.3) for each of these ϕ -states.

4.3.7.1 Assembly boundaries

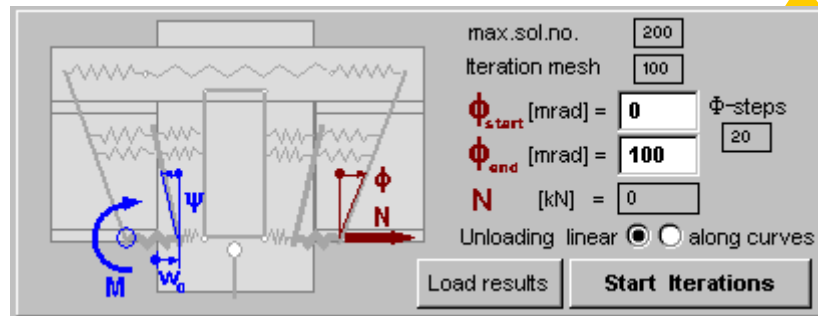


Fig.4-127 Definition of assembly boundaries

First some assembly boundaries have to be defined using the input tools collected in Fig.4-127:

- During the increase of joint rotation it may occur that some individual spring deformations are decreasing. The user has the opportunity to decide whether the corresponding spring force in such a case of component unloading should be calculated using the unloading stiffness (“Unloading linear”, see Fig.4-108) or if the force should always be taken as lying on the w-F curve itself (Unloading “along curves”, see Fig.4-107).
- The rotation limits can be defined as ϕ_{start} and ϕ_{end} . In view of the iterative rotation increase from step to step (deformation history of all contributing components) in the case of a “linear unloading” ϕ_{start} has to be set zero. In case of an unloading “along curves” the iterations may even be started with any arbitrary value of ϕ_{start} . The number of ϕ -states between ϕ_{start} and ϕ_{end} can be defined with the “ ϕ -step” input box. A higher number of ϕ -states increases the resolution of the aimed M- ϕ curve and therefore also its accuracy.
- For each ϕ -state all possible solutions fulfilling joint equilibrium (see fundamental iteration procedure) will be stored. So for a high number of ϕ -states also the number of solutions increases. A maximum number of solutions to be stored to an internal data field can be defined with “max.sol.nr.”
- The mesh width used for each “fundamental iteration” can be defined as “Iteration mesh” (see Fig.4-124).
- An acting normal force at the joint edge (“N”) can be entered as well. However attention has to be paid that an existing normal force drastically restricts the valid ϕ -range where the compression rows are still exposed to compression and the tension rows are still in tension. Whereas the influence of that effect has been taken into consideration within the Eurocodes [60] by a general upper normal force limit of 10% of the plastic beam resistance, those invalid joint deformation states with “invalid force signs” automatically will be high-lightened by CoBeJo-Joint for the actual joint configuration. Any normal force is assumed to act at the layer of the compression row ($y=0$) and therefore the joint moment also will be linked to that special point in case of $N \neq 0$ ($M' \neq M$, see also Fig.4-44)!

4.3.7.2 Component assembly

Now the assembly of all translational spring curves can be launched with “Start iterations”. Alternatively a recently performed assembly calculation may be loaded: Instead of the iterations described afterwards the same type of results can directly be taken from a previously saved output file (file type *.jo2; see 4.3.7.4 “joint curves”) followed by the result presentation (Fig.4-130). Loading a result file requires that the actual joint configuration has already got a unique ID (joint identification, see 4.3.4) and that this agrees with the ID of the saved results to ensure coherence between the actual joint configuration and the results.

The assembly procedure is built up quite similar to the “fundamental iteration procedure” however with a further external loop changing ϕ within the limits ϕ_{start} and ϕ_{end} in steps of $(\phi_{\text{start}} - \phi_{\text{end}})/(\phi \text{ steps})$. The iteration process is indicated by a flood box. A time consuming assembly may be interrupted with a “Stop” button.

For each ϕ -state the following calculations are carried out (for further explanations the previous ϕ -state will be called ϕ_p , the actual one is ϕ_a):

- First a data field of M_i and dN values is calculated depending on the variables w_0 and Ψ .
- Then all possible solutions are searched. Apart from the corresponding spring deformations, spring forces, joint deformations and joint forces also the following data will be stored for each found solution:

Internal work (W_i):

The work done by all the internal component forces is calculated to come from the relevant deformations related to the previous rotation state (ϕ_p) to those of the actual one (ϕ_a), see Fig.4-128.

$$W_i = \sum_{\text{components } k} \int_{w_{p,k}}^{w_{a,k}} F_k(w_k) \cdot dw_k$$

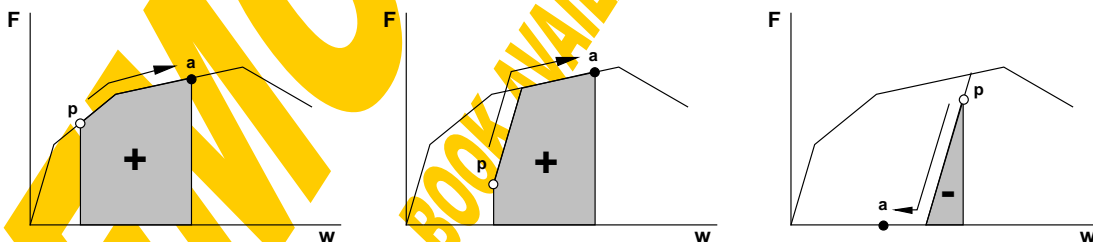


Fig.4-128 Examples for the work done by internal forces

External work (W_a):

The work done by the external joint moment is calculated to come from the previous rotation state (ϕ_p) to the actual one (ϕ_a), see Fig.4-129. As the calculation of the M - ϕ curve is done in ϕ -steps the gained “curve” strictly is only a polygon and therefore the calculated external work to come from ϕ_p to ϕ_a is only an approximation by a linear interpolation. The deviation to the exact value

increases if one component undergoes a drastic change of stiffness within this ϕ -step ϕ_p to ϕ_a (little deviation for higher number of “ ϕ -steps”).

$$W_e = \left| \frac{M_p + M_a}{2} \right| \cdot (\phi_a - \phi_p)$$

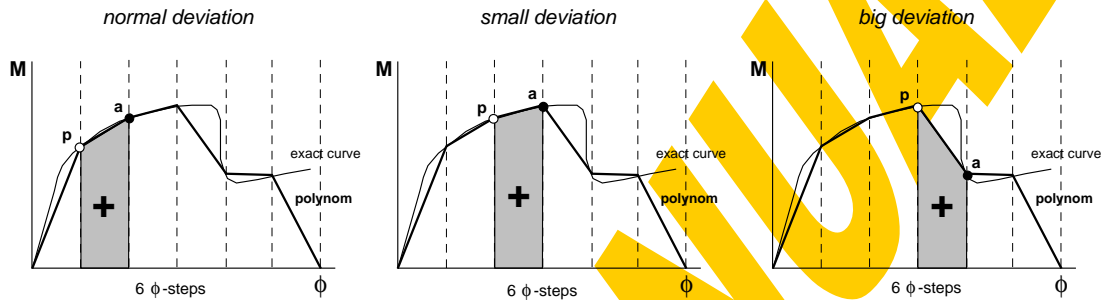


Fig.4-129 Example for the work done by external moments

Work difference ($\Delta W = |W_i - W_d|$):

Finally the difference between internal and external work is determined as an indicator for the accuracy of a solution. For a perfectly small resolution of the M- ϕ curve (infinite number of ϕ -steps) the work difference for the decisive solution would be zero.

- If only one solution could be found for the actual ϕ -state no further investigations are necessary. Otherwise the one decisive solution has to be gained with the criterion that the work difference should be zero (or at least a minimum).
If already for an arbitrary starting rotation ($\phi_a = \phi_{start}$) more than one solution could be found the user will be asked to define one of the gained solutions as the decisive one (so this should already be known from a previous assembly starting with $\phi = 0$).
- For the so-gained decisive solution the corresponding work difference will be converted into the following reference value, which afterwards will be displayed together with the results as an indicator for the reliability of the curves.

$$\overline{\Delta W} = \frac{\Delta W}{\left| \frac{M_p + M_{a,decisive}}{2} \right|} \quad [\% / \text{mrad}]$$

- Finally also the corresponding translational spring deformations are stored for this decisive solution to serve as reference points ($w_i(\phi_p)$) for the next ϕ -state.

Now the above procedure is repeated for the next ϕ -state.

4.3.7.3 Warnings

After the calculations have been finished for the last ϕ -state (ϕ_{end}) it will be checked if the maximum observed work deviation $\overline{\Delta W}_{max}$ exceeds an info limit of 2%/mrad or even a warning limit of 10%/mrad. In such cases the following messages will be displayed:

- The difference between internal and external work is bigger than 2%/mrad. This indicates a deviation of the real M- ϕ curve from its linear interpolation polygon

(stiffness change of spring). So you could try to reduce the ϕ -intervals by increasing the number of ϕ -steps to improve accuracy.

- The difference between internal and external work is bigger than 10%/mrad. This indicates a considerable deviation of the real M- ϕ curve from its linear interpolation polygon (remarkable stiffness change or even failure of one spring). So try to reduce the ϕ -intervals by increasing the number of ϕ -steps to get a more reliable solution. (In the case of a component failure $\overline{\Delta W}_{\max} > 10\%/mrad$ commonly cannot be avoided and therefore this warning then may be ignored.)

Before disregarding such a warning it should be checked if a refinement of ϕ -steps helps to improve accuracy by a closer approximation of the polygon to the real curve. The info and warning limits as well as the default data for the ϕ -steps so far have defined based on the experience with a set of check calculations. Further comprehensive parameter studies using typical joint configurations should help to improve these values.

If some warnings have been observed for one of the several ϕ -states during the procedures "iteration_w0" and "iteration_psi" due to more than one solution within an iteration rectangle or due to a spring failure they will now be displayed in a collected informative message box. In the case of multi-solutions a more dense iteration mesh is recommended (increase "iteration mesh"; attention: doubling the mesh factor quadruples the iteration time!). If the reason really is a spring failure this warning can be ignored. Such a decision can easily be taken from the "basic joint calculations" (see 4.3.6.2).

DEMO - FULL BOOK AVAILABLE AT ERNST & SOHN BERLIN

4.3.7.4 Presentation of results

At the end the calculation window (Fig.4-126) will be modified for the presentation of the results as shown in Fig.4-130. To come back to the definition of assembly boundaries (Fig.4-127) for a new calculation the button “Done” has to be pressed.

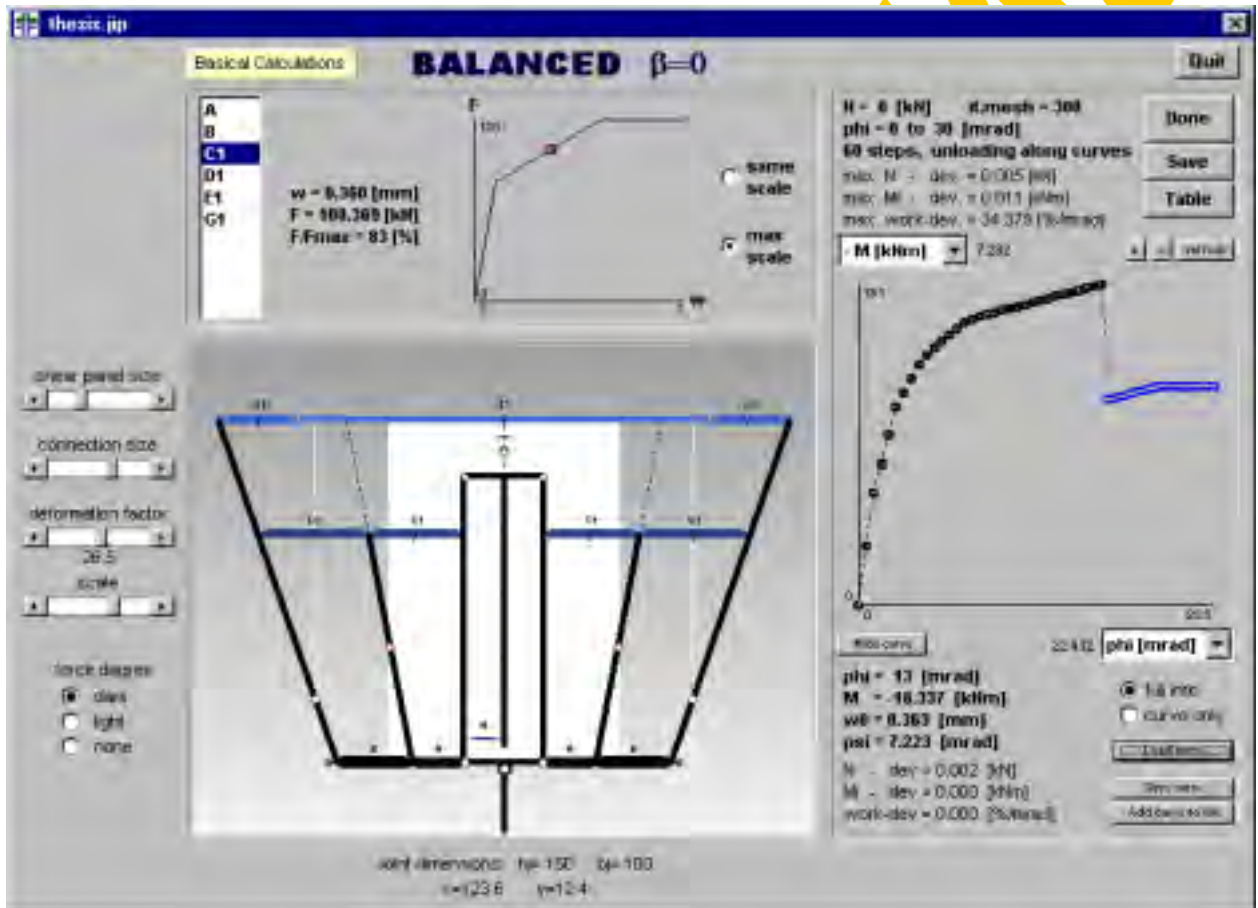


Fig.4-130 Presentation of main calculation results

The several presentation tools should now be described in detail to take maximum profit of the results: Fig.4-131 shows the joint curve window, Fig.4-135 shows the joint deformation window and Fig.4-136 shows the component response window (all these three being part of the overall presentation window shown in Fig.4-130).

Joint curves

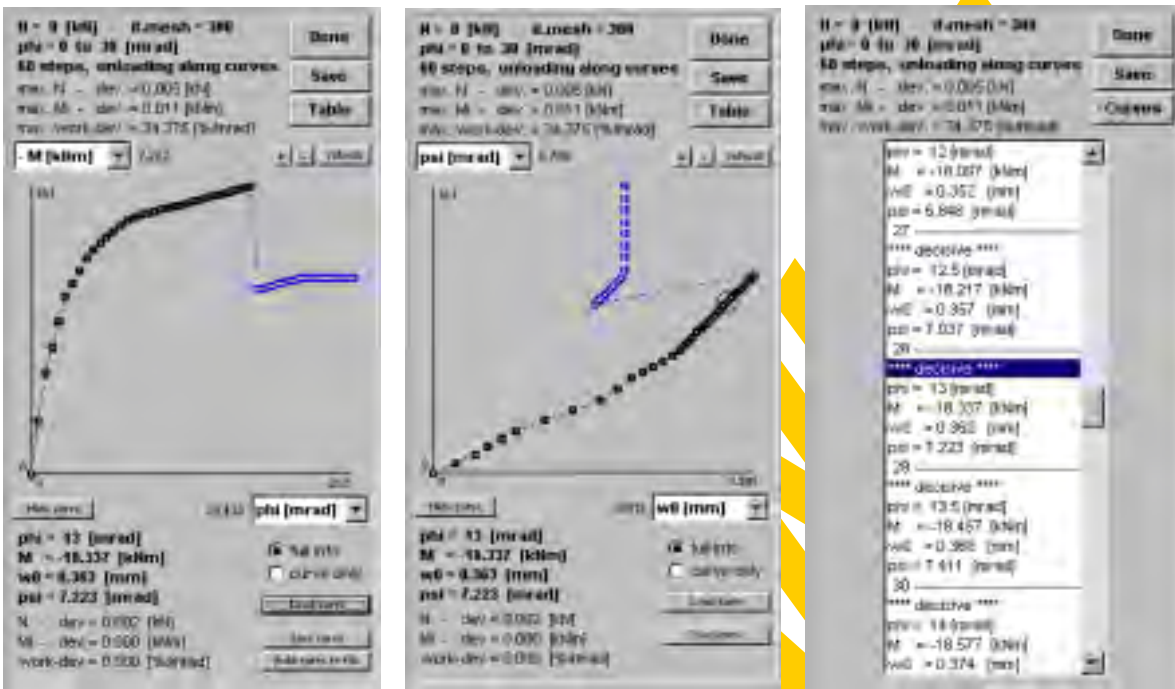


Fig.4-131 Joint curve window

At the top of this window the chosen assembly boundaries such as the normal force, the iteration mesh, the ϕ -range including the number of steps and the type of unloading (linear or along the curve) are stated, followed by the maximum deviation values in view of the normal force, the internal joint moment and the work difference considering all solutions for the whole ϕ -range.

The core of Fig.4-131 is represented by the joint curves themselves. For both of the two axes list boxes enable to select between the joint rotation ϕ [mrad], the joint moment $-M$ [kNm] (hogging positive), the compression dent w_0 [mm] and the rotation of the loadintroduction separation bar Ψ [mrad]. The variety of different axes combinations helps to get an immediate idea about the joint response. All decisive solutions are indicated with thick circles, the other (non-decisive) solutions are drawn as small points. The colour of these circles or points represents the corresponding joint state: black is normal, blue indicates a spring failure and red indicates an invalid force within a component. If $\Delta W_{max} < 2\%/mrad$ the polygon connecting the decisive solution circles is draw with a thick line, if $\Delta W_{max} > 2\%/mrad$ the polygon is a thin line and if $\Delta W_{max} > 10\%/mrad$ the polygon is a dashed line as a kind of warning in view of reliability. For each decisive solution (circles) the corresponding work difference ΔW is indicated by a vertical white bar; the longer this bar the higher is this deviation. This gives an idea within which ϕ -range a refinement of the curve would be recommendable.

With the option buttons "full info" and "curve only" it can be decided whether all the mentioned additional information should be given in the graphs or if it should be focused on the bare curve itself. "Load curve" enables to give an additional reference curve drawn in light green for a direct comparison. Such a reference curve can be loaded from a *.spr-file (Fig.4-90). The values stored in the first column are taken for

the horizontal axis, those of the second column are taken for the vertical axis. The reference curve can be hidden or shown again with the buttons “Hide curve” or “Show curve”. Analogously an actual solution curve (polygon) can be saved to such a *.spr file for a later comparison with other calculations or for an export to other programs. The name of the curve will automatically be set together by the joint file name and the actual axes. The first column is filled with the values of the horizontal axis, the second column stores the vertical axis. To refine an $M-\phi$ curve only in such ϕ -ranges where the observed work deviation has been relatively high the actual $M-\phi$ solutions may be added to an already saved $M-\phi$ curve using the button “Add curve to file”. This might help to save iteration time, however generally it is recommended to start a completely new joint calculation just with a higher number of ϕ -steps but covering again the full ϕ -range.

If the MS Windows clipboard has been used in the meantime it may be necessary to “refresh” the graph. With the “+” button followed by a mouse click definition of two points within the graph a zoomed view can be realised. The “-” button restores the graph within the maximum axes boundaries of all found solutions. Pressing “Shift” and the “-” button simultaneously sets the axes limits to those of the actually loaded reference curve.

With the button “Table” it can be switched from the graphs to a table collecting all solution data in view of the corresponding ϕ , M , w_0 and Ψ values (see Fig.4-131, right side). “Curve” changes back to the graphs. A double click with the mouse on one of the solutions either in the graph or the table also cause a switch between graphical and tabular result representation. The double clicked solution will be high-lightened.

Moving the mouse over the graph (mouse pointer is a crosshair) gives the axis values of the actual mouse position next to the axes list boxes. However one of the most interesting tools certainly is the possibility to see **the direct coherence** between a solution point and both the corresponding joint deformation as well as the corresponding component’s response. So when moving the mouse over the graph whilst the left mouse button is kept pressed (or clicking on a solution in the table) will cause the following procedure: the closest decisive solution point to the actual mouse position is evaluated, high-lightened by a big circle and the corresponding data such as ϕ , M , w_0 , Ψ and all corresponding deviation values are displayed within the lower part of the joint curve window (Fig.4-131). Furthermore the corresponding joint deformation state (Fig.4-135) is updated as well as the corresponding component responses (Fig.4-136). If one of the axis is defined to display the joint rotation ϕ the mouse pointer becomes a horizontal or vertical arrow if the mouse button is pressed, indicating that only that mouse movement in the direction of the ϕ -axis will be considered for the search of the closest decisive solution (this eases to follow the full load history from ϕ_{start} to ϕ_{end} without any unintended jumps). Otherwise the mouse pointer remains a crosshair and both the actual horizontal and vertical mouse position are of interest for the search of the closest decisive solution. When pressing “Shift” additionally (plus left mouse button, plus mouse move) not only the closest decisive but any closest solution can be caught (however those non-decisive solutions normally are not of further interest). Fig.4-132 shows a kind of film representing the graphs resulting from a mouse move along the ϕ - M curve.

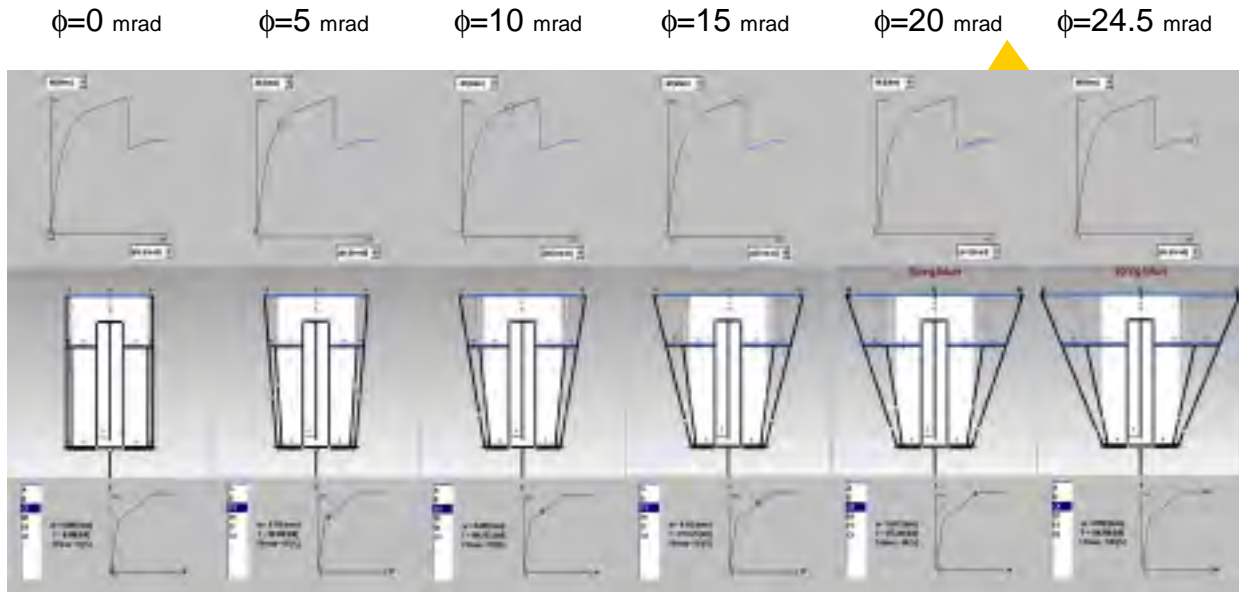


Fig.4-132 Corresponding joint deformation to respective ϕ -M points

Finally the overall gained assembly results can be saved to an output file with the help of the button "Save". First the file name has to be defined with the file management window (Fig.4-86). If the actual joint configuration has ever been saved and therefore has already got its unique joint-ID (see 4.3.4); which enables a clear assignment between joint input and corresponding joint output file, it can be decided between three different output types (if no joint-ID is available type 0 will be chosen automatically):

- type 0 = SHORT file version (*.jo1): As shown on page 306 only a very short file will be produced containing ϕ , M , w_0 and Ψ for the decisive solutions only. Such an output file is intended for a data transfer to other applications but cannot be loaded later instead of carrying out the same assembly iterations again (too little data available).
- type 1 = LONG file version (*.jo2): As shown on page 307 an extended file will be produced containing ϕ , M , w_0 and Ψ as well as all provisional component results (corresponding w -F points and force degrees) however only for the decisive solutions. Such a result file can be loaded later instead of carrying out the same iterations again (see 4.3.7.2).
- type 2 = FULL file version (*.jo2): As shown on page 308 a complete file will be produced containing ϕ , M , w_0 and Ψ as well as all provisional component results (corresponding w -F points and force degrees) for all solutions. Also such a result file can be loaded later instead of carrying out the same iterations again (see 4.3.7.2).

Together with MS Excel these output files e.g. may be used to draw relationships such as between ϕ and the corresponding component deformations w_i or component forces F_i (examples are illustrated in Fig.4-133 and Fig.4-134).

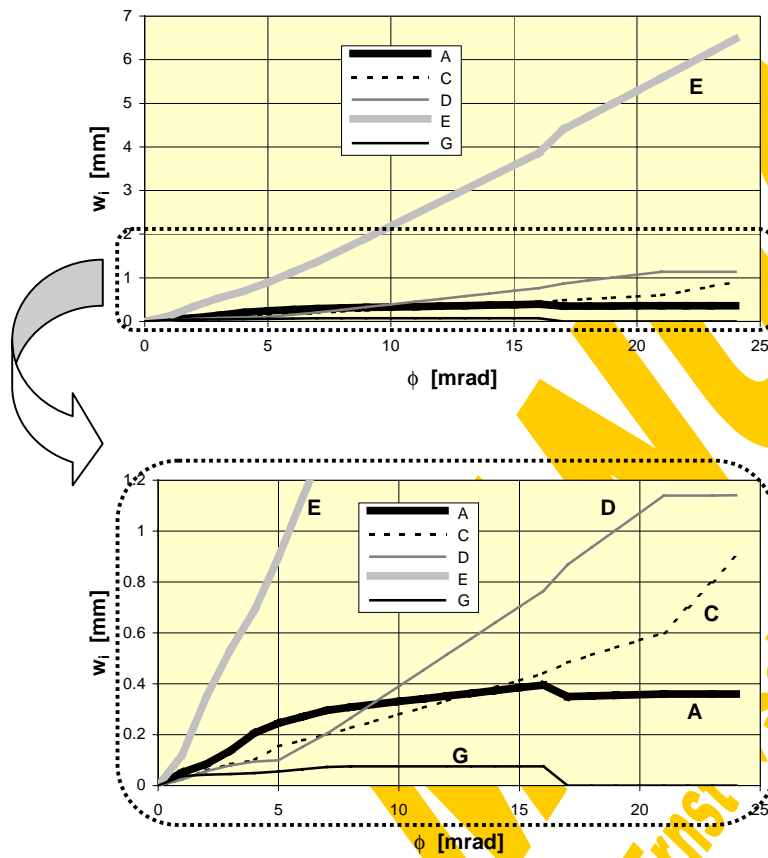


Fig.4-133 Coherence example ϕ - w_i gained from saved output file

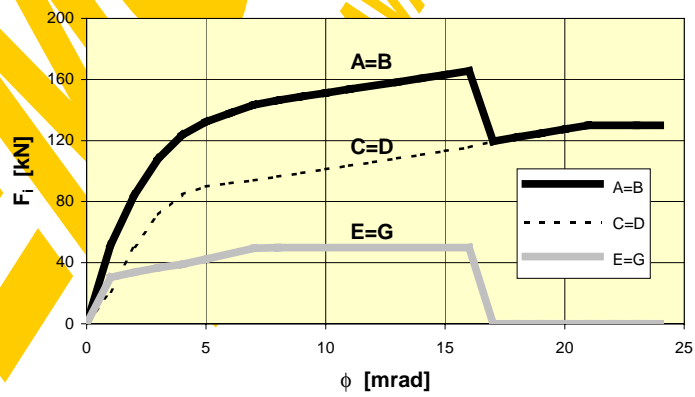


Fig.4-134 Coherence example ϕ - F_i gained from saved output file

SHORT result file version: DECISIVE solutions only

Joint file = thesis.jip
 Joint name = Thesis
 ID-Number 990319183637
 phi-range [mrad] = 0 30
 phi-steps = 30
 LINEAR unloading
 N [kN]= 0
 iteration mesh = 50
 max. deviation of
 N [kN]= 0.0088
 max. deviation of
 Mi [kNm]= 0.0065
 max. deviation of
 work [%/mrad]= 19.0747

 No.of solutions 26
 No.of decisive
 solutions 25

no.	ϕ [mrad]	M [kNm]	w_0 [mm]	Ψ [mrad]	comment
1	0	0	0	0	
2	1	-6.666	0.0515	0.7647	
3	2	-10.1253	0.0844	1.4382	
4	3	-12.6472	0.1366	2.2063	
5	4	-14.3142	0.2065	3.0606	
6	5	-15.3399	0.245	4.0003	
7	6	-16.0768	0.2703	4.4809	
8	7	-16.8135	0.2955	4.9569	
9	8	-17.1356	0.3086	5.3475	
10	9	-17.376	0.3194	5.7223	
11	10	-17.616	0.3303	6.0984	
12	11	-17.8566	0.341	6.4728	
13	12	-18.0971	0.3518	6.8475	
14	13	-18.3373	0.3627	7.2231	
15	14	-18.5773	0.3735	7.5989	
16	15	-18.8179	0.3843	7.9734	
17	16	-19.0579	0.3951	8.3495	
18	17	-11.9515	0.3491	8.326	spring failure
19	18	-12.2143	0.3517	8.6428	spring failure
20	19	-12.4765	0.3543	8.9612	spring failure
21	20	-12.7386	0.3569	9.2797	spring failure
22	21	-12.9996	0.3596	9.6009	spring failure
23	22	-13.0008	0.3596	10.5978	spring failure
24	23	-12.9998	0.3596	11.5979	spring failure
25	24	-13.0011	0.3596	12.5972	spring failure

LONG result file version: DECISIVE solutions PLUS provisional spring results

Joint file = thesis.jp
 Thesis ID-Number = 990319103657
 ID-Number = 30
 iterations = 30
 LINEAR unloading
 N [kN]= 0
 iteration mesh = 50
 max. deviation of N [kN]= 0.0088
 max. deviation of M [kNm]= 0.0065
 max. deviation of work [%/mm]= 19.0747
 No. of solutions = 26
 No. of decisive solutions = 25

no.	ϕ [mm]	decisive	M [kNm]	w_0 [mm]	Ψ [mm]	N joint [kN]	M internal [kNm]	dev. of work [%/mm]	comment
1	0	***	0	0	0	0	0	4.5465	
2	1	***	-6.666	0.0515	0.7647	0.0088	-0.0036	0.0001	
3	2	***	-10.625	0.1344	2.4582	-0.0055	-0.0075	0.0001	
4	3	***	-14.584	0.2173	5.1457	-0.0086	-0.0111	0.0001	
5	4	***	-18.542	0.2995	7.8332	-0.0096	-0.0059	0.0215	
6	5	***	-22.500	0.3817	10.5207	-0.0046	-0.0018	0.0867	
7	6	***	-26.458	0.4639	13.2060	0.0018	0.0033	0.0023	
8	7	***	-30.416	0.5461	15.8913	-0.0049	-0.0002	0.0015	
9	8	***	-34.374	0.6283	18.5766	0.0003	0.0003	0.0018	
10	9	***	-38.332	0.7105	21.2619	0.0006	0.0002	0.2012	
11	10	***	-42.290	0.7927	23.9472	-0.0042	0.0007	0.0009	
12	11	***	-46.248	0.8749	26.6325	-0.0025	-0.0030	0.0001	
13	12	***	-50.206	0.9571	29.3178	-0.0039	-0.0009	0.0001	
14	13	***	-54.164	1.0393	32.0031	-0.0011	0.0009	0.0013	
15	14	***	-58.122	1.1215	34.6884	-0.0017	0.0004	0.0013	
16	15	***	-62.080	1.2037	37.3737	0.0021	-0.0003	0.0001	
17	16	***	-66.038	1.2859	40.0590	0.0003	0.0004	0.0001	
18	17	***	-70.000	1.3681	42.7443	-0.0024	-0.0004	0.0001	
19	18	***	-73.962	1.4503	45.4296	-0.0037	-0.0002	19.0747	spring failure
20	19	***	-77.924	1.5325	48.1149	-0.0045	-0.0001	0.0008	spring failure
21	20	***	-81.886	1.6147	50.8002	-0.0045	0.0013	0.0008	spring failure
22	21	***	-85.848	1.6969	53.4855	-0.0036	-0.0007	0.0006	spring failure
23	22	***	-89.810	1.7791	56.1708	-0.0022	-0.0004	0.0067	spring failure
24	23	***	-93.772	1.8613	58.8561	-0.0022	0.0008	0.0019	spring failure
25	24	***	-97.734	1.9435	61.5414	-0.0022	-0.0002	0.0024	spring failure
26	25	***	-101.696	2.0257	64.2267	-0.0022	0.0011	0.0033	spring failure

spring defl. w [mm], spring force F [kN], percentage of use u [%]

no.	ϕ	w_0	F_0	U_0	F_{01}	U_{01}	W_{01}	F_{01}	U_{01}	W_{01}	F_{01}	U_{01}	W_{01}	F_{01}	U_{01}	W_{01}	F_{01}	U_{01}	W_{01}
1	0	0	0	0	0	0	0	0	0	0	0	0	0	0	0	0	0	0	0
2	1	-0.05	-51.52	17	0.02	21.21	0.02	21.17	15	0.12	30.33	51	0.04	30.33	51	0.04	30.33	51	0
3	2	-0.10	-103.04	34	0.04	42.42	0.04	42.34	30	0.24	60.66	81	0.08	60.66	81	0.08	60.66	81	0
4	3	-0.14	-154.56	51	0.08	63.63	0.08	63.51	45	0.36	90.99	121	0.12	90.99	121	0.12	90.99	121	0
5	4	-0.21	-231.84	71	0.12	95.45	0.12	95.27	63	0.54	136.48	181	0.16	136.48	181	0.16	136.48	181	0
6	5	-0.25	-304.80	95	0.16	127.27	0.16	127.05	84	0.72	181.92	241	0.20	181.92	241	0.20	181.92	241	0
7	6	-0.27	-377.76	121	0.20	158.18	0.20	157.92	108	0.90	226.36	301	0.24	226.36	301	0.24	226.36	301	0
8	7	-0.30	-450.72	148	0.24	189.09	0.24	188.79	136	1.08	270.80	361	0.28	270.80	361	0.28	270.80	361	0
9	8	-0.31	-523.68	176	0.28	220.00	0.28	219.66	164	1.26	315.24	421	0.32	315.24	421	0.32	315.24	421	0
10	9	-0.32	-596.64	204	0.32	250.91	0.32	250.53	192	1.44	359.68	481	0.36	359.68	481	0.36	359.68	481	0
11	10	-0.34	-669.60	232	0.36	281.82	0.36	281.40	220	1.62	404.12	541	0.40	404.12	541	0.40	404.12	541	0
12	11	-0.34	-742.56	260	0.36	312.73	0.36	312.27	248	1.80	448.56	601	0.44	448.56	601	0.44	448.56	601	0
13	12	-0.35	-815.52	288	0.36	343.64	0.36	343.14	276	1.98	493.00	661	0.48	493.00	661	0.48	493.00	661	0
14	13	-0.36	-888.48	316	0.36	374.55	0.36	374.01	304	2.16	537.44	721	0.52	537.44	721	0.52	537.44	721	0
15	14	-0.37	-961.44	344	0.36	405.46	0.36	404.88	332	2.34	581.88	781	0.56	581.88	781	0.56	581.88	781	0
16	15	-0.38	-1034.40	372	0.36	436.37	0.36	435.74	360	2.52	626.32	841	0.60	626.32	841	0.60	626.32	841	0
17	16	-0.40	-1107.36	400	0.36	467.28	0.36	466.59	388	2.70	670.76	901	0.64	670.76	901	0.64	670.76	901	0
18	17	-0.35	-1180.32	428	0.36	498.19	0.36	497.45	416	2.88	715.20	961	0.68	715.20	961	0.68	715.20	961	0
19	18	-0.35	-1253.28	456	0.36	529.10	0.36	528.31	444	3.06	759.64	1021	0.72	759.64	1021	0.72	759.64	1021	0
20	19	-0.35	-1326.24	484	0.36	560.01	0.36	559.17	472	3.24	804.08	1081	0.76	804.08	1081	0.76	804.08	1081	0
21	20	-0.36	-1400.00	512	0.36	590.92	0.36	590.03	500	3.42	848.52	1141	0.80	848.52	1141	0.80	848.52	1141	0
22	21	-0.36	-1473.76	540	0.36	621.83	0.36	620.89	528	3.60	892.96	1201	0.84	892.96	1201	0.84	892.96	1201	0
23	22	-0.36	-1547.52	568	0.36	652.74	0.36	651.75	556	3.78	937.40	1261	0.88	937.40	1261	0.88	937.40	1261	0
24	23	-0.36	-1621.28	596	0.36	683.65	0.36	682.61	584	3.96	981.84	1321	0.92	981.84	1321	0.92	981.84	1321	0
25	24	-0.36	-1695.04	624	0.36	714.56	0.36	713.47	612	4.14	1026.28	1381	0.96	1026.28	1381	0.96	1026.28	1381	0

Warnings:

FULL result file version(ALL) solutions PLUS provisional spring results

Joint file = thesis.jit
 ID-Number = 990319183637
 phi-range [mm] = 0 30
 phi-steps = 30
 N [mm] = 0
 N [mm] unloading = 50
 iteration mesh = 0.0068
 max.deviaton of N [kN]=
 max.deviaton of M [kNm]=
 max.deviaton of work [%/mm]= 19.0747
 No. of solutions = 26
 No. of decisive solutions = 25

no.	phi [mm]	W0 [mm]	psi [mm]	N joint [kN]	M internal [kNm]	dev.of work [%/mm]	comment
1	0	0	0	0	0	0	
2	1	-6.666	0.7647	0.0088	-0.0036	4.5465	
3	2	-10.1207	1.4387	0.0016	-0.0065	0.0383	
4	3	-10.1263	1.4382	-0.0055	-0.0007	0.011	
5	4	-12.6472	2.2063	0.0007	-0.0006	1.956	
6	5	-15.3399	3.246	0.0018	-0.0023	0.879	
7	6	-16.0768	4.0003	0.0018	-0.0023	0.8667	
8	7	-16.8135	4.4809	-0.0049	-0.0002	0.0015	
9	8	-17.1356	4.9569	0.0003	-0.0008	0.0018	
10	9	-17.376	5.3475	0.0005	-0.0002	0.2012	
11	10	-17.616	5.7223	-0.0042	-0.0007	0.0008	
12	11	-17.856	6.0984	-0.0038	-0.0003	0.0001	
13	12	-18.096	6.4728	-0.0037	-0.0005	0.0001	
14	13	-18.337	6.8471	-0.0037	-0.0004	0.0001	
15	14	-18.5773	7.2215	-0.0017	-0.0004	0.0013	
16	15	-18.8179	7.5959	0.0021	-0.0003	0.0001	
17	16	-19.0579	7.9734	0.0003	-0.0004	0.0001	
18	17	-19.2979	8.3495	-0.0024	-0.0004	0.0001	spring failure
19	18	-19.5379	8.7256	-0.0037	-0.0002	19.0747	spring failure
20	19	-19.7779	9.1017	-0.0049	-0.0009	0.0001	spring failure
21	20	-20.0179	9.4778	-0.0045	-0.0003	0.0016	spring failure
22	21	-20.2579	9.8539	-0.0035	-0.0007	0.0006	spring failure
23	22	-20.4979	10.2299	-0.0022	-0.0008	0.0019	spring failure
24	23	-20.7379	10.6060	-0.0022	-0.0008	0.0019	spring failure
25	24	-20.9779	10.9821	-0.0022	-0.0002	0.0024	spring failure
26	25	-21.2179	11.3582	-0.0022	-0.0011	0.0033	spring failure
27	26	-21.4579	11.7343	-0.0022	-0.0011	0.0033	spring failure

spring deflo w [mm], spring force F [kN], percentage of use u [%]

no.	phi	Ws	Fs	Us	Fb	Ub	Wd1	Fd1	Ud1	Wt1	Ft1	Ut1	Wg1	Fg1	Ug1
1	0	0	0	0	0	0	0	0	0	0	0	0	0	0	0
2	1	-0.05	-51.52	17	-51.49	26	0.02	21.21	16	0.02	0.12	15	0.04	30.33	51
3	2	-0.09	-84.37	28	-84.31	42	0.06	50.59	39	0.06	0.21	36	0.04	33.80	56
4	3	-0.14	-117.22	38	-117.14	62	0.06	50.55	39	0.06	0.35	36	0.04	33.80	56
5	4	-0.21	-150.07	48	-149.95	82	0.06	50.55	39	0.06	0.50	36	0.04	33.80	56
6	5	-0.25	-182.92	58	-182.81	102	0.10	84.60	65	0.09	0.69	60	0.05	39.07	65
7	6	-0.27	-215.77	68	-215.62	122	0.10	84.60	65	0.09	0.80	64	0.06	42.26	70
8	7	-0.30	-248.62	78	-248.44	142	0.15	92.00	71	0.15	1.13	66	0.06	45.65	76
9	8	-0.31	-281.47	88	-281.25	162	0.20	94.02	72	0.20	1.36	67	0.07	49.42	82
10	9	-0.32	-314.32	98	-314.06	182	0.23	96.35	74	0.27	1.63	69	0.08	50.00	83
11	10	-0.33	-347.17	108	-346.77	202	0.25	98.75	76	0.33	1.91	71	0.08	50.00	83
12	11	-0.34	-380.02	118	-379.48	222	0.28	101.16	78	0.39	2.19	72	0.08	50.00	83
13	12	-0.35	-412.87	128	-411.34	242	0.33	103.56	80	0.45	2.47	74	0.08	50.00	83
14	13	-0.35	-445.72	138	-443.14	262	0.33	105.96	82	0.55	2.75	76	0.08	50.00	83
15	14	-0.36	-478.57	148	-475.94	282	0.33	108.37	83	0.65	3.02	77	0.08	50.00	83
16	15	-0.37	-511.42	158	-508.74	302	0.39	110.77	85	0.64	3.30	79	0.08	50.00	83
17	16	-0.37	-544.27	168	-541.64	322	0.41	113.18	87	0.64	3.58	81	0.08	50.00	83
18	17	-0.38	-577.12	178	-574.51	342	0.44	115.58	89	0.77	3.86	83	0.08	50.00	83
19	18	-0.40	-610.00	188	-606.88	362	0.44	115.58	89	0.77	4.14	85	0.08	50.00	83
20	19	-0.35	-642.85	198	-639.68	382	0.48	119.52	92	0.87	4.40	87	0.08	50.00	83
21	20	-0.35	-675.70	208	-672.53	402	0.51	122.13	94	0.94	4.70	89	0.08	50.00	83
22	21	-0.36	-708.55	218	-705.42	422	0.51	124.74	96	0.94	5.00	91	0.08	50.00	83
23	22	-0.36	-741.40	228	-738.27	442	0.57	127.35	98	1.00	5.29	93	0.08	50.00	83
24	23	-0.36	-774.25	238	-771.12	462	0.60	130.00	100	1.14	5.58	95	0.08	50.00	83
25	24	-0.36	-807.10	248	-804.00	482	0.70	130.00	100	1.14	5.88	97	0.08	50.00	83
26	25	-0.36	-840.00	258	-836.88	502	0.80	130.00	100	1.14	6.18	99	0.08	50.00	83
27	26	-0.36	-872.85	268	-869.73	522	0.90	130.00	100	1.14	6.48	101	0.08	50.00	83

Warnings:

Joint deformation

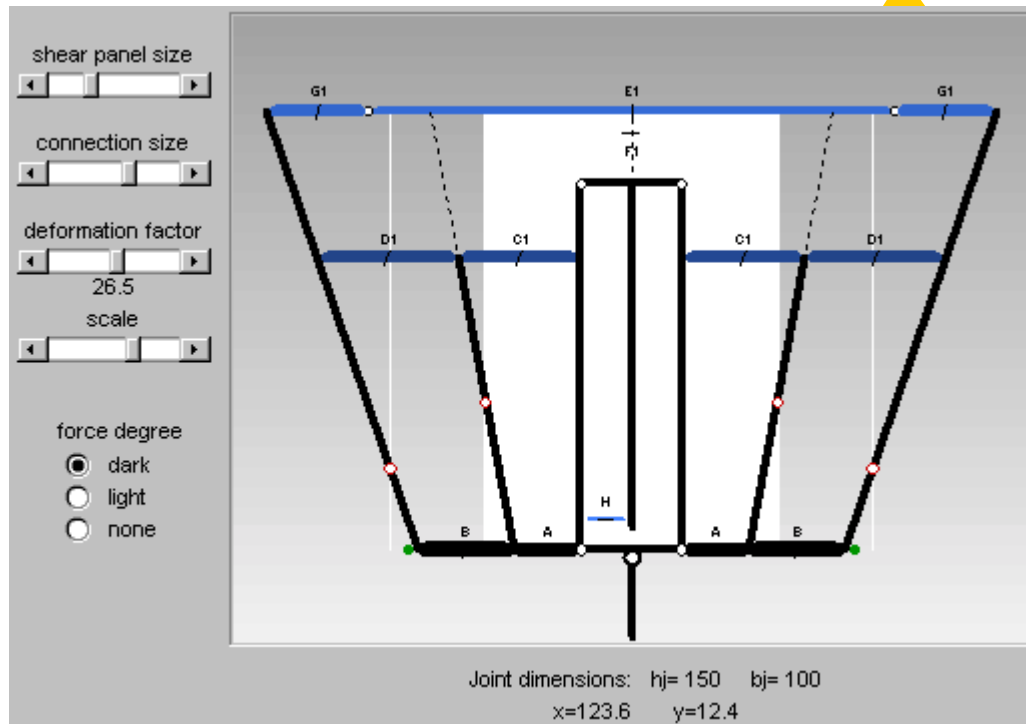


Fig.4-135 Joint deformation window

The graphical presentation of the actual joint deformation state has already been described in detail in chapter 4.3.6.1 (presentation of results, Fig.4-112). It comprises the actual component deformations including the force degrees (incl. eventual spring failures) and the rotation centres of the separation bars.

Moving the mouse over the graph displays the actual geometrical values x and y below the graph. The shear panel size, the connection size, the deformation factor and the joint scale may be varied using the relevant scroll bars. The presentation of the force degrees can be manipulated with option buttons: either “dark” or “light” bars are indicating the actual force degree (percentage of use) for each component or this additional information can be switched off.

Component response

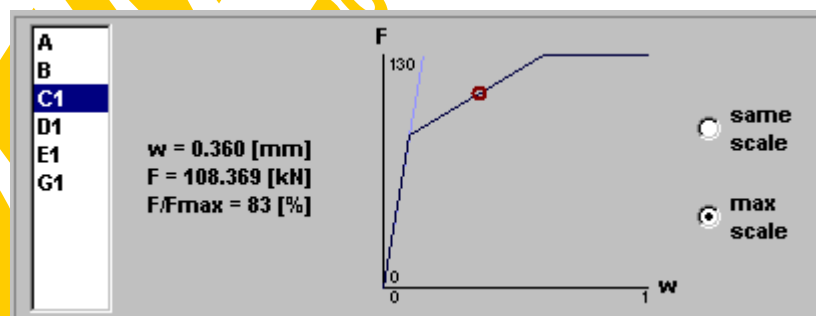


Fig.4-136 Component response window

The w-F values corresponding to the presently chosen solution is drawn for each contributing component as a red point within the relevant w-F curve. Due to an eventual linear unloading this point must not always lie on the curve itself. By clicking on the table of contributing components one being of present interest can be chosen. The state of the option buttons “same scale” or “max. scale” decides whether all component curves are drawn with the same axes limits or if for each one the scale should be stretched to fill the full diagram area.

4.3.7.5 Final comparisons

Fig.4-137 shows a comparison between the results gained for the described example joint (“thesis.jip”, see page 263) and those results from the same joint, however where only the layer of reinforcement in tension has been removed. So this is a comparison between a composite joint and its steelwork counterpart (final state ↔ erection state). The gain of stiffness and resistance by adding and activating the slab reinforcement for the joint action is obvious. In this composite joint example (“thesis.jip”) the ductility of the reinforcement deliberately has been reduced just to demonstrate a spring failure. However in normal practice the composite joint will provide a clear moment plateau for plastic redistribution (thick line in Fig.4-137 with modified spring E with 8mm ductility instead of 4mm).

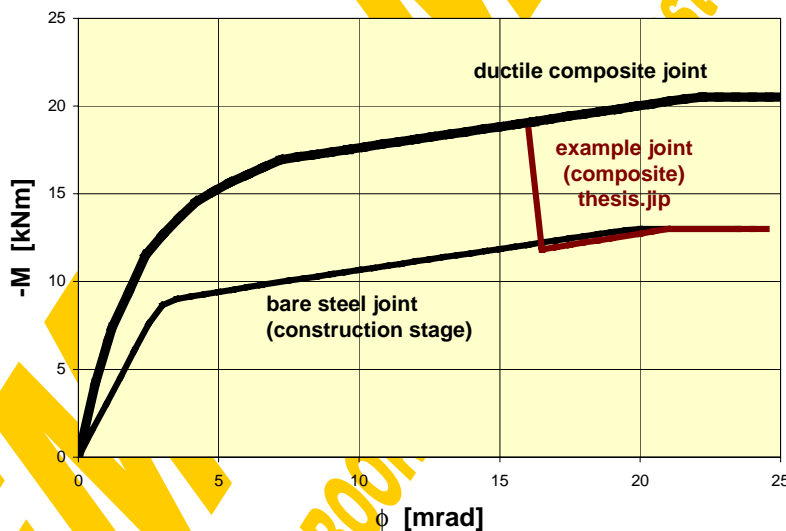


Fig.4-137 Composite joint compared to bare steel joint counterpart

The difference in view of the M- ϕ curve once calculated with a linear component unloading and once with an unloading along the F-w curve can be seen in Fig.4-138. As for the example joint “thesis.jip” only the component A will be unloaded the difference in the resulting curves is not really important.

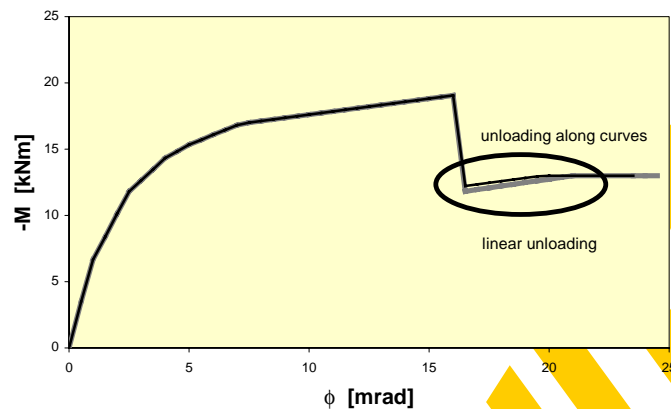


Fig.4-138 Different M - ϕ curves due to different component unloading types

Finally a comparison should be performed between the sophisticated curve gained with the help of CoBeJo and the joint's key values (initial stiffness S_{ini} and moment resistance M_R) according to the Eurocode [49,60] assembly procedures. The EC-calculation for the example joint "thesis.jip" is given in Fig.4-139. A comparative graph can be seen in Fig.4-140.

c ... spring stiffness [kN/mm], F ... spring resistance [kN]

compression row A+B:

$$c_{AB} = \frac{1}{\frac{1}{1000} + \frac{1}{\infty}} = 1000 \quad F_{AB} = \min(300; 200) = 200$$

steelwork tension row C+D ($y = 100\text{mm}$):

$$c_{CD} = \frac{1}{\frac{1}{850} + \frac{1}{900}} = 437 \quad F_{CD} = \min(130; 140) = 130$$

reinforcement row E/2+G ($y = 150\text{mm}$):

$$c_{EG} = \frac{1}{\frac{1}{2 \cdot 300} + \frac{1}{800}} = 343 \quad F_{EG} = \min(50; 60) = 50$$

$$z_{eq} = \frac{437 \cdot 100^2 + 343 \cdot 150^2}{437 \cdot 100 + 343 \cdot 150} = 127 \text{ mm} \quad [\text{see EC3 - Annex J (J.38)}]$$

$$c_{eq} = \frac{437 \cdot 100 + 343 \cdot 150}{127} = 749 \text{ kN/mm} \quad [\text{see EC3 - Annex J (J.36)}]$$

$$S_{ini} = \frac{127^2}{\frac{1}{1000} + \frac{1}{749}} = 6910 \text{ kNm}$$

$$M_R = 50 \cdot 150 + 130 \cdot 100 = 20.5 \text{ kNm} \quad (50 + 130 < 200 \text{ ok})$$

Fig.4-139 Main joint characteristics calculated according to the Eurocodes [49,60]

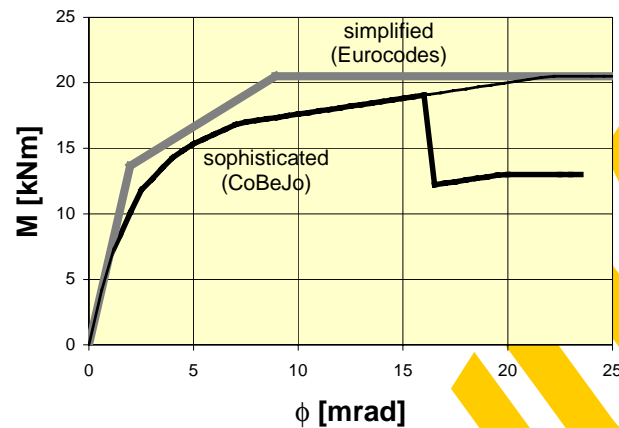


Fig.4-140 Graphical comparison between sophisticated and simplified spring assembly results

4.3.7.6 Unbalanced joint loading

The present program version only enables the assembly for balanced joint moments ($\beta=0$, see Fig.4-141). In the future this will be extended to fully unbalanced joints ($\beta=1$, single-sided) including the behaviour of the components F and H as well as the frame spring SYS. Finally it will be enlarged to $0 < \beta < 1$.

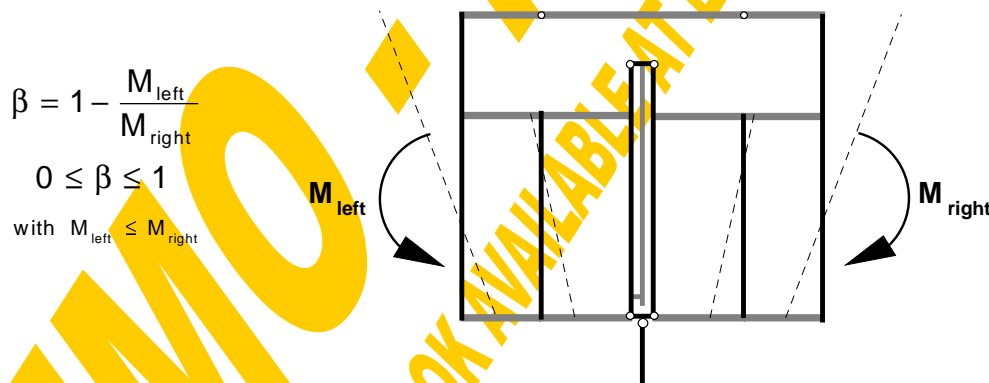


Fig.4-141 Ratio of moment imbalance

For $\beta=0$ only three (w_{0r}, Ψ_r, ϕ_r) of the overall seven ($w_{0\ell}, \Psi_{\ell}, \phi_{\ell}, w_{0r}, \Psi_r, \phi_r, \phi_s$) degrees of freedom (Fig.4-142) had to be varied within the iterations, because due to symmetry the deformations on the left and right hand side are equal and the shear deformation even is zero. However the general structure of the program has already been built up in view of such an extension to unbalanced joint loading.

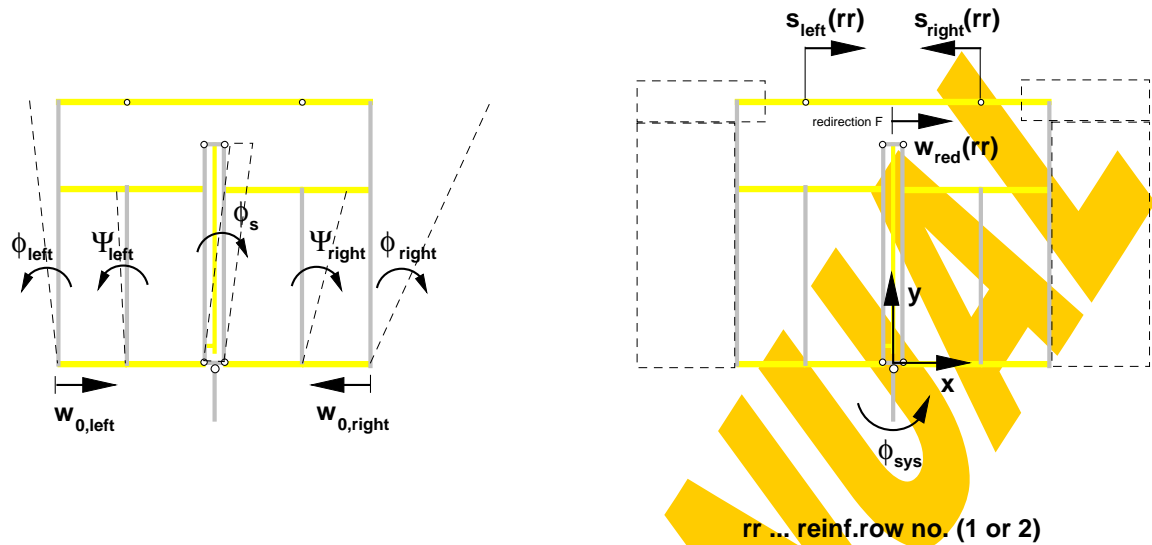


Fig.4-142 Joint degrees of freedom and remaining variables

4.3.8 Conclusions

Both the theoretical background as well as the handling of the CoBeJo-module “Joint characterisation” have been described. This program represents a powerful tool for the non-linear assembly of component springs according to the Innsbruck component model. As the pre- and post-processing possibilities have especially been adopted to the requirements of joint calculations it is a real alternative to conventional FE-programs, which have been used for check calculations [137]. In the present version, where the component characteristics have to be taken from tests or mechanical models this program is primarily intended to researchers and advanced practitioners. Integrating this sophisticated assembly procedure into an overall joint characterisation package like the Module Bank Program [122] could increase its common use drastically.

Using comprehensive parameter studies the assembly procedure CoBeJo-Joint will now serve to investigate the applicability of the simplified Eurocode component assembly as well as the influence of overstrength effects on failure modes and joint rotation capacity.

REFERENCES

References

A

- 1 Acker, A.: *Recommendations for the design of precast prestressed hollow core floors*. ECCS/TC11, Düsseldorf (1996)
- 2 Aigner, M.: *Detailuntersuchungen für Anschlußprobleme von Flachdecken an runde Stahlprofile und Verbundprofile*. Master thesis, Innsbruck (1996)
- 3 Ampferer, G.: *Detailuntersuchungen für Anschlußprobleme von Flachdecken an rechteckige Stahlstützen bzw. Verbundstützen*. Master thesis, Innsbruck (1996)
- 4 Aribert, J.M.: *Effect of the structural steel grade on the design of partial shear connections. Specific investigation of steel grade S460*. ECCS/TC11-8/96 (1996)
- 5 Aribert, J.M.: *Influence of slip of the shear connection on composite joint behaviour*. Third International Workshop on Connections in Steel Structures, Trento (1995)

B

- 6 Badran, M.Z.: *Modelling of the connection zone of composite joints*. Doctoral thesis, Innsbruck (1995)
- 7 Badran, M.Z.: *Tests on semi-rigid composite joints*. COST C1-Workshop Prague (1994)
- 8 Baehre, R., Pepin, R.: *Flachdecken mit Stahlträgern in Skelettbauweise*. Bauingenieur 70 p.65-71 (1995)
- 9 Bakker, C.; Voorn, W.: *Gelaste Hoekverbindingen in Raamwerken*. Amsterdam/Brussels (1974)
- 10 Bauberatung Stahl: *Geschoßbau in Stahl. Flachdecken-Systeme*. Dokumentation 605, Düsseldorf (1996)
- 11 Bauberatung Stahl: *Neue Wege im Stahl- und Verbundbau*. Dokumentation 601, Düsseldorf.
- 12 BCSA; SCI: *Joints in steel construction: Moment connections*. Publication no.207/95 (1995)
- 13 Bernuzzi, C.; Gadotti, F.; Zandonini, R.: *Joint Action in Slim Floor Systems*. COST C1-WG 2 (1995)
- 14 Bijlaard, F.; Steenhuis, M.: *Prediction of the influence of connection behaviour on the strength, deformations and stability of frames, by classification of connections*. AISC, Connections in steel structures II, Pittsburgh (1991)

- 15 Bjorhovde, R.; Brozzetti, J.; Colson, A.: *Connections in steel structures. Behaviour, strength and design*. Cachan (1987)
- 16 Bode, H.: *Verbundbau. Konstruktion. Berechnung*. Werner-Verlag (1987)
- 17 Bode, H.: *Versuche mit Verbundträgern bei niedrigem Verdübelungsgrad*. Stahlbau, 60.Jahrgang, Heft 9 (1991)
- 18 Bode, H.: *Zur Verdübelung von Verbundkonstruktionen*. Der Prüfeningenieur (1992)
- 19 Bode, H.; Kronenberger, H.-J.: *Behaviour of composite joints and their influence on semi-continuous composite beams*. Engineering Foundation Conference, Composite Construction III, Irsee (1996)
- 20 Bode, H.; Kronenberger, H.-J.: *Zum Einfluß teiltragfähiger, verformbarer Verbundanschlüsse auf das Tragverhalten von Verbundträgern*. Stahlbau 67 p.501-515 (1998)
- 21 Bode, H.; Minas, F.: *Bemessungsdiagramme zur Vordimensionierung von Geschoßdecken in Stahlverbundbauweise*. Bautechnik, 72.Jahrgang, Heft 11 (1995)
- 22 Bode, H.; Schanzenbach, J.: *Das Tragverhalten von Verbundträgern bei Berücksichtigung der Dübelnachgiebigkeit*. Stahlbau, 58.Jahrgang, Heft 3 (1989)
- 23 Bode, H.; Stengel, J; Sedlacek, G; Feldmann, M; Müller, C.: *Untersuchung des Tragverhaltens bei Flachdecken-Systemen mit verschiedener Ausbildung der Platten und verschiedener Lage der Stahlträger*. Endbericht P261; Forschungsprojekt, Universität Kaiserslautern, RWTH Aachen (1996)
- 24 Bozzo, E.; Piazza, M.; Ballerini, M.; Occhi, F.: *Il sistema flowdrill per la giunzione di elementi tubolari in acciaio. (The flowdrill system in hollow steel section joints.)* Giornate italiane della costruzione in acciaio (1993)
- 25 Braun, Ch.: *Das Momenten-Rotationsverhalten von geschweißten, steifenlosen Rahmenknoten bei Querkraftbeanspruchung*. Doctoral thesis, Innsbruck (1987)
- 26 Brugger, E.: *Zur lokalen Krafteinleitung bei IPE-Profilen*. Master thesis, Innsbruck (1994)
- 27 Brugger, R.: *Zur Schubtragfähigkeit von Verbundknoten*. Doctoral thesis, Innsbruck (1993)
- 28 Bucheli, P.; Crisinel, M.: *Verbundträger im Hochbau. Theoretische Grundlagen, Beispiele, Bemessungstabellen*. SZS Schweizerische Zentralstelle für Stahlbau (1982)
- 29 Bürkner, K.-E.: *Elasto-plastische Berechnung von nachgiebig verdübelten Verbundtragwerken - FE-Berechnungen und Versuche*. Mitteilung Nr.81-1 des Instituts für Konstruktiven Ingenieurbau - Ruhr-Universität Bochum (1981)

C

- 30 CEB-FIP: *Model Code 1990 - Design code*. Lausanne (1993)
- 31 Commission of the European Communities: *Frame design including joint behaviour (Vol.1-3)*. Executive Committee Ref.no. 93-F6.05, ECSC no.7210-SA/212+320 (1997)
- 32 Cosenza, E.; Fabbrocino, G.; Manfredi, G.: *Some remarks on the development of rotation capacity of composite joints*. COST C1/WD2-97-27 (1997)
- 33 Cosenza, E.; Fabbrocino, G.; Manfredi, G.: *The influence of the rebar ductility on the rotational capacity of composite beams*. SDSS'97, Nagoya (1997)
- 34 Cosenza, E.; Manfredi, G.; Mazzolani, S.: *Some remarks on the modelling of the interaction between the reinforcing steel - concrete in tension - shear connectors and structural steel in composite joints*. COST C1-Workshop, Prague (1994)
- 35 Cosenza, E.; Mazzolani, S.; Pecce M.: *Ultimate limit state checking of continuous composite beams designed to Eurocode recommendations*. Costruzioni Metalliche, No.5 (1992)
- 36 COST C1: *Recent advances in the field of structural steel joints and their representation in the building frame analysis and design process*. Brussels/Luxembourg (1999)
- 37 COST C1: *Semi rigid behaviour of civil engineering structural connections*. Proceedings of the 1st state of the art workshop, Straßbourg (1992)
- 38 COST C1: *Semi rigid behaviour of civil engineering structural connections*. Proceedings of the 2nd state of the art workshop, Prague (1994)
- 39 COST C1: *Semi rigid behaviour of civil engineering structural connections*. Proceedings of the International Conference, Liège (1997)
- 40 COST C1: *Composite steel-concrete joints in braced frames for buildings*. Brussels/Luxembourg (1996)
- 41 Couchman, G; Lawson, M.: *The use of composite connections in practice*. International Conference "Composite Construction - Conventional and Innovative" in Innsbruck, Report p.451-456, IABSE Zürich (1997)

D

- 42 Dabaon, M.A.: *Beitrag zur teilweisen Verdübelung bei Verbundträgern*. Doctoral thesis, Innsbruck (1993)
- 43 Dabaon, M.A.; Tschemmerneegg, F.; Hassan, K.; Lateef, T.A.: *Zur Tragfähigkeit von Verbundträgern bei teilweiser Verdübelung*. Stahlbau, 62.Jahrgang, Heft 1 (1993)

- 44 Demetz, St.: *Vereinfachte Verbundrahmenberechnung nach ENV1994-1-1 anhand der Rahmensysteme aus den Diplomarbeiten von Hudritsch D. und Hächl M. mit anschließendem Vergleich*. Master thesis, Innsbruck (1999)
- 45 Deutsches Institut für Bautechnik: *FEDU-Verbundelement*. Allgemeine bauaufsichtliche Zulassung, Zul.nr. Z-26.4-33, Berlin (1997)
- 46 DIN 18800, Teil 5: *Verbundtragwerke aus Stahl und Beton. Bemessung und Konstruktion*. 3.Entwurf (1996)
- 47 Dornetshuber, J.: *Zur Krafteinleitung in Verbundknoten mit Rohrprofilen*. Master thesis, Innsbruck (1990)
- 48 DStV - Deutscher Stahlbau-Verband: *Bemessung und Konstruktion von Verbundtragwerken aus Stahl und Beton*. Deutsche Fassung der EKS-Veröff. No.72 (1994)

E

- 49 ECCS: *Design of composite joints for buildings (incl. Model code provisions for composite joints in building frames)*. TC11, Brussels (1999)
- 50 ECCS: *Analysis and design of steel frames with semi-rigid joints*. ECCS TC8, report no.67 (1992)
- 51 ECCS: *Composite beams and columns to Eurocode 4*. Report no.72, Brussels (1993)
- 52 ECCS: *Design manual for composite slabs*. Report no.87, Brussels (1995)
- 53 ECCS: *Design tables for composite beams*. TC11, Brussels (1999)
- 54 ECCS: *Examples to Eurocode 3*. Report no.71, Brussels (1993)
- 55 ECCS: *Geschoßbau in Stahl: Eine schwedische Bauweise. (Multi-storey building in steel - The swedish development)*. Report no.74, Brussels (1996)
- 56 ECCS: *Multi-storey buildings in steel - Design guide for slim floors with built-in beams*. Report no.83, Brussels (1995)
- 57 Ellmerer, P.: *Ermittlung der charakteristischen Kennwerte der Krafteinleitungsfedern für HEA-Profile*. Master thesis, Innsbruck (1988)
- 58 ENV 1993-1-1: *Eurocode 3 - Bemessung und Konstruktion von Stahlbauten (Design of steel structures)*.
- 59 ENV 1994-1-1: *Eurocode 4 - Bemessung und Konstruktion von Verbundtragwerken aus Stahl und Beton (Design of composite steel and concrete structures)*.
- 60 ENV-1993-1-1/pr A2: Revised annex J (version Nov.94): *Joints in building frames*. (1994)
- 61 ENV-1993-1-1:1992/A2: Annex Z: *Determination of design resistance from tests*. (1998)

- 62 ENV-1994-2: *Design of composite steel and concrete structures - Bridges*. (1997)

F

- 63 Fabbrocino, G.; Manfredi, G.; Pecce, M.: *Modelling of steel-concrete composite beams with partial shear connection subjected to hogging moment* (in Italian). XI th C.T.E. Symposium, Napels (1996)
- 64 Fink, A.: *Das Momentenrotationsverhalten von Verbundknoten mit Verbundstützen aus Rechteckhohlprofilen*. Doctoral thesis, Innsbruck (1997)
- 65 Fink, A.: *Die Krafteinleitung in Stahlstützen unter Berücksichtigung einer Stützennormalkraft*. Master thesis, Innsbruck (1992)
- 66 Fontana, M., Borgogno, W.: *Brandverhalten von Slim-Floor-Verbunddecken*. Stahlbau 64 p.168-174 (1995)

G

- 67 Gomes, F.: *Proposal for the classification of beam-to-column joints*. COST C1/WD2-95-20 (1995)
- 68 Grimus, W.: *Die Krafteinleitung in Verbundstützen*. Master thesis, Innsbruck (1989)

H

- 69 Hächl, M.: *Berechnung eines unverschieblichen Verbundrahmens mit ausbetonierten Kreis-Hohlprofilstützen und Verbundflachdecken*. Master thesis, Innsbruck (1998)
- 70 Haensel, J.: *Kriechen und Schwinden des Betons in Stahlträger-Verbundkonstruktionen*. Werner-Verlag (1977)
- 71 Haller, R.: *Kalibrierung von Komponenten für Knoten in Mischbauweisen mit Walzprofilstützen für ENV1994-1-1, Annex J*. Master thesis, Innsbruck (1998)
- 72 Hanswille, G.: *Cracking of concrete - mechanical models of the design rules in EC4*. Engineering Foundation Conference, Composite Construction III, Irsee (1996)
- 73 Hanswille, G.: *Zur Rißbreitenbeschränkung bei Verbundträgern*. Mitteilung Nr.86-1 des Instituts für Konstruktiven Ingenieurbau - Ruhr-Universität Bochum (1986)
- 74 Herzog, M.: *Steifigkeitskalibrierung von Komponenten für Knoten in Mischbauweise mit Hohlprofilstützen für ENV1994-1-1, Annex J*. Master thesis, Innsbruck (1998)
- 75 Hittenberger, R.: *Zur Durchdringung von Stützen und Deckenplatten bei Verbundknoten*. Doctoral thesis, Innsbruck (1992)

- 76 Holzner, B.: *Die Krafteinleitung in Verbundstützen unter Berücksichtigung einer Stützennormalkraft*. Master thesis, Innsbruck (1992)
- 77 Höß, P.: *Optimierung von Stockwerkrahmen aus Stahl mit biegesteifen und biegeweichen Rahmenknoten*. Doctoral thesis, Karlsruhe (1994)
- 78 Huber, G.: *Report of STSM to Liège*. COST C1/WD2-97-28 (1997)
- 79 Huber, G.; Kronenberger, H-J.; Weynand, K.: *Representation of joints in the analysis of structural systems*. COST-C1 International Conference Liège (1997)
- 80 Huber, G.; Tschemmerneegg, F.: *Classification and assessment of joints*. COST C1/WD2-98-02 (1998)
- 81 Huber, G.; Tschemmerneegg, F.: *Modellbildung für Riegel-Stützen-Verbindungen*. Fachseminar & Workshop Verbundbau 2, FH München (1998)
- 82 Huber, G.; Tschemmerneegg, F.: *Modelling of beam-to-column joints*. Journal of Constructional Steel Research, 45 p.199-216 (1998)
- 83 Huber, G.; Tschemmerneegg, F.: *Verbindungen - Komponentenmethode. Fachtagung Verbundkonstruktionen*, DFG-Forschergruppe Verbundbau, Universität Kaiserslautern (1997)
- 84 Hudritsch, D.: *Berechnung eines unverschieblichen Verbundrahmens mit ausbetonierten Rechteck-Hohlprofilstützen und Flachdecken*. Master thesis, Innsbruck (1997)
- 85 Humer, C.: *Das Momenten-Rotationsverhalten von steifenlosen Rahmenknoten mit Kopfplattenanschlüssen*. Doctoral thesis, Innsbruck (1987)
- 86 Huter, M.: *Internationale Versuchsdatenbank für Stahl- und Verbundknoten*. Doctoral thesis, Innsbruck (1997)
- I**
- 87 IABSE: *International Conference "Composite Construction - Conventional and Innovative"* in Innsbruck. Zürich (1997)
- 88 INTAS: *Slim floor construction. Periodic Progress Report 09/97-08/98*. Intas project 96-2154 (1998)
- J**
- 89 Jaspert, J.-P.: *Etude de la semi-rigidite des noeuds poutre-colonne et son influence sur la resistance et la stabilite des ossatures en acier*. Doctoral thesis, Liège (1991)
- 90 Johnson, R.; Molenstra, N.: *Partial shear connection in composite beams in building*. Proceedings Institute of Civil Engineers, Part 2, vol.91 (1991)

K

- 91 Kindmann, R.; Bergmann R.: *Auswertung der Versuche zum Tragverhalten von Verbundprofilen mit ausbetonierten Kammern - Verbundträger*. Bericht No.9202, Lehrstuhl für Stahlbau - Bochum (1992)
- 92 Klein, H.: *Das elastisch-plastische Last-Verformungsverhalten steifenloser, geschweißter Knoten für die Berechnung von Stahlrahmen mit HEB-Stützen*. Doctoral thesis, Innsbruck (1985)
- 93 Krings, W.: *Berechnungstafel für die Momenten-Krümmungs-Beziehung im Zustand II beim Rechteckquerschnitt nach EC2*. Bautechnik, 71.Jahrgang, Heft 6 (1994)
- 94 Kronenberger, H.J.: *Ein Beitrag zum Verhalten von Anschlüssen im Verbundbau unter besonderer Berücksichtigung von Nachgiebigkeiten in der Verbundfuge und des Einflusses der Herstellung*. Doctoral thesis, Kaiserslautern (in preparation)

L

- 95 Larcher, Th.: *Versuche zur Krafteinleitung der Trägersauflagerkräfte bei Hohlprofilverbundstützen mit Setznägeln*. Master thesis, Innsbruck (1997)
- 96 Leitner, H.: *Die Querkraftdeformation bei Verbundknoten*. Master thesis, Innsbruck (1989)
- 97 Lener, G.: *Berechnung räumlicher Stahlrahmen mit nichtlinearem Knotenverhalten unter Berücksichtigung der Normalkraftsinteraktion*. Doctoral thesis, Innsbruck (1988)
- 98 Lener, G.: *Programmsystem Plan. Traglastberechnung räumlicher Stabtragwerke unter Berücksichtigung der Nachgiebigkeit der Verbindungselemente, von geometrischen und physikalischen Nichtlinearitäten sowie geometrischen und strukturellen Imperfektionen. Version 3.43*, Feldkirch (1996)
- 99 Leon, R.T.: *Theories of incomplete interaction*. Engineering Foundation Conference, Composite Construction III, Irsee (1996)
- 100 Leon, R.T.; Hoffman J.J.; Staeger, T.: *Partially restrained composite connections*. Design guide, AISC, Chicago (1996)
- 101 Lindner, J.; Bergmann, R.: *Zur Bemessung von Verbundstützen nach DIN 18800 Teil 5*. Stahlbau 67 p.536-546 (1998)

M

- 102 Meixner, G.: *Tragfähigkeitsuntersuchungen an slim-floor-Trägern*. Master thesis, Innsbruck (1995)

- 103 Müller, G.: *Das Momentenrotationsverhalten von Verbundknoten mit Verbundstützen aus Rohrprofilen*. Doctoral thesis, Innsbruck (1998)

N

- 104 Najafi, A.; Anderson, D.: *Ductile steel-concrete composite joints*. International Conference "Composite Construction - Conventional and Innovative" in Innsbruck, Report p.427-432, IABSE Zürich (1997)
- 105 Nethercot, D.A.: *Semi-rigid joint action and the design of nonsway composite frames*. Engineering Structures, Vol.17, No.8, Great Britain (1995)
- 106 Neulichedl, A.: *Zum Verhalten von Verbundplatten aus Stahlprofilblechen und Stahlbeton unter Berücksichtigung des nichtlinearen Verhaltens der Verbundfuge*. Doctoral thesis, Innsbruck (1990)
- 107 Niederwanger, G.: *Experimentelle Spannungsanalysen*. Lecture, Innsbruck

O

- 108 ÖNORM ENV 1993-1-1: *Eurocode 3 - Bemessung und Konstruktion von Stahlbauten (Design of steel structures)*. Vornorm (1993)
- 109 ÖNORM ENV 1994-1-1: *Eurocode 4 - Bemessung und Konstruktion von Verbundtragwerken aus Stahl und Beton (Design of composite steel and concrete structures)*. Vornorm (1994)
- 110 ÖStV - Österreichischer Stahlbauverband: *Richtlinien für Verbundkonstruktionen im Hochbau*. Wien (1988)

P

- 111 Pajari, M.: *Shear resistance of prestressed hollow core slabs on flexible supports*. VTT publication 228, Espoo (1995)
- 112 Pajari, M.; Yang, L.: *Shear capacity of hollow core slabs on flexible supports*. VTT research note 1587, Espoo (1994)
- 113 Petersen, C.: *Stahlbau*. pp.820, Braunschweig (1988)

Q

- 114 Queiroz, G.: *Estudo do Comportamento e Sistematizacão do Projeto de Ligacoes Rígidias entre Perfis I com Almas Coplanares*. Doctoral thesis, Innsbruck/Brasil (1992)

R

- 115 Rangetiner, E.: *Einfluß der Knotennachgiebigkeit auf die Stabilität von verschieblichen Portalrahmen*. Master thesis, Innsbruck (1998)
- 116 Ren, P.: *Numerical modelling and experimental analysis of steel beam-to-column connections allowing for the influence of reinforced-concrete slabs*. Doctoral thesis, Lausanne (1995)
- 117 Roik, K.: *Verbundkonstruktionen*. Stahlbau-Handbuch. Band 1. pp. 627, Köln (1982)
- 118 Rubin, D.: *Knoten für die Mischbauweise - Assembly, Transformation und Klassifikation*. Doctoral thesis, Innsbruck (in preparation)

S

- 119 Sattler, K.: *Theorie der Verbundkonstruktionen. Spannbeton. Stahlträger in Verbund mit Beton. Band 1+2*. Verlag Wilh.Ernst&Sohn, Berlin (1959)
- 120 Sauerborn, I.: *Zur Grenztragfähigkeit von durchlaufenden Verbunddecken*. Doctoral thesis, Kaiserslautern (1995)
- 121 Schanzenbach, J.: *Zum Einfluß von Dübelnachgiebigkeit und Unterverdübelung auf das Tragverhalten von Verbunddurchlaufträgern im Hoch- und Industriebau*. Doctoral thesis, Kaiserslautern (1988)
- 122 Schaur, B.C.: *Entwicklung einer Modulbank für Stahl- und Verbundknoten*. Doctoral thesis, Innsbruck (1995)
- 123 Schlaich, E.J.; Schäfer, K.: *Konstruieren im Stahlbetonbau*. Betonkalender 1993 II, Berlin (1993)
- 124 SCI: *Composite beam design to Eurocode 4*. SCI publication 121, Berkshire (1994)
- 125 SCI: *Composite column design to Eurocode 4*. SCI publication 142, Berkshire (1994)
- 126 SCI: *Design aspects of precast hollow core slabs used with structural steelwork*. ECCS/TC11, Düsseldorf (1996)
- 127 SCI: *Design of asymmetric slimflor beams using deep composite decking*. SCI publication 175, Berkshire (1997)
- 128 SCI: *Design of semi-continuous braced frames*. SCI publication 183, Berkshire (1997)
- 129 SCI: *Moment connections in composite construction: Interim guidance for end-plate connections*. Technical report 143, Berkshire (1995)
- 130 Sedlacek, Weynand, Kong, Saal, Klinkenberg, Bode, Kronenberger: *Research work done in Germany in the field of semi-rigid connections*. COST C1-Workshop, Prague (1994)

- 131 Seeber, W.: *Versuche mit Slim-floor-Trägern - Erfahrungen mit der Datenbank*. Master thesis, Innsbruck (1995)
- 132 Sprint RA351: *Steel moment connections according to Eurocode 3. Simple design aids for rigid and semi-rigid joints*. European Community strategic programme for innovation and technology transfer (1995)
- 133 Stahl-Informations-Zentrum; Bergmann, R.; Breit, M.: *Verbundstützen aus einbetonierten Walzprofilen*. Merkblatt 217, Düsseldorf (1989)
- 134 Stahl-Informations-Zentrum; Bode, H.; Bergmann, R.: *Betongefüllte Stahlhohlprofilstützen*. Merkblatt 167, Düsseldorf (1989)
- 135 Stahl-Informations-Zentrum; Schanzenbach, J.: *Verbundträger im Hochbau*. Merkblatt 267, Düsseldorf (1991)
- 136 Steiner, M.: *Teiluntersuchungen zu Verbundknoten mit Hohlprofilstützen - Großversuche und Komponentenversuche*. Master thesis, Innsbruck (1997)
- 137 Stippler, P.: *Nichtlineare Vergleichsrechnungen zum Knotenverhalten*. Master thesis, Innsbruck (in preparation)
- 138 Stoiberer, H.: *Zur Querkraftdeformation von Verbundknoten mit Rohrprofilen*. Master thesis, Innsbruck (1990)

T

- 139 Taus, M.: *Näherungsmethoden zur Bemessung von Rahmen unter Berücksichtigung des nichtlinearen Knotenverhaltens*. Doctoral thesis, Innsbruck (1987)
- 140 Thor, J.: *A new fire-safe composite steel beam*. Steel Construction Today 4 p.137-140 (1990)
- 141 Tschemmernegg, F.: *A nonlinear joint model for the design of structural steel frames*. ACAI 1/1988 pp.31-41, Milano (1988)
- 142 Tschemmernegg, F.: *Composite frames with slim floors*. Second World Conference on Steel in Construction, San Sebastian (1998)
- 143 Tschemmernegg, F.: *Connection of floor systems to columns - Conventional and Advanced*. International Conference "Composite Construction - Conventional and Innovative" in Innsbruck, Report p.445-450, IABSE Zürich (1997)
- 144 Tschemmernegg, F.: *Die Mischbauweise - eine Bautechnologie für die Zukunft*. Stahlbau 68 p.155-160 (1999)
- 145 Tschemmernegg, F.: *Entwicklung von Bauelementen und deren Verbindung im Verbundbau*. Stahlbau, 63.Jahrgang, Heft 1 (1994)
- 146 Tschemmernegg, F.: *First building in Austria with a composite frame designed acc. to ENV1994-1*. Engineering Foundation Conferences, Composite Construction III, Irsee (1996)

- 147 Tschemmernegg, F.: *Mischbauweisen Brückenbau*. Lecture, Innsbruck (1997)
- 148 Tschemmernegg, F.: *Mischbauweisen Hochbau*. Lecture, Innsbruck (1993)
- 149 Tschemmernegg, F.: *Steifenlose Konstruktionen im Stahlhochbau. DStV - Das moderne Stahlbauunternehmen - Wandlung in Entwurf und Konstruktion*. Dt.Stahlbautag, Stuttgart (1976)
- 150 Tschemmernegg, F.: *Steifenlose Stahlskeletttragwerke und dünnwandige Vollwandträger - Berechnung und Konstruktion - Europäische Empfehlungen*. Verlag Wilh.Ernst&Sohn, Berlin (1977)
- 151 Tschemmernegg, F.: *The design of structural steel frames under consideration of the nonlinear behaviour of joints*. Journal of Constructional Steel Research (1987)
- 152 Tschemmernegg, F.: *The non-linear behaviour of composite joints*. Journal of Constructional Steel Research, 21 p.59-70 (1992)
- 153 Tschemmernegg, F.: *Zur Bemessung von Schenkeldübeln, eines neuen Dübels für Verbundkonstruktionen im Hochbau*. Bauingenieur 60 p.351-360 (1985)
- 154 Tschemmernegg, F.; Beck, H.: *Nailed shear connection in composite tube columns*. ACI-paper, Houston Convention (1997)
- 155 Tschemmernegg, F.; Bergmann, J.; Marcher, S.: *Zur Berechnung von Verbundrahmen mit nachgiebigen Verbundknoten*. Stahlbau 67 p.516-524 (1998)
- 156 Tschemmernegg, F.; Brugger, R.; Hittenberger, R.; Wiesholzer, J.; Huter, M.; Schaur, B.C.; Badran, M.Z.: *Zur Nachgiebigkeit von Verbundknoten*. Stahlbau, 63.Jahrgang/ Heft 12 (1994), 64.Jahrgang/Heft 1 (1995)
- 157 Tschemmernegg, F.; et.al.: *Neue Innsbrucker Mischbautechnologie mit Erfolg beim Millennium Tower in Wien angewandt*. Stahlbau, 68.Jahrgang, Heft 8 (1999)
- 158 Tschemmernegg, F.; Huber, G.: *Component method for joints*. COST C1/WD2-96-16 (1996)
- 159 Tschemmernegg, F.; Huber, G.: *Gutachten über die Tragfähigkeit von Stanzdübeln*. Innsbruck (1995)
- 160 Tschemmernegg, F.; Huber, G.: *Joint transformation*. COST C1/WD2-96-09 (1996)
- 161 Tschemmernegg, F.; Huber, G.: *Technical papers T1 to T15. Calibration work within COST-C1/ECCS TC11 Drafting Group for Composite Connections for ENV 1994-1-1, Annex J*. Innsbruck (1995-1998)
- 162 Tschemmernegg, F.; Huber, G.: *To the development of composite and mixed connections*. International Conference on Steel and Composite Structures, Delft (1999)

- 163 Tschemmernegg, F.; Huber, G.: *Flachdecken mit Stanzdübeln (Slim-floors with punched shear connectors)*. Bauingenieur 71 p.425-436 (1996)
- 164 Tschemmernegg, F.; Huber, G.; Huter, M.; Rubin, D.: *Komponentenmethode und Komponentenversuche zur Entwicklung von Baukonstruktionen in Mischbauweise*. Stahlbau 66 p.624-638 (1997)
- 166 Tschemmernegg, F.; Huber, K.: *Rahmentragwerke in Stahl unter besonderer Berücksichtigung der steifenlosen Bauweise*. Österreichischer Stahlbauverband, Schweizerische Zentralstelle für Stahlbau, Wien/Zürich (1987)
- 167 Tschemmernegg, F.; Huter, M.: *Classification of beam-to-column joints*. COST C1/WD2-93-16 (1993)
- 168 Tschemmernegg, F.; Lener, G.; Taus, M.: *Zur Nachgiebigkeit von Rahmenknoten Teil 2*. Stahlbau 58 p.45-52 (1989)
- 169 Tschemmernegg, F.; Neulichedl, A.: *Entwicklung einer ankerlosen, duktilen Verbundplatte*. Bauingenieur 68 p.313-322 (1993)
- 170 Tschemmernegg, F.; Tautschnig, A.; Klein, H.; Braun, Ch.; Humer, Ch.: *Zur Nachgiebigkeit von Rahmenknoten*. Stahlbau 56 p.299-306 (1987)

W

- 171 Wahlberg, H.: *Bestimmung der plastischen Grenzkennwerte für Krafteinleitung bei HEA-Profilen St360*. Master thesis, Innsbruck (1987)
- 172 Wald, F.: *Column bases*. Prag (1995)
- 173 Weger, A.: *Geschweißte Innenknoten mit IPE-Profilen*. Master thesis, Innsbruck (1994)
- 174 Wegscheider, J.: *Geschweißte Randknoten mit IPE-Profilen*. Master thesis, Innsbruck (1994)
- 175 Weynand, K.: *SERICON - Databank on joints in building frames*. COST-C1 Workshop, p.465, Strasbourg (1992)
- 176 Weynand, K.: *Sicherheits- und Wirtschaftlichkeitsuntersuchungen zur Anwendung nachgiebiger Anschlüsse im Stahlbau*. Doctoral thesis, Aachen (1997)
- 177 Wicke, M.: *Betonbau - Grundlagen - Bemessung im Stahlbeton*. Lecture, Innsbruck
- 178 Wicke, M.; Münger, F.; Randl, N.: *Design of Shear Transfer in Concrete-Concrete Composite Structures*. International Conference "Composite Construction - Conventional and Innovative" in Innsbruck, Report p.163-168, IABSE Zürich (1997)
- 179 Wiesholzer, J.: *Zur Krafteinleitung bei Verbundknoten*. Doctoral thesis, Innsbruck (1992)

- 180 Winkler, B.J.: *Versuche zur Ermittlung des Schub- und Krafteinleitungsverhaltens von Rechteckhohlprofilen mit und ohne Betonfüllung*. Master thesis, Innsbruck (1995)

Z

- 181 Zangerl, O.: *Versuche zur Ermittlung des Schub- und Krafteinleitungsverhaltens von Rohrprofilen mit und ohne Betonfüllung*. Master thesis, Innsbruck (1995)
- 182 Betonkalender 1993, Teil II.: Verbundkonstruktionen. 82.Jahrgang, Berlin (1993)
- 183 Beton-Kalender 1993. Teil II. p.551-680, Ernst&Sohn, Berlin (1993)
- 184 Connections in steel structures. Behaviour, strength and design. Proceedings of the Third International Workshop, Elsevier, Trento (1995)
- 185 Stahlbaujahrbuch 1999. Verlag Wilh.Ernst&Sohn, Berlin (1999)